

EXCITONS IN CRYSTALLINE BENZENE

Thesis by
Steven Douglas Colson

In Partial Fulfillment of the Requirements
For the Degree of
Doctor of Philosophy

California Institute of Technology
Pasadena, California

1968

(Submitted August 4, 1967)

To My Parents

ACKNOWLEDGMENTS

I thank Professor G. Wilse Robinson for his help and guidance during the past four years. His contribution to my scientific education is gratefully acknowledged and his interest in my future is sincerely appreciated.

I also wish to acknowledge my colleagues who have contributed either directly or indirectly to the present study. Special thanks are due to Mr. Elliot R. Bernstein who worked closely with me on numerous occasions and who was always willing to take time out to discuss various aspects of this work. The contributions of Mr. David M. Hanson, Dr. Raoul Kopelman, and Dino S. Tinti to those respective portions of this work which are presented as co-author reprints and preprints are also acknowledged.

I am grateful to the California Institute of Technology, the National Science Foundation, the U.S. Atomic Energy Commission, and the U.S. Army Research Office for financial support.

I am especially appreciative of the support of my wife, Donna, who has been a continuing source of encouragement and has helped extensively in the preparation of this thesis.

ABSTRACT

PART I. EXPERIMENTAL PROCEDURE

The spectrographs and excitation sources used to study the absorption and emission spectra of crystalline benzene are described and their relative merits discussed.

A new purification method is also described. This method, in which the benzene is vacuum refluxed over an $\sim 100^{\circ}\text{C}$ cesium mirror, can be used in conjunction with zone refining techniques to reduce the spectroscopic impurity level to $\sim 10^{-6}$ mole percent. Also see Part III in this regard.

A modified Bridgman type crystal growing technique that is used to produce high quality, low temperature crystals is described in detail. The development of these experimental techniques was essential to the success of the experiments described in Parts II and III.

PART II. SINGLET EXCITON BAND STRUCTURE
OF CRYSTALLINE BENZENE

The Frenkel theory for localized excitations in molecular crystals is redeveloped and extended for the case of benzene to lay a consistent theoretical framework for the interpretation of pure and mixed crystal spectra. Three types of dipole selection rules are proved for $\underline{k} \neq 0$ transitions in a restricted Frenkel limit. They are: 1) $\Delta \underline{k} = 0$; 2) general selection rules

based on interchange symmetry; and 3) the $\underline{g} \leftrightarrow \underline{u}$ selection rule for centrosymmetric crystals. These are particularly important in the interpretation of exciton band \leftrightarrow exciton band transitions. Furthermore, the interchange group and ideal mixed crystal concepts are introduced to provide a clear, precise definition of the static and dynamic contributions to the energy of the crystal states. Emphasis is placed upon the relative signs and magnitudes of the dynamic coupling constants rather than on crystal splittings since these constants give directly the anisotropy of the resonance interactions in the crystal.

Experimental data from the absorption and emission spectra of the ${}^1B_{2u}$ state of pure and isotopic mixed benzene crystals are also presented. From these data it can be concluded that the line shapes and transition energies are very sensitive to the effects of crystal strain. Exciton band \leftrightarrow exciton band transition line shapes are interpreted in terms of the density of states function of the ${}^1B_{2u}$ exciton band. This experimental function is found to be inconsistent with that predicted from the data obtained from the variation of energy denominators method of analysis of this exciton band by Nieman and Robinson. The variation of energy denominators method is investigated with more extensive and improved experiments. It is found to be inappropriate for the study of the ${}^1B_{2u}$ state of crystalline benzene, and these new experiments lead to a different interpretation

of this band. The resonance coupling constants obtained from this new interpretation are used to calculate the density of states function for a crystal of 32,000 molecules. This calculated function is in excellent agreement with that obtained from the exciton band \longleftrightarrow exciton band transition line shapes. Exciton band \longleftrightarrow exciton band transitions involving the lowest singlet of crystalline naphthalene are also reported and discussed.

PART III. TRIPLET EXCITONS IN CRYSTALLINE BENZENE;
LOCATION OF THE FIRST AND SECOND TRIPLETS;
PHOSPHORESCENCE AND TRAP - TRAP ENERGY TRANSFER
IN ISOTOPIC MIXED CRYSTALS.

The first and second triplets of solid benzene are observed using O_2 and NO perturbation techniques. The absorption spectra of long benzene crystals of ultrahigh spectroscopic purity are discussed in terms of the unperturbed transition to the second triplet state.

The phosphorescence spectrum of isotopic mixed benzene crystals is analyzed with special emphasis being placed on the effects of the static crystal field. The fluorescence and absorption spectra are used to supplement this analysis.

The phosphorescence and fluorescence spectra of three component isotopic mixed benzene crystals are studied as a function of guest concentration, excitation lamp intensity, and temperature. Some very interesting effects are observed at high lamp intensities and interpreted

in terms of triplet - triplet annihilation of trapped excitation. Triplet excitation is found to be transferred between two different traps which are not more than $\sim 20 \text{ \AA}$ apart in this system.

TABLE OF CONTENTS

PART	TITLE	PAGE
I.	EXPERIMENTAL PROCEDURES.....	1
	A. Basic Setup.....	2
	B. Sample Preparation.....	6
II.	SINGLET EXCITON BAND STRUCTURE OF CRYSTALLINE BENZENE.....	15
	A. Frenkel Exciton Selection Rules for $k \neq 0$ Transitions in Molecular Crystals.....	16
	References.....	32
	B. Electronic and Vibrational Exciton Structure in Crystalline Benzene.....	35
	References.....	92
	C. Absorption Spectra of Strained Benzene Crystals at Low Temperatures.....	96
	References.....	97
	D. Direct Observation of the Entire Exciton Band of the First Excited Singlet States of Crystalline Benzene and Naphthalene.....	98
	References.....	159
	E. Location of the Fourth, Forbidden Factor Group Component of the ${}^1B_{2u}$ State of Crystalline Benzene.....	164
	References.....	196
III.	TRIPLET EXCITONS IN CRYSTALLINE BENZENE: LOCATION OF THE FIRST AND SECOND TRIPLETS; PHOSPHORESCENCE AND TRAP-TRAP ENERGY TRANSFER IN ISOTOPIC MIXED CRYSTALS.....	198
	A. First and Second Triplets of Solid Benzene.....	199

PART	TITLE	PAGE
B.	Observation of the Second Triplet of Solid Benzene Using NO Perturbation.....	208
	References.....	208
C.	Static Crystal Effects on the Vibronic Structure of the Phosphorescence, Fluorescence, and Absorption Spectra of Benzene Isotopic Mixed Crystals.....	209
	References.....	288
D.	Trap-Trap Triplet Energy Transfer in Isotopic Mixed Benzene Crystals.....	290
	References.....	322
	PROPOSITIONS.....	323

PART I

EXPERIMENTAL PROCEDURES

A. Basic Experimental Setup

A number of different spectrographs and spectrometers were used for the experiments reported in this thesis. Since they are all standard spectroscopic equipment, they will not be discussed in detail but will only be compared with respect to dispersion, aperture and detection method as tabulated in Table 1. The photographic aperture (speed) of these instruments is proportional¹ to the area of the grating (A) divided by the square of focal length f of the collimating mirror (lense); since $A = (\pi/4)d^2$ for a circular grating with diameter d, this gives the familiar camera rule that the exposure is inversely proportional to $(f/d)^2$, or the "f/-number" squared. The effective f/-number, calculated from the speed A/f^2 of the instruments (all of which contain rectangular gratings) is given in parenthesis in Table I. The photoelectric speed depends upon the slit height and width and, therefore, will not be a characteristic constant of a given spectrometer but will depend upon the values chosen for these parameters.

The experimental setup for each instrument was basically the same and has been adequately described by previous theses from this laboratory.² However the proper selection of new light sources and filtering systems was essential to the success of this research. For

Table I

SPECTROGRAPH	MOUNT	PHOTOGRAPHIC SPEED A/f ²	BLAZE ANGLE	GRATING GROOVES per mm	1 st ORDER DISP.	METHOD OF DETECTION
0.75M J-A	Czerny-Turner	1.9×10^{-2} (f/6.5)	$1/\mu$	600	40 Å/mm	Photographic Photoelectric
2.0M Caltech	Czerny-Turner	5.5×10^{-3} (f/12)	$1/\mu$	600	8 Å/mm	Photographic
1.83M J-A	Ebert	-	$1/\mu$	600	9 Å/mm	Photoelectric
3.4M J-A	Ebert	6.5×10^{-4} (f/35)	0.9μ	600	5 Å/mm	Photographic
		9.1×10^{-4} (f/29)	3μ	300	5 Å/mm	Photographic
		5.3×10^{-4} (f/38)	5.7μ	300	9 Å/mm	Photographic
Medium Quartz B&L		1.1×10^{-2} (f/8)	Prism	~ 1 Å/mm	at 2650 Å	Photographic

example, when this research was initiated, the standard source for the excitation of the benzene emission spectrum was an 800 watt Hanovia high pressure xenon source which was filtered by a 2600 \AA interference filter and gaseous Cl_2 and Br_2 filters. With this source and the 2 M spectrograph, several hours were required to photograph the weak 0,0 transition of the phosphorescence spectrum. In addition, the fluorescence spectrum, which required comparable exposure times, was partially overlapped by continuum from the lamp. In contrast, it was found that the fluorescence and phosphorescence 0,0 transitions could easily be photographed in less than 5 min. when using a 4 watt GE germicidal low pressure mercury lamp which had been filtered by a $\text{NiSO}_4 - \text{CoSO}_4$ Kasha³ filter solution and a dilute solution of diphenylbutadiene in methanol. The significance of this advantage was not just that it saved time. Without such an intense source, it would have been nearly impossible to accurately measure the intensity distribution of the broad emission lines characteristic of exciton band \leftrightarrow exciton band transitions (See Part II), to photograph the benzene phosphorescence on the 3.4 M J-A spectrograph (See Part III), or to make the accurate intensity measurements necessary for the energy transfer experiments (See Part III). In fact, the measurements of the emitted intensity as a function of lamp intensity required the use of several of the more intense lamps simultaneously (See Part III).

A number of different light sources were found to be necessary, depending upon the purpose of the particular experiment. They will each be discussed separately below.

1. PEK High Pressure Mercury Arc Lamp (200 watt)

This lamp was particularly useful for exciting the benzene fluorescence spectrum. Because of the Hg resonance reabsorption, there is effectively no output in the 2500 - 2700 Å region even though there is considerable output at 2450 - 2500 Å. Thus, this lamp could easily be filtered with a Bausch and Lomb fast (f/3.5) monochromator and used to give a fluorescence spectrum which was free from any overlying continuum in the region of the 0,0 transition (2650 Å). The scattered light in the monochromator was high enough to require the use of Cl₂ and Br₂ gas filters, the combination of which transmits from 2200 to 2800 Å, in addition to the monochromator in order to obtain a clean spectrum in the rest of the fluorescence region. This source likewise provided a clean phosphorescence spectrum, however, in this case the monochromator and gas filters could be replaced by a NiSO₄ - CoSO₄ Kasha filter solution to obtain more intensity. Using these combinations of source and filters, the fluorescence and phosphorescence 0,0 transitions of isotopically mixed benzene crystals could be photographed in 5-10 min. on the 2M spectrograph.

2. GE Low Pressure Germicidal Mercury Lamp (4 watt).

Approximately 80% of the total output of this lamp is in the lines at 2537 Å. Thus, even though it has ~50 times less power output than the PEK high pressure arc lamp, it is about three times more effective for exciting the benzene emission. Because of its size (~5 in. long) and very sharp emission lines, it was much more difficult to filter than the arc lamp, but the lack of continuous emission in its output made it useable in some cases where more intensity was required. For instance, for the energy transfer experiments, where only a few emission lines were measured, the high intensity was used to increase the accuracy of the phosphorescence and fluorescence intensity measurements. Because the sharp mercury lines did not overlap the benzene emission lines of interest, the lamp could be used without any filters. The intensity of the Hg lines in the fluorescence region could be markedly reduced by using a very dilute solution of diphenylbutadiene in methanol and a filter before the sample. However, this solution, which has an ~100 Å window at 2600 Å, was found to be unstable to UV excitation and had to be changed after each half hour of use.

3. Hanovia Model LO 735A-7 Low Pressure, Confined Discharge Mercury Lamp (12 watt)

The output of this lamp is easier to collect and

filter than that of the germicidal lamp since the discharge is confined to a volume of $\sim 1 \text{ cm}^3$. However, the discharge pressure is somewhat higher than that of the germicidal lamp. Consequently, there is some continuum output and the percentage of the output in the 2537 \AA region is reduced such that the total usable UV light is about the same as that obtained from the 4 watt lamp.

4. PEK High Pressure Xenon Arc Lamp (150 watt)

The smooth continuous output of the xenon arc lamp was used for photographing the benzene absorption spectrum. Lamp intensity was usually not a problem for the absorption spectra (exposure times were often $\sim 1 \text{ sec.}$) and, thus, this lamp was chosen primarily because of its small arc. The small arc made it possible to focus the light on small samples without necessitating additional baffling to prevent stray light from reaching the spectrograph.

B. Sample Preparation

Extremely high sample purity was essential to almost all of the experiments which comprised this research. That none of the standard purification methods would be adequate can be easily seen by considering the fact that $\sim 10^{-8}$ parts of phenol in benzene could have been detected in the long crystals ($\sim 5 \text{ cm}$) used to observe the second triplet of solid benzene in absorption (Part III). Furthermore, $>10^{-7}$ parts of phenol would have made it

impossible to accurately measure the intensity distribution of the exciton band \leftrightarrow exciton band absorption (Part II. Thus, new purification techniques had to be devised before the research could be successfully completed. The most successful procedure developed is described in detail and compared to other techniques in Part III, however, some more recent findings concerning the results of the method will be discussed at this time for completeness. The preparation of high quality crystals also played an essential role in this research and will be discussed below.

1. Preparation of Very High Purity Benzene

The most successful method involved the treatment of benzene with pure cesium metal. The benzene was refluxed, under vacuum, over the surface of a cesium film which was heated to about 100°C. Any impurities which were more reactive than benzene (and some of the benzene) reacted with the cesium to form a black non-volatile deposit in the reaction vessel. The purified benzene could then easily be separated from the deposit by one vacuum distillation. It was found that effectively all of the phenol and several other impurities were removed by this technique. However, certain unidentified impurities (one in the region of the lowest triplet state and some in the region of the lowest singlet) were difficult to eliminate. This problem can effectively be overcome

by combining zone refining techniques with the cesium treatment. A sample of benzene which had been extensively zone refined by G.J. Sloan of the Central Research Laboratories of du Pont was found to contain almost no impurities except phenol which was present at about 10^{-3} percent. The spectrum of a 4 cm crystal of this sample, after treatment with cesium, only showed a very faint trace of impurity absorption in the singlet region. The 99.93 mole percent pure Phillips research grade benzene used in Part III was almost completely free of the troublesome impurities in the first singlet region and, thus, the cesium treatment produced extremely pure benzene.

2. Crystal Growth

The preparation of large benzene crystals which were transparent at 4.2°K was a very challenging experimental task. Large (1 cm X 10 cm) crystals at -20°C were relatively easy to grow from the melt using a Bridgman furnace (See Part III). However, the samples cracked extensively when cooled to liquid helium temperatures, even though they were mounted in a Teflon holder and cooled over a period of several hours by radiation. They remained translucent, but one to two hours were required to obtain an absorption spectrum with the 2 M instrument.

The development of a considerably superior method

was made possible because of the artistry of Erich W. Siegel and Learco Minghetti of the Cal. Tech. chemistry glass shop. They were able to prepare the ingenious quartz crystal growing cell shown in Fig. 1. This cell could be used for growing crystals as thin as 10μ and as thick as 5cm. Not only did this cell construction allow one to prepare near perfect crystals at 4.2°K (see below), but the sample could be vacuum degassed in the cell and left in the cell during the entire experiment. This was found to improve the phosphorescence yield by at least a factor of two.

The crystals were prepared as follows: The benzene was usually purified by the cesium reflux method and then vacuum distilled directly into the crystal growing cell. The cell was then sealed off under vacuum and removed from the vacuum system. The crystal was grown from the melt by lowering the cell at the rate of ~ 1 cm/day into a modified Bridgman furnace (Fig. 2), the lower half of which was a liquid nitrogen filled dewar. The key to the success of this method was the development of a continuous temperature gradient down the crystal from $\sim 0^{\circ}\text{C}$ to almost liquid nitrogen temperature. As the crystal was slowly lowered, a given horizontal cross-section could then be maintained at an almost even temperature since the heat is being removed from the bottom. In contrast, radiation cooling of the crystal would cool the outside more rapidly than its inside and, since

Figure 1. Modified Bridgman Type
Sample Cell.

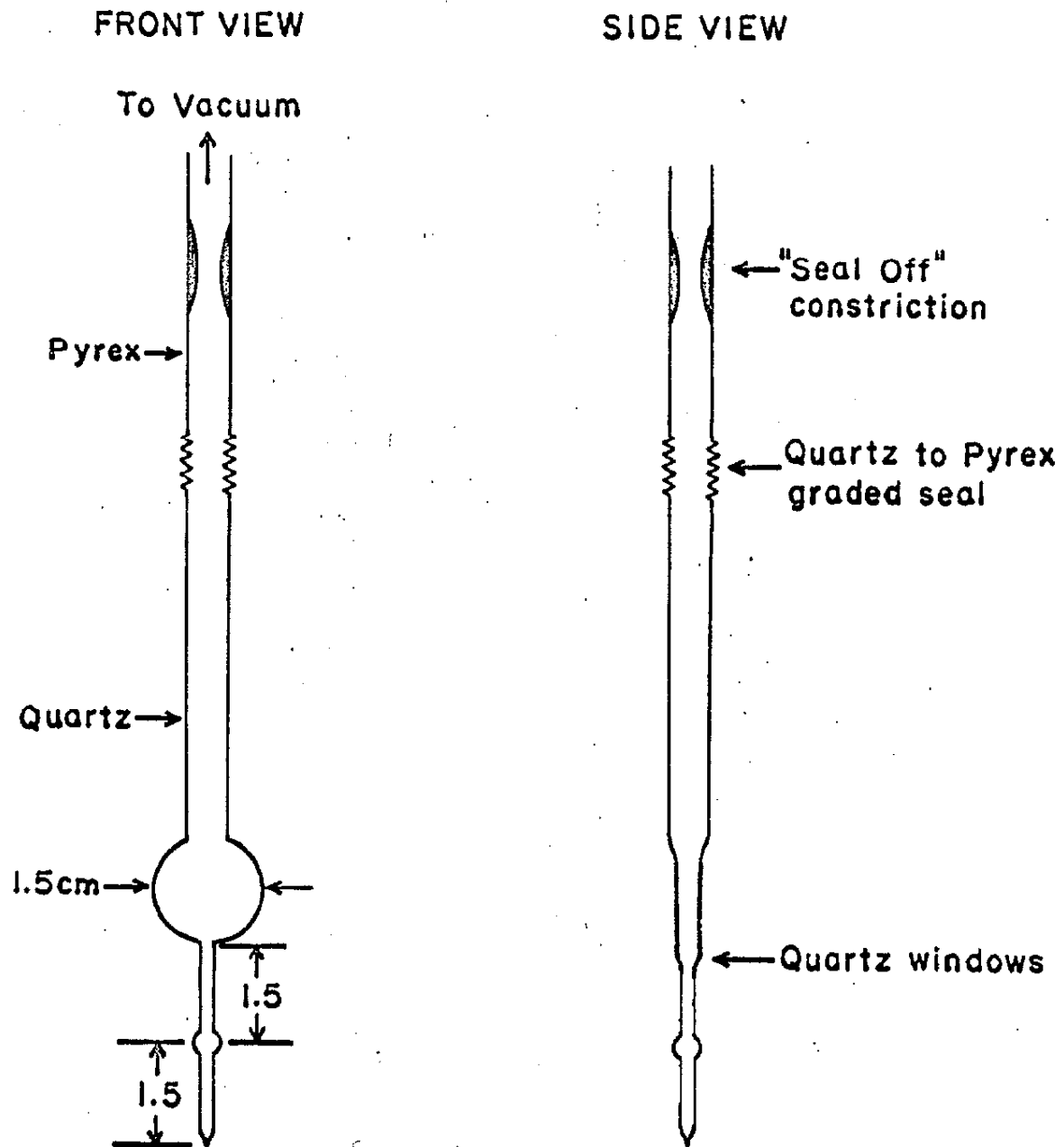
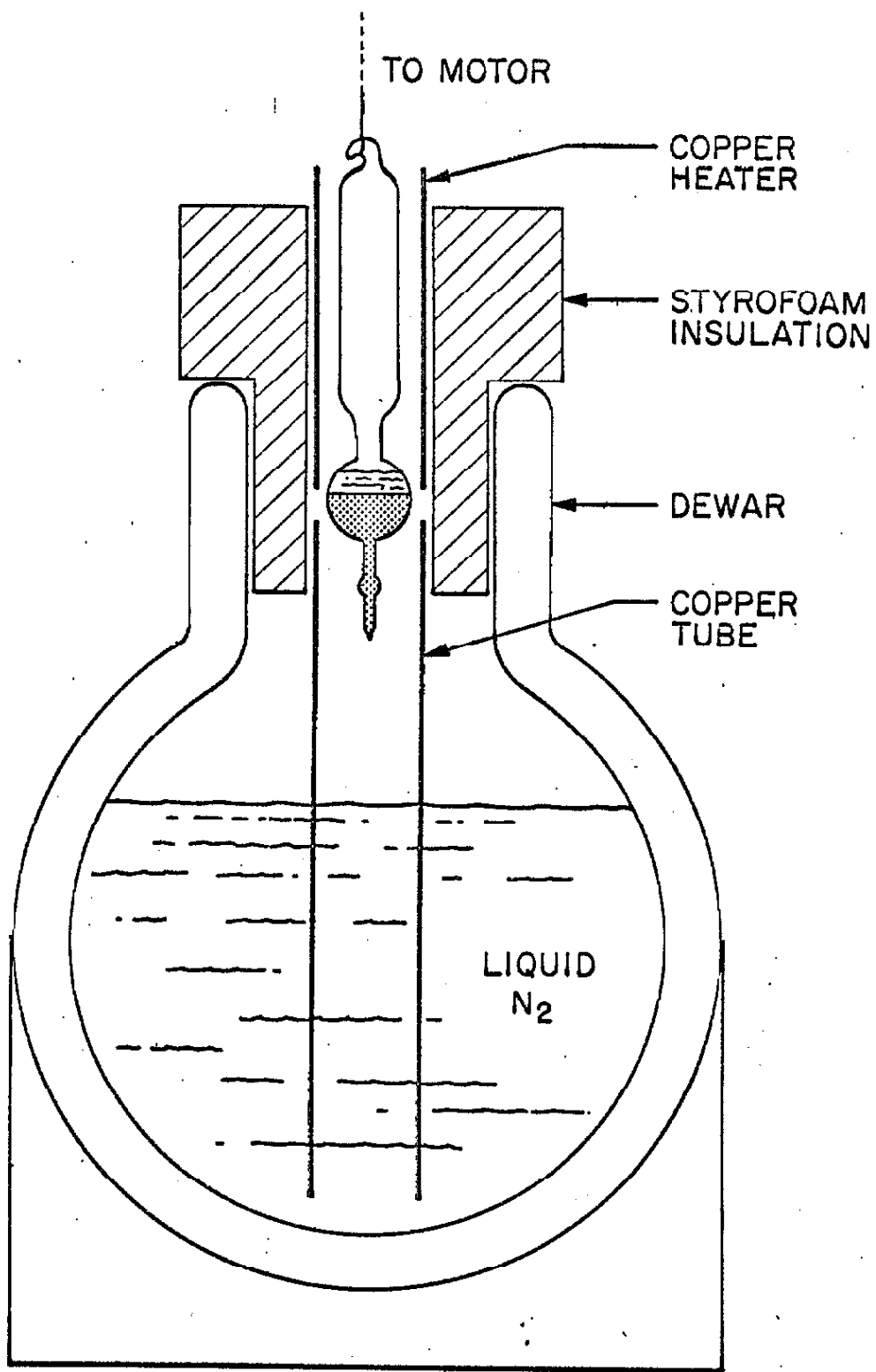
SAMPLE CELL

Figure 2. Modified Bridgman Type
Crystal Growing Furnace.



benzene crystals are poor heat conductors, large strains would result as the cool outside attempts to contract around the "hot" inside of the crystal. Placing the temperature gradient down the length of the crystal requires that it be able to contract linearly, which it is free to do as long as it does not adhere to the sides of the vessel. Nearly perfect crystals up to 5 cm in length, which could be cooled to 4.2°K with little or no additional cracking, have been grown by this technique.

REFERENCES

1. R.A. Sawyer, Experimental Spectroscopy (Dover Publications, Inc., New York, 1963) p.48.
2. G.C. Nieman, Thesis (California Institute of Technology, 1965).
3. M. Kasha, J. Opt. Soc. Am. 38, 929 (1948).

PART II

SINGLET EXCITON BAND STRUCTURE OF
CRYSTALLINE BENZENE

Frenkel Exciton Selection Rules for $k \neq 0$ Transitions
in Molecular Crystals

S.D. COLSON, R. KOPELMAN,* AND G.W. ROBINSON

Gates and Crellin Laboratories of Chemistry,**

California Institute of Technology,

Pasadena, California 91109

ABSTRACT

Three types of dipole selection rules are proved for $k \neq 0$ in a restricted Frenkel exciton limit. They are: 1) $\Delta k = 0$; 2) general selection rules based on interchange symmetry; and 3) the $\underline{g} \leftrightarrow \underline{u}$ selection rule for centrosymmetric crystals. Even though the latter two selection rules are generally valid only for special values of k , and in particular for $k \neq 0$, they can be shown to be valid for all k in crystals where restrictions are placed on the magnitude of interactions between certain translationally equivalent molecules. For benzene and naphthalene, and probably for many other organic crystals, the translationally equivalent interactions that ruin the selection rules are non-nearest neighbors and are now known to be very small. The

* Present address: Department of Chemistry, University of Michigan, Ann Arbor, Michigan.

** Contribution No. 3422

selection rules are therefore excellent approximations for these crystals. It is also shown that the transition matrix element in this restricted Frenkel limit is \underline{k} -independent, a fact that is important in analyzing the intensity distribution of band \leftrightarrow band transitions in terms of the density-of-states function. Inability to detect a $\underline{u} \leftrightarrow \underline{u}$, band \leftrightarrow band transition experimentally in crystal-line benzene is consistent with the theoretical results.

INTRODUCTION

In centrosymmetric crystals, only transitions between states that belong to the totally symmetric representation of the translation group ($\underline{k} = 0$) have been generally believed¹ to be governed by $\underline{g} \leftrightarrow \underline{u}$ selection rules. Such conclusions were based upon considerations of the group of the wave vector,² as only this group is applicable for $\underline{k} = 0$ energy levels. In centrosymmetric crystals, the inversion symmetry is generally included in the group of the wave vector only for certain special values of \underline{k} .^{2,3} However, by using additional theoretical considerations it can be shown that electric dipole transitions between all \underline{k} levels of Frenkel exciton bands are expected to obey $\underline{g} \leftrightarrow \underline{u}$ selection rules provided inversion is a site, not an interchange,^{4,5} operation, and furthermore provided that interactions between certain translationally equivalent molecules in the crystal are small. This selection rule is valid even though the inversion symmetry is not

included in the group of the wave vector. In addition, other symmetry-based selection rules for $\mathbf{k} \neq 0$ emerge from a consideration of this restricted Frenkel limit. A few of these selection rules will be discussed in this paper.

THEORETICAL

The arguments leading to the selection rules may be sketched out in the following way. Since the translational subgroup of the space group is Abelian, only one-dimensional irreducible representations occur.⁸ Thus, as is well known, in the Bloch representation^{8,9} the Hamiltonian matrix describing the energy levels associated with the set of all translationally equivalent molecules in a crystal contains no off-diagonal elements. Each diagonal element is related to a specific value of the reduced wave vector \mathbf{k} . If there are \underline{t} different translationally equivalent sets corresponding to \underline{t} molecules per primitive unit cell, the full $N \times N$ Hamiltonian matrix describing the crystal energies consists of N/t $t \times t$ Hermitian submatrices along the main diagonal, each submatrix being labeled by a unique \mathbf{k} . Off-diagonal elements $\mathcal{L}_{qq}^f(\mathbf{k})$ within each submatrix arise because of interactions between the \underline{t} sets of translationally equivalent molecules. The $\mathcal{L}_{qq}^f(\mathbf{k})$ are composed of the M_{qq}' 's of many earlier papers¹⁰ modified by phase factors and summed over the whole lattice. The diagonal elements

$\mathcal{L}_{qq'}^f(\underline{k})\delta_{qq'}$, of the submatrices depend upon a k -independent term which defines the position of the exciton band "origin", plus k -dependent terms that arise from interactions among molecules belonging to one of the translationally equivalent subsets of molecules in the crystal.

The \underline{k} -dependent diagonal terms have the form

$$L_{qq}^f(\underline{k}) = \sum_{n'=1}^{N/t} \exp i\underline{k} \cdot (\underline{r}_{n'} - \underline{r}_n) \int \phi_{nq}^{f*} H \phi_{n'q}^f dR, \quad (1)$$

where \underline{r}_n is a radius vector from the crystal origin to an equivalent point (the "unit cell origin") in the n^{th} unit cell. ϕ_{nq}^f are vibronic functions, having the symmetry of the site, representing localized excitation f at the q^{th} site in the n^{th} unit cell,¹¹ all other molecules in the crystal being unexcited; H is the crystal Hamiltonian composed of Coulombic interactions among all the nuclear and electronic charges in the crystal.^{7,12} Integration is carried out over the entire crystal, but for Frenkel excitons, where the basis functions extend very little beyond the site, the practical range of integration is over just the sites nq and $n'q$, and the only important part of the integral arises from that term in the crystal Hamiltonian H that couples the nq^{th} site with the $n'q^{\text{th}}$ site.

As both Davydov¹² and Knox¹³ independently have pointed out, the diagonal elements $\mathcal{L}_{qq'}^f(\underline{k})\delta_{qq'}$ are not equal for $q = 1, 2, \dots, t$ except for certain values of the reduced

wave vector; $\underline{k} = 0$, or, in benzene and naphthalene crystals, \underline{k} lying along a crystallographic axis containing only translationally equivalent molecules, being examples. The inequivalence of the $\mathcal{L}_{qq}^f(\underline{k})\delta_{qc}$, arises even though every molecule in the crystal lies at an equivalent location with respect to its own surroundings. In this case, summing over the translationally equivalent interactions without the phase factors (i.e., for $\underline{k} = 0$) would give the same value for all $q = 1, 2, \dots, t$. However, for general values of \underline{k} one must, according to Eq. (1), compare for different q the magnitudes of the interaction matrix elements along certain fixed directions specified by the vector \underline{r}_n , in the crystal. Since intermolecular interactions are angular dependent and since the different sets of translationally equivalent molecules are oriented differently in space, these interactions for the various q are, in general, different for each value of $\underline{k} \cdot (\underline{r}_n - \underline{r}_n)$. Thus the $L_{qq}^f(\underline{k})$ are different for each q . A simple two-dimensional diagram in Knox's book¹⁴ illustrates the point.

Since the diagonal elements of the submatrices are not equal for general values of \underline{k} , the eigenvalues and eigenvectors of the submatrices are in general complicated functions of the matrix elements. In the event, however, that these elements were all equal, the eigenvalues and eigenvectors would take a simple form; or if

they were not quite equal but if their differences were small compared with the magnitude of the off-diagonal elements, the same situation would hold. Neglecting antisymmetrization, which is not important to the arguments, one could then write the normalized Frenkel exciton wavefunction in this limiting case as:

$$\Psi^{f\alpha}(\underline{k}) = N^{-\frac{1}{2}} \sum_{n=1}^{N/t} \sum_{q=1}^t a_q^{\alpha} \exp(i\underline{k} \cdot \underline{r}_n) \exp(i\underline{k} \cdot \underline{\tau}_q) \phi_{nq}^f, \quad (2)$$

where $\underline{\alpha}$ designates the interchange state formed from different linear combinations of one-site excitons, $\underline{\tau}_q$ is the displacement vector of the q^{th} site from the origin of its own unit cell, and a_q^{α} designates the appropriate coefficient ($\pm 1, \pm i$) derived from the interchange representation⁵ $\underline{\alpha}$. The coefficient a_1^{α} can always be taken as +1. For example, in the case of crystalline benzene (space group D_{2h}^{15} , $t = 4$) the four interchange states $\Psi^{f\alpha_1}(\underline{k})$, $\Psi^{f\alpha_2}(\underline{k})$, $\Psi^{f\alpha_3}(\underline{k})$, and $\Psi^{f\alpha_4}(\underline{k})$ may be constructed from the four sets of coefficients

$$a_q^{\alpha_1} = +1, +1, +1, +1; a_q^{\alpha_2} = +1, +1, -1, -1;$$

$$a_q^{\alpha_3} = +1, -1, +1, -1; a_q^{\alpha_4} = +1, -1, -1, +1$$

where for each set, $q = 1, 2, 3, 4$, respectively, and with $\alpha_1 = A$, $\alpha_2 = B_1$, $\alpha_3 = B_2$, $\alpha_4 = B_3$. The A, B₁, B₂, B₃ labeling of these functions is by no means unique. The above choice is generated from the D_2 interchange group whose elements are the identity E and the three screw

axis operations C_2^a , C_2^b , C_2^c , defined in the usual way.¹⁵ The choice of convention will be discussed more fully in another paper.⁷

In the case where all translationally equivalent interactions vanish, the eigenfunction given by Eq. (2) is exact. The situation is even more favorable for certain crystals, benzene and naphthalene being examples, where translationally equivalent interactions, skew to the crystallographic a, b, and c axes, need to be large in order to destroy the approximation. Such molecules are fairly distant neighbors in the benzene and naphthalene crystals and are expected to lead to small coupling except, of course, when the interactions are long range as for dipole-dipole terms. Experimental results¹⁶ on benzene have shown that even the nearest-neighbor, translationally equivalent interactions (along the a, b and c axes) in the low-lying electronic states of these crystals, where the transition dipoles for combining with the ground state are small, are less than 2 cm^{-1} , compared with around 10 cm^{-1} for the translationally inequivalent interactions. One therefore expects Eq. (2) to be an excellent approximation. This situation probably pertains for low-lying π - π^* transitions in many organic crystals.

For Frenkel excitons, the transition dipole operator \underline{M} has the form

$$\underline{M} = \sum_{q=1}^t \underline{M}_q \quad (3)$$

where $\underline{M}_q = \sum_{n=1}^{N/t} \underline{M}_{nq}$, a sum of dipole operators at the q^{th} site over the N/t unit cells. We approximate the wave vector of the radiation field as zero, a good approximation for visible and infrared radiation. The matrix element of the crystal moment for a transition $f''\alpha''k'' \leftrightarrow f\alpha k$ becomes

$$\langle \Psi^{f''\alpha''}(\underline{k}'') | \underline{M} | \Psi^{f\alpha}(\underline{k}) \rangle \quad (4)$$

Furthermore, for Frenkel excitons, each term of this matrix element is, for all practical purposes, non-vanishing only if $\phi_{n',q'}^{f''}$, ϕ_{nq}^f , and $\underline{M}_{n',q'}$, all belong to the same site in the same unit cell. In this case, using the eigenfunction given by Eq. (2), the matrix element Eq. (4) simplifies to

$$\begin{aligned} N^{-1} \sum_{n,n',n''=1}^{N/t} \sum_{q,q',q''=1}^t \exp(-i\underline{k}'' \cdot \underline{r}_{n''}) \exp(i\underline{k} \cdot \underline{r}_n) \\ \times (a_{q''}^{\alpha''*} a_q^\alpha) \exp(-i\underline{k}'' \cdot \underline{\tau}_{q''}) \exp(i\underline{k} \cdot \underline{\tau}_q) \\ \times \left[\int \phi_{n''q''}^{f''*} \underline{M}_{n'q'} \phi_{nq}^f dR \right] \delta_{nn'} \delta_{nn''} \delta_{qq'} \delta_{qq''} . \end{aligned} \quad (5)$$

where dR is a volume element associated with electronic and nuclear coordinates in a region of the crystal that

spans the space occupied by the functions in the integrand. Thus, the crystal transition moment becomes

$$N^{-1} \sum_n \sum_{q=1}^{N/t} a_q^{\alpha'} \left[\int \phi_{nq}^{f''*} \tilde{M}_{nq} \phi_{nq}^f dR \right]$$

where $\alpha' = \alpha'' \times \alpha$.

SELECTION RULES

It is easy to see from Eq. (5) that the matrix element is nonvanishing only under very special conditions. The first of these is that $\underline{k} = \underline{k}''$, a result that yields the $\Delta \underline{k} = 0$ selection rule, valid for all \underline{k} . It should also be noted that, because of this, the matrix element is k -independent. It has the same value for all \underline{k} provided $\underline{k}'' = \underline{k}$. This latter property is important in the discussion of band-band transitions,^{17,18} the result here being that in this restricted, but important, Frenkel limit the intensity distribution in such a transition will be determined only by the exciton density-of-states function in the upper and lower bands.

The matrix element of the crystal moment also vanishes identically¹⁰ in the case where the direct product representation $\alpha'' \times \alpha = \alpha'$ does not transform as a crystal dipole moment operator under the interchange group operations. Thus, transitions where $\alpha' = A$ will be forbidden for the D_2 interchange group of benzene. Again, one should note that this type of selection rule holds for our specialized Frenkel limit for all \underline{k} . For the benzene

case, for instance, $\underline{M}^{\alpha'}$ transforms as B_1 , B_2 , and B_3 , and the selection rule shows that, for all $\underline{k} = \underline{k}''$, $A \leftrightarrow B_1$, $B_2 \leftrightarrow B_3$, $A \leftrightarrow B_2$, $B_1 \leftrightarrow B_3$, $A \leftrightarrow B_3$, $B_1 \leftrightarrow B_2$ transitions are allowed, while others, e.g., $A \leftrightarrow A$, $B_1 \leftrightarrow B_1$, etc., are forbidden by interchange symmetry. This selection rule is also important in the interpretation of band-to-band transitions in molecular crystals having more than one molecule per unit cell.

Since the transition moment matrix element is \underline{k} -independent, it also follows easily that the $\underline{g} \leftrightarrow \underline{u}$ selection rule holds for all \underline{k} providing that inversion is included in the site group. In this case, the ϕ_{nq}^f functions have the symmetry of the site, and therefore their sum taken over the whole crystal transforms as either \underline{g} or \underline{u} under site inversion. In addition, the \underline{M}^{α} 's change sign under such a symmetry operation. The $\underline{g} \leftrightarrow \underline{u}$ selection rule is therefore preserved for all \underline{k} in the special Frenkel limit, whether inversion belongs to the group of the wave vector or not; and, in general, the analysis shows that, since the matrix element Eq. (5) is \underline{k} -independent, $\Delta \underline{k} = 0$ transitions for any \underline{k} are governed by the same selection rules as those governing $\underline{k} = 0$ states.

EXPERIMENTAL

Unfortunately, because of the requirement of a negative experimental result, selection rules forbidding transitions are often difficult to establish

especially since there are factors other than the selection rule that can cause the transition to be weak. Limits on the validity of the selection rules, however, can sometimes be set. In this experimental section, an attempt is made to observe a $\underline{u} \leftarrow \underline{u}$ transition for $\underline{k} \neq 0$. A limited number of vibronic transitions provide the only method of testing the theory as the observation of a transition involving $\underline{k} \neq 0$ states ("band-to-band transitions") requires thermal excitation of vibrational bands of the crystal. In order to resolve the resulting hot band from the cut-off absorption of the crystal, the thermally populated modes must have frequencies larger than the electronic exciton bandwidth, i.e., they must be crystal vibrations that correspond to free molecular vibrations, not to phonons. In addition, only a limited number of final vibronic states for the transition are observable since the transition energy must remain smaller than the cut-off energy. In particular, thermally accessible hot-band transitions to the zeroth vibrational level in the upper electronic state provide the most convenient (sometimes the only) examples of vibronic band-to-band transitions that can be studied. Thus, to establish the selection rules outlined in this paper, not only are negative experiments required, but also there is the further condition that only an extremely limited number of transitions are available for this kind of study, at least as far as vibronic transitions are concerned.

Perhaps pure vibrational transitions in very long, highly purified crystals would provide a better way of testing the theory, but such experiments are a little more difficult and have not yet been carried out.

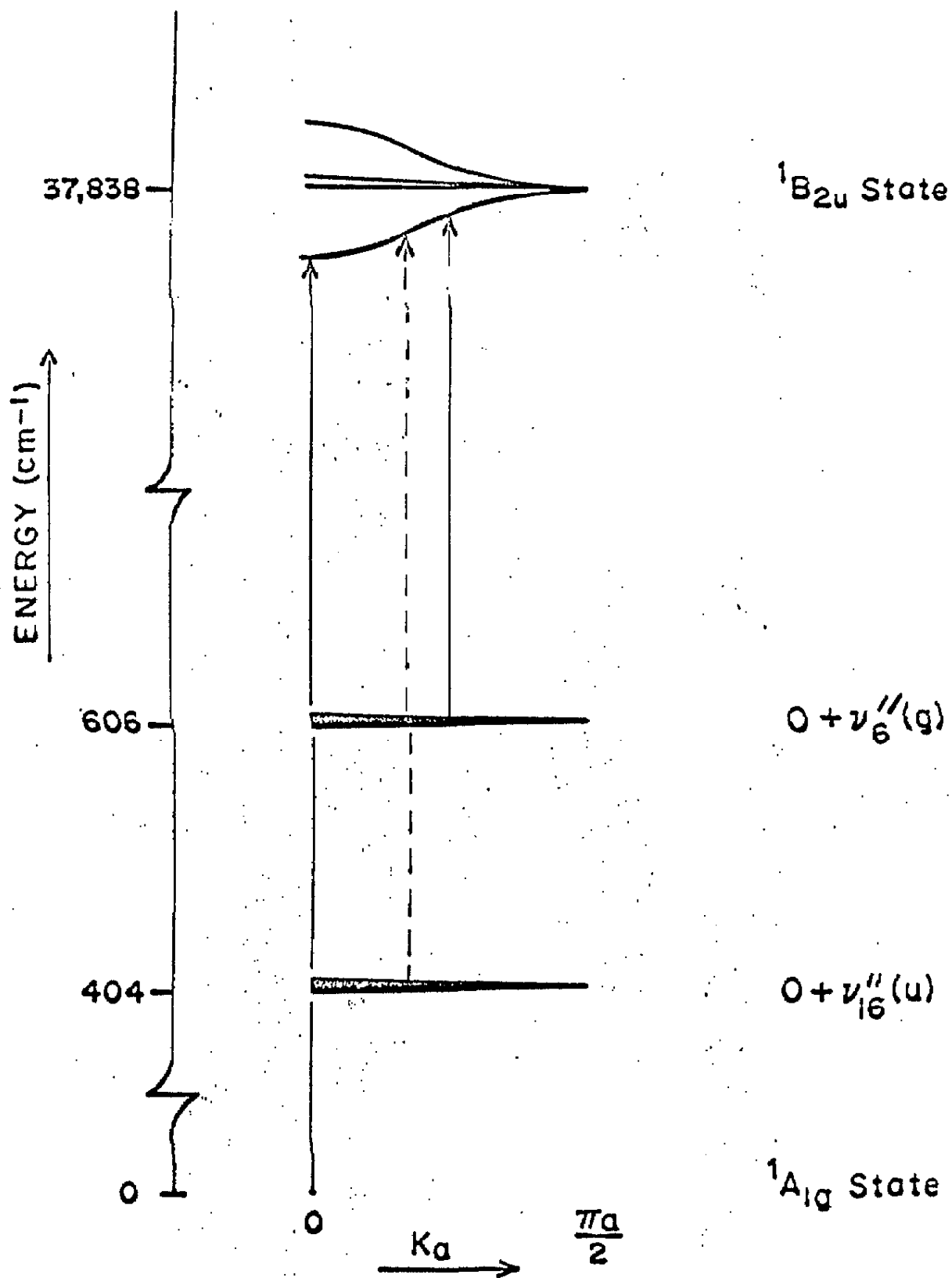
In the case of crystalline benzene, long-range interactions related to the ${}^1B_{2u}$ electronic exciton band are thought to be weak.¹⁶ This crystal therefore should provide an example of the transitions described by the theory. Because of the nature of the experiments, it is to be emphasized that the results certainly do not "prove" the theory. At the moment, they seem to be the only available experiments pertinent to the question, and for this reason they are briefly mentioned here. In the future, when sufficiently pure anthracene can be prepared, the experiments will be repeated with this crystal. The lowest-lying anthracene singlet transition might provide an example where long-range interactions are sufficiently large to spoil the selection rules derived here.

The benzene crystal¹⁹ is centrosymmetric with site group C_1 . Exciton band \leftarrow exciton band absorptions, where all the k levels of a lower energy band are thermally populated, have been studied. In this case the $\Delta k = 0$ selection rules are not present. In 5 cm crystals of highly purified benzene²⁰ the $u \leftarrow g$, band \leftarrow band absorption to the ${}^1B_{2u}$ ($37,800 \text{ cm}^{-1}$) electronic exciton band originating from the $\nu_6''(e_{2g}, 606 \text{ cm}^{-1})$ vibrational exciton band in the ${}^1A_{1g}$ electronic ground state was observed.²¹

See Fig. 1. The spectra were taken at liquid nitrogen and lower temperatures, the relatively long crystal path length being required for detection of the weak hot-band absorptions at such temperatures. The details of the experiments and the resulting analysis of the ${}^1B_{2u}$ exciton band will be published later. The main point here is that the $\underline{u} \leftarrow \underline{u}$ hot band corresponding to a ${}^1B_{2u} \leftarrow \nu''_{16}$ (e_{2u} , 404 cm^{-1}) transition was not observed even though the $\underline{u} \leftarrow \underline{g}$ hot band absorption ${}^1B_{2u} \leftarrow \nu''_6$ was easily detectable. Under these conditions most hot band transitions are expected to originate from other than $k = 0$ states. At 65°K the Boltzmann population of the ν''_{16} band is about 80 times that of the ν''_6 band. It is estimated from the spectra that at this temperature an absorption 100 times weaker than the ν''_6 hot band could have been observed. Thus the strength of the ${}^1B_{2u} \leftarrow \nu''_6$ transition is at least 8000 times weaker than the corresponding one involving the ν''_6 vibration. Using relative strengths estimated from the fluorescence spectrum, it can be shown that the ${}^1B_{2u} \leftarrow \nu'_{16}$ transition is at least 1000 times weaker than the 0-0 transition.

It should be pointed out that some $\underline{u} \leftarrow \underline{g}$ transitions in crystalline benzene are also extremely weak compared with the 0-0 transition. Thus not observing the ν'_{16} hot band does not prove the validity of the theory but is certainly consistent with it.

Figure 1. Schematic band structure of crystalline benzene showing some allowed (—) and forbidden (---) transitions.



ACKNOWLEDGEMENTS

We gratefully acknowledge the support of the National Science Foundation. The criticisms of David M. Hanson helped to sharpen a number of points presented in the paper.

FOOTNOTES

¹D.P. Craig and S.H. Walmsley, Physics and Chemistry of the Organic Solid State, I., ed. by Fox, Labes and Weissberger (Interscience, New York, 1963), p. 585.

²L.P. Bouckaert, R. Smoluchowski and E. Wigner, Phys. Rev. 50, 58 (1936).

³H. Winston and R.S. Halford, J. Chem. Phys. 17, 607 (1949).

⁴R. Kopelman, manuscript in preparation.

⁵Roughly speaking interchange operations permute translationally inequivalent molecules. More specifically, interchange operations correspond to elements of the factor group not included in the site group.⁴ Together with the identity, which here is defined modulo translation for nonsymmorphic space groups,⁶ certain sets of interchange elements may form a group. For the benzene crystal, interchange operations include glide plane (σ) and screw axis (C_2) operations, but not inversion. The set E, C_2^a, C_2^b, C_2^c , which forms a group, is not unique but it develops that it is the most convenient set to use.^{4,7} It is used here as well as in our other papers concerning the benzene crystal.⁷

⁶C. Herring, J. Franklin Inst., 233, 525 (1942).

⁷E.H. Bernstein, S.D. Colson, R. Kopelman and G.W. Robinson, manuscript in preparation.

⁸See, for example, R.M. Hochstrasser, Molecular

Aspects of Symmetry (W.A. Benjamin, Inc., New York, 1966), p.288 et seq.

⁹R.S. Knox, Theory of Excitons (Academic Press, New York, 1963), Chap. II.

¹⁰See, for example, D.Fox and O. Schnepp, J. Chem. Phys., 23, 767 (1955), but see footnote 11 below. See also forthcoming paper⁷ where the relationship between $\mathcal{L}_{qq'}^f$, and $M_{qq'}$ is discussed in more detail.

¹¹See, for example, H. Winston, J. Chem. Phys., 19, 156 (1951) where the symmetry properties of the "site functions" are discussed. Note that the site functions used here are different from those of Fox and Schnepp¹⁰ in their Eq. (3) in that they used molecular functions to approximate the site functions.

¹²A.S. Davydov, Soviet Phys., Usp. 82, 145 (1964).

¹³Ref. 9, p.32

¹⁴Ref. 9, p.30.

¹⁵ C_2^a , for example, corresponds to a rotation by π about the crystallographic \underline{a} axis followed by a nonprimitive translation $\mathcal{T}_a = \frac{1}{2}\underline{a}$ in a positive direction along the \underline{a} axis.

¹⁶E.R. Bernstein, S.D. Colson, and D.S. Tinti, manuscript in preparation.

¹⁷E.I. Rashba, Soviet Phys., Solid State, 5, 757 (1963).

¹⁸S.D. Colson, D.M. Hanson, R. Kopelman and G.W. Robinson, manuscript in preparation.

¹⁹E.G. Cox, Rev. Mod. Phys. 30, 159 (1958).

²⁰S.D. Colson and E.R. Bernstein. J. Chem. Phys. 43, 2661 (1965).

²¹The use of molecular point group representations ${}^1A_{1g}$, ${}^1B_{2u}$, etc., for the description of states in the crystal is not really correct. Not only is the molecular symmetry reduced in the Frenkel functions $\Psi^{f\alpha}(k)$, which are characterized by interchange symmetry, but it is even reduced in the localized excitation functions ϕ_{nq}^f because of the distortion of the molecular eigenfunctions by the crystal field. For this reason, the integral in Eq. (5) does not vanish, for example, when f corresponds to a B_{2u} state of molecular benzene and f corresponds to an A_{1g} state of molecular benzene, even though the integral would vanish if the full symmetry of the molecule were retained in the crystal. We retain the notation ${}^1B_{2u}$ and ${}^1A_{1g}$ not only as a convenient labeling device, but also because in the Frenkel limit distortions of the molecular wavefunctions are not very severe.

Electronic and Vibrational Exciton Structure
in Crystalline Benzene*

ELLIOT R. BERNSTEIN, STEVEN D. COLSON,
RAOUL KOPELMAN,[†] and G. WILSE ROBINSON

Gates and Crellin Laboratories of Chemistry,[‡]
California Institute of Technology, Pasadena, California 91109

(Received 10 April 1967)

ABSTRACT

Although much work has been done on vibrational and electronic excitons in crystalline benzene, emphasis in the past has mostly been placed on "splittings" rather than on the magnitudes and relative signs of the intermolecular interaction energies (i. e., matrix elements or coupling constants) causing these splittings. Not only do the splittings and associated polarization studies in neat (pure) crystals shed light on these interaction energies, but also important in this regard are band-to-band ($\underline{k} \neq 0$) transitions in neat crystals; and orientational effects, site splittings, shifts, and resonance pair spectra in isotopic mixed crystals. Using a diversity of these kinds of complimentary experimental results, we shall in future papers present new information about magnitudes and relative signs of many of the pertinent coupling

* Supported in part by the National Science Foundation.

[†] Present address: Department of Chemistry, University of Michigan,
Ann Arbor, Michigan 48104.

[‡] Contribution No. 3512.

constants for vibrational and electronic excitons in crystalline benzene. The purpose of this particular paper is to lay a consistent theoretical framework for the discussion of these experimental papers.

Emphasis will be placed on $\underline{k} \neq \underline{0}$ states, isotopic mixed crystals, and translationally equivalent interactions, as well as the Davydov splittings. The interchange group concept is introduced in order to simplify the theoretical analysis. From the four possible interchange groups \underline{D}_2 , \underline{C}_{2V}^a , \underline{C}_{2V}^b , \underline{C}_{2V}^c , the \underline{D}_2 group is found to be the most convenient for the classification of benzene exciton functions. A differentiation between static and dynamic interactions is made in the limit of Frenkel excitons, and the concepts of site distortion energy and the ideal mixed crystal are introduced to aid in this distinction. Data pertaining to site shifts and splittings and resonance and quasisresonance interaction terms for the ${}^1B_{2U}$ electronic exciton band and the vibrational $\nu_{12}(b_{1U})$, $\nu_{15}(b_{2U})$ and $\nu_{18}(e_{1U})$ exciton bands are discussed in order to illustrate the theoretical concepts.

I. INTRODUCTION

The benzene molecule has long served as a prototype for the study of π -electron systems. The benzene crystal has been of similar importance in the study of intermolecular interactions. The experimental investigation of vibrational¹ and electronic² transitions in solid benzene paralleled the theoretical development of symmetry considerations³ and exciton theory⁴ for molecular crystals. Several review articles discuss much of this past work.⁵ More recently, a powerful approach to the investigation of exciton interactions, first mentioned by Hiebert and Hornig,⁶ using off-resonance techniques in isotopic mixed crystals, has been utilized⁷ in the study of the electronic exciton structure of benzene.

Certainly for vibrational excitons and probably for those electronic excitons associated with the lowest singlet and triplet states of benzene, the Frenkel limit applies. Even though the theory of Frenkel excitons has been discussed many times before, both in general and with particular reference to the benzene crystal, the presently available literature on this subject has many shortcomings for our purposes. Not only is there the usual wide range of notational differences, but unfortunately there have been a number of confusing or incorrect statements made. Most confusion seems to arise in the symmetry classification of the crystal wave functions, the Davydov "D-term", the approximations leading to closed-form expressions for eigenfunctions and eigenvalues of $\underline{k} \neq 0$ states and transition probabilities involving these states, the meaning of site-group splittings, and the causes of breakdown of oriented-gas model polarization properties. It is partly for this reason that we undertake to redevelop and extend the subject. In doing this we develop the concepts of the ideal mixed crystal and the site distortion energy, and clarify the meaning of the Davydov D term. We further emphasize the possible shortcomings of a first-order theory.

One of the specific purposes of this paper is to emphasize the importance of discussing exciton interactions in terms of precisely defined exciton coupling constants rather than splittings, band shapes, or overall bandwidths. While it is possible to derive uniquely these characteristics of the exciton band from the coupling constants, the converse is not generally true. In particular, for the case of benzene, merely giving the splittings among the observed three Davydov components, as has been done for both electronic and vibrational bands, in no way fixes the magnitude or relative signs of the excitation exchange interactions responsible for this splitting. This is so because one transition from the totally symmetric ground state to one of the Davydov components is dipole-forbidden. It should be further noted that the relative signs of the coupling constants have significance only if the convention used in defining the crystal wave functions is given explicitly. The interchange group concept is introduced for this purpose. Not only do the magnitudes and signs of the coupling constants uniquely define the Davydov splittings, but they also give detailed information concerning the directional properties of the excitation exchange interaction. This provides a much more sensitive test of theoretical calculations, which in the past have been compared only to overall splittings, and thus presents a means of determining the origin of these interactions (i. e., in the case of electronic excitations, mixing with ion-pair exciton states,⁸ octopole-octopole interactions,^{4b} exchange interactions,⁷ etc.).

Using the theory we illustrate, with specific examples from the benzene crystal spectra, how to extract the exciton coupling constants. The band structure of the ${}^1B_{2u}$ electronic state and a few ground state vibrational bands of C_6H_6 are discussed in detail. While the magnitudes and relative signs of the exciton coupling constants (see Sec. II-F) can be obtained from studies

with unpolarized light, assignments of each coupling constant to an interaction among a specific set of molecules in the crystal requires polarization properties of the transitions to be known. Because of the difficulty of identification of crystal faces in benzene, in addition to depolarization caused by cracking and straining at low temperatures, polarization assignments are more apt to be unreliable than those in other crystals of aromatic molecules. It is hoped that unambiguous polarized light experiments can be carried out in the near future, in order that reliable assignments of the coupling constants can be made.

II. THEORY

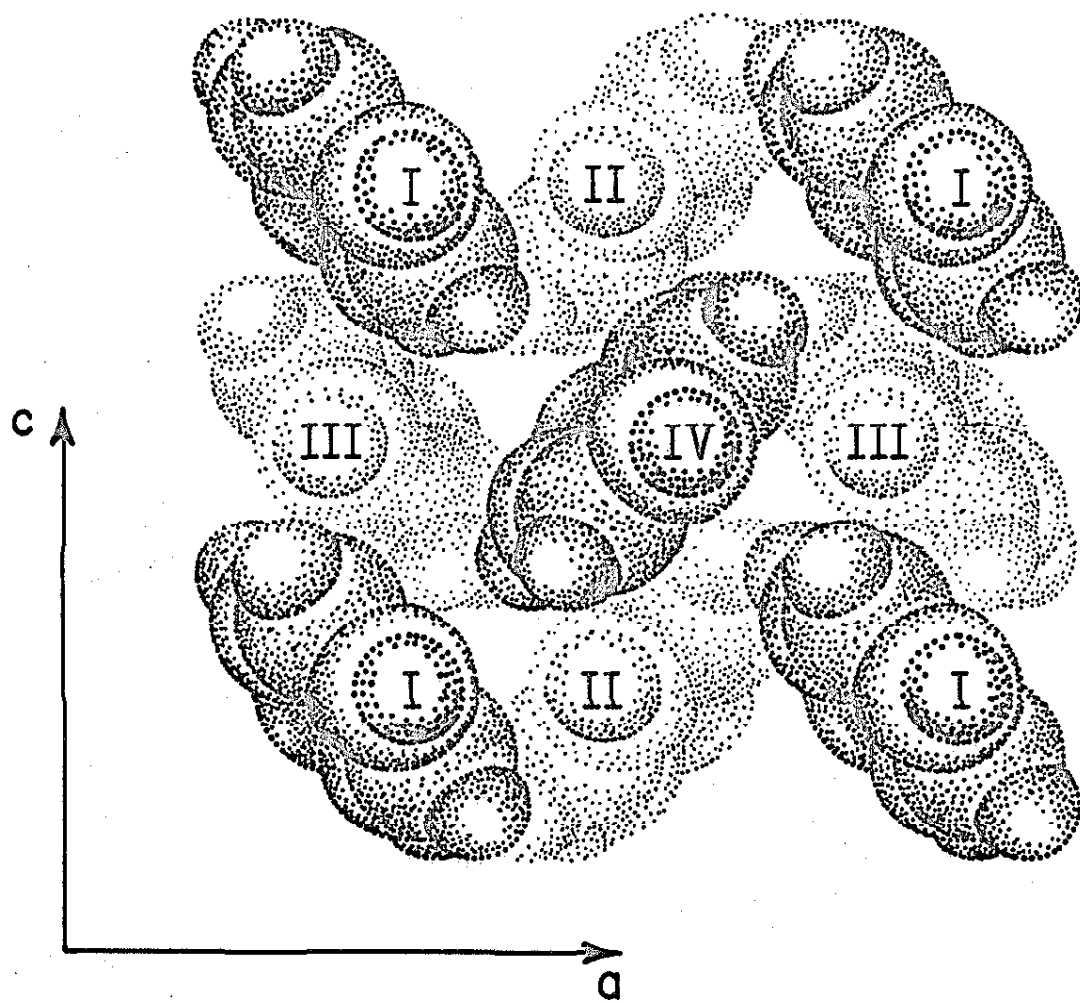
A. Site, Interchange, and Factor Group Symmetry

The symmetry of crystals can be considered as made up of the following types of operations: (1) site operations, describing the local "point" symmetry, where the "point" of interest usually is the center of the molecular building block; and (2) transport operations, carrying a given molecular unit into a physically identical location and orientation. The transport operations can be classified further into two categories: (a) the translational operations; and (b) the interchange operations. The latter includes both proper and improper rotations, screw rotations, and glide reflections. The so-called static field interactions are related to the site symmetry, while the dynamic interactions are related to the transport symmetry. Dynamic interactions have gone under names such as excitation exchange, resonance, or exciton interactions, or by the term "the coupling of oscillators".

In the case of the benzene crystal the space group is $D_{2h}^{15}(P_{bca})$, and there are four molecules per primitive unit cell occupying sites of inversion symmetry⁹ (see Fig. 1). The site group is therefore C_i . The four sets of translationally inequivalent molecules corresponding to the four sites

Figure 1

Diagram of crystalline benzene viewed down the \underline{b} -axis. The R_{ij} are the center-to-center distances at 77 °K between molecules i and j .



$$a = 7.37 \text{ \AA}$$

$$b = 9.35 \text{ \AA}$$

$$c = 6.77 \text{ \AA}$$

$$R_{\text{I II}} = 5.95 \text{ \AA}$$

$$R_{\text{I III}} = 5.76 \text{ \AA}$$

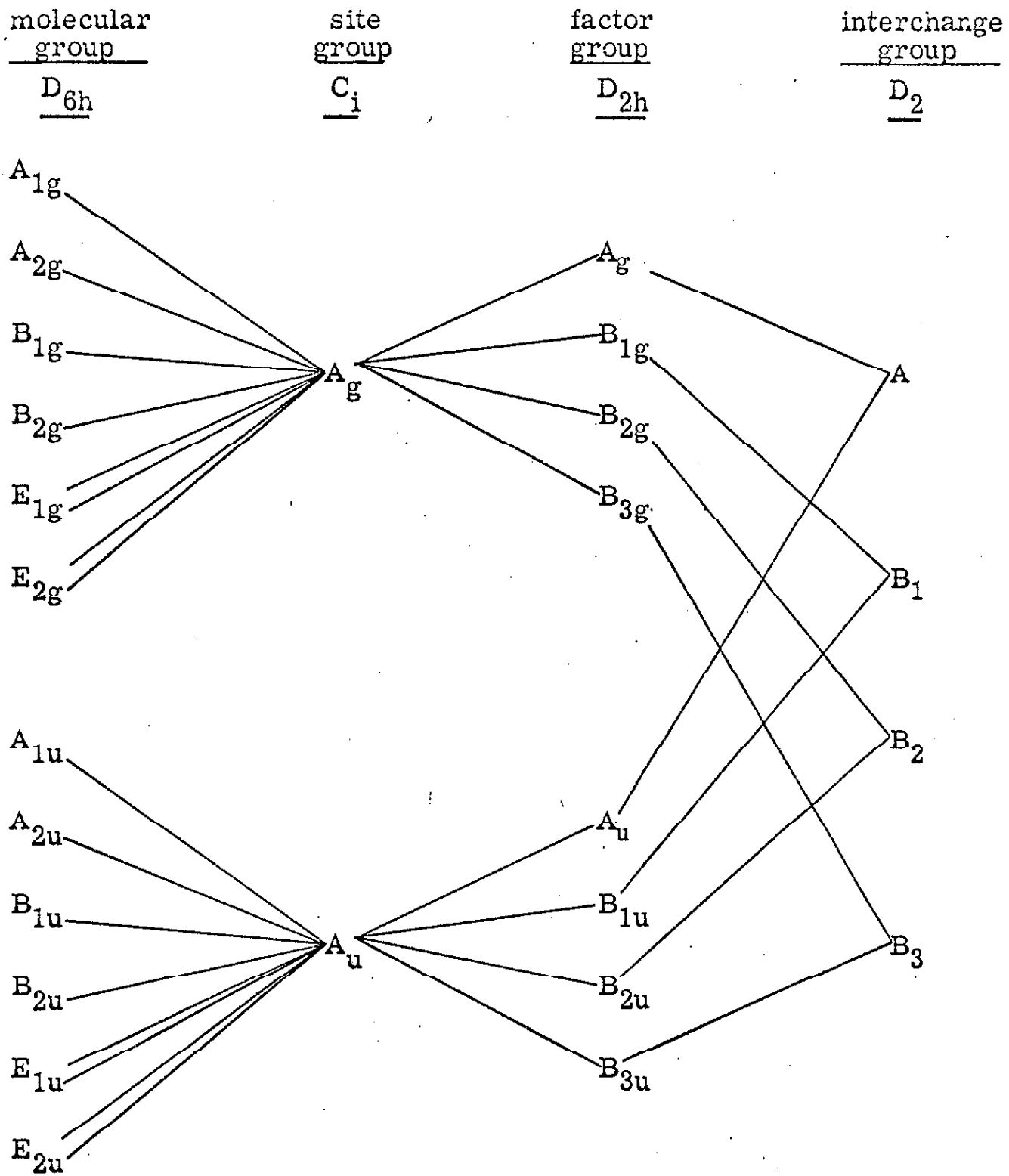
$$R_{\text{I IV}} = 5.00 \text{ \AA}$$

per unit cell are labeled I, II, III, IV. The interchange operations in the benzene crystal are the screw axis rotations C_2^a , C_2^b , and C_2^c ; and the glide plane reflections $\sigma^a (\equiv iC_2^a)$, $\sigma^b (\equiv iC_2^b)$, and $\sigma^c (\equiv iC_2^c)$. Considering the translations as interchange-identity operations E, certain sets of the above mentioned operations generate groups of order four¹⁰ which we call interchange groups. The four interchange operations associated with an interchange group permute the four sets of translationally inequivalent molecules among themselves. There are four possible interchange groups for the benzene crystal: $\underline{C}_{2V}^a = \{E, C_2^a, \sigma^b, \sigma^c\}$; $\underline{C}_{2V}^b = \{E, \sigma^a, C_2^b, \sigma^c\}$; $\underline{C}_{2V}^c = \{E, \sigma^a, \sigma^b, C_2^c\}$; and $\underline{D}_2 = \{E, C_2^a, C_2^b, C_2^c\}$. The particular set $\{E, C_2^a, C_2^b, C_2^c\}$ is unique in that it has the virtue that the right or left handedness of a coordinate system attached to a site is preserved upon such permutations. We therefore call the set \underline{D}_2 the proper interchange group for the benzene crystal.

The factor group \underline{D}_{2h} for the benzene crystal is generated as the direct product of the site group and the interchange group, $\underline{D}_2 \times \underline{C}_i$ for the particular case of the proper interchange group. This relationship among site, interchange, and factor group symmetry holds, however, for all interchange groups, proper as well as improper. The space symmetry of the crystal is generated from the factor group symmetry and the translational symmetry; or, alternatively, from the site and transport symmetries, or the interchange and site-translation symmetry $\underline{S}(\alpha^1)$ defined by Vedder and Hornig.^{5b} The correlation among the benzene molecular point group and the site, interchange, and factor groups in the benzene crystal is depicted in Fig. 2. It should be noted that the only non-trivial symmetry of the molecule that is carried over to the site, and therefore to the factor and space groups, is inversion.

Figure 2

Correlation among groups pertinent to the benzene crystal.



B. Generation of Exciton Functions

In the limit of the tight-binding (Frenkel) approximation for a crystal containing N molecules with four molecules per unit cell, we construct antisymmetrized functions representing localized electronic or vibrational excitation f on a particular molecule at a given site in the crystal,

$$\phi_{nq}^f = \mathcal{A} \chi_{nq}^f \prod_{n' \neq n}^{N/4} \chi_{n'q}^0 \quad (1)$$

where \mathcal{A} is the electronic antisymmetrizing operator, n labels the unit cell, q labels the site (I, II, III, IV) in the unit cell, and χ_{nq} is a crystal site function (see below). From these functions one can generate the one-site exciton functions in the Bloch representation,^{3e}

$$\phi_q^f(\underline{k}) = (N/4)^{-\frac{1}{2}} \sum_{n=1}^{N/4} \exp(i\underline{k} \cdot \underline{R}_{nq}) \phi_{nq}^f, \quad (2)$$

where \underline{R}_{nq} denotes the position of the center of a molecule located at the q^{th} site in the n^{th} unit cell with respect to a common crystal origin, and \underline{k} is the reduced wave vector. It is convenient to write,

$$\underline{R}_{nq} = \underline{r}_n + \underline{\tau}_{nq}, \quad (3)$$

with \underline{r}_n defining some convenient local origin in the n^{th} unit cell and $\underline{\tau}_{nq}$ being a vector from this local origin to site q ($=$ I, II, III, IV) in this same unit cell. Note that because of translational symmetry, $\underline{\tau}_{nq}$ is identical for all n . Therefore, we shall hereafter drop the subscript n .

Before going further one must be specific about the site numbering. One scheme is as good as another, but it is important to be consistent and always to state explicitly which convention is used, since the appearance

of the results depends on the numbering scheme used. Using the operations of the proper interchange group D_2 , we define the numbering scheme for benzene as in Table I such that for $\underline{k} = \underline{0}^{11}$: $C_2^a \phi_I^f(\underline{0}) \rightarrow \phi_{II}^f(\underline{0})$; $C_2^b \phi_I^f(\underline{0}) \rightarrow \phi_{III}^f(\underline{0})$; and $C_2^c \phi_I^f(\underline{0}) \rightarrow \phi_{IV}^f(\underline{0})$. In the same way C_2^a "interchanges" sites III and IV, C_2^b "interchanges" sites II and IV, while C_2^c "interchanges" sites II and III. This is the same numbering scheme as used by Cox but is different from that of Ref. 4b and Ref. 7.

C. The Crystal Hamiltonian

We now proceed to determine the Hamiltonian matrix elements for the specific case of the benzene crystal. The manner in which one divides up the total crystal Hamiltonian H into a zero-order part and a perturbation Hamiltonian part depends upon the representation to be employed. In the tight-binding limit, where excitation is localized primarily at the site, it is convenient to divide H into a one-site Hamiltonian H^0 and an intersite interaction Hamiltonian H' :

$$H^0 = \sum_{n=1}^{N/4} \sum_{q=1}^{IV} H^0(nq) \quad (4)$$

$$H' = \frac{1}{2} \sum_{n=1}^{N/4} \sum_{q=1}^{IV} \sum_{n'=1}^{N/4} \sum_{q'=1}^{IV} (1 - \delta_{nn'} \delta_{qq'}) H'(nq; n'q') \quad (5)$$

where $\delta_{nn'} \delta_{qq'} = 1$ for $n = n'$ and $q = q'$ simultaneously, and zero otherwise. The eigenfunctions of $H^0(nq)$ are just the crystal site functions χ_{nq} introduced in Eq. (1). It should be emphasized that Eq. (4) does not provide for multiple excitations of two or more sites, and therefore places at least a part (for example, the R^{-6} part) of the van der Waals energy in H' . Mixing with Wannier exciton states or ion-pair states must also come from H' when using the tight-binding representation.

Table I

Symmetry transformations of the $\underline{k} = \underline{0}$ one-site excitons

	E	C_2^a	C_2^b	C_2^c	i	σ_a	σ_b	σ_c
ϕ_I^g	ϕ_I^g	ϕ_{II}^g	ϕ_{III}^g	ϕ_{IV}^g	ϕ_I^g	ϕ_{II}^g	ϕ_{III}^g	ϕ_{IV}^g
ϕ_{II}^g	ϕ_{II}^g	ϕ_I^g	ϕ_{IV}^g	ϕ_{III}^g	ϕ_{II}^g	ϕ_I^g	ϕ_{IV}^g	ϕ_{III}^g
ϕ_{III}^g	ϕ_{III}^g	ϕ_{IV}^g	ϕ_I^g	ϕ_{II}^g	ϕ_{III}^g	ϕ_{IV}^g	ϕ_I^g	ϕ_{II}^g
ϕ_{IV}^g	ϕ_{IV}^g	ϕ_{III}^g	ϕ_{II}^g	ϕ_I^g	ϕ_{IV}^g	ϕ_{III}^g	ϕ_{II}^g	ϕ_I^g
ϕ_I^u	ϕ_I^u	ϕ_{II}^u	ϕ_{III}^u	ϕ_{IV}^u	$-\phi_I^u$	$-\phi_{II}^u$	$-\phi_{III}^u$	$-\phi_{IV}^u$
ϕ_{II}^u	ϕ_{II}^u	ϕ_I^u	ϕ_{IV}^u	ϕ_{III}^u	$-\phi_{II}^u$	$-\phi_I^u$	$-\phi_{IV}^u$	$-\phi_{III}^u$
ϕ_{III}^u	ϕ_{III}^u	ϕ_{IV}^u	ϕ_I^u	ϕ_{II}^u	$-\phi_{III}^u$	$-\phi_{IV}^u$	$-\phi_I^u$	$-\phi_{II}^u$
ϕ_{IV}^u	ϕ_{IV}^u	ϕ_{III}^u	ϕ_{II}^u	ϕ_I^u	$-\phi_{IV}^u$	$-\phi_{III}^u$	$-\phi_{II}^u$	$-\phi_I^u$

Since the translational subgroup of the space group is Abelian, only one-dimensional irreducible representations occur.¹² Thus, as is well known, in the Bloch representation the Hamiltonian matrix describing the energy levels associated with a set of translationally equivalent molecules in a crystal contains no off-diagonal elements. The matrix is therefore diagonal in the reduced wave vector \underline{k} , each diagonal element being characterized by one specific value of this "quantum number". If only a single non-degenerate excited state of the molecule is considered and if the crystal structure is such that there is only one molecule per unit cell, i. e., if all N molecules in the crystal are translationally equivalent, then the $N \times N$ Hamiltonian matrix simply consists of N diagonal terms of the type $\langle f, \underline{k} | H | f, \underline{k} \rangle$, where f, \underline{k} represents the function (and its complex conjugate) $\phi_{\underline{q}}^f$ of Eq. (2) for a single \underline{q} , and where $H = H^0 + H'$.

If two molecular states, say f' and f'' , in such a crystal are considered, then the Hamiltonian matrix consists of $2N$ diagonal terms, $\langle f', \underline{k} | H | f', \underline{k} \rangle$ and $\langle f'', \underline{k} | H | f'', \underline{k} \rangle$. Since in general $\phi_{\underline{q}}^f(\underline{k})$ need not be an exact eigenfunction of H because of the choice of χ_{nq}^f , there may be "configuration interaction" terms $\langle f', \underline{k} | H | f'', \underline{k} \rangle$, giving rise to a matrix consisting of N 2×2 blocks along the main diagonal. Many such singly excited configurations $f', f'', f''' \dots$ may have to be considered. In addition, again depending upon the choice of representation, there may be multiply excited configurations of the crystal that must be included for energy or intensity calculations. For example, the doubly excited configurations constructed from localized excitation functions,

$$\phi_{n', n''}^{f' f''} = e^{\chi_{n'}^{f'} \chi_{n''}^{f''}} \prod_{n \neq n', n''}^N \chi_n^0 \quad (6)$$

(for one molecule per unit cell) may be very important in the consideration of van der Waals energies and spectral shifts through the matrix elements $\langle f'f'', \underline{k} | H | 00, \underline{k} \rangle$ and $\langle f'f'', \underline{k} | H | f0, \underline{k} \rangle$.

When there are 4 molecules per unit cell (4 different sets of translationally equivalent molecules) and the possibility exists of doubly degenerate molecular states, as in the benzene crystal, the Hamiltonian matrix is a little more complicated. Considering only a single, non-degenerate excited



state \underline{f} , the full $N \times N$ Hamiltonian matrix consists of $N/4$ 4×4 Hermitian submatrices, each submatrix labeled by a unique \underline{k} , along the main diagonal. Off-diagonal elements within each submatrix arise because of interactions among the four sets of translationally inequivalent molecules (i. e., sites). Matrices of higher-order than four would have to be considered if \underline{f} described a doubly degenerate molecular state (in which case the $N/4$ submatrices are 8×8) or if interaction of the f^{th} configuration with other singly or multiply excited configurations were to be included.

D. First-Order Frenkel Theory

Using the one-site exciton functions of Eq. (2) as zero-order functions, the first-order Hamiltonian matrix elements for the excited state of crystal-line benzene, corresponding to the f^{th} excited state of the molecule, are,

$$\mathcal{L}_{qq'}^f(\underline{k}) = \sum_{n'=1}^{N/4} \exp i\underline{k} \cdot (\underline{\tau}_{q'} - \underline{\tau}_q) \exp i\underline{k} \cdot (\underline{r}_{n'} - \underline{r}_n) \times \int \phi_{nq}^{f*} H \phi_{n'q'}^f dR. \quad (7)$$

It is convenient in Eq. (7) to separate the \underline{k} independent terms, for which $q = q'$ and $n = n'$, from the \underline{k} dependent terms, and write,

$$\mathcal{L}_{qq'}^f(\underline{k}) = (\epsilon^f + D^f) \delta_{qq'} + L_{qq'}^f(\underline{k}), \quad (8)$$

where

$$\epsilon^f = \int \phi_{nq}^{f*} H^0 \phi_{nq}^f dR \quad (9)$$

$$D^f = \int \phi_{nq}^{f*} H' \phi_{nq}^f dR. \quad (10)$$

Using an approximate Hamiltonian matrix, in which certain non-nearest translationally equivalent interactions are assumed negligible,¹³ the normalized crystal eigenfunctions $\Psi^{f\alpha}(\underline{k})$ may be expressed in terms of the representations $\underline{\alpha}$ of the \underline{D}_2 interchange group. They are:

$$\Psi^{f\alpha}(\underline{k}) = \frac{1}{2} \sum_{q=I}^{IV} a_q^{\alpha} \phi_q^f(\underline{k}) \quad (11)$$

where the a_q^{α} are coefficients corresponding to the $\underline{\alpha}^{\text{th}}$ representation of \underline{D}_2 . For $\alpha = A$, $a_q^A = +1, +1, +1, +1$ when $q = I, II, III, IV$, respectively. Similarly, $a_q^{B_1} = +1, +1, -1, -1$; $a_q^{B_2} = +1, -1, +1, -1$; and $a_q^{B_3} = +1, -1, -1, +1$. In the particular case of $\underline{k} = \underline{0}$ one need not call upon the above approximation, and in our first-order tight-binding limit, the eigenfunctions may be written exactly:

$$\begin{aligned} \Psi^{fA}(\underline{0}) &= \frac{1}{2}(\phi_I^f(\underline{0}) + \phi_{II}^f(\underline{0}) + \phi_{III}^f(\underline{0}) + \phi_{IV}^f(\underline{0})) \\ \Psi^{fB_1}(\underline{0}) &= \frac{1}{2}(\phi_I^f(\underline{0}) + \phi_{II}^f(\underline{0}) - \phi_{III}^f(\underline{0}) - \phi_{IV}^f(\underline{0})) \\ \Psi^{fB_2}(\underline{0}) &= \frac{1}{2}(\phi_I^f(\underline{0}) - \phi_{II}^f(\underline{0}) + \phi_{III}^f(\underline{0}) - \phi_{IV}^f(\underline{0})) \\ \Psi^{fB_3}(\underline{0}) &= \frac{1}{2}(\phi_I^f(\underline{0}) - \phi_{II}^f(\underline{0}) - \phi_{III}^f(\underline{0}) + \phi_{IV}^f(\underline{0})) \end{aligned} \quad (12)$$

The functions $\Psi^{f\alpha}(\underline{0})$ map into gerade or ungerade functions of the \underline{D}_{2h} factor group depending on whether χ^f is gerade or ungerade. The complete correlation diagram is given in Fig. 2.

It is important to note that the $\underline{k} = \underline{0}$ crystal function transformations under \underline{D}_2 are independent of the symmetry \underline{g} or \underline{u} of the site function χ^f . This is not the case for the other three possible interchange groups, all of which contain two glide-plane reflection operations that change the sign of \underline{u} functions but not of \underline{g} functions, if right handed coordinate systems are used throughout.¹⁰ This is an example of the kind of ambiguity that may arise when an improper interchange group is used. Group theoretically such improper groups are correct, but they can certainly lead to

confusion in practice. In any case, both for those who use the proper interchange group and for those who insist on using improper ones, it is important in molecular crystal spectroscopy that the convention, whatever it is, be stated explicitly. Even though the difference of results is only a matter of phasing, in order to compare calculated and experimental quantities it is important to know just what phase relation is used by any particular author!

It should perhaps be pointed out how not to form interchange or factor group representations. Symmetry elements present in the molecule but absent in the site have no significance in the crystal! Using them to find the interchange or factor group representations is definitely incorrect in principle and, at best, misleading in practice. This procedure, introduced by Davydov (see p. 43 of Ref. 4a), has consistently given wrong or inconsistent results for the benzene crystal; though usually the results have been correct for systems such as naphthalene and anthracene where there are only two molecules per unit cell. For instance, Davydov (p. 56 of Ref. 4a) gives only a pair of factor group components (and different ones at that!) for B_{1u} and B_{2u} electronic states of benzene even though he employs four molecules per unit cell. The reason that Davydov obtained incorrect results for benzene was not, as is often stated,^{2e,4b} that he employed the old crystal structure, since that had the correct space group. It was because he tried to make use of the molecular point group operations in the crystal, where, except for those preserved by the site, they have no meaning.

In the paper of Fox and Schnepf,^{4b} an attempt was made to follow Davydov's method of constructing factor group representations by using molecular point group operations. These authors did, however, use carefully selected coordinate systems on each molecule in conjunction with the refined crystal structure data of Cox.⁹ They correctly found four factor group components for each nondegenerate state of molecular benzene in

agreement with Winston^{3d}; but the crystal functions they obtained for the molecular B_{1u} state belonged to different factor group representations than those for the molecular B_{2u} state! Both B_{1u} and B_{2u} states, and for that matter all u states of benzene, have identical site and factor group representations and should therefore all be described by the same type of crystal wave function insofar as symmetry is concerned. It is easy to see from what we have presented here and in Section II-A that the treatment of Fox and Schnepf actually amounts to the use of the C_{2v}^b interchange group for the ${}^1B_{1u}$ molecular electronic state, and the C_{2v}^c interchange group for the ${}^1B_{2u}$ state. The use of such conventions is mathematically correct, but, unless they are stated explicitly, the meaning of the factor group wave functions and the relative signs (vide infra) of the coupling constants become obscure.

One last thing should be pointed out. The use of projection operators¹⁴ does indeed guarantee that the crystal functions are eigenfunctions, but does not specify a convention, unless the phases of the functions used in this method are explicitly identified with certain interchange operations.¹⁰

E. Site Functions

For small site distortions, like those for crystalline benzene, distinguishing between site functions and molecule functions is not expected to make large differences in energy. It is, however, extremely important to differentiate between site functions and free-molecule functions when considering intensities and polarization properties of transitions. A breakdown of the

oriented gas model for intensities can occur because of site distortion even in the absence of large energy perturbations by intersite interactions. This model, for example, would be obviously inappropriate in cases where a weak or forbidden gas phase transition is greatly enhanced in the crystal. Such enhancement can occur even though the intermolecular forces causing the intensity enhancement are so weak that they do not cause a measurable breakdown of the first-order Frenkel limit with respect to energy.

Unfortunately, the concept of the site function as introduced by Winston and Halford^{3c} and further discussed by Winston^{3d} is somewhat ambiguous. These authors envisioned the distortion at the site as arising from a general "crystal field". This sort of language is convenient for many problems, and in particular for the discussion of the vibrational states of crystals, with which Winston and Halford were primarily concerned. For the vibrational problem it is easy to separate crystal field effects in H^0 from interaction terms in H' . One merely considers in H^0 a molecule in the crystal where not only the nuclei but also the electrons have been distorted. This leads to different equilibrium nuclear positions and different (intramolecular) force constants than in the free molecule; H' , which also has the symmetry of the site, is written in terms of intermolecular force constants coupling these distorted molecules. For the electronic exciton problem, however, the crystal field idea does not allow a very clear separation of H^0 and H' . Which intermolecular interaction terms in H should be considered part of the "crystal field" and which should be included in H' ?

Three possible choices of electronic basis functions χ_{nq}^f come to mind:

- 1) the χ_{nq}^f could be eigenfunctions of a free, undistorted benzene molecule;
- 2) χ_{nq}^f could be eigenfunctions of a distorted benzene molecule in some "average field" of all the other molecules in the crystal; or
- 3) χ_{nq}^f could be eigenfunctions

of a free benzene molecule whose nuclear framework has been distorted to match that of the molecule in the crystal.

The first choice is undesirable since the symmetry of the terms in H^0 is higher than that of the crystal site. Terms in H' would have to contain the effect of the nuclear distortion on the electronic energies in addition to the usual interaction terms. The advantage of this approach, however, lies in the relative simplicity of the basis functions. It is the one that has been used in theoretical calculations. We shall not use this model here since one of our objectives is to emphasize the consequences of the low symmetry of the crystal site functions. It should be emphasized that the higher order effects of configuration interaction and van der Waals energy must be taken care of separately in this approach. Thus, a strictly first-order theory may be inadequate to explain "shifts" and other contributions to the crystal energies. Such contributions are expected to be particularly important for electronic excitation.

The second type of basis function may lead to the kind of ambiguity mentioned earlier since terms in H^0 representing the "crystal field" contain intermolecular interelectronic interactions usually included in H' . It would be desirable to choose H^0 to be an "effective Hamiltonian" such that the eigenvalues $\langle 0 | H^0 | 0 \rangle$ and $\langle f | H^0 | f \rangle$ already include the k -independent configuration interaction and van der Waals terms. However, such an effective Hamiltonian cannot be written down in terms of one-site functions as in Eq. (4); and to include multisite functions in H^0 would destroy the useful Frenkel exciton formalism upon which the above theoretical results are based. We therefore abandon this extreme approach in the case of vibrational and low-lying electronic states of benzene, which we feel lie very close to the Frenkel limit.

To employ a less extreme crystal field model, where only one-site terms appear in H^0 is possible, but difficult to prescribe precisely. Qualitatively the electrons and nuclei at the site are distorted by some effective electrical field caused by the rest of the crystal, the field being chosen so as to minimize contributions from higher-order effects. The van der Waals terms and terms arising from configuration interaction with, say, Wannier or ion-pair states of the crystal must be taken into account separately by perturbation theory.

A still less extreme crystal field model would be the third one above -- the distorted nuclei model. It would again give rise to van der Waals and configuration interaction contributions since the electronic eigenfunctions of a free molecule, even though its nuclei have been distorted, are not necessarily equivalent to eigenfunctions of any of the zero-order Hamiltonians in the second model. Thus, the distorted-nuclei model gives rise to the same kind of energy contributions as the \underline{D}_{6h} model, but the value of each energy contribution differs for the two models. Even the \underline{k} -dependent energies differ for the three models. One therefore must realize that, just as in other problems, individual terms in a total energy expression have different values depending upon what representation is used, and the terms add up to the true total energy only in the highest order of approximation.

F. Band Energies

The \underline{k} -dependent energies of the exciton band can be obtained in closed form to first-order in crystal site wavefunctions from the approximate Hamiltonian matrix discussed in Ref. 13. This first-order energy, expressed in a manner similar to the original Davydov form,^{4a} is

$$E^{f\alpha}(\underline{k}) \equiv \mathcal{E}^{f\alpha}(\underline{k}) - \mathcal{E}^0 = \epsilon + D + L^{f\alpha}(\underline{k}). \quad (13a)$$

When higher order effects are taken into account Eq. (13a) becomes

$$E^{f\alpha}(\underline{k}) = \epsilon + D + L^{f\alpha}(\underline{k}) + W + w(\underline{k}). \quad (13b)$$

In these equations $\mathcal{E}^{f\alpha}(\underline{k})$ and \mathcal{E}^0 are, respectively, the excited and ground state energies of the crystal; $\epsilon = \epsilon^f - \epsilon^0$ where ϵ^f and ϵ^0 are the excited and ground state energies of a molecule at the site whose eigenfunctions χ_{nq}^f are specified by some particular site representation; $D = D^f - D^0$ is a \underline{k} -independent band shift term; and $L^{f\alpha}(\underline{k})$ is the \underline{k} -dependent energy associated with the α^{th} irreducible representation of the interchange group. The quantities ϵ^f and D^f were defined in Sec. II-D; ϵ^0 and D^0 are analogously defined except that ground state site functions ϕ_{nq}^0 are employed. To first order, the \underline{k} -dependent energy $L^{f\alpha}(\underline{k})$, which is of primary importance in the consideration of the exciton band structure, is a function of the \underline{k} -dependent matrix elements $L_{qq}^f(\underline{k})$ defined in the last section:

$$L^{f\alpha}(\underline{k}) = L^f(\underline{k}) + a_{\text{II}}^{\alpha} L_{\text{I II}}^f(\underline{k}) + a_{\text{III}}^{\alpha} L_{\text{I III}}^f(\underline{k}) + a_{\text{IV}}^{\alpha} L_{\text{I IV}}^f(\underline{k}). \quad (14)$$

We have dropped the subscripts on the diagonal element $L_{qq}^f(\underline{k})$ since the

approximation from which Eq. (14) is derived rests on the fact that

$$L_I \overset{f}{I}(\underline{k}) = L_{II} \overset{f}{II}(\underline{k}) = L_{III} \overset{f}{III}(\underline{k}) = L_{IV} \overset{f}{IV}(\underline{k}), \quad (15)$$

for each \underline{k} . Equation (15) is not an approximation, of course, for some special values of \underline{k} such as $\underline{k} = 0$.^{4g}

The quantities W and $w(\underline{k})$ in Eq. (13b) represent the contributions from higher-order \underline{k} -independent shift terms and higher-order \underline{k} -dependent energies, respectively. Again, it is to be emphasized that, while the value of $E^{f\alpha}(\underline{k})$ in Eq. (13b) is independent of representation, the values of the individual parts vary with representation. If free-molecule eigenfunctions are used for the site functions χ_{nq}^f , then ϵ is the free-molecule excitation energy, the D and L integrals are written in terms of free-molecule functions, and W and $w(\underline{k})$ must contain not only the usual configuration interaction and van der Waals terms, but also terms, both \underline{k} -independent and \underline{k} -dependent, arising from energy changes caused by nuclear distortions at the crystal site. If the χ_{nq}^f represent functions for a free molecule whose nuclei have been distorted, then ϵ , D , and $L^{f\alpha}(\underline{k})$ all have different values than if determined from undistorted free-molecule functions; and W and $w(\underline{k})$ are also different.

Rather than specifying any particular representation in this paper, for the purpose of fitting the experimental data we shall simply adopt the form of Eqs. (13a) and (13b) with the understanding that the theoretical values of the parameters depend upon the particular representation chosen.

If the higher-order \underline{k} -dependent terms $w(\underline{k})$ are negligible, the simple form of $L^{f\alpha}(\underline{k})$ discussed in the preceding sections is preserved. We shall assume this to be the case for vibrational as well as low-lying electronic excitations in crystalline benzene, and shall show in this and subsequent papers that

such an assumption does not conflict with experimental evidence. Even though the higher-order \underline{k} -dependent terms must be ignored to preserve the simple form of our equations, for the purpose of fitting experimental data all the higher-order \underline{k} -independent shift terms, such as the van der Waals terms, may be included without difficulty. Neglecting the $w(\underline{k})$,
 |———— a good approximation when perturbing bands are far removed from the Frenkel exciton band under study, we rewrite Eq. (13b) as,

$$E^{f\alpha}(\underline{k}) = \bar{\epsilon} + L^{f\alpha}(\underline{k}) + \Delta, \quad (16)$$

where

$$\Delta = \epsilon - \bar{\epsilon} + D + W.$$

The quantity $\bar{\epsilon}$ is just the gas phase excitation energy. In some of our future papers it will be convenient to introduce a "site distortion energy" $P = \epsilon - \bar{\epsilon}$. In Eq. (16) the quantities $L^{f\alpha}(\underline{k})$ and Δ can be imagined by the experimentalist as the \underline{k} -dependent energy and site shift term that give the best fit of the observed exciton band energies relative to the free-molecule energy, and by the theorist as quantities to be calculated using first- and higher-order perturbation theory starting with the best available site functions χ_{nq}^f . It is possible further to decompose Δ for degenerate states into a shift term and an intrasite resonance shift contribution. This approach will be taken in a future paper from this laboratory concerning crystal site effects for the benzene system.¹⁵ Knowing $E^{f\alpha}(\underline{k})$ and $\bar{\epsilon}$, experiments can generally shed light only on the overall values of $L^{f\alpha}(\underline{k})$ and Δ , not on the source of these terms.¹⁶

It is necessary to make a final comment upon the D-term in Δ . The reader should note that the D-term does not contain contributions from site states other than the ground and particular excited state with which one is

dealing, and is representation-dependent. There has been some ambiguity in the literature about this D-term. Some workers, while using a definition of D similar to ours, and free-molecule basis functions, have tried to equate it to the total experimental gas-to-crystal band shift for the transition. This, of course, is a highly erroneous kind of correlation, especially for electronic excitations, because of the possible presence of relatively large second-order shift terms and the difference between D at the site and D calculated with molecular functions. In some cases, but not benzene, there is also the possible presence of large $\underline{k} = \underline{0}$ shift terms $L^f(\underline{0})$, that cause the mean value of the $\underline{k} = \underline{0}$ Davydov components not to be related to the mean energy of the whole band. Still other workers have tried to equate the entire gas-to-crystal shift to the $\underline{k} = \underline{0}$ shift terms. The reader should note that the shifts in neat crystals, in isotopic mixed crystals, and in chemical mixed crystals (i. e., benzene in hexane) are often all of similar size and direction. The effect of resonance interactions is nearly lost in the second case and completely lost in the latter case, indicating that resonance interactions must give a relatively minor contribution to the shift. For some molecular crystal transitions, where the exciton interactions are strong, such correlations between experimental and theoretical band shift terms may be more nearly correct than for the benzene transitions discussed here. However, even in these cases, neglect of site distortion energy and in particular second-order contributions to Δ is probably not justified.

G. Coupling Constants and Davydov Splittings

Some earlier papers^{4b, 4f, 7} concerned with the exciton structure of crystalline benzene expressed ^{first-order} energies in terms of coupling constants, M_a , M_b , M_c , $M_{I II}$, $M_{I III}$, and $M_{I IV}$, dropping the superscript f , whence,

$$\begin{aligned}
 L^f(\tilde{\omega}) &= 2M_a(\tilde{\omega}) + 2M_b(\tilde{\omega}) + 2M_c(\tilde{\omega}) \\
 L_{I II}^f(\tilde{\omega}) &= 4M_{I II}(\tilde{\omega}) \\
 L_{I III}^f(\tilde{\omega}) &= 4M_{I III}(\tilde{\omega}) \\
 L_{I IV}^f(\tilde{\omega}) &= 4M_{I IV}(\tilde{\omega})
 \end{aligned}
 \tag{17}$$

there being an identical set of translationally equivalent interactions along each positive and negative crystallographic direction \underline{a} , \underline{b} , and \underline{c} and a set of four identical interactions between any molecule and its translationally inequivalent neighbors. While Ref. 7 considered the M 's in Eq. (17) to be nearest-neighbor interactions, they are really summed quantities over all members of each set in accordance with Eq. (7). Since translationally

equivalent interactions lying skew to the crystallographic axes have been omitted,¹³ the energy contribution $L^f(\underline{0})$ in Eqs.(17) is approximate even for $\underline{k} = \underline{0}$. However, for the ${}^1B_{2u}$ and ${}^3B_{1u}$ electronic states of benzene, and undoubtedly also for vibrational states of benzene, the approximation is an excellent one because of the smallness of the omitted terms (vide infra).

For the particular case of $\underline{k} = \underline{0}$, the resulting four energy levels associated with each nondegenerate molecular state are the Davydov components. These are important since they are the only ones that can be reached by interaction with radiation from the $\underline{k} = \underline{0}$ ground state of the crystal. In terms of the coupling constants, and with respect to a common origin, $\bar{\epsilon} + \Delta + L^f(\underline{0})$, the $\underline{k} = \underline{0}$ energies are:

$$\begin{aligned}
 E(A) &= 4(+M_{I\ II} + M_{I\ III} + M_{I\ IV}) \\
 E(B_1) &= 4(+M_{I\ II} - M_{I\ III} - M_{I\ IV}) \\
 E(B_2) &= 4(-M_{I\ II} + M_{I\ III} - M_{I\ IV}) \\
 E(B_3) &= 4(-M_{I\ II} - M_{I\ III} + M_{I\ IV}),
 \end{aligned}
 \tag{18}$$

where it is understood that the M_{qq} 's refer to $\underline{k} = \underline{0}$. These equations are exact for the Frenkel model. It should be noted that the mean value $\bar{\epsilon} + \Delta + L^f(\underline{0})$ of the Davydov components lies at the mean value $\bar{\epsilon} + \Delta$ of the exciton band only in the case where all \underline{k} -dependent translationally equivalent interactions are negligible. $L^f(\underline{0})$ will be referred to as the $\underline{k} = \underline{0}$ shift (or the translational shift). This point is important in the analysis of isotopic mixed crystal data, since it is $\bar{\epsilon} + \Delta$, not $\bar{\epsilon} + \Delta + L^f(\underline{0})$, that determines the position of the guest energy levels in the ideal case (vide infra).

H. Site Group Splitting and the Ideal Mixed Crystal

Direct manifestation of the reduction in symmetry of molecular quantities in the site is the site group splitting. Symmetry arguments show that degenerate states of the molecule often map into nondegenerate irreducible representations of the site group. This is true in benzene where the molecular symmetry is much higher than the site symmetry (see Fig. 2). Degeneracies present in the molecular state can therefore be removed by the site. The splitting has been called site group splitting^{3a} and has been primarily studied in the vibrational spectrum of molecular crystals, but is certainly not limited to vibrations alone.

In order to be able to discuss site group splitting without complications due to interchange group splitting it is suggested that site group splitting be defined phenomenologically as the splitting obtained for the guest in an ideal mixed crystal. The ideal mixed crystal is defined as one in which: (a) the guest is infinitely dilute; (b) the only difference between guest and host is one of isotopic substitution; (c) guest and host have the same symmetry and dimensions; (d) quasi-resonance interactions between guest and host and the effects of isotopic substitution on Δ are negligible. Isotopic mixed crystals approximate fairly closely this definition. In addition small correction terms to be discussed later can be applied to bring the isotopic mixed crystal even closer to the concept of the ideal mixed crystal. The phenomenological definition of the ideal mixed crystal brings into agreement, as close as is thought possible, the observed site group splitting in isotopic mixed crystals and the original idea^{3a} that site group splitting is the result of the static field (\underline{k} -independent) interactions at the site. In the ideal mixed crystal the site group splitting of a degenerate gas phase band will therefore be _____

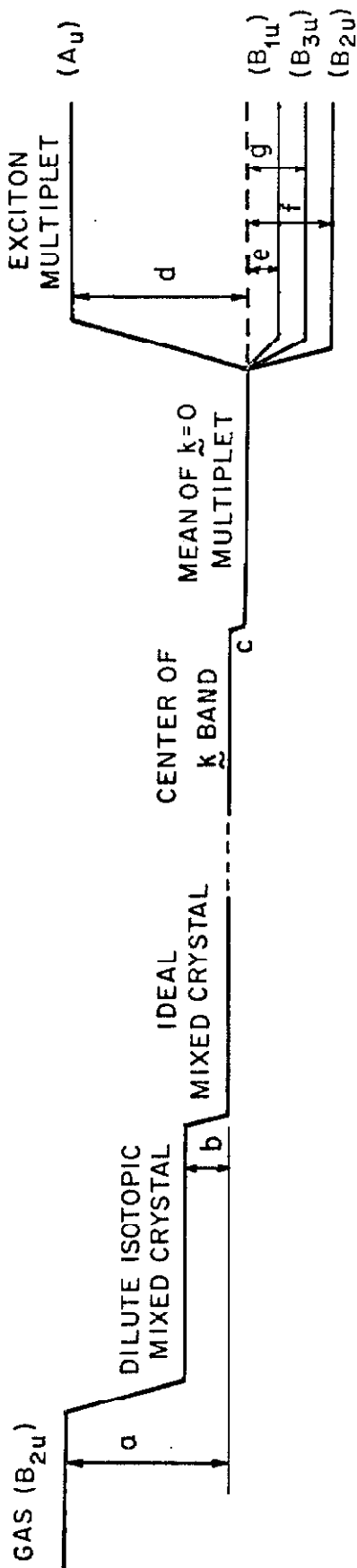
Figure 3

Schematic exciton structure--benzene.

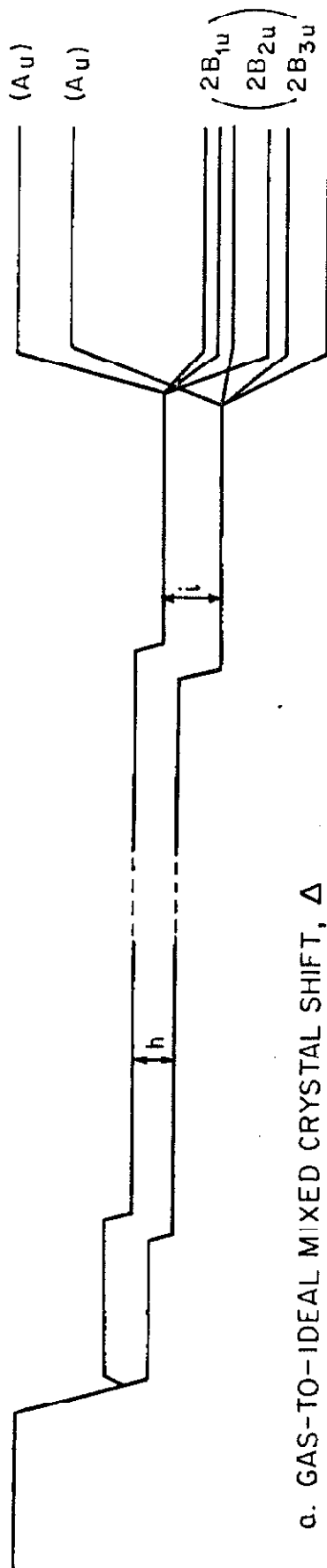
MOLECULE (\tilde{D}_{6h})

SITE ($\tilde{\zeta}_i$)

FACTOR (\tilde{D}_{2h})



GAS (E_{1u})



a. GAS-TO-IDEAL MIXED CRYSTAL SHIFT, Δ
 b. QUASI-RESONANCE CORRECTION (SEE REF. 7)

c. $\tilde{k} = 0$ SHIFT, L^f (0)

d. $4(M_{I,II} + M_{I,III} + M_{I,IV})$

e. $4(M_{I,I} - M_{I,II} - M_{I,III} - M_{I,IV})$

f. $4(-M_{I,II} + M_{I,III} - M_{I,IV})$

g. $4(-M_{I,I} - M_{I,II} + M_{I,III})$

h. $(\Delta x - \Delta y)$

INTERCHANGE SPLITTING

i. h PLUS ADDITIONAL NEAT CRYSTAL RESONANCE TERMS

quantitatively identical to the difference in the Δ terms of the originally degenerate components. Symbolically this can be written as $(\Delta_x - \Delta_y)$, where x and y designate the degenerate components. (See Fig. 3.)

In the neat crystal there are additional resonance contributions to the splitting of free-molecule degenerate states. Excitation exchange interactions will couple not only site group components of one kind (say x) among different sites, but may also couple site group components of different kinds (x and y) among the various sites. The last statement is certainly true when both "kinds" belong to the same site group species (benzene!) but also in some cases where the two "kinds" belong to different site group species.¹⁷ In other words, any degenerate or nearly degenerate levels present after the static interactions have been introduced may be further coupled together by the dynamic (k -dependent) interactions in the neat crystal, or by quasisresonance interactions in the mixed crystal (vide infra). This statement holds whether the near degeneracy arises from site group splitting or from accidental degeneracies present in the system. The latter case when applied to vibrational levels resembles Fermi resonance.¹⁸ It is different from typical Fermi resonance in that the effect is an intermolecular one and that anharmonicities of the usual type need not be present to effect the interaction.

The essence of the last paragraph is that whenever site group splitting and interchange group splitting are expected together, the total effect cannot be handled even conceptually as a simple superposition of two independent effects. For the benzene crystal, the full 8×8 submatrix must be considered leading to ten independent off-diagonal coupling constants, whose values are not determinable from the limited experimental data obtainable. A separation of the two effects would be justified as a first approximation only if: (a) The site group interaction is an order of magnitude larger than the resonance

interactions, or (b) the site group components are of different symmetry (see, however, footnote 17). Except for these two cases, the so-called site group splitting in a neat crystal will contain contributions not only from the phenomenological site group splitting in the ideal mixed crystal but also from resonance interactions usually discussed within the space group.

The ideal mixed crystal is also a useful concept for discussing non-degenerate states. If, for a real mixed crystal, the deviations from the idealizing conditions can be evaluated quantitatively, the mean value $\bar{\epsilon} + \Delta$ of the exciton band can be found from the mixed crystal energy. This technique allows one to evaluate $L^f(\underline{0})$ if the mean value $\bar{\epsilon} + \Delta + L^f(\underline{0})$ of the Davydov components is independently known. Similarly, if $L^f(\underline{0})$ is known to be negligible, the ideal mixed crystal level can be equated to $\bar{\epsilon} + \Delta$. For the case of benzene vibrations where the $L^f(\underline{0})$ are expected to be small, this provides a technique for finding the position of the "forbidden" Davydov component. While these concepts were implicitly utilized by Nieman and Robinson⁷ for the determination of the Davydov structure of the lowest excited electronic states of the benzene crystal, their usefulness was neglected in the concurrent interpretation of both electronic and vibrational^{5e} exciton structure.

III. EXPERIMENTAL METHODS AND RESULTS

The experiments of Nieman and Robinson⁷ on the ${}^1B_{2u}$ electronic exciton band were repeated. These results will be discussed in some detail to illustrate the theory and to derive the exciton coupling constants using the D_2 interchange group. Infrared transitions in neat and isotopic mixed benzene crystals were also obtained and a few of these spectra will be discussed for further illustration.

The deuterated benzene was obtained from Merck, Sharp, and Dohme, Ltd., Canada, and was vacuum distilled before use. The C_6H_6 was obtained from Phillips Petroleum Co. (99.89 mole % pure) and was used without further purification. The neat crystals for the infrared experiments were made by placing liquid benzene between two CsI windows, which were pressed together in a sample holder. The holder was made from brass and was fitted with indium in order to apply firm, uniform pressure to the soft salt windows. A few drops of benzene were placed on the CsI window, and the sample holder was assembled and attached to the bottom of a "cold-finger" helium dewar in a dry nitrogen atmosphere. The dewar was then assembled, and the sample was frozen to liquid nitrogen temperature (77°K) while the dewar was being evacuated. At this temperature one could see through the sample, and even

upon subsequent cooling to 4.2°K the sample remained clear. Sample thickness, estimated from measurements of absolute absorption intensities¹⁹ in the infrared, was about 5-10 μ . For the ultraviolet experiments, a technique similar to that used by Nieman and Robinson⁷ was employed.

The concentration of the isotopic mixed samples was about 1% guest in 99% host. This low concentration was used in order that complete isolation of the guest in the host crystalline lattice could be effected even though to detect infrared absorption this meant that larger, less convenient sample thicknesses were necessary. The thicker samples were made with a 0.050 inch indium wire gasket placed between the CsI windows. When compressed, this spacing was approximately 0.75 to 1.0 mm thick. The gasket was not made into a closed circle, allowing an entrance into which the liquid sample could be introduced. However, indium "tails", with which the sample holder could be sealed after it is filled with benzene, were left attached. The well-mixed²⁰ sample was then placed in the holder, sealed, and solidified as discussed above. After cooling to 77°K the sample was heavily cracked, although it was possible to see through some portions of it. Some of the infrared spectra were taken at 77°K and some at 4.2°K with no apparent differences observed. These data are presented in Table II and in Figs. 4, 5, 6, and 7. The neat crystal infrared spectra are virtually identical with those already reported in the literature.¹⁹

IV. DISCUSSION OF EXPERIMENTAL RESULTS

As explained in the Theoretical Section, in order to understand fully molecular crystalline interactions, it is necessary to study both neat and isotopic mixed crystals. With the data obtained from mixed crystals it is possible to isolate and to study separately crystalline interactions arising from different "sources." By varying the isotopic substitution, guest energy states

TABLE II. Some u-vibrational levels of C_6H_6 (in cm^{-1})

Symmetry	Gas ^a	C_6H_6 in C_6D_6 ^b	Neat Crystal ^b	Polarization and Symmetry ^c	
$e_{1u}(\nu_{18})$	1037	1034.8 1038.6	1030.0		
			1032.5		
			1033.3		
			1034.6		
			1038.9		
$b_{1u}(\nu_{12})$	1010	1011.3	1006.9	c	B_{3u}
			1008.6	b	B_{2u}
			1009.7	a	B_{1u}
$b_{2u}(\nu_{15})$	1146	1146.9	1142.5	c	B_{3u}
			1148.6	a	B_{1u}
			1150.3	b	B_{2u}

^a S. Brodersen and A. Langseth, Mat. Fys. Skr. Dan. Ved. Selsk 1, 1 (1956).

^b Our measurements.

^c S. Zwerdling and R. S. Halford, J. Chem. Phys., 23, 2221 (1955).

Figure 4

Infrared spectrum of the e_{1u} (ν_{18}) fundamental of 1% C_6H_6 in C_6D_6 at 4.2°K, showing 3.8 cm^{-1} site group splitting.

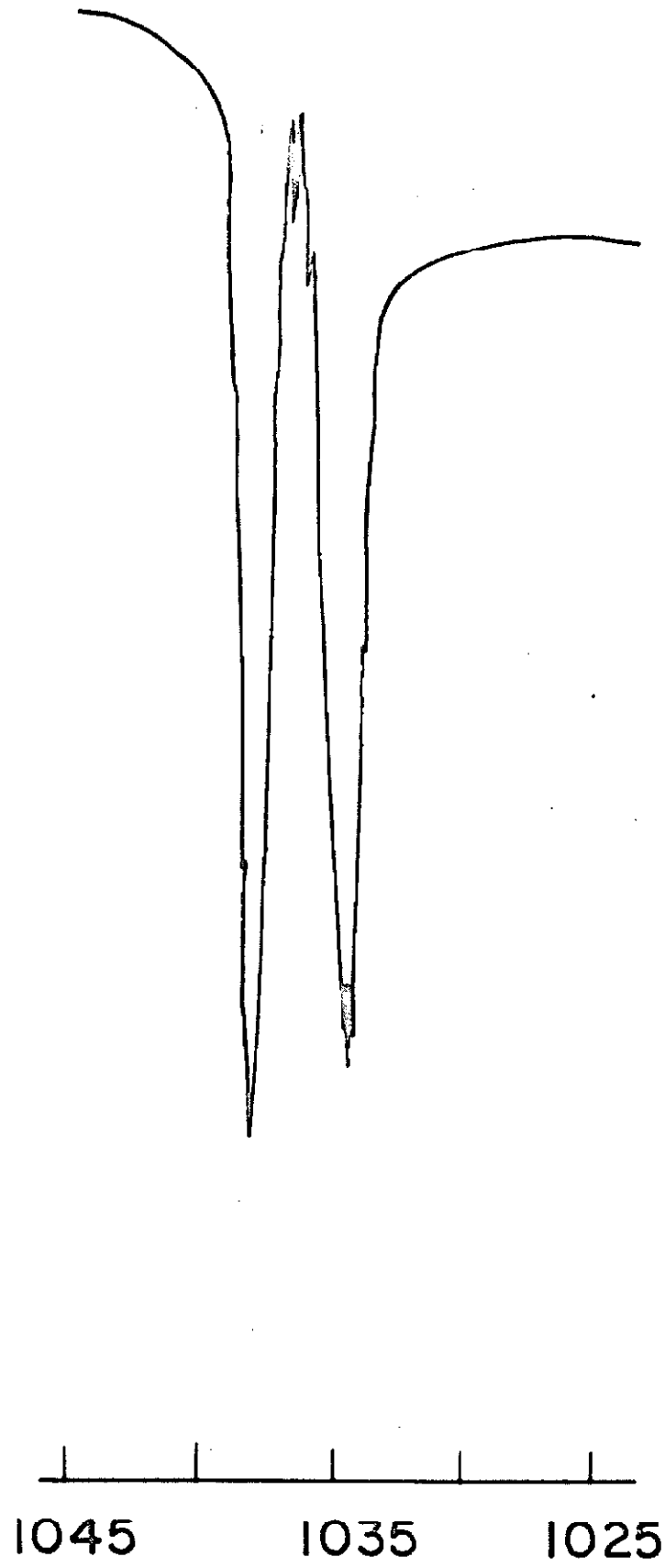


Figure 5

Infrared spectrum of the e_{1u} (ν_{18}) fundamental of neat C_6H_6 at $4.2^\circ K$.

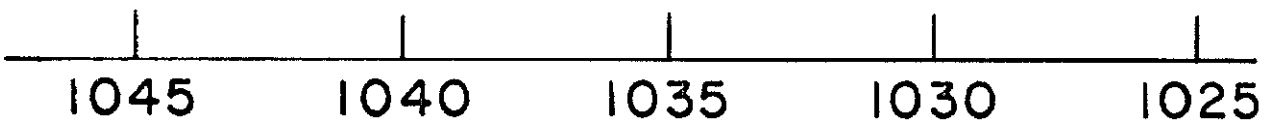
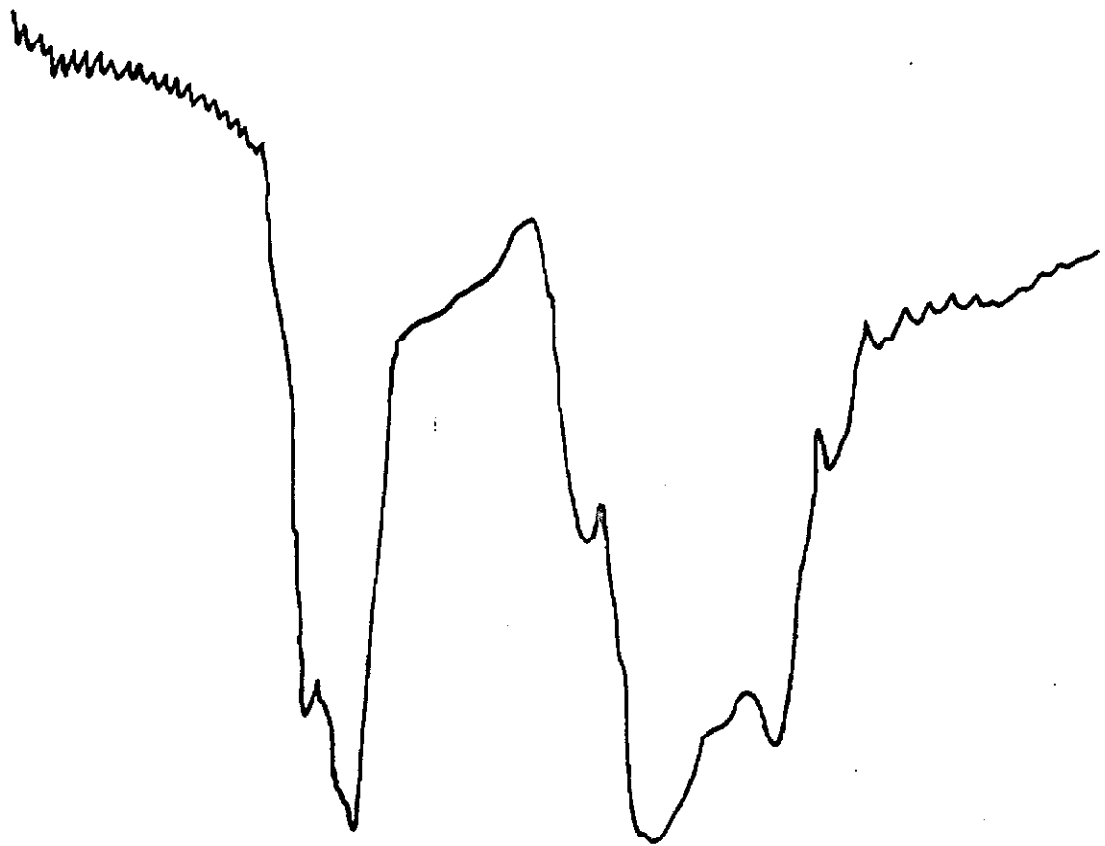


Figure 6

Infrared spectra of the b_{1u} (ν_{12}) fundamental of neat C_6H_6 and
1% C_6H_6 in C_6D_6 at 77°K.

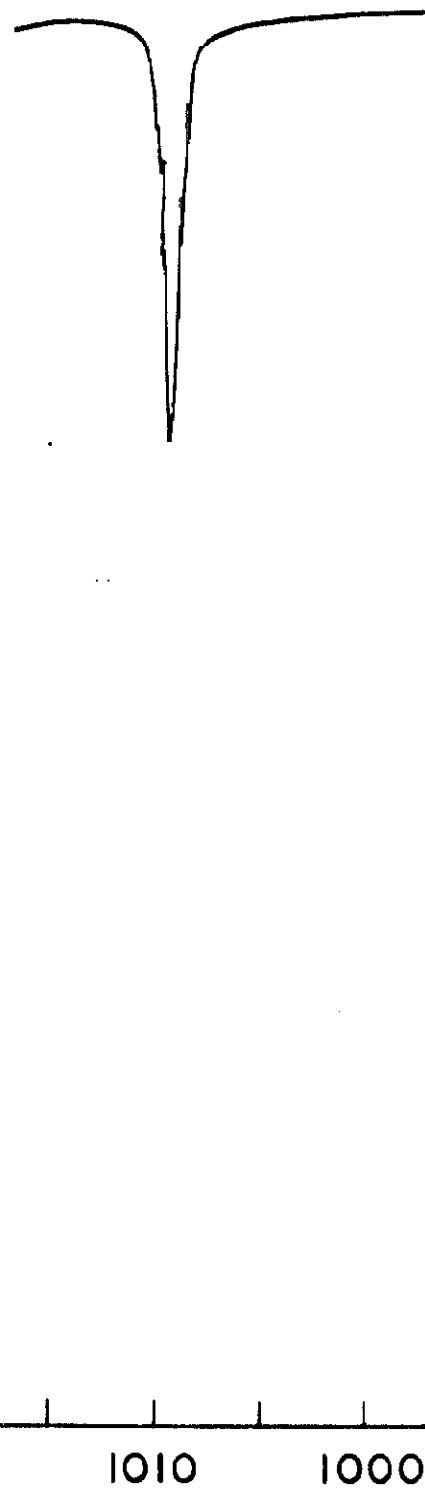
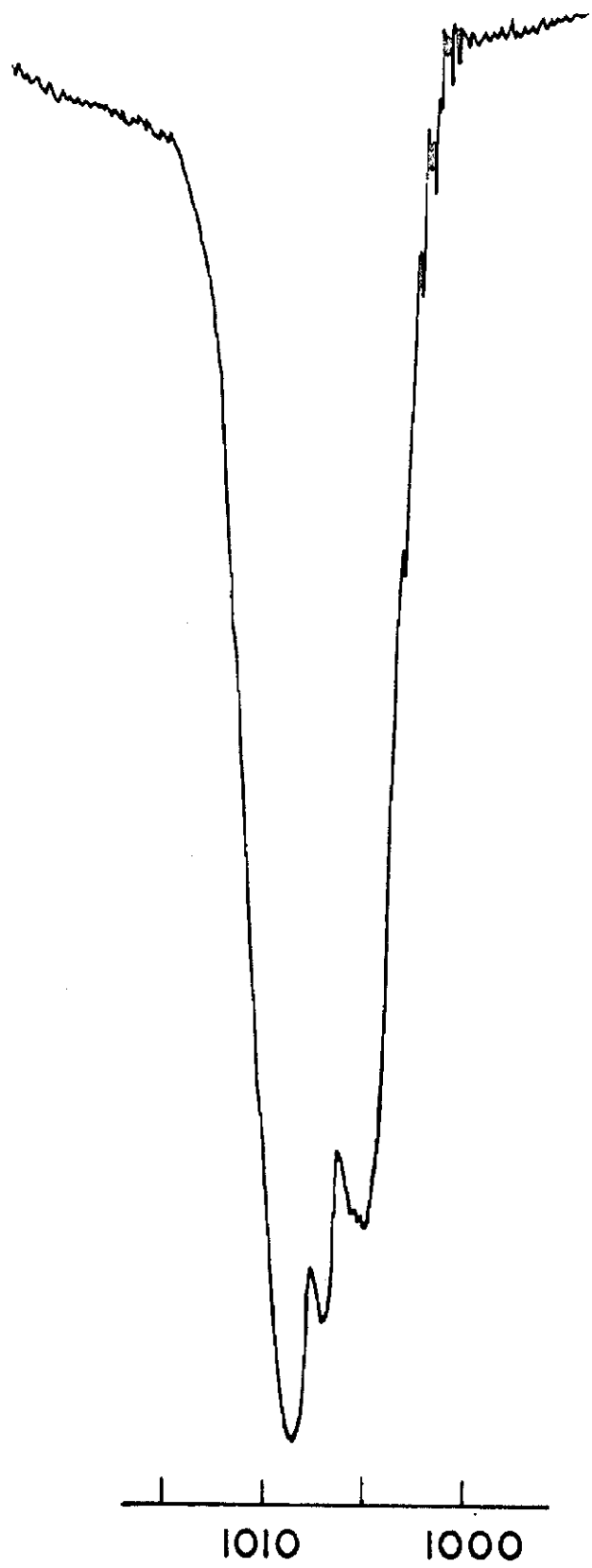
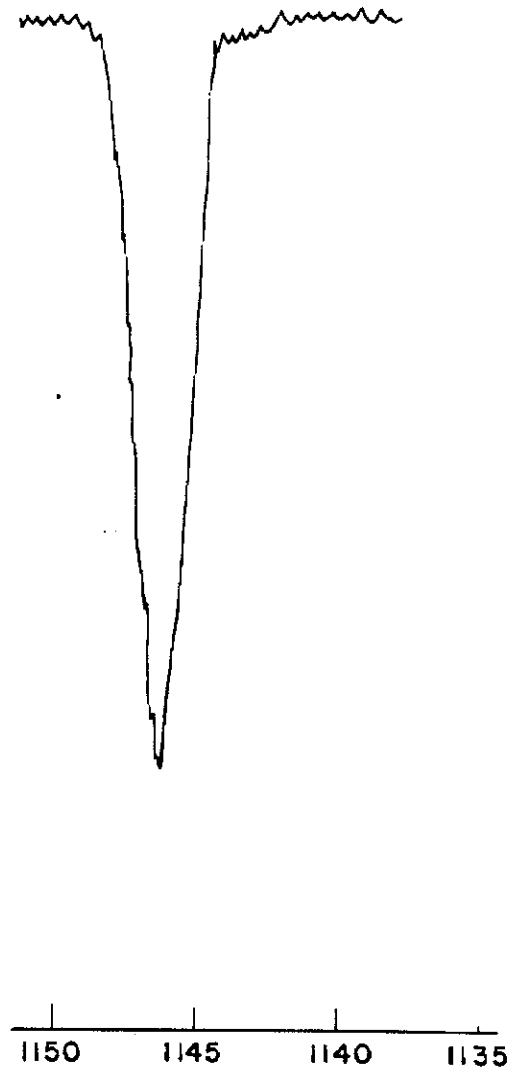
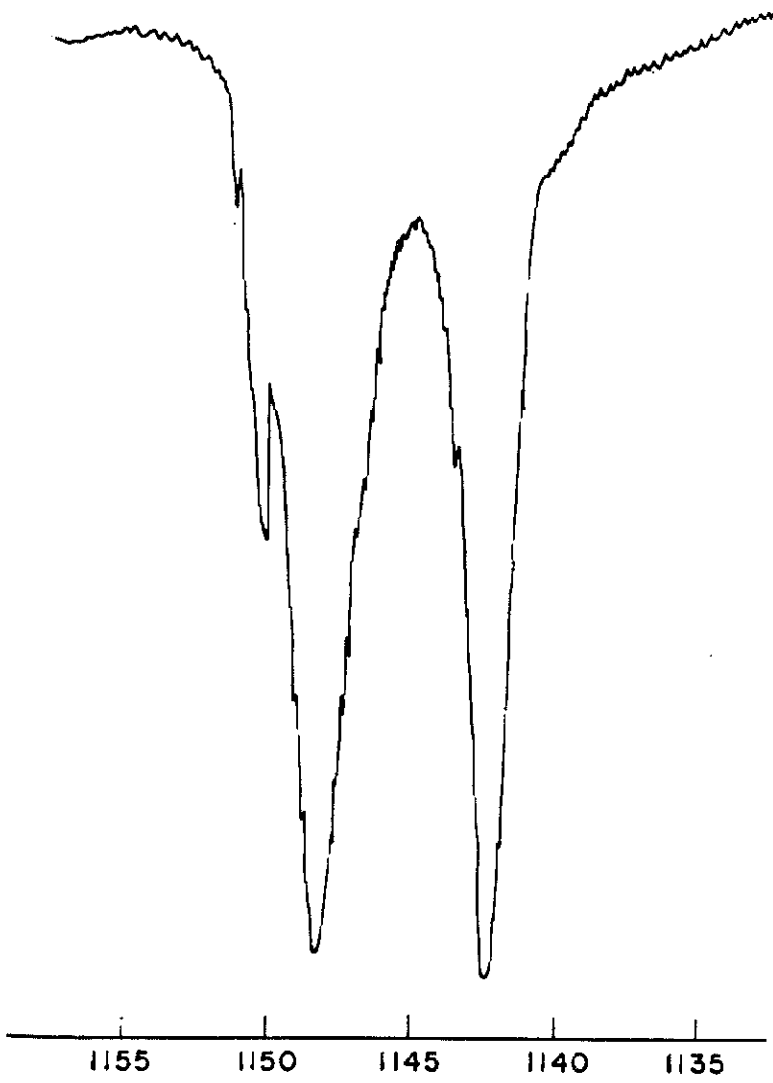


Figure 7

Infrared spectra of the b_{2u} (ν_{15}) fundamental of neat C_6H_6 and 1% C_6H_6 in C_6D_6 at 77°K.



in such samples can be brought into near resonance with host levels. Therefore, it is not only possible to gain knowledge about the static field interactions but also about the dynamic interactions.

A. C₆H₆ Electronic Band ⁻¹B_{2u}

The interchange group structure of this state, as obtained from neat and isotopic mixed crystal absorption spectra, is given in Table III and Fig. 8. In neat crystalline C₆H₆, the 0-0 line of the ¹B_{2u} - ¹A_{1g} transition²¹ has been observed both in absorption and emission. Because of the interchange group selection rules for these processes¹³ ($\Delta k = 0$; B₁ ↔ B₂; B₁ ↔ B₃; B₂ ↔ B₃; A ↔ B₁, B₂, B₃), only the $\underline{k} = \underline{0}$ components of the B₁, B₂, and B₃ bands can be observed for transitions involving the totally symmetric ($\underline{k} = \underline{0}$, A_g) ground state of the crystal. Thus the E(A) level, or alternatively the mean value of the Davydov components, must be located by an indirect method to obtain the M values in Eq. (17).

The 0-0 component in emission is found to be coincident within 5 cm⁻¹ with the lowest interchange group component observed in absorption. From the selection rules, one can/therefore conclude that the lowest interchange component has B symmetry and that its $\underline{k} = \underline{0}$ level is at or near the bottom of the band. If a state of B_u symmetry were not the lowest factor group component, or, if the $\underline{k} = \underline{0}$ level were not its lowest state, we would not have observed the 0-0 transition in emission, but would have observed only transitions terminating in vibrational exciton bands of the ground electronic state.¹³ (In agreement with this expectation is the fact that only a slight increase in temperature is necessary for complete removal of the 0-0 band in emission.¹³) Without making extensive polarization studies, it is impossible further to assign this state to any one of the three possible B levels (B_{1u}, B_{2u}, B_{3u}). The assignment of the lowest level to one of the B_u levels is consistent with the conclusions reached by Nieman and Robinson.⁷

TABLE III. Benzene ${}^1B_{2u} \leftarrow {}^1A_{1g}$ electronic (0-0) transition (in cm^{-1}) according to the ideal mixed crystal model.

Gas phase ^a C_6H_6 in C_6D_6	Ideal mixed crystal ^b	Algebraic mean of k band in neat crystal	Algebraic mean of Davydov components ^c	Davydov components ^d	Coupling constants ^e
38086.1	37862 ± 2	37862 ± 2	37872 ± 16	$A_u = 37,996 \pm 48$ $B_{2u} = 37,847.1 \pm 1.0$ $B_{3u} = 37,841.8 \pm 1.0$ $B_{1u} = 37,803.2 \pm 1.0$	$M_{I,II} = +6.9 \pm 2$ $M_{I,III} = +12.4 \pm 2$ $M_{I,IV} = +11.7 \pm 2$

^aJ. H. Callomon, T. M. Dunn, J. M. Mills, Phil. Trans. Roy. Soc. (London) 259A, 499 (1966)

^bCorrected for quasi resonance Eq. (18) plus 2 cm^{-1} for the interaction with the lowest vibronic level (ref. 7a).

^cCorrected for $L_f(Q)$, the " $k = 0$ shift". See Eq. (15) and the following two paragraphs of discussion.

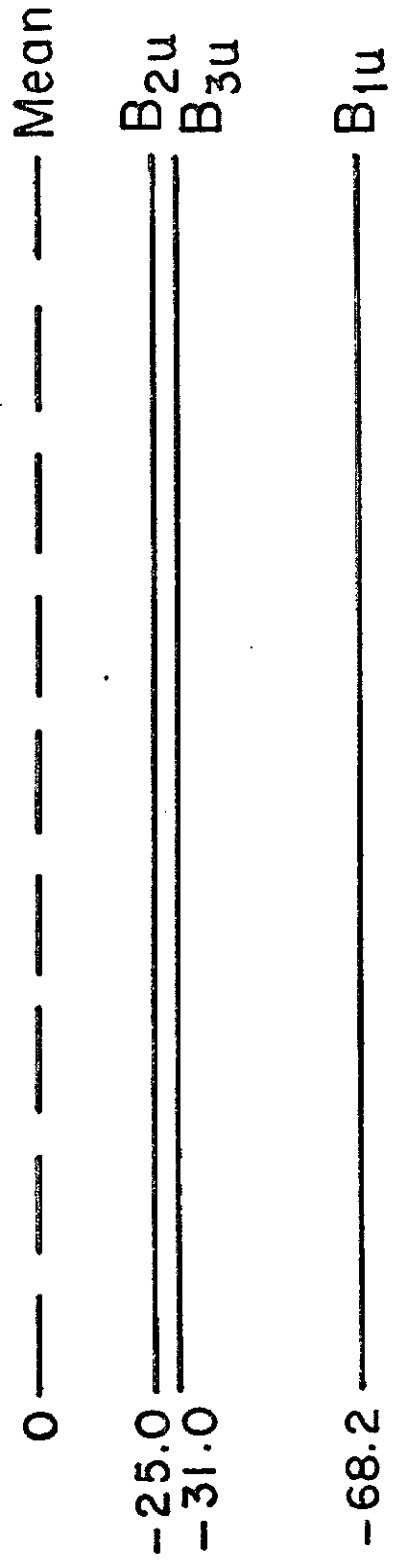
^dAssignment of symmetry (B_{1u} , B_{2u} or B_{3u}) is based on polarization data of Broude, ref. 2c.

^eNew data suggest that for benzene isotopic mixed crystals do not closely approach the ideal mixed crystal limit. In particular there seems to be an isotope effect on the Δ term of Eq. (17).

Figure 8

Davydov structure of the ${}^1B_{2u}$ electronic state of C_6H_6 using data of Nieman and Robinson. The mean lies at $37,872\text{ cm}^{-1}$. See Table III.

124.2-----A_u



As mentioned above, in order to obtain the M values from the experimental data, either the position of the A level or the mean value of the Davydov components must be known. Following the method of Nieman and Robinson,⁷ and providing the ideal mixed crystal limit can be approached in this way,

the latter quantity can be evaluated from isotopic mixed crystal data to which small corrections due to quasiresonance shifts and the $\underline{k} = \underline{0}$ shift term $L^f(0)$ have been applied. First, the supposed ideal mixed crystal value of the transition energy ($\bar{\epsilon} + \Delta$) is obtained by correcting the observed 0-0 transition of the isotopic mixed crystal C_6H_6 in C_6D_6 for the quasiresonance shift,⁷

$$\delta \approx 4\beta^2/\Delta E, \quad (18)$$

where,

$$\beta^2 = M_{I\ II}^2 + M_{I\ III}^2 + M_{I\ IV}^2 + \frac{1}{2}(M_a^2 + M_b^2 + M_c^2). \quad (19)$$

The β of Nieman and Robinson is used, i. e., $\beta = 18\text{ cm}^{-1}$. The $\underline{k} = \underline{0}$ shift is then determined such that the β calculated from the splitting and shift terms $[L^{f\alpha}(0)]$ agrees with the measured value. Using the D_2 interchange group and accepting with reservations the interchange group assignments of the observed levels obtained from polarized absorption experiments^{2c} with reservations as discussed in Ref. 7, we then calculate from Eq. (17),

$$\begin{aligned} M_{I\ II} &= + 6.9\text{ cm}^{-1} \\ M_{I\ III} &= + 12.4\text{ cm}^{-1} \\ M_{I\ IV} &= + 11.7\text{ cm}^{-1}. \end{aligned}$$

This calculation is outlined in Tables III and IV. The site shift term $\Delta = -224\text{ cm}^{-1}$ can be found from the ideal mixed crystal 0-0 transition energy ($37,862\text{ cm}^{-1}$), determined as above, and the gas phase 0-0 transition energy ($36,086\text{ cm}^{-1}$). Thus we find that the average \underline{k} -independent crystal binding energy is about 6.0% larger for an excited state molecule than for a ground state molecule in the normal crystal.²² It should be noted that the calculated M values differ in sign from those of Nieman and Robinson, who give -6.9 cm^{-1} , -12.4 cm^{-1} ,

and $+11.7 \text{ cm}^{-1}$, as they did not use the \underline{D}_2 interchange group but instead used the method of Fox and Schnepf^{4b} in the determination of the symmetry of their wave functions.²³

More recent data are apparently inconsistent with the interpretation of Nieman and Robinson. Data on the reverse isotopic mixed crystal, C_6D_6 in C_6H_6 , and on band-to-band transitions seem to suggest a total exciton bandwidth only about $1/3$ that given by the above M values. This discrepancy, thought to be caused by an isotope effect on the electronic Δ term, is presently the object of further investigation. The new results, which indicate that in benzene the ideal mixed crystal cannot be approximated accurately by the technique of isotopic substitution, will be discussed in a separate paper.²⁴ All translationally equivalent interactions are found to be small, justifying the assumptions made above and in Ref. 13.

B. Ground State Ungerade Vibrations

Ungerade vibrations can be observed in infrared absorption. In the gas phase only a_{2u} and e_{1u} vibrations are dipole-allowed within the \underline{D}_{6h} symmetry group of benzene. In the crystal, because of the loss of exact \underline{D}_{6h} symmetry, a partial relaxation of the selection rules occurs, and vibrations of original molecular symmetry a_{2u} , b_{1u} , b_{2u} , e_{1u} , and e_{2u} are observed. One degenerate (e_{1u}) and two nondegenerate vibrations (one b_{1u} and one b_{2u}) will be discussed in detail below.

Degenerate Vibrations -- We have defined site group splitting as the splitting that occurs in degenerate vibrations of guest molecules in an ideal mixed crystal. In order to approach the ideal as closely as possible, the real mixed crystal should be an isotopic mixed crystal in which the guest-host quasi-resonance interactions are reduced to a minimum (i. e., for our case, C_6H_6 guest in a C_6D_6 host or vice versa). Such a choice essentially eliminates contributions from resonance interactions to the observed site splitting. Using this mixed crystal, a 3.8 cm^{-1} site group splitting in crystalline benzene for

the e_{1u} vibration ν_{18} is observed. See Fig. 4. Since the interchange splitting for nondegenerate ungerade vibrations is about 10 cm^{-1} , a quantitative treatment, using site group and interchange group concepts of the degenerate vibrations in the neat crystal does not appear possible. The neat crystal spectrum of the $e_{1u}(\nu_{18})$ band is given in Fig. 5.

Nondegenerate Vibrations -- For these vibrations, in which no site group splitting occurs, the mixed crystal data can be used, as in the case of the ${}^1B_{2u}$ electronic band, to aid in the interpretation of the pure crystal spectrum. Dilute mixed crystal experiments,¹⁵ using solvents of isotopically modified benzene other than C_6H_6 and C_6D_6 , indicate that the quasi-resonance corrections are negligible (less than 1 cm^{-1}) and that Δ is small and independent of the isotopic substitution of the host. Recent calculations of the Davydov structure of benzene vibrational bands,^{25, 26} that are successful in predicting the correct order of magnitude of the overall splittings would predict negligible interactions between the translationally equivalent molecules. Thus, as a first approximation, we assume the mean value of the Davydov components in the pure crystal to be the value of that vibration in the isotopic mixed crystal. With this assumption, the three observed B levels allow a calculation of the complete interchange group structure (see Figs. 9 and 10). Using, with reservations, the polarization results of Zwerdling and Halford^{1e} we can find $M_{I \text{ II}}$, $M_{I \text{ III}}$, and $M_{I \text{ IV}}$ for both the $b_{2u}(\nu_{15})$ and $b_{1u}(\nu_{12})$ vibrational bands. The calculated energies, M values and β values [Eq. (19)] are given in Table IV, and the interchange structures are presented in Figs. 9 and 10. It should be noted, as will be reported later,²⁷ that the factor group structures corresponding to the same normal mode in crystals of C_6H_6 and C_6D_6 are nearly identical. From the calculated β values it is now possible to check the assumption that the quasi-resonance correction to the mixed crystal data, used to obtain the band centers, is indeed small. Applying Eq. (18) one finds that the quasi-resonance correction is less than the

Figure 9

Vibrational Davydov structure of the $b_{1u}(\nu_{12})$ band of C_6H_6 . The mean lies at 1011.3 cm^{-1} .

8.7 - - - - - Au

0 - - - - - Mean

-1.6 - - - - - B_{1u}

-2.7 - - - - - B_{2u}

-4.4 - - - - - B_{3u}

Figure 10

Vibrational Davydov structure of the b_{2u} (ν_{15}) band of C_6H_6 . The mean lies at 1146.9 cm^{-1} .

3.4 ————— B_{2u}

1.7 ————— B_{1u}

0 ————— Mean

-0.7 ————— Au

-4.4 ————— B_{3u}

TABLE IV. Various contributions to the energy of some exciton states.

State	Gas to mixed crystal shift ^a	Quasi-resonance shift ^b	Static field term (Δ) ^c	$L^f(0)$, the " $\tilde{k}=0$ shift"	β	Exciton coupling constants ^d			
						I, II	M	I, III	I, IV
${}^1B_{2U}$ ^e	-232.8 ± 1	$+9 \pm 2$	-224 ± 3	$+8 \pm 4$	$+18 \pm 2$	$+6.9 \pm 2$	$+12.4 \pm 2$	$+11.7 \pm 2$	
$b_{1U}(\nu_{12})$	$+1.3 \pm .5$	~ 0.0	$+1.0 \pm 1$	~ 0.0	$+1.7 \pm .3$	$+0.89 \pm .2$	$+0.75 \pm .2$	$+0.54 \pm .2$	
$b_{2U}(\nu_{15})$	$+0.9 \pm .5$	~ 0.0	$+1.0 \pm 1$	~ 0.0	$+0.5 \pm .3$	$+0.12 \pm .2$	$+0.34 \pm .2$	$-0.64 \pm .2$	

^a C_6H_6 in C_6D_6 values compared with indirectly derived gas phase values.

^bObtained from β of Nieman and Robinson, ref.7.

^cObtained by adding the first and second columns.

^dElectronic and vibrational polarization assignments taken from

V. L. Broude, Usp., 4, 584 (1962), and S. Zwerdling and R. S. Halford, J. Chem. Phys. 23, 2221 (1955).

^e See footnote e of Table III.

experimental error, as was assumed. A discussion of the interaction terms will be given elsewhere.^{15, 26, 27}

V. SUMMARY

The major points made in this paper are:

- 1) The concept of the interchange group is introduced and is applied to the molecules in the primitive unit cell. This group provides a convenient and unambiguous way of discussing the relative signs of the exciton coupling constants.
- 2) The site distortion energy P and band-shift term Δ are introduced, and together with the D -term are discussed relative to the experimental band-shift.
- 3) It is emphasized that site wave functions χ_{nq}^f , and not molecular wave functions, are the ones of greater significance.
- 4) Static and dynamic interactions are distinguished and are associated, respectively, with \underline{k} -independent and \underline{k} -dependent terms of the Davydov energy equation. These interactions are associated with site operations and transport operations, respectively.
- 5) The ideal mixed crystal is defined and its importance in the determination of site splittings, band shifts, and forbidden Davydov components is emphasized.
- 6) The exciton structure of molecular degenerate, or nearly degenerate, states cannot be described simply as site group splitting plus interchange group splitting. We have therefore used the term site group splitting to describe the splitting of molecular degenerate states associated with guest molecules in an ideal mixed crystal.
- 7) Experimental data, interpreted within the framework of the foregoing theoretical ideas, are presented for the ${}^1B_{2u}$ electronic exciton band and for a few vibrational exciton bands in the electronic ground state.

REFERENCES

¹(a) R. S. Halford and O. A. Schaeffer, *J. Chem. Phys.* 14, 141 (1946); (b) R. Mair and D. F. Hornig, *J. Chem. Phys.* 17, 1236 (1949); (c) A. Fröhling, *Ann. de Phys.* 12^e Série, t. 6, 26 (1951); (d) S. C. Sirkar and A. K. Ray, *Ind. J. Phys.* 24, 189 (1950); (e) S. Zwerdling and R. S. Halford, *J. Chem. Phys.* 23, 2221 (1955).

²(a) V. L. Broude, V. S. Medvedev, and A. F. Prikhotko, *J. Exptl. Theoret. Phys. (U. S. S. R.)* 21, 665 (1951); (b) V. L. Broude, V. S. Medvedev, and A. F. Prikhotko, *Opt. i. Spektr.* 2, 317 (1957); (c) V. L. Broude, *Usp. Fiz. Nauk* 74, 577 (1961) [Engl. Transl. *Sov. Phys. --USP* 4, 584 (1962)]; (d) V. N. Vatulev, N. I. Sheremet, and M. T. Shpak, *Opt. i. Spektr.* 16, 315 (1964); (e) A. Zmerli, *J. Chim. Phys.*, 56, 387 (1959).

³(a) R. S. Halford, *J. Chem. Phys.* 14, 8 (1946); (b) D. F. Hornig, *J. Chem. Phys.* 16, 1063 (1948); (c) H. Winston and R. S. Halford, *J. Chem. Phys.* 17, 607 (1949); (d) H. Winston, *J. Chem. Phys.* 19, 156 (1951); (e) L. P. Bouckaert, R. Smoluchowski, and E. Wigner, *Phys. Rev.* 50, 58 (1936).

⁴(a) A. S. Davydov, *Theory of Molecular Excitons*, (McGraw-Hill, N. Y., 1962); (b) D. Fox and O. Schnepp, *J. Chem. Phys.* 23, 767 (1955); (c) D. P. Craig and P. C. Hobbins, *J. Chem. Soc.* 1955, 539; (d) D. P. Craig, *J. Chem. Soc.* 1955, 2302; (e) D. P. Craig and S. H. Walmsley, *Mol. Phys.* 4, 113 (1961); (f) D. P. Craig and J. R. Walsh, *J. Chem. Soc.* 1958, 1613; (g) A. S. Davydov, *Usp. Fiz. Nauk* 82, 393 (1964). [*Sov. Phys. --USP* 7, 145 (1964).]

⁵(a) D. S. McClure, *Solid State Phys.* 8, 1 (1958); (b) W. Vedder and D. F. Hornig, *Adv. Spectry.* 2, 189 (1961); (c) O. Schnepp, *Ann. Rev. Phys. Chem.* 14, 35 (1963); (d) D. P. Craig and S. H. Walmsley in *Physics and*

Chemistry of Organic Solid State, Vol. I, ed. by Fox, Labes, and Weissberger, (Interscience, N. Y., 1963), p. 586; (e) D. A. Dows, ibid., p. 609.

⁶G. L. Hiebert and D. F. Hornig, J. Chem. Phys. 20, 918 (1952).

⁷G. C. Nieman and G. W. Robinson, J. Chem. Phys. 39, 1298 (1963).

⁸R. Silbey, S. A. Rice, and J. Jortner, J. Chem. Phys. 43, 3336 (1965).

⁹E. G. Cox, Rev. Mod. Phys. 10, 159 (1958); E. G. Cox, D. W. J. Cruickshank, and J. A. S. Smith, Proc. Roy. Soc. (London) A247, 1 (1958); G. E. Bacon, N. A. Curry, and S. A. Wilson, Proc. Roy. Soc. (London) A279, 98 (1964).

¹⁰R. Kopelman, J. Chem. Phys. 00, 0000 (1967).

¹¹These relations do not hold for all values of k .

¹²(a) E. P. Wigner, Group Theory (Academic Press, New York, 1959), p. 59; (b) G. F. Koster, Solid State Phys. 5, (1957), reprinted by Academic Press, N. Y.; C. Kittel, Quantum Theory of Solids (John Wiley and Sons, Inc., New York, 1963), Chap. 9.

¹³S. D. Colson, R. Kopelman and G. W. Robinson, J. Chem. Phys. 00, 0000 (1967).

¹⁴Ref. 12(a), p. 118.

¹⁵E. R. Bernstein, manuscript in preparation.

¹⁶This point is discussed by T. Thirunamachandran [Thesis (University College, London, 1961)]. He points out that the importance of the octapole-octapole interactions in determining the Davydov splitting can be evaluated by determining the polarizations of the Benzene exciton components.

¹⁷This will happen when one or more symmetry operations of different, physically equivalent sites are not parallel. This points out the usefulness of

the interchange group, as some interactions "allowed" by the interchange group appear to be forbidden by the factor group. This apparent contradiction arises because similar but non-parallel operations of different sites may all map into the same class of operations of the factor group. It should be remembered that the site group is only isomorphous with a subgroup of the factor group, not identical with it.

¹³R. Kopelman, J. Chem. Phys. 44, 3547 (1966) and references therein.

¹⁹W. B. Person and C. A. Swenson, J. Chem. Phys. 33, 233 (1960);
J. L. Hollenberg and D. A. Dows, J. Chem. Phys. 39, 495 (1963).

²⁰Poorly mixed samples of 1% guest in 99% host and a well mixed sample of higher concentration were studied. The absorptions, while not having the complete exciton structure of the neat crystals, were not as sharp as those of the low concentration isotopic mixed crystals and some bands even exhibited residual splittings. This tends to indicate that, in general, mixed crystal studies, designed to eliminate guest-guest interactions, should be carried out at guest concentrations of less than 2%. The concentrated (5-10%) mixed crystal spectra of J. L. Hollenberg and D. A. Dows [J. Chem. Phys. 39, 495 (1963)] appear much like the above-mentioned poorly mixed samples.

²¹As the molecular symmetry is not conserved in the site, the use of D_{6h} designations for the symmetry of crystal states is not really correct. However, we will retain the notation here merely as a convenient labelling device.

²²The heat of sublimation for benzene is about 3800 cm^{-1} . G. Milazzo, Ann. Chim. Rome 46, 1105 (1956).

23

Note that the designation of molecules II and IV has also been changed from that of Nieman and Robinson (also Fox and Schnepf^{4b} and Craig and Walsh^{4f}) to agree with the crystallographic work of Cox, Cruickshank, and Smith.⁹ Because of the restrictions due to the interchange group it would be very awkward to accept the designations of the a, b, and c, axes of Cox, et al. without accepting their numbering of molecules. This designation is

consistent with the benzene ac projection shown in Fig. 2.

²⁴ S. D. Colson, manuscript in preparation.

²⁵ I. Harada and T. Shimanouchi, *J. Chem. Phys.* 44, 2016 (1966).

²⁶ E. R. Bernstein, manuscript in preparation.

²⁷ E. R. Bernstein and G. W. Robinson, manuscript in preparation.

Absorption Spectra of Strained Benzene Crystals at Low Temperatures*

STEVEN D. COLSON

Gates and Crellin Laboratories of Chemistry, † California Institute of Technology, Pasadena, California

(Received 1 August 1966)

IN very thin crystals attached to a substrate and cooled, large crystal stresses are produced. The effects of these stresses on the $2600\text{-}\text{\AA}$ ${}^1B_{2u} \leftarrow {}^1A_{1g}$ $[0-0 + \nu_6'(e_{2g})]$ absorptions of crystalline benzene have been observed previously.¹⁻³ While six Davydov components are expected⁴ for transitions into a doubly degenerate vibronic state, only a doublet has thus far been resolved in the $[0-0 + \nu_6'(e_{2g})]$ transition in strained¹ or unstrained³ crystals. The predominant effects reported for these transitions, and interpreted as being caused by strain, are a broadening of the absorption lines, an increase in the doublet splitting from 9 to 29 cm^{-1} , and a pronounced "induced" polarization of one of the components. These components show only weak polarization in unstrained crystals. No interpretation of the remarkable induced polarization has been proposed to date. It could be that the stress on the crystal separates out from the others one or a particular pair of the exciton components that polarizes sharply.

The 0-0 band itself and the totally symmetric progressions built on the 0-0 transition, though potentially interesting, are weaker and were not reported in the Russian work.

A number of benzene crystals $\sim 1\text{-}5 \mu$ thick were

grown by pressing liquid benzene between two quartz optical flats and then cooling them either slowly by suspension over liquid N_2 or rapidly by direct immersion into liquid N_2 . Both methods result in strained crystals as evidenced by their absorption spectra. The spectra of these crystals are compared in Fig. 1 with that of a thicker crystal ($\sim 30 \mu$) that was grown by slowly cooling a sample in a quartz cell. A grating spectrograph utilizing the fourth order of a 15 000-lines/in. grating in a 2-m mount was used to take all the spectra. Since the spectrograph is stigmatic, the vertical direction on the photographic plate represents the vertical direction of the crystal. The apparently slanted absorptions of Crystal B actually are piecewise vertical, the vertical portions representing regions of the sample that are subject to different stresses. The half-widths of the absorption lines in the strained crystals are $\sim 6 \text{ cm}^{-1}$. Shifts as great as $10 \pm 2 \text{ cm}^{-1}$ to both high and low energy have been observed. The splitting between the mean of the b and c polarized components and the a component of the 0-0 band changed from $41 \pm 1 \text{ cm}^{-1}$ in the unstrained crystal⁵ to $34 \pm 2 \text{ cm}^{-1}$ in Crystal B and to $44 \pm 2 \text{ cm}^{-1}$ in Crystal C.

That the energy shifts are indeed due to strain and

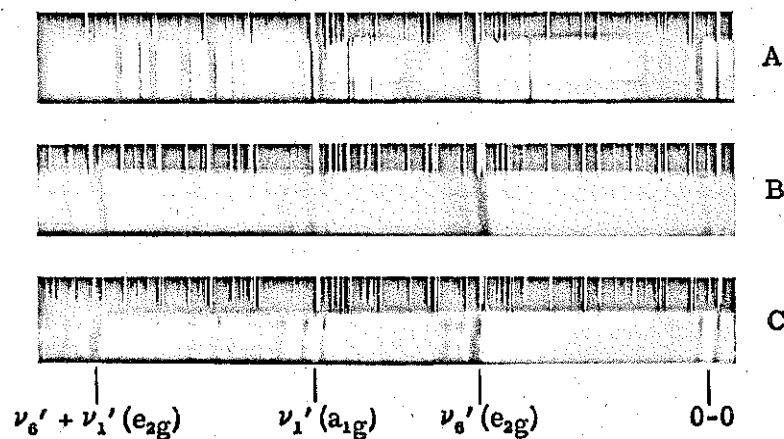


FIG. 1. Absorption spectra of unstrained (A) and two different strained (B and C) crystals of C_6H_6 . The high-energy member of the 0-0 doublet in the strained crystals represents the unresolved b and c polarized absorptions.

not to the effect of crystal thickness on the energy of the exciton components¹ is evidenced by the fact that the strains give shifts either to higher or to lower energy for crystals of comparable thickness. Compare Crystal B with C. In addition, a portion of the thin crystals B and C absorb at the same energy as the thicker sample. As one might expect, the effect of strain on the 0-0 progression is not always of the same magnitude as that on the 0-0+ ν_6' series. See Crystal B. The large increase in the doublet splitting of the 0-0+ ν_6' transition observed by Broude *et al.*¹⁻³ was not seen in our thin crystal. We would have been able to detect the splitting if it had been greater than 15 cm⁻¹. The probable reason for the differences between our observations and those of Broude *et al.* is that their crystals were apparently thinner and more strained than ours.

These same effects, but of smaller magnitude, have also been observed for thicker ($\sim 30\text{-}\mu$) crystals constrained between quartz windows and cooled rapidly.

From these results it can be concluded that the measurement of absorption line shapes and line positions in organic crystal spectroscopy require near-perfect crystals. Intrinsic linewidths are of interest, say, in the study of relaxation phenomena. One may also conclude that observation of "true" exciton emission from pure crystals at low temperatures is difficult at best. Unless the crystal is essentially strain free the highly mobile exciton will migrate to crystal regions where the strains have produced a red shift, relax into these "traps," and subsequently emit from these sites. This is likely to be particularly troublesome in crystals such as anthracene where, because of the large oscillator

strength, most of the absorption is near the crystal surface where strains are more apt to occur.

The shifts and changes in the exciton splittings are most likely caused by anisotropic changes in the intermolecular distances and resultant changes in van der Waals and resonance interactions.⁴ As one of the $k=0$ exciton components of the 0-0 band cannot be observed because of selection rules, the magnitude of the changes in van der Waals and resonance interactions are not separable. Even an isotropic stress applied to the crystal would not result in an isotropic change in the unit cell dimensions, as the compressibilities along the various axes are not the same.⁶ It seems that experiments where the stresses were applied along crystallographic axes in a more controlled manner could be very helpful in assigning the absorptions seen in the pure crystal spectra. This would be much like studying the polarization of the absorption but would perhaps be more sensitive and give additional information.

The author is grateful to Professor G. W. Robinson for his support and helpful discussions.

⁴ Financed in part by the National Science Foundation.

[†] Contribution No. 3403.

¹ V. I. Broude, M. M. Pakhomova, and M. M. Prikhod'ko, *Opt. Spectry*, **2**, 323 (1957).

² V. I. Broude and M. I. Onoprienko, *Opt. Spectry*, **8**, 332 (1960).

³ V. I. Broude, *Soviet Phys.—Usp.*, **4**, 584 (1962) [*Usp. Fiz. Nauk* **74**, 577 (1961)].

⁴ E. R. Bernstein, S. D. Colson, R. Kopelman, and G. W. Robinson (to be published).

⁵ G. C. Nieman and G. W. Robinson, *J. Chem. Phys.*, **39**, 1298 (1963).

⁶ E. G. Cox, D. W. J. Cruickshank, and J. A. S. Smith, *Proc. Roy. Soc. (London)* **A247**, 1 (1958).

Direct Observation of the Entire Exciton Band of the First Excited
Singlet States of Crystalline Benzene and Naphthalene*

S. D. COLSON,** D. M. HANSON, R. KOPELMAN[†] AND
G. W. ROBINSON

Gates and Crellin Laboratories of Chemistry,[‡] California Institute of
Technology, Pasadena, California 91109

ABSTRACT

The density-of-states functions for the exciton bands of the first excited singlet states of crystalline benzene and naphthalene have been determined experimentally. The experimental density functions were derived from spectral data involving exciton band \rightarrow exciton band transitions. The experimental results for naphthalene have been compared with calculations based on the octopole model. Using a Frenkel dispersion relation and various sets of coupling constants, density functions have been calculated and compared with the experimental results. For benzene these calculations show that the "optically forbidden" A_u component lies between 37,815 and 37,875 cm^{-1} . From the temperature dependence of transitions, phonon contributions have been estimated. It is found that the experimentally derived density function is temperature independent below $\sim 30^\circ\text{K}$.

* Supported in part by the National Science Foundation.

** Present address: Division of Pure Physics, National Research Council, Ottawa 7, Ontario, Canada.

[†] Present address: Department of Chemistry, University of Michigan, Ann Arbor, Michigan 48104.

[‡] Contribution No. 3567.

I. INTRODUCTION

The stationary states of condensed systems such as crystals are characterized as energy bands. The individual states within these bands for periodic systems are designated by \underline{k} , the reduced wave number vector.¹ The standard spectroscopic data concerning the low energy electronic states of molecular crystals consists of a few lines (Davydov components) corresponding to some or all of the $\underline{k} = 0$ levels. Only these levels are observed in transitions from the crystal ground state ($\underline{k} = 0$) because of the selection rule² $\Delta\underline{k} = 0$. In certain cases even some $\underline{k} = 0$ levels cannot be observed because of additional selection rules, e.g., the restrictions of factor group symmetry in the benzene crystal.

Within the framework of the Frenkel approach, the physical quantities that determine the band structure are the intermolecular resonance interactions. If all of the Davydov components are spectroscopically allowed, one can directly determine the magnitudes and relative signs of the interactions between interchange equivalent molecules. From this data alone nothing can be said about the interactions between translationally equivalent molecules. The latter may, in principle, be the dominant interactions responsible for the band structure.

An indication of the magnitude of the translationally equivalent interactions has been obtained recently from isotopic mixed crystal experiments.^{3,4} A more direct approach is given in the present work and utilizes exciton band \leftrightarrow exciton band spectroscopic transitions.

This technique allows all \underline{k} states to be observed since the initial state is no longer restricted to $\underline{k} = 0$. This method was first proposed by Rashba;⁵ however, its practical and detailed utilization depends upon the special Frenkel exciton selection rules⁶ and the use of extremely pure and high quality crystals.⁷ We are thus able to find the density of states in the electronic exciton band as well as the total band width which depends upon all of the intermolecular interactions in the crystal.

Even though the complete exciton band structure in molecular crystals has been the object of several calculations,^{3,8} it has not yet been presented experimentally and discussed in terms of these theoretical models. It is of interest to compare experiment and theory, especially concerning the applicability of multipole expansions and the assumption of pairwise interactions, the location of ion-pair states,⁹ and the quality of the available atomic and molecular eigenfunctions^{3,9} as well as the fundamental concepts of an elementary excitation in a static lattice.

II. GENERAL DISCUSSION

Exciton band \leftrightarrow exciton band transitions involving the first excited singlet states of crystalline benzene and naphthalene are observed in both absorption and emission. The benzene and naphthalene crystals are good candidates for such an investigation for several reasons.

(1) These systems are of general interest since the electronic and vibrational states have been extensively studied both experimentally and theoretically in the molecule as well as in the crystal.

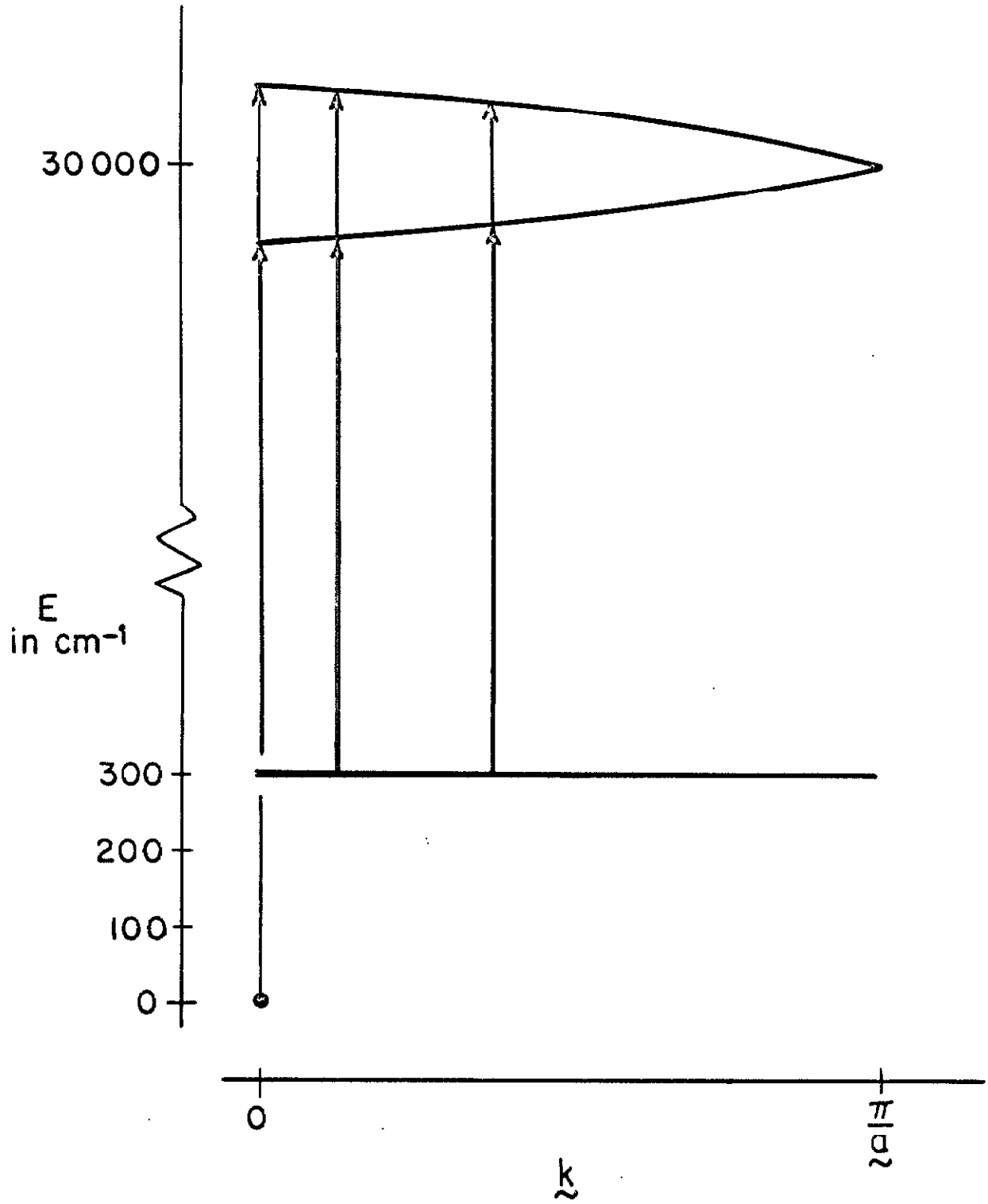
(2) Naphthalene is a case where the extremes of the electronic exciton band are approximately known, while benzene is an intriguing case where the extent of the exciton band is unknown. The predicted locations of the forbidden Davydov component have ranged from the bottom to the top of the band.^{3, 10, 11}

(3) They are some of the few compounds which have been purified to the degree necessary for such experiments.

The transitions shown schematically in Fig. 1 are exciton band--exciton band transitions. In absorption, this method relies upon the thermal population of all the \underline{k} levels of the ground state vibrational exciton band. The absorption process, then, involves all these levels as initial states and all the \underline{k} levels of the electronic exciton band as final states. In emission, the initial states are the thermally populated¹² \underline{k} states of the electronic exciton band while the \underline{k} states of the vibrational exciton band serve as the final states. The intensity distributions in both the absorption and emission bands are proportional to the density of \underline{k} levels in the electronic exciton band provided (1) the width of the vibrational exciton band is negligible, (2) an equilibrium population of the levels in the electronic exciton band is attained, (3) intensity contributions from phonon transitions are negligible, (4) the transition probability is \underline{k} independent and the $\Delta\underline{k} = 0$ selection rule is valid, (5) the differences in branch to branch¹³ transition probability does not alter this intensity distribution.

The width of vibrational exciton bands in molecular crystals is known¹⁴ to be approximately $1-10 \text{ cm}^{-1}$. The vibrational exciton band of benzene which is utilized in the present experiment is the $\nu_6''(e_{2g})$ which is known to have an exciton splitting¹⁵ of $\sim 5 \text{ cm}^{-1}$. This finite

Fig. 1. Schematic diagram of band structure of a linear crystal comparing an exciton band \leftarrow exciton band transition with the 0, 0 transition.



width may introduce an uncertainty in the energy of the density function $\rho(E)$ of a few wavenumbers. However, the maximum of the density function determined from ν_6'' coincides with that determined from $\nu_1''(a_{1g})$ for which no exciton splitting has been observed.¹⁵ The band \leftrightarrow band transition involving ν_1'' is not intense enough to accurately give the entire density function. For naphthalene, the vibrational exciton bands at 510 and 514 cm^{-1} are used. The total width of these two bands¹⁶ is less than 6 cm^{-1} , which is small compared to the 160 cm^{-1} exciton splitting in the electronic state. In the absorption experiment, the finite width of the vibrational exciton band also results in a Boltzmann population distribution of the \underline{k} levels in the initial state; however, for a 600 cm^{-1} vibration at liquid nitrogen temperature, the population ratio between the highest and the lowest energy \underline{k} state will cause a $\leq 10\%$ deviation in the absorption band intensity distribution from the hypothetical case reflecting only the density of \underline{k} states in the electronic exciton band.

Boltzmann statistics describe the population of energy levels in a dilute system provided there is sufficient time for equilibrium to be attained. The fact that relaxation within the manifold of \underline{k} levels is fast relative to the fluorescence lifetime is shown by the temperature dependence of the fluorescence lineshapes (vida infra).

Optical transitions involving lattice vibrations or phonons are expected to contribute to the shape and width of the observed band \leftrightarrow band transitions. The magnitude of this contribution can be estimated from the temperature dependence of the fluorescence spectra and the comparison of it with the absorption spectra (vida infra). It should be

emphasized that we use the term phonons synonymously with lattice vibrations as distinguished from the internal vibrations of the molecule.

The electric dipole transition moments involved in a band \leftrightarrow band transition have been shown⁶ to be independent of \underline{k} , the reduced wave number vector, provided certain long-range interactions can be neglected. Within the use of this approximate Hamiltonian, it has also been shown that the $\Delta\underline{k} = 0$ selection rule as well as the factor group selection rules⁶ are valid for all \underline{k} . The validity (within the above approximation) of the $\underline{g} \leftrightarrow \underline{u}$ selection rule in centrosymmetric crystals for all \underline{k} is of special interest. For, if a breakdown of this selection rule is observed, one knows that the above approximation is not valid and thus the interpretation of the intensity distribution in the band \leftrightarrow band transition is no longer straightforward. Unfortunately, the converse is not necessarily true.

Since the factor group selection rules are valid for all \underline{k} , it can easily be shown, assuming an oriented site¹⁷ model, that the transition probability from any single branch to all bands is a constant. For benzene the factor group selection rules show that only the following transitions are allowed: $A \leftrightarrow B_1$, $A \leftrightarrow B_2$, $A \leftrightarrow B_3$, $B_1 \leftrightarrow B_2$, $B_1 \leftrightarrow B_3$, $B_2 \leftrightarrow B_3$. Thus in a band to band transition there are three distinct transitions originating from each branch. For the case where all branches of the vibrational band are degenerate, three of the allowed transitions occur at the same energy. The sum of the intensity of these three is independent of the symmetry classification of the initial branch. Thus, the intensity distribution of the band to

band transition gives the density of states in the electronic exciton band within the other limitations cited above.

It is of interest now to consider how this density of states is determined by the intermolecular interactions in the crystal. This derivation is straightforward within the formalism of first order perturbation theory using one site basis functions. This first order theory has formed the basis for the development and application of the Frenkel approach by Davydov and others.¹⁹ Although a higher order formalism has been suggested,⁹ there exists no experimental evidence which demonstrates the failure of this first order approach. On the other hand, the higher order formalism as presently applied to naphthalene disagrees with several experimental observations.^{4, 20} As Craig and Philpott,^{8b} and Sarti-Fantoni²⁰ have pointed out, it is unfortunate that the complete band structure has not been calculated from this approach. It would be of interest to compare those results with that of the octopole model and with the present experimental results. However, it should be pointed out that when higher order terms are considered the transition probability may be \underline{k} dependent. This possibility must be considered before comparison with the present experiments can be made. Because of its simplicity, historical development, and apparent accuracy, we treat the exciton band structure for the ${}^1B_{2u}$ states of benzene and naphthalene within the framework of the simple first order theory.

The density function, $\rho(E)$, which gives the number of exciton or \underline{k} states per unit of energy can be determined from the dispersion relation. In the restricted Frenkel limit,⁶ the dispersion relation, $E(\underline{k})$, which gives the energy of the state with wave number vector \underline{k} , has an especially simple form.

$$E^{f\alpha}(\underline{k}) = \sum_{q=1}^m a_q^\alpha L_{Iq}^f(\underline{k}) \quad (1)$$

The zero of energy for this equation is the algebraic mean of the exciton band in a hypothetical crystal in which all resonance interactions are zero.²²

Here, m is the number of molecules per unit cell, a_q^α are the coefficients corresponding to the α^{th} representation of the interchange group,²³ and the $L_{Iq}^f(\underline{k})$ are the \underline{k} dependent sums of excitation exchange matrix elements for the f excited state as defined by Ref. 21.

$$L_{Iq}^f(\underline{k}) = \sum_{n'=1}^{n/m} \exp i\underline{k} \cdot (\underline{\tau}_{q'} - \underline{\tau}_q) \cdot \exp i\underline{k} \cdot (\underline{r}_{n'} - \underline{r}_n) \times \int \phi_{nq}^{f*} H' \phi_{n'q'}^f dR \cdot (1 - \delta_{nn'}) \quad (2)$$

where \underline{r}_n defines the origin of the n^{th} unit cell, $\underline{\tau}_q$ is a vector from that origin to the q^{th} molecule in that unit cell, and ϕ_{nq}^f is the localized excitation function²⁴ representing the nq^{th} molecule in its f excited state.

The density of states is obtained then by computing $E(\underline{k})$ and tabulating the number of states per energy interval. Such a computation requires evaluation of the excitation exchange integrals (\mathcal{M}_{ij}) . These can be evaluated from theoretical or semi-empirical models and

compared with experiments. The Davydov splittings place restrictions on the possible values of the interchange equivalent interactions since these splittings depend upon sums of the \mathcal{M}_{ij} over the entire lattice.²¹ It should be noted that we reserve the term Davydov splitting for the exciton splitting at $\underline{k} = 0$. Data from the spectra of isotopic mixed crystals provide similar information about the sums of translationally equivalent interactions.^{3,4} In contrast, the density function depends upon \underline{k} dependent sums of all these interactions and thus provides an independent measure of the intermolecular resonance interactions.

For weak transitions such as the lowest singlet states of benzene and naphthalene, the lattice sums are expected to converge rapidly. Then, by considering only interactions with the nearest translationally and interchange equivalent molecules, it can easily be shown that for benzene

$$\begin{aligned}
 E^{f\alpha}(\underline{k}) = & 2 m_a \cos(k_a a) + 2 m_b \cos(k_b b) + 2 m_c \cos(k_c c) \\
 & + 4 a_{II}^{\alpha} m_{III} \cos\left(k_a \frac{a}{2}\right) \cos\left(k_b \frac{b}{2}\right) \\
 & + 4 a_{III}^{\alpha} m_{I III} \cos\left(k_b \frac{b}{2}\right) \cos\left(k_c \frac{c}{2}\right) \\
 & + 4 a_{IV}^{\alpha} m_{I IV} \cos\left(k_a \frac{a}{2}\right) \cos\left(k_c \frac{c}{2}\right)
 \end{aligned} \tag{3}$$

where $\mathcal{M}_{Iq} = \int \phi_I^{f*} |H'| \phi_q^f dR$ ($\mathcal{M}_{a, b, c}$ represent the interaction of molecule I with its translationally equivalent neighbors along the a, b, and c axes, respectively) and where

$$\begin{aligned}
 \underline{k} &= \underline{k}_a + \underline{k}_b + \underline{k}_c \\
 \underline{k}_a &= \frac{\pi}{a} \frac{n_a}{N_a}, \quad -N_a < n_a \leq N_a
 \end{aligned}$$

etc.

The number of values of \underline{k}_a is equal to the number of molecules ($2N$) along the \underline{a} crystal axis.

Naphthalene is an example of a crystal with two molecules per unit cell. The dispersion relation for such crystals has been considered in detail by Davydov²⁵ and Knox.²⁶ Assuming only certain near neighbor interactions contribute, the following dispersion relation is obtained for the two branches of the lowest singlet exciton band of naphthalene.

$$\begin{aligned}
 E^{\pm}(\underline{k}) &= 2\mathcal{M}_a \cos(k_a a) + 2\mathcal{M}_b \cos(k_b b) + 2\mathcal{M}_c \cos(k_c c) \\
 &\pm 4\mathcal{M}_{I\Pi} \cos(k_a \frac{a}{2}) \cos(k_b \frac{b}{2}) \\
 &\pm 4\mathcal{M}_{I\Pi'} \cos(k_c c) \cos(k_a \frac{a}{2}) \cos(k_b \frac{b}{2}) \\
 &\mp 4\mathcal{M}_{I\Pi'} \sin(k_c c) \sin(k_a \frac{a}{2}) \cos(k_b \frac{b}{2})
 \end{aligned} \tag{4}$$

III. EXPERIMENTAL TECHNIQUES

As already mentioned, these experiments were made possible by the recent advancements in purification techniques for benzene and naphthalene.^{27, 28} Purified crystals 1 to 5 cm long were grown from the melt by slowly lowering the cells through a sharp temperature gradient directly into a liquid nitrogen cooled chamber. Using this technique, one obtains crystals with few or no cracks at 77°K which could be cooled to 4.2°K with little or no additional cracking. As the resultant crystal is in an evacuated container, several hours

are required from the time the container is immersed in liquid He until the crystal cools from 77°K to 4.2°K. The hot band absorption was monitored during this period, and while no marked change in the structure of the absorption was observed upon cooling, its intensity gradually decreased until no residual absorption could be detected at liquid helium temperature. The 0,0 absorptions in thin crystal were also observed at 77°K, 27°K (benzene only), and 4°K. The spectra were taken utilizing a 150 W Xe arc lamp and the 3rd order of a 600 lines/mm Bausch and Lomb grating in a 2 m Czerny-Turner mount. Tracings of the photographic plates were taken on a Joyce and Loebel model E12 MK III microdensitometer and a Jarrell-Ash model 23-500 microphotometer.

The fluorescence spectra of benzene and naphthalene were observed at 77°K, 27°K (benzene only), and 4.2°K on the two meter instrument. The intensity distribution of the 0,0 - ν_6'' fluorescence band in benzene and the 0,0 - "512" fluorescence band in naphthalene was determined at 77°K and 20.4°K using 3rd order of a 600 lines/mm grating in a 1.83 M Jarrell-Ash Ebert spectrometer. Both the photoelectric and photographic line positions were determined by reference to an iron-neon standard.

The thin crystals (20 μ to 2 mm) used for the 0,0 absorption and all fluorescence studies were grown in a manner similar to that used for the band - band absorption spectra. The respective temperatures were maintained by immersing the sample in boiling N₂, Ne, H₂, or He. It was necessary to open the crystal cell, exposing the

crystal to the cryogenic liquid, to prevent the excitation source from heating the sample.

IV. EXPERIMENTAL RESULTS

The experimental results are given in Figs. 2 through 5, 9, 10, and 12. Figure 2 shows the microdensitometer tracings of the fluorescent band→ band transition at temperatures of 77 to 4°K in benzene. Also included in Fig. 2 is the corresponding transition of a benzene guest in a deuterobenzene host. This isotopic mixed crystal technique demonstrates the sharpness of these transitions when they are not associated with exciton bands. The J-A 1.83 M spectrometer tracings are shown in Figs. 3, 4, and 5. Figure 4 includes the neat crystal and the isotopic mixed crystal transition for naphthalene at 4.2°K taken with a 300 lines/mm grating in 18th order. The two accidentally degenerate vibrations are nearly resolved. These are easily resolved in mixed crystal phosphorescence.

The density functions for both benzene and naphthalene were derived from the fluorescence lines by assuming the lowest energy level in the electronic exciton bands is coincident with the lowest Davydov component. This assumption is believed to be valid since the 0,0 transition is observed in fluorescence at 1.8°K, and since fluorescence lines involving vibrational exciton bands are shifted only by the value of the vibrational quantum. For example, in benzene the $0' - \nu_6''$ transition does not extend to the red of $31,003 - 606 \text{ cm}^{-1}$ where $38,003 \text{ cm}^{-1}$ is the location of the lowest Davydov component

Fig. 2. Microdensitometer tracings of the $0,0 - \nu_6''$ fluorescence band - band transition of crystalline benzene at 77, 27, and 4.2°K, illustrating the temperature dependence of the linewidth and shape. Also included is the corresponding transition for ~1% C_6H_6 in C_6D_6 showing the 3.1 cm^{-1} splitting of the ground state $e_{2g}(\nu_6)$ vibration. The mixed crystal transition has been shifted to account for the difference in the neat and mixed crystal origins.

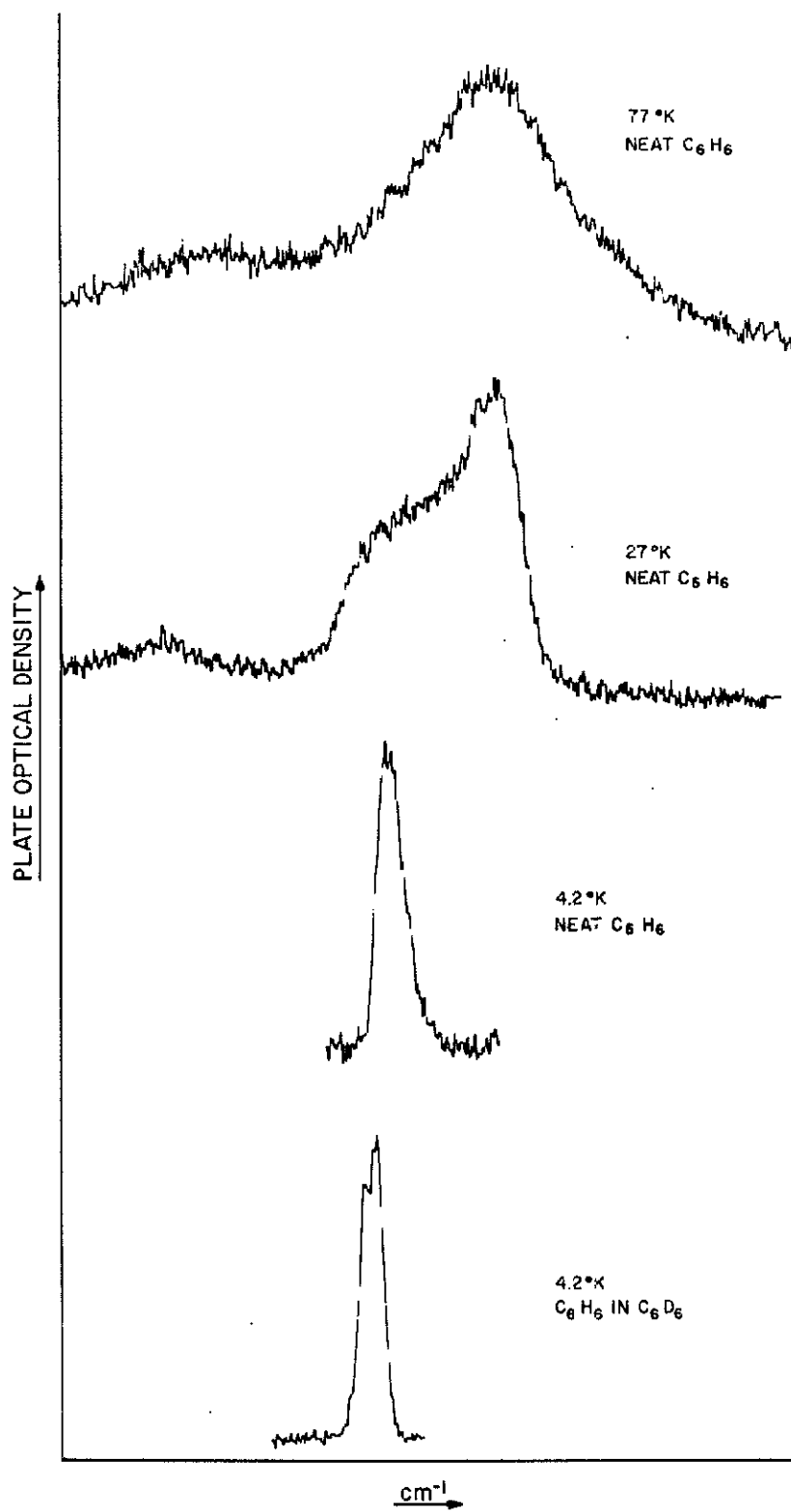


Fig. 3. The $0,0 - \nu_6''$ transition of crystalline benzene observed with the 1.83 M J-A spectrometer at 77 and 20.4°K. The solid curves represent the average of the noise as determined by repeating the spectrum several times.

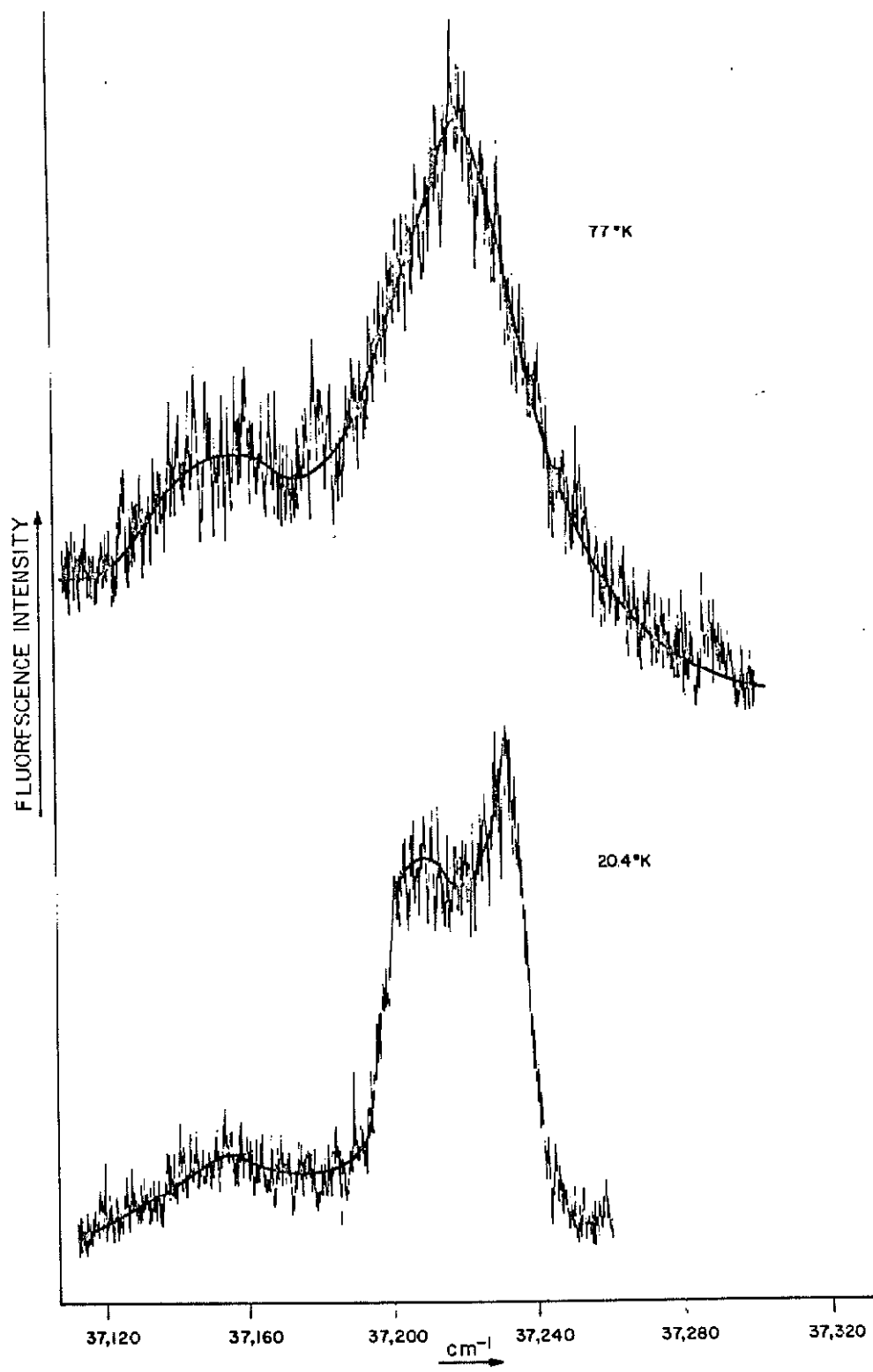


Fig. 4. The 0,0 - "512" transition of crystalline naphthalene observed with the 1.83 M J-A spectrometer. The band at 20°K was graphed from Fig. 5 in order to correct for the different recorder speed. The neat and mixed (1% C₁₀H₈ in 99% C₁₀D₈) crystal transitions at 4.2°K were observed using the higher resolution grating in 18th order. A comparison of these transitions illustrates the participation of $\underline{k} \neq 0$ levels, even at 4.2°K.

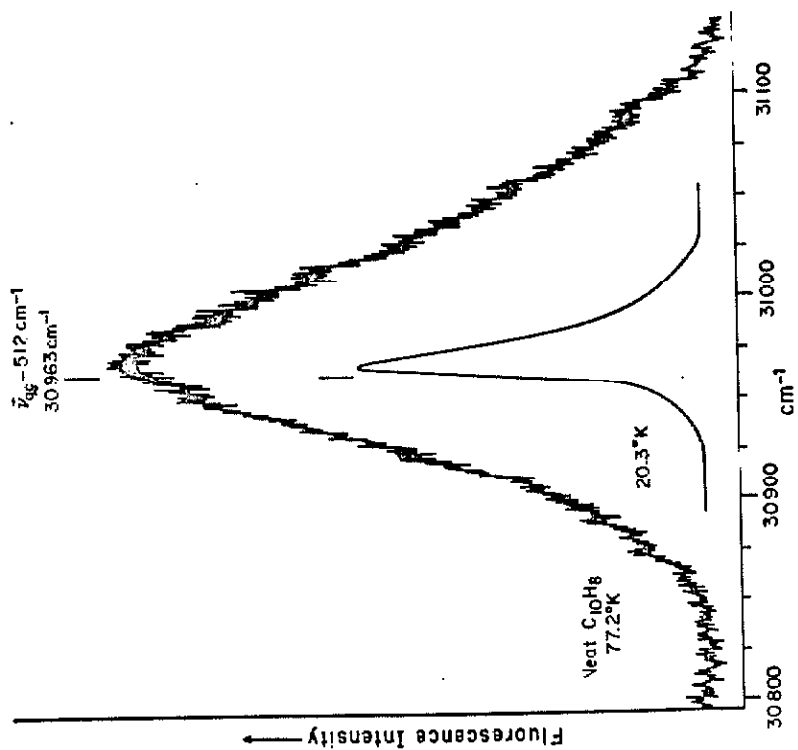
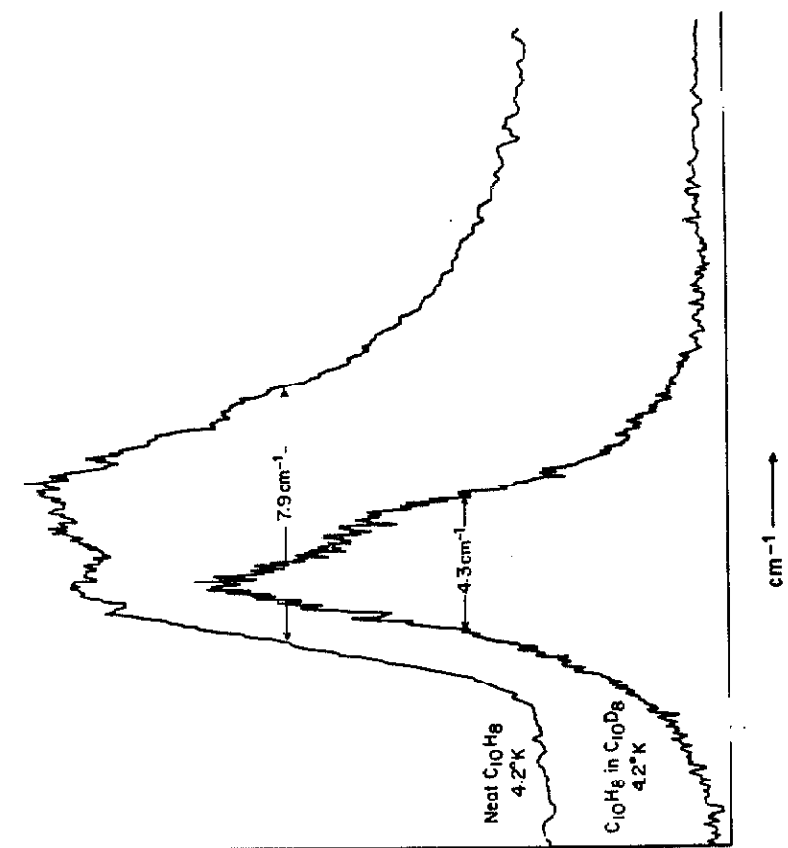
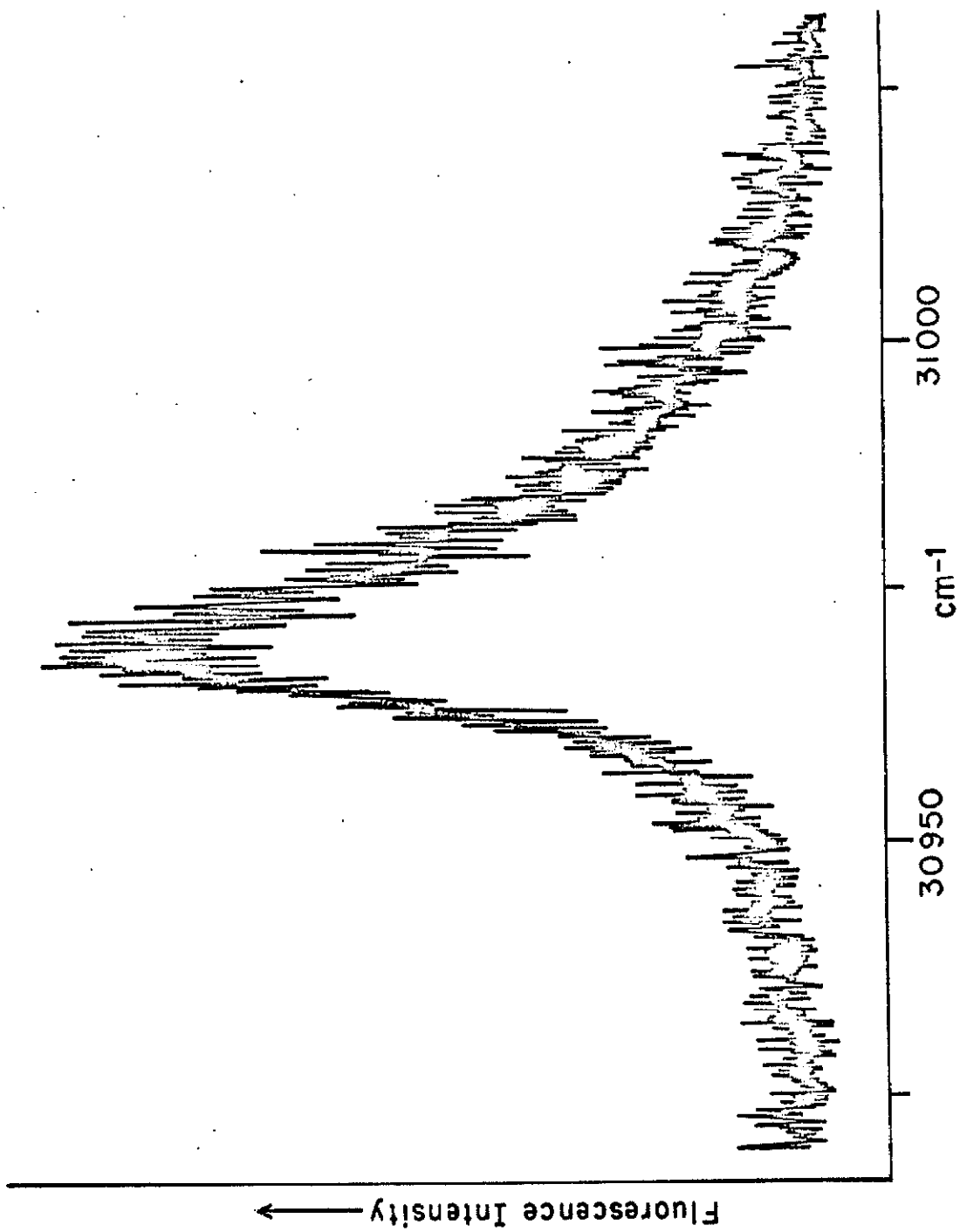


Fig. 5. The 0,0 - "512" transition in neat crystalline naphthalene at 20.4 °K.



above the ground state. If the exciton band extended far below this Davydov component, the transition would be red shifted by more than 606 cm^{-1} . Additional evidence has been presented for the case of naphthalene by experiments with isotopic mixed crystals.²⁹ Within this assumption and the assumption of Boltzmann equilibrium within the band, the density function can be calculated from the fluorescence lineshape by multiplying the intensity at a given energy by the appropriate Boltzmann factor. The plate optical density was converted to intensity before making the calculation for the 27°K benzene fluorescence. These density functions are shown in Figs. 6, 7, and 8 for benzene and naphthalene.

Microdensitometer tracings of the absorption band-band transitions in benzene and naphthalene are shown in Figs. 9 and 10. In Figs. 7 and 11, the plate optical density has been converted to sample optical density for each case. The sample optical density is linearly proportional to the density function, $\rho(E)$.

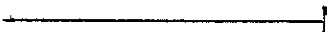
The contribution of lattice vibrations or phonons to the experimentally derived density functions can be evaluated from the temperature dependence of these density functions, from the temperature dependence of the 0,0 absorptions in thin crystals, and from a comparison of density functions derived from absorption and emission data at the same temperature. The 0,0 absorptions which are shown in Figs. 10 and 12. Phonons are expected to contribute to these experimental results in two ways. Transitions 

Fig. 6. Density of states function of the lowest singlet exciton band of crystalline benzene as determined from the 20.4 °K (\blacksquare) and 27 °K (\circ) fluorescence shown in Figs. 2 and 3. The observed Davydov components are indicated symbolically and designated by their polarizations.

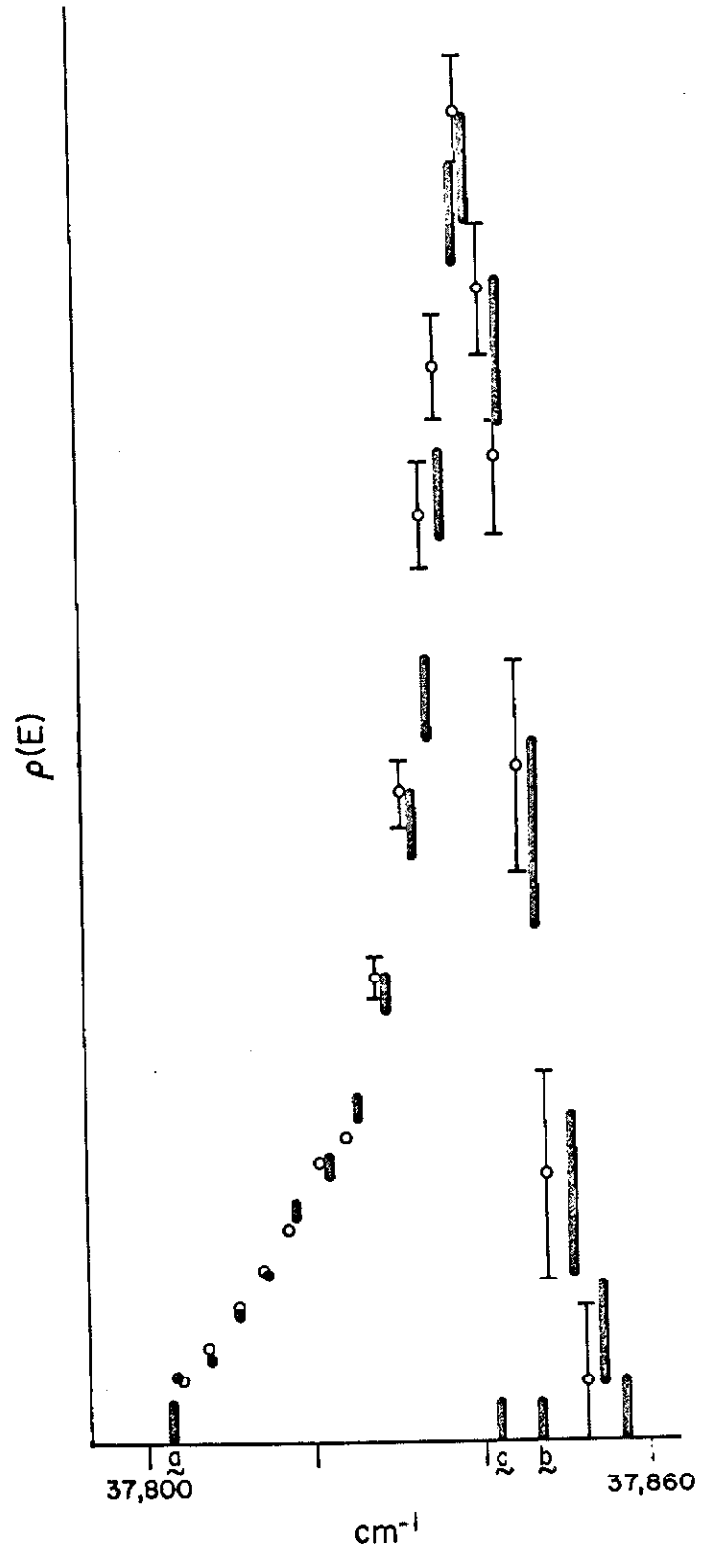




Fig. 7. Density of states function of the ${}^1B_{2u}$ benzene exciton band as determined from the 77 °K fluorescence () and the $\sim 60^\circ\text{K}$ absorption () band \leftrightarrow band transitions. The \underline{a} polarized Davydov component is taken as the bottom of the band and, thus, the fluorescence intensity to lower energy is attributed to phonons and is shown as a dashed line. The different rules of the addition phonons in absorption and emission can be clearly seen in the wings of the respective functions.

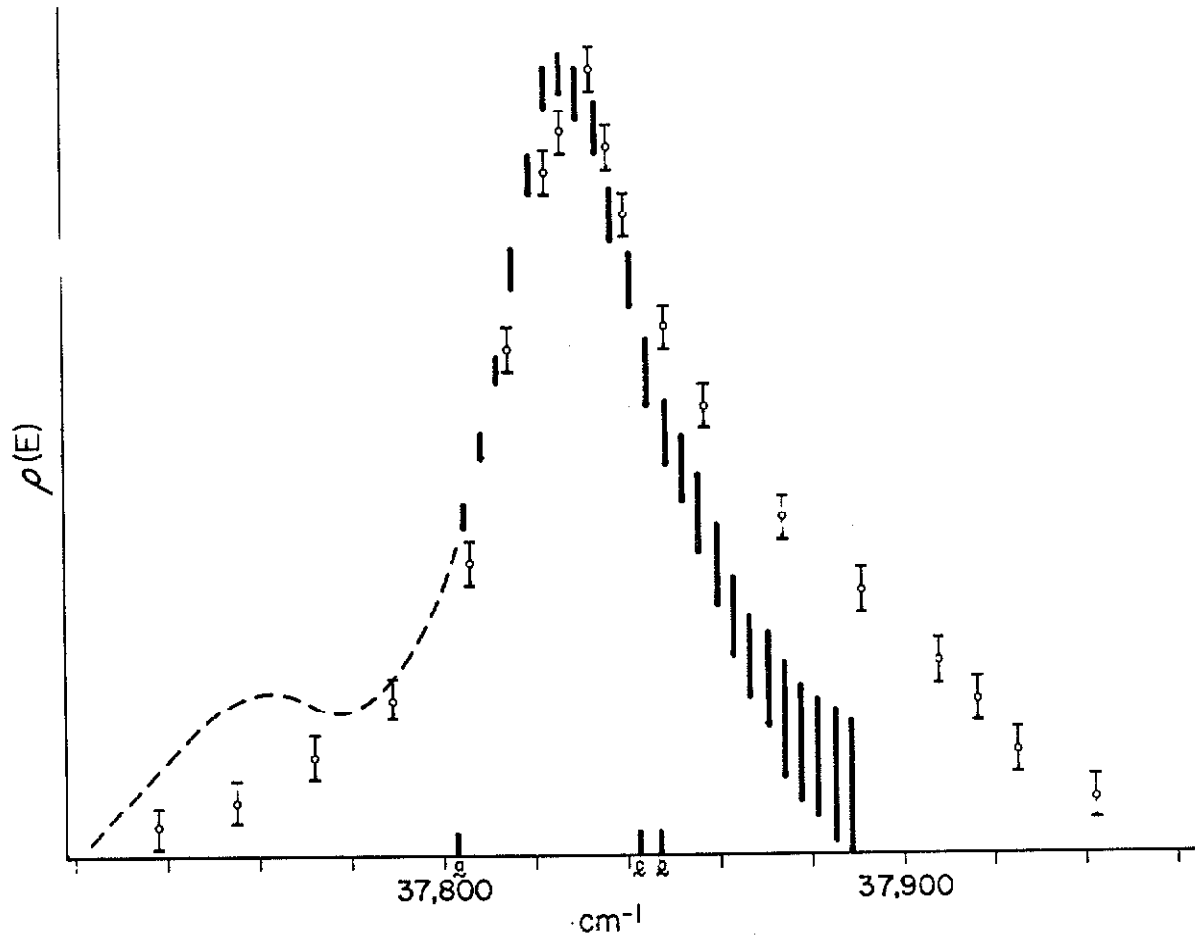


Fig. 8. Density-of-states function for the naphthalene exciton band derived from the 77 °K (\blacksquare) and 20 °K (\circ) fluorescence shown in Fig. 4. The Davydov components are indicated symbolically and designated by their polarizations. The \underline{ac} component is assumed to be at the bottom of the exciton band, and intensity at lower energy is attributed to phonons and shown with the dashed lines. The density function is obtained from the fluorescence intensity by multiplying by the appropriate Boltzmann factor. This multiplication also magnifies the experimental uncertainty in the fluorescence lines. The intensities below the \underline{ac} Davydov component are not corrected for a thermal distribution.

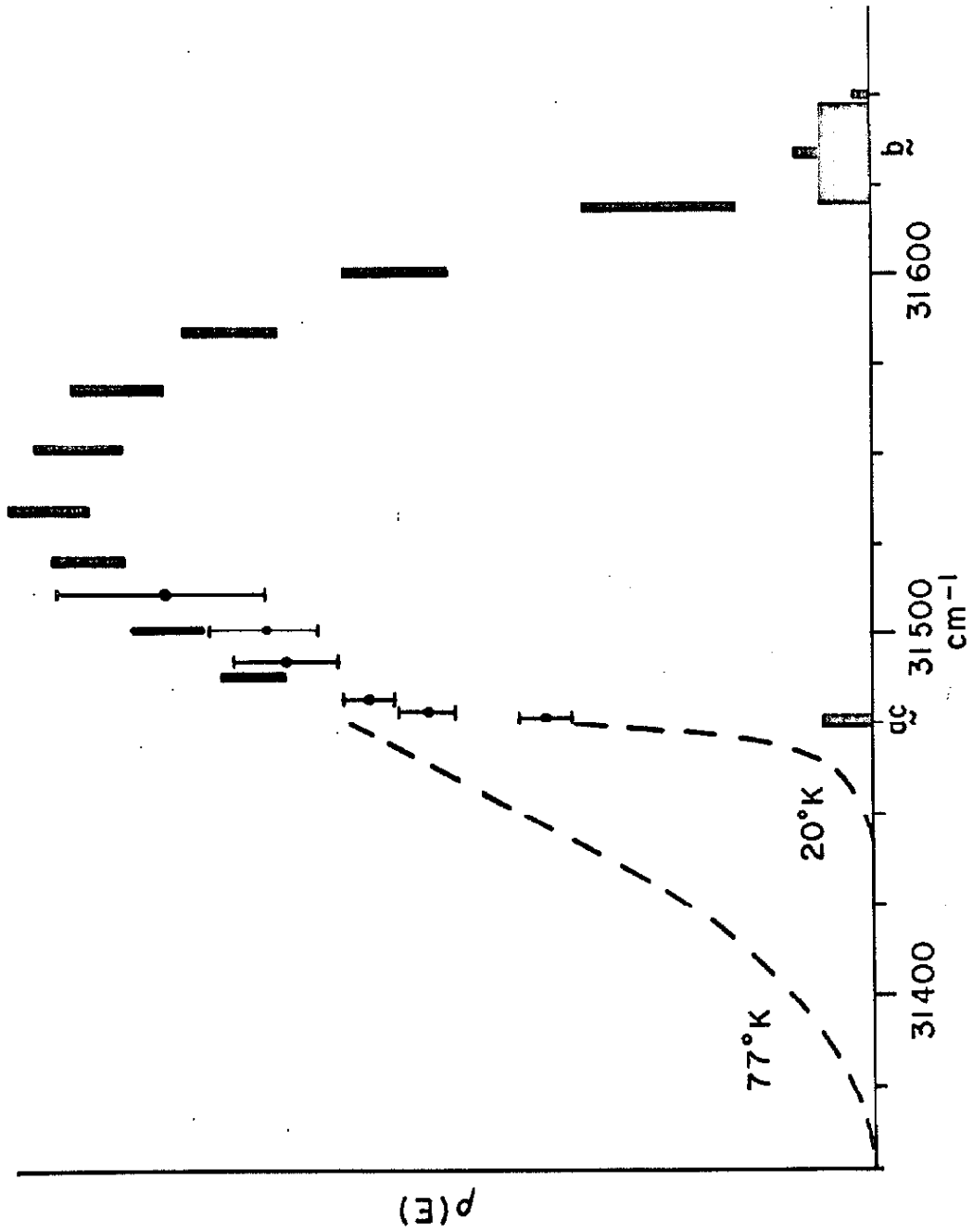


Fig. 9. Microdensitometer tracings of the absorptions to the pure electronic ${}^1B_{2u}$ state of crystalline benzene from the 606 cm^{-1} vibrational band at $\sim 60^\circ\text{K}$ (top) and the crystal ground state at 4.2°K (bottom).

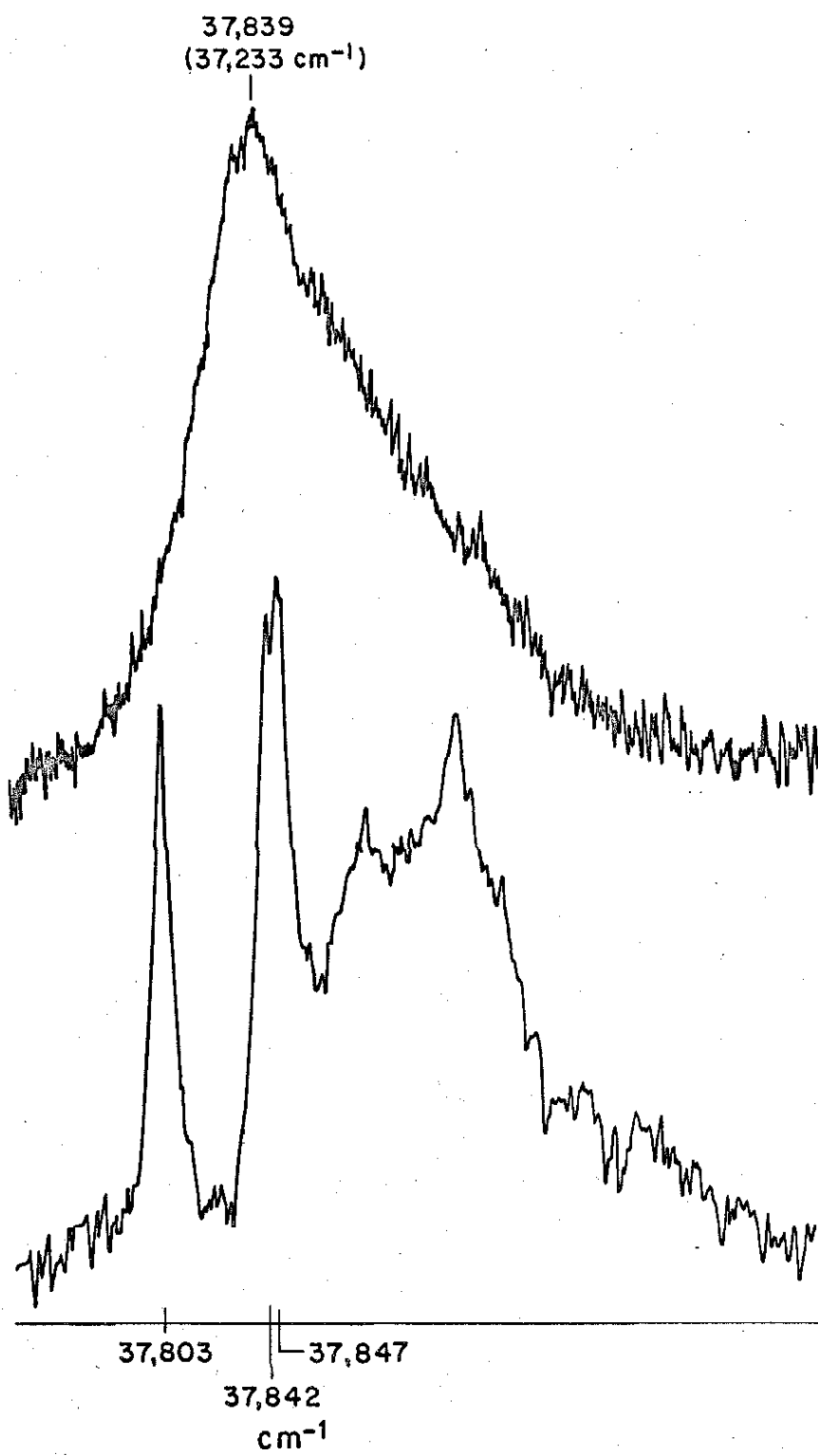


Fig. 10. Microdensitometer tracings of the 0,0 transition in crystalline naphthalene at (i) 4.2°K and (ii) 77°K. (iii) The exciton band ← exciton band transition (absorption) observed in a 1 cm crystal at 77°K. This tracing has been shifted to higher energy by the value of the vibrational quantum in order to compare it with the Davydov splitting.

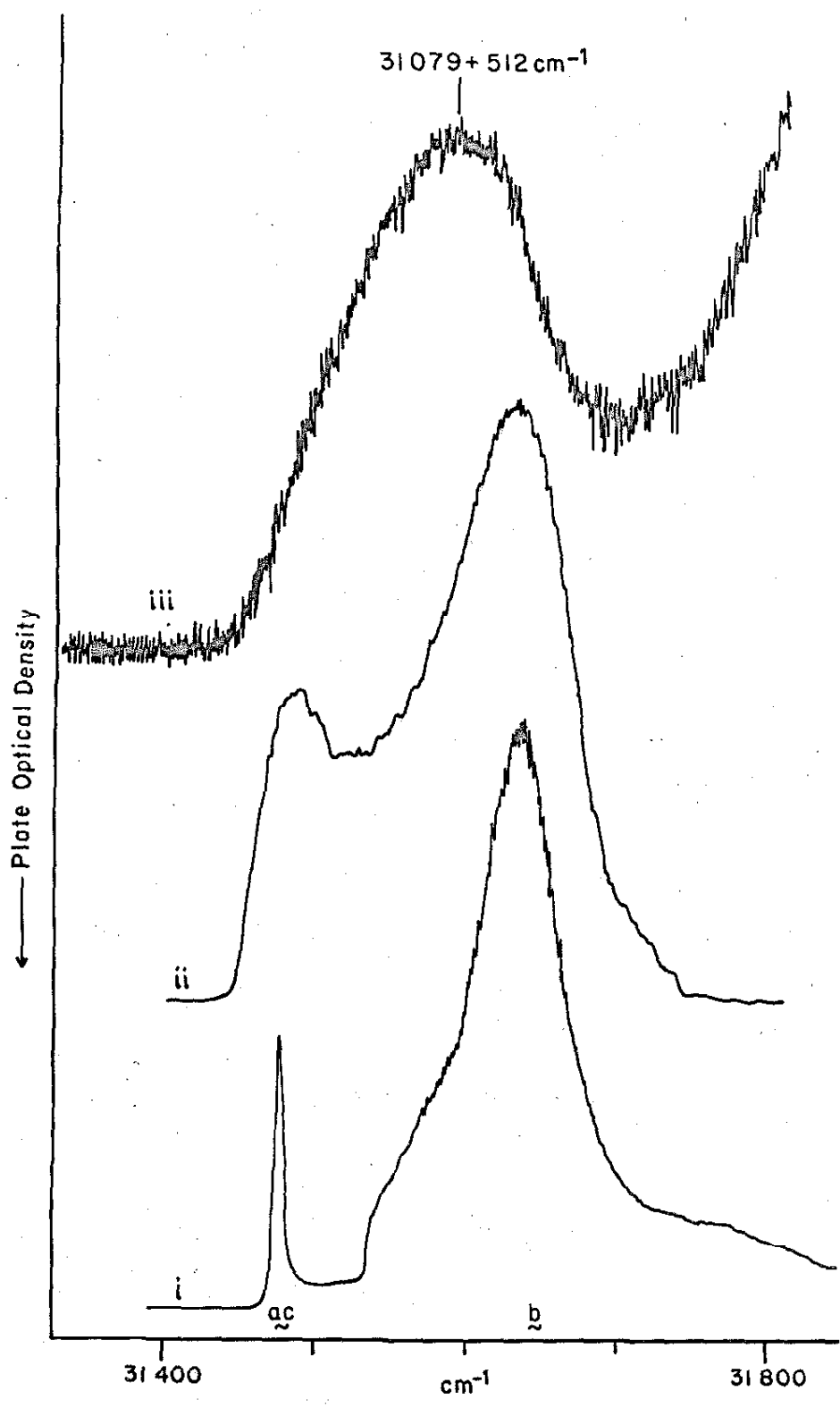


Fig. 11. Sample optical density for the band ← band transition which is shown in Fig. 10. A consideration of Lambert's law ————— } shows that the density function is linearly proportional to sample O. D. within the restrictions discussed in this paper. The background absorption on which the band ← band transition of interest is observed is accounted for as a change in I_0 . The difficulty in determining I_0 is represented by the shading of the curve.

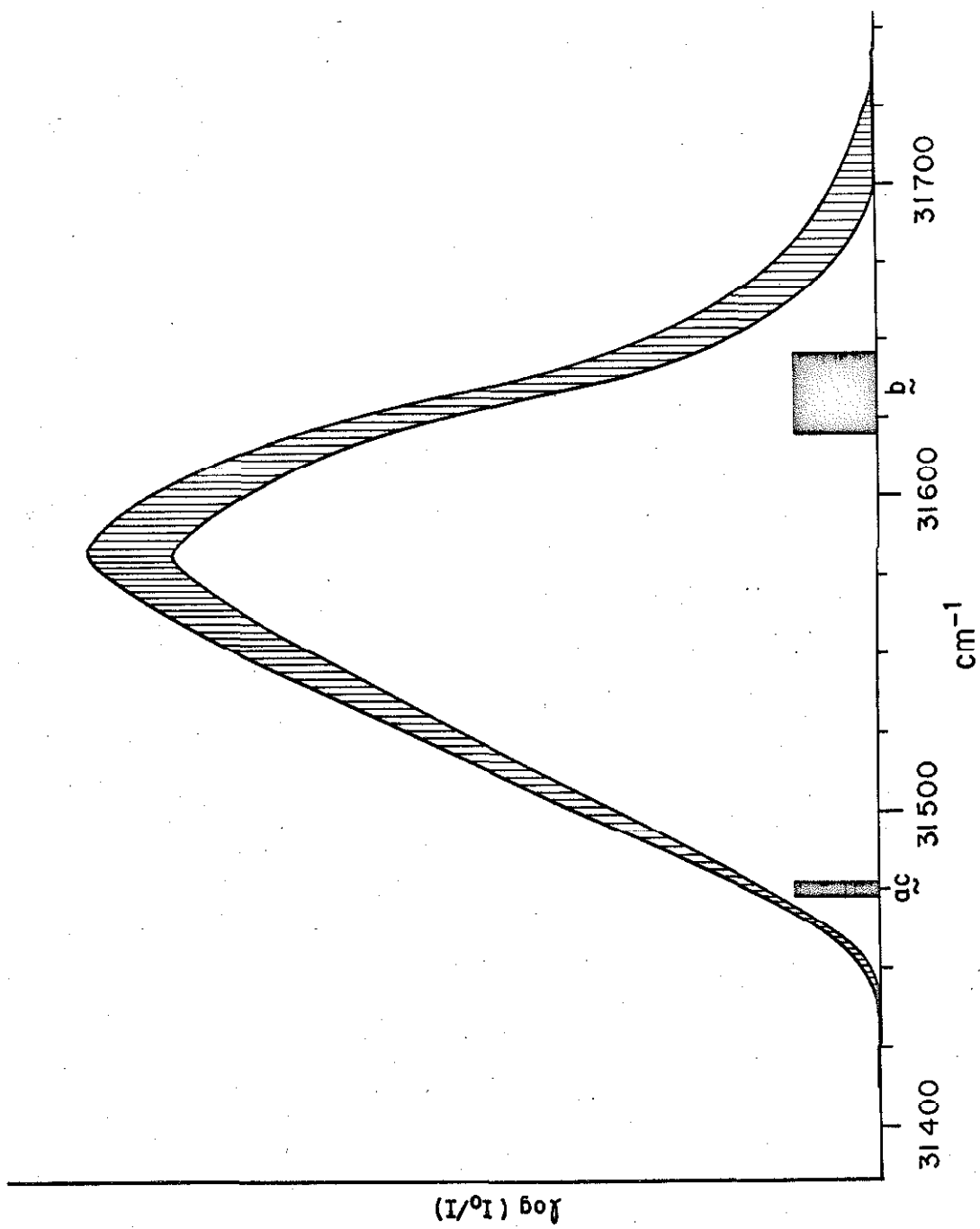
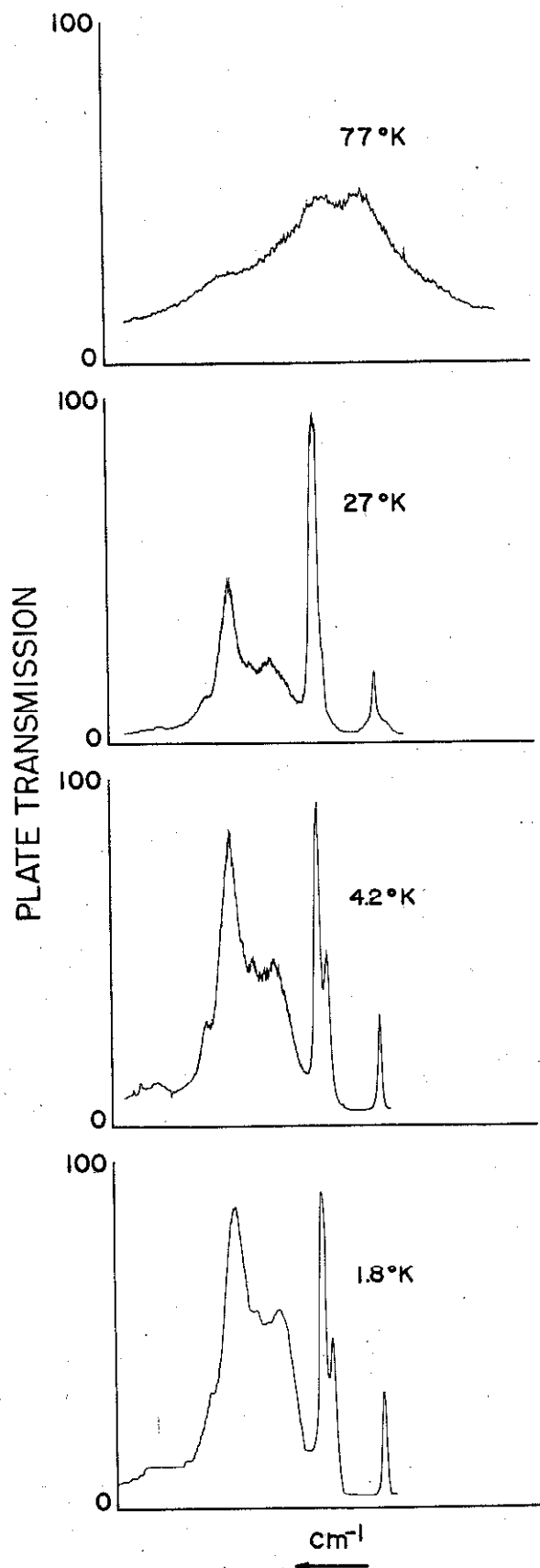


Fig. 12. Microphotometer tracing of the $0, 0 \ ^1B_{2u} \leftarrow \ ^1A_{1g}$ tracings of crystalline benzene at 77, 27, 4.2 and 1.8°K. The spectra were taken from different samples whose thicknesses ($\sim 20 \mu$) were not accurately determined. The middle Davydov component can be seen on the photographic plate as a shoulder on the highest energy one at 27°K.



involving phonons in either the initial or final states may contribute to the observed intensities and line shapes. The band structure itself may depend upon the motion of the molecules in the lattice.

A comparison of the benzene density functions at several temperatures (Figs. 6 and 7) shows that the temperature effect is not negligible. Relative to the density function at 20.4°K, the maximum of the density function at 77°K has shifted $\sim 12 \text{ cm}^{-1}$ to the red, its half-width has increased from 15 to 45 cm^{-1} and the wings are considerably extended. In contrast, the effect of changing the temperature from 20.4° to 27°K is within experimental error and thus may indicate that the effects of thermal phonons can be neglected at these low temperatures. This suggestion is supported by the temperature dependence of the 0,0 absorption spectra as shown in Fig. 12. There, it can be seen that the change in line width between 1.8° and 27°K is very small. The highest energy Davydov component broadens $\sim 4 \text{ cm}^{-1}$ nearly masking the middle component assigned to a shoulder which is clearly visible on the photographic plates but is poorly reproduced in Fig. 12. A broad absorption develops under the lowest Davydov component. No measurable change in the Davydov splitting occurs in this temperature range. On the other hand, at 77°K the absorption is quite different; the line width of the Davydov components is 30-50 cm^{-1} and their splitting appears to have decreased, the upper components (now unresolvable) being shifted toward lower energy. As they are not clearly resolved, the actual splitting of two such broad absorptions will be larger than the separation between their maxima ($\sim 30 \text{ cm}^{-1}$). The overlapping wings will tend to shift the maxima

toward one another. This data is not at complete variance with the findings of Maria and Zahlan³⁰ (MZ) but it differs in several significant respects. 1) The line widths of the Davydov components observed here at low temperatures ($T < 27^\circ\text{K}$) are, in agreement with the findings of Broude,³¹ two to four times narrower than those of MZ at corresponding temperatures. 2) The change in these line widths in going from 4.2 to 1.8°K is not outside the normal crystal to crystal fluctuations ($\leq 1\text{ cm}^{-1}$) in contrast to the "sudden 50% increase in band width at temperatures below 4.2°K " observed by MZ. Such an increase would make it impossible to resolve the splitting between the upper Davydov components at 1.8°K , contrary to what is seen in Fig. 12. 3) The relative intensities of the Davydov components and their intensity relative to that of the phonon addition bands appear to be very different from the findings of MZ. This, however, is felt to nearly be an indication of the difficulty in making accurate intensity measurements of intrinsically very sharp intense bands. Little significance should be attached to the apparent intensities of the sharp Davydov components relative to the intensity of these phonon bands or even in relation to one another.³² There is considerable reason to believe that the $0,0$ transition in crystalline benzene is not primarily phonon induced. In the crystal, the benzene molecule is at a site of C_1 symmetry. The $0,0$ transition is therefore no longer forbidden provided there is an interaction between the molecule and its environment. These crystal interactions are sufficiently strong to induce all ten of the ungerade benzene vibrations in the infra-red spectrum of

the crystal¹⁴ even though only four of these are allowed in the gas phase. The IR crystal spectra are independent of temperature²¹ between 4.2 and 77°K indicating that the crystal perturbation is not dependent upon the occupation of phonon states. The broadness of the absorptions of MZ could easily be due to crystal imperfections and strains.³³

For the case of benzene, then, it is felt that the band-band transitions at temperatures below $\sim 30^\circ\text{K}$ give a qualitatively accurate description of the density function associated with the $^1\text{B}_{2u}$ state. The low energy tail in fluorescence has a mirror image relationship to the broad absorptions to the blue of the Davydov components (Fig. 12) which have been assigned as phonon addition bands by several authors.^{31a, 34} These can therefore be omitted from the density function.

Likewise for naphthalene, the spectroscopic transitions are not temperature independent. Unfortunately because of the width of the naphthalene exciton band, the high energy portion of the density function cannot be accurately determined at low temperatures from the fluorescence. Thus, the temperature effects due to phonons must be evaluated, at least qualitatively, in order to learn about the density function.

The 0,0 absorption for naphthalene at 77 and 4.2°K is shown in Fig. 10. This transition has been studied as a function of temperature by Maria,³⁵ and Prikhot'ko and Soskin.³⁶ It should be noted that Maria's absorption bands (his Fig. 1) are much broader than ours or those of Prikhot'ko and Soskin. The distortion of this spectra, as

pointed out by Prikhot'ko and Soskin is caused by crystal strains and defects. Conclusions regarding the intensity, shape, and temperature dependence of such distorted and overlapping spectra must be made cautiously. The data of Prikhot'ko and Soskin show, that as for the case of benzene, the 0,0 absorption of naphthalene is independent of temperature below $\sim 30^\circ\text{K}$. The half-widths of the Davydov components increase $10\text{-}30\text{ cm}^{-1}$ in going from 4° to 77°K . The spectra remain, however, qualitatively the same and no change occurs in the Davydov splitting. This fact indicates the temperature independence of the band structure. In addition, Prikhot'ko and Soskin have shown, through good polarization measurements, that phonon addition bands analogous to those in benzene underlie the \underline{b} polarized Davydov component. Their data indicate that these increase in intensity with increasing temperature.

From the above considerations of the phonon contribution to $\underline{k} = 0$ transitions, the phonon contribution to a band - band transition at 77°K can be estimated. The transition involving each \underline{k} state will be broadened roughly 25 cm^{-1} . There will also be an intensity contribution from the phonon addition bands. In absorption these transitions will contribute intensity roughly 70 cm^{-1} above the center of the exciton band just as they do in the 0,0 transition. In fluorescence these transitions will retrace the density function modified by the Boltzmann factor but $\sim 70\text{ cm}^{-1}$ to lower energy. The observed band \leftrightarrow band fluorescence and absorption lineshapes in both benzene and naphthalene are consistent with these expectations.

Within the above model, which is analogous to the weak coupling model¹⁸ for vibronic transitions in molecular crystals, the phonon contribution is a minimum at the low energy edge of the band-band absorption and the high energy edge of the 77 °K fluorescence. The composite density function calculated from these portions of the respective lines is shown in Fig. 13. The lower Davydov component is taken as the bottom of the band. The 20.4 ° and 77 °K fluorescence lines calculated from this density function are shown in Figs. 14/ and 15. The 20.4 °K fluorescence indicates that the density function rises even more sharply to its maximum than is indicated in Fig. 13.

Although the interpretation of the above experimental results is unique, the experimental spectra are not. Band - band transitions of benzene have been observed, and interpreted as such by A. Zmerli,³⁴ and by V. N. Vatulov, N. I. Sheremet, and M. T. Shpak.³⁷ However, neither group attempted to interpret them in terms of the density-of-states function of the excited state; in fact, Zmerli interprets the spectra in terms of emission from the $k = 0$ states only. Vatulov, et al., interpret the spectra in terms of emission from an exciton band containing two branches instead of four. The small difference between our fluorescence lineshape at 20.4 °K and that of Vatulov, et al., could be caused by the change in the Boltzmann equilibrium due to the presence of lower lying traps (benzene molecules at defect sites or chemical impurities) in their samples. A considerable portion of their emitted intensity comes from defects and impurities while no such emission is observed in our spectrum.

Pröpstl and Wolf³⁸ measured the fluorescence of crystalline naphthalene between 2 ° and 100 °K. At low temperatures (4-20 °K) they

Fig. 13. The composite density function for naphthalene, determined roughly from the high-energy edge of the band \rightarrow band fluorescence and the low-energy edge of the band \leftarrow band absorption; Figs. 8 and 11, respectively.

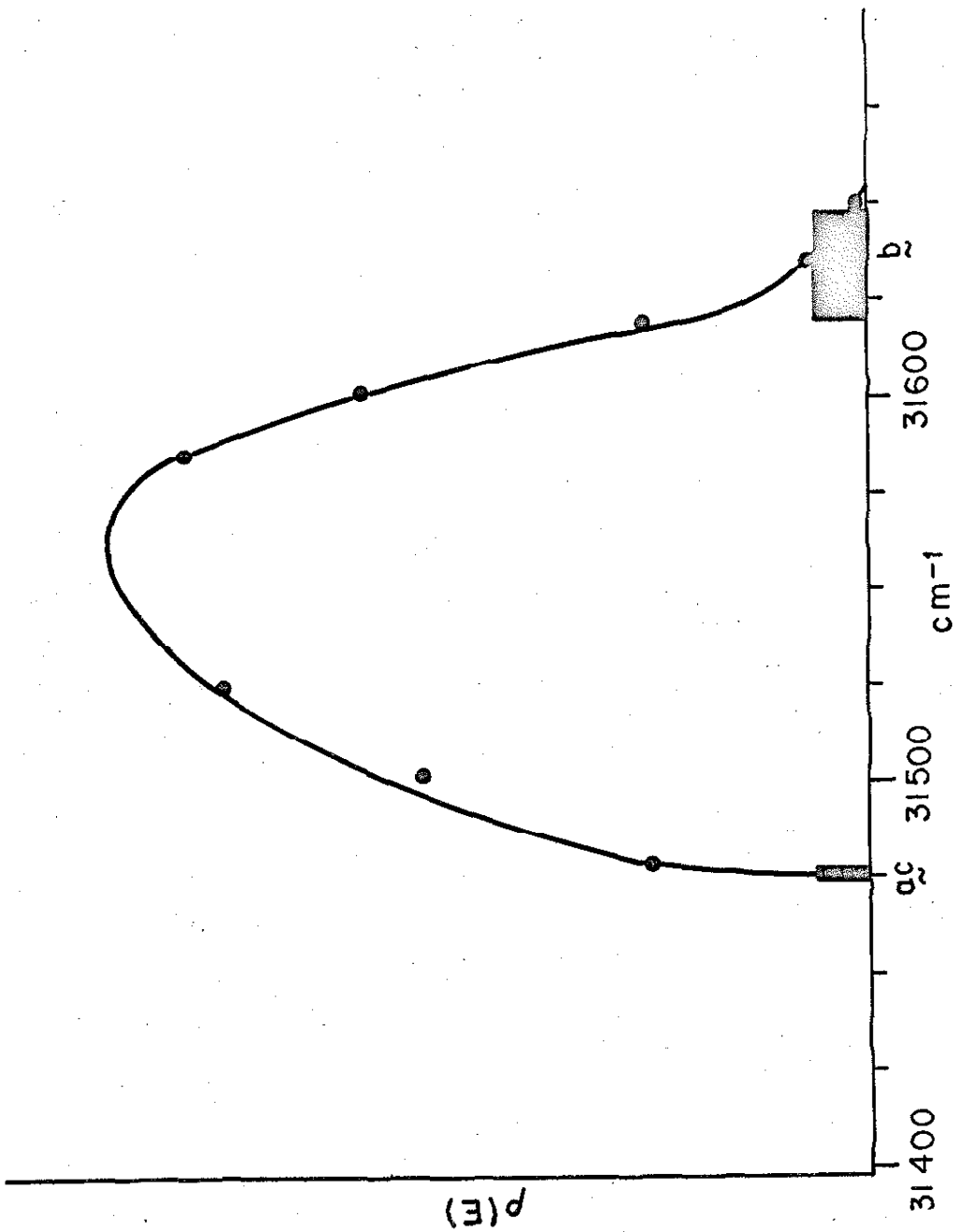


Fig. 14. (A) The experimental fluorescence band ($0, 0 - "512"$) at 20°K . The halfwidth, neglecting the phonon contribution, is shown by the arrow and is 16 cm^{-1} . (B) This fluorescence band as predicted from the density function of the octopole model, see Fig. 18. The fluorescence intensity is obtained from $\rho(E)$ by multiplying by the appropriate Boltzmann factor. The halfwidth equals 15 cm^{-1} . (C) This fluorescence band predicted from the composite density function, see Fig. 13. The halfwidth equals 24 cm^{-1} . This disagreement may indicate that the density function rises even more rapidly to its maximum than the composite function shows.

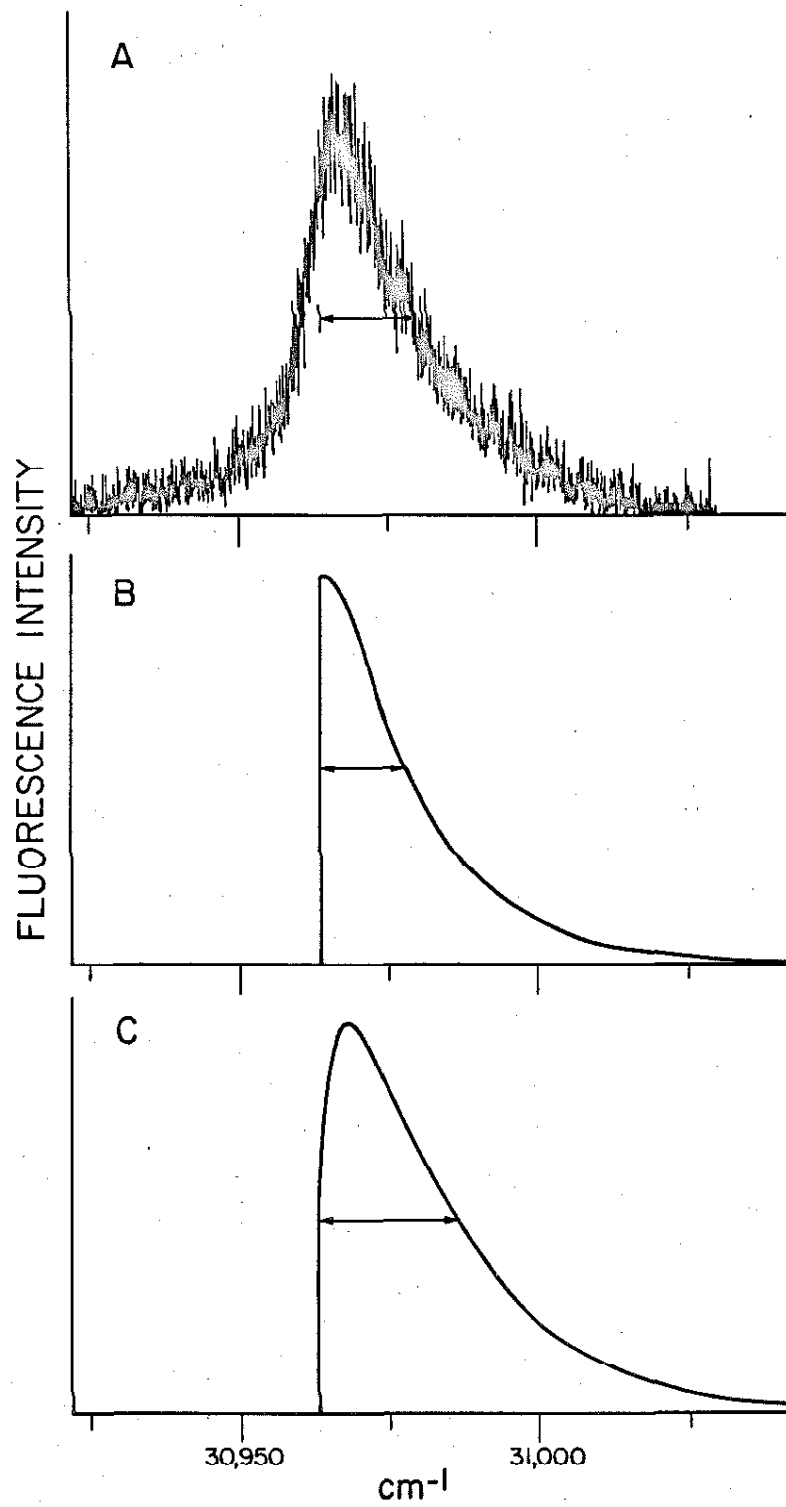
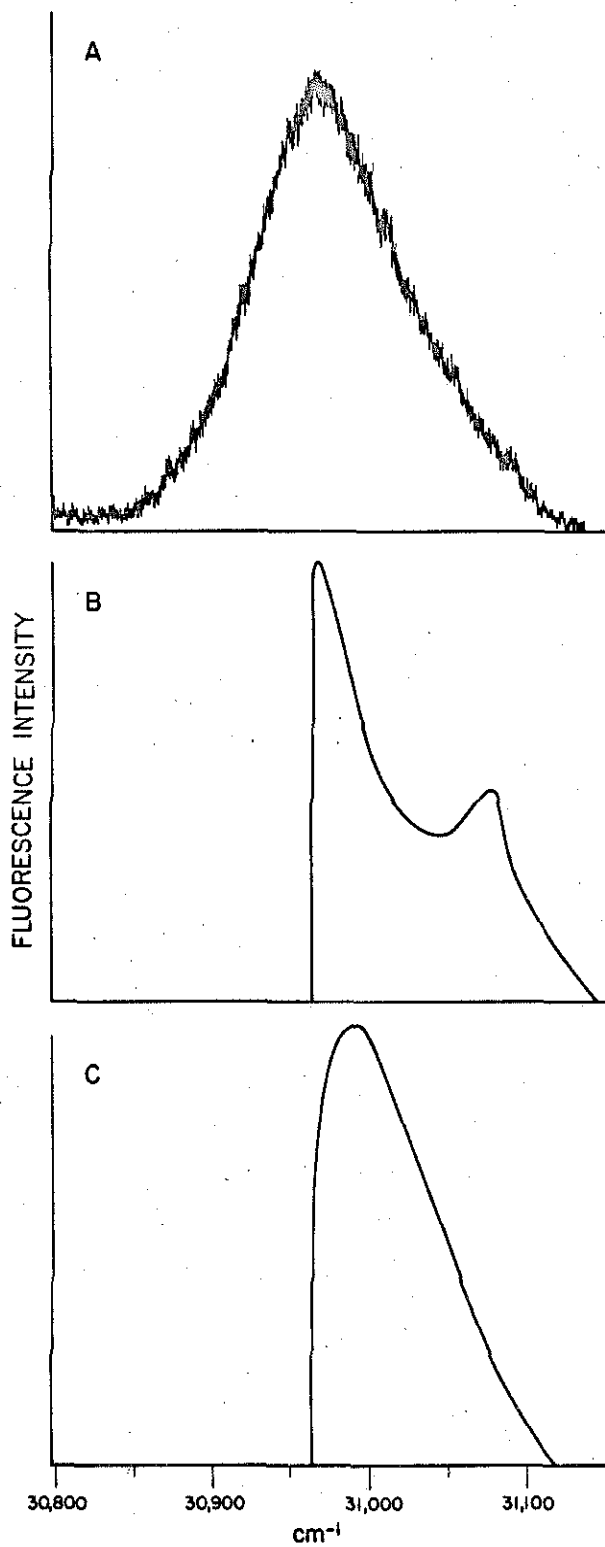


Fig. 15. (A) The experimental fluorescence band at 77 °K. The intensity below 30,963 cm^{-1} is attributed to phonons and is neglected in the calculated lineshape. (B) This fluorescence band as predicted from the octopole model, and (C) from the composite function. Although the octopole model disagrees with the experimental result, with respect to both the width and shape of the fluorescence line, this disagreement may be due only to the effect of phonons.



observed fluorescence only from the lower (ac) Davydov component. At higher temperatures (50-90°K) the $0' - 0''$ emission came from both high (b) and low (ac) Davydov components while the $0' - \nu''$ emissions seemed to originate from about the mean of the Davydov components. Although it was recognized by Pröpstl and Wolf that emission originates from the upper regions of the exciton band at high temperatures, they did not appreciate the role of the vibrational exciton band in explaining the difference between the $0' - 0''$ and $0' - \nu''$ emission. It is precisely this difference which allows the phonon contribution to be estimated and the density function of the electronic exciton band to be determined.

Following the theoretical development of Rashba,⁵ several Russian researchers have discussed exciton band \leftrightarrow exciton band transitions. Davydov²⁵ has summarized these results for the case of naphthalene and applied Rashba's ideas to predict the emission curve from the absorption curve. However, in view of the temperature dependence of the band \leftrightarrow band transitions in both benzene and naphthalene, Davydov's assumption that phonon contributions can be neglected is not justified. The low energy broadening of the fluorescence with increasing temperature cannot be explained using only electronic exciton states provided the vibrational exciton band is narrow. We therefore have been unable to reproduce Davydov's calculation of the fluorescence lineshape using his formulism because such a calculation must use transitions originating at energies lower than the bottom of the exciton band (his E_0 which equals $E_a(Q)$ in naphthalene).

Furthermore, this treatment assumes a \underline{k} dependence in the transition matrix element, and thus these spectra could not be related to the exciton band structure. It is only the approximations discussed earlier that remove such \underline{k} dependence and allow the density function to be discussed directly and simply in terms of the band - band transitions.

Recently Broude, Rashba, and Sheka³⁹ have interpreted the broad absorptions above the ${}^1B_{2u} 0, 0$ transition in crystalline naphthalene in terms of double exciton states.³ These states have been previously discussed in footnote 31 of Ref. 3. The interpretation of Broude, et al., required the knowledge of $\rho(E)$ which they approximated (without justification) from absorption band - band transition data taken at 90°K. Such theories illustrate the usefulness of an accurate density function in the interpretation of the entire crystal spectrum.

V. DISCUSSION

The density of states functions of benzene and naphthalene have been calculated using the first order Frenkel theory as described in Sec. II. Sets of M_{ij} have been chosen in accordance with the restrictions of the Davydov splittings and the isotopic mixed crystal data. For benzene, the assignments of the Davydov components are in question. The most recent work of Broude^{31a} gives one line at 37,803 cm^{-1} polarized parallel to the \underline{a} crystal axis and three lines (37,839; 37,846; and 37,847 cm^{-1}) polarized parallel to the \underline{c} axis at 20°K. This is consistent with the work of Zmerli but he was unable to resolve the

splittings of the \underline{c} -polarized lines. Recently, Wolf⁴⁰ has been quoted^{9b} as observing the \underline{a} and \underline{c} polarizations to be reversed from the above findings. However, as he states, his assignment is taken to be in agreement with Broude's earlier work⁴¹ which Broude has since revised in light of additional experimental results which give the data quoted above. We have been unable to resolve any splitting in the highest energy component, observing lines at $37,803 \text{ cm}^{-1}$, $37,8418 \text{ cm}^{-1}$, and $37,8471.1 \text{ cm}^{-1}$. In light of the above discussion of the spectral data, we have assigned the polarizations of our lines as \underline{a} , \underline{c} , \underline{b} in order of increasing energy to be consistent with the choice of Nieman and Robinson and the experimental finding of Claxton.⁴² The results of the density of states calculations will be independent of this choice, provided one of the higher energy components is \underline{b} polarized, but the \mathcal{M}_{ij} will not be uniquely related to a specific excitation exchange integral until the polarizations are clarified. The highest energy component reported by Davydov does not appear in his published spectra nor in higher resolution spectra taken in this laboratory at 4.2°K with a 3.4 M Jarrell-Ash Ebert spectrograph. For lack of independent confirmation of its presence, this line will be ignored in this work. The \mathcal{M}_{ij} for the benzene calculation have been determined by assuming an energy for the fourth (A_u) component, solving Eq. (18) of Ref. 21 for $M_{I\text{II}}$, $M_{I\text{III}}$, and $M_{I\text{IV}}$ and then assuming that only the nearest-neighbor interchange equivalent interactions contributed to the splitting, i. e., $M_{ij} \equiv \mathcal{M}_{ij}$. The interaction among the translationally equivalent molecules shift all the Davydov components

equivalently and thus have to be determined separately. Recent experiments in our laboratory⁴⁴ have shown that the interpretation of isotopic mixed crystal data by Nieman and Robinson is subject to question as the energies of isotopic guests of higher energy than the host are not given by a normal extension of the mixed crystal theory. This merely indicates that their stated assumptions must be reevaluated. We, therefore, have no independent measure of the translationally equivalent interactions \mathcal{M}_a , \mathcal{M}_b , \mathcal{M}_c and, as a result, they have been chosen to give the best fit to the experimental $\rho(E)$ for each choice of the energy of the A_u level. In order to approximately account for the different \underline{a} , \underline{b} , and \underline{c} crystal axis lengths, the relative magnitudes of \mathcal{M}_a , \mathcal{M}_b , and \mathcal{M}_c have been chosen to agree with the predictions of Nieman and Robinson based on an electron exchange model for the excitation exchange integrals, i. e., $\mathcal{M}_a : \mathcal{M}_b : \mathcal{M}_c = 1 : 0 : 3$. The results of these calculations for a crystal of 32,000 molecules, for various values of the A_u level, are given in Fig. 16. Two choices of \mathcal{M}_a , \mathcal{M}_b , and \mathcal{M}_c are given in one case to illustrate the effect of such interactions. $\rho(E)$ is also calculated from the \mathcal{M}_{ij} given from the isotopic mixed crystal data of Nieman and Robinson, and the poor agreement with experiment is consistent with the complications mentioned above. See Fig. 17 in which this $\rho(E)$ is compared to that obtained from the 20.4°K fluorescence. From these calculations it can be concluded that, if Frenkel theory is applicable, the A_u level is most likely between 37,815 cm^{-1} and 37,875 cm^{-1} .

The density function of naphthalene has been calculated from Eq. (4) for several choices of _____

Fig. 16. Density-of-states function giving the number of states per wavenumber interval as determined by the dispersion relation [Eq. (3)] for various values of the excitation exchange integrals. The position of the allowed (■) and forbidden (□) are indicated along the horizontal axis. (A) $\mathcal{M}_{I\ II} = -0.90$, $\mathcal{M}_{I\ III} = 4.85$, $\mathcal{M}_{I\ IV} = 4.25$, and $\mathcal{M}_a = \mathcal{M}_b = \mathcal{M}_c = 0\ \text{cm}^{-1}$. (B) $\mathcal{M}_{I\ II} = -1.55$, $\mathcal{M}_{I\ III} = 3.93$, $\mathcal{M}_{I\ IV} = 3.28$, $\mathcal{M}_a = -0.25$, $\mathcal{M}_b = 0$, $\mathcal{M}_c = -0.75\ \text{cm}^{-1}$. (C) $\mathcal{M}_{I\ II} = -2.03$, $\mathcal{M}_{I\ III} = 3.45$, $\mathcal{M}_{I\ IV} = 2.80$, and $\mathcal{M}_a = \mathcal{M}_b = \mathcal{M}_c = 0\ \text{cm}^{-1}$. (D) $\mathcal{M}_{I\ II} = -2.96$, $\mathcal{M}_{I\ III} = 2.51$, $\mathcal{M}_{I\ IV} = 1.86$, $\mathcal{M}_a = -0.60$, $\mathcal{M}_b = 0$ and $\mathcal{M}_c = -1.80\ \text{cm}^{-1}$. (E) $\mathcal{M}_{I\ II} = -3.69$, $\mathcal{M}_{I\ III} = 1.89$, $\mathcal{M}_{I\ IV} = 1.24$, $\mathcal{M}_a = -0.75$, $\mathcal{M}_b = 0$, and $\mathcal{M}_c = -2.25\ \text{cm}^{-1}$. (F) $\mathcal{M}_{I\ II} = -4.22$, $\mathcal{M}_{I\ III} = 1.26$, $\mathcal{M}_{I\ IV} = 0.60$, $\mathcal{M}_a = -1.00$, $\mathcal{M}_b = 0$, and $\mathcal{M}_c = -3.00\ \text{cm}^{-1}$. (G) $\mathcal{M}_{I\ II} = -4.82$, $\mathcal{M}_{I\ III} = 0.65$, $\mathcal{M}_{I\ IV} = 0$, and $\mathcal{M}_a = \mathcal{M}_b = \mathcal{M}_c = 0$. (H) $\mathcal{M}_{I\ II} = -4.82$, $\mathcal{M}_{I\ III} = 0.65$, $\mathcal{M}_{I\ IV} = 0$, $\mathcal{M}_a = -1.00$, $\mathcal{M}_b = 0$, and $\mathcal{M}_c = -3.00\ \text{cm}^{-1}$.

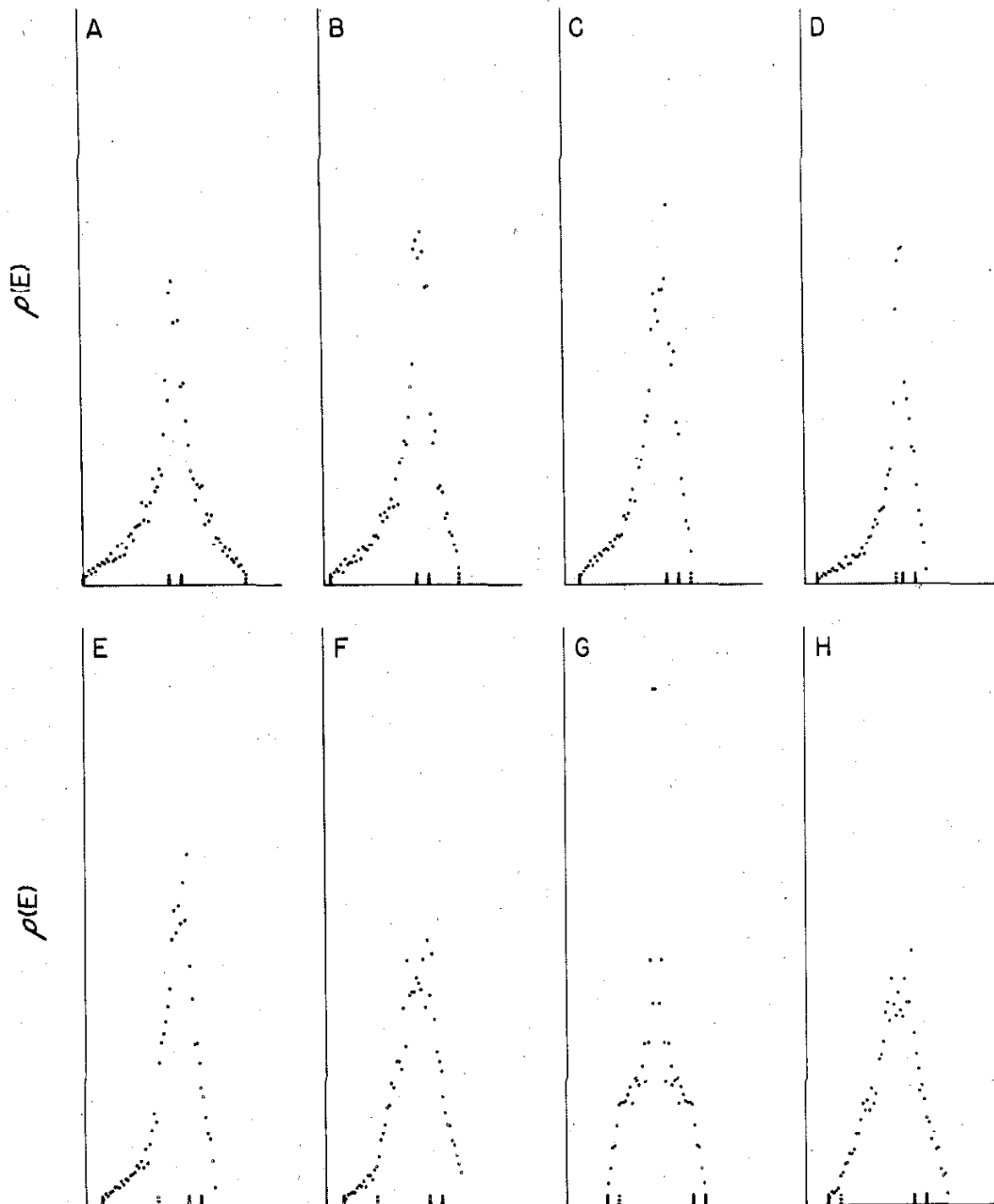


Fig. 17. Comparison of the 20.4°K experimental (\square) density-of-states function with that calculated from the \mathcal{M}_{ij} of Nieman and Robinson (\cdots) [$\mathcal{M}_{I\ II} = 6.90$, $\mathcal{M}_{I\ III} = 12.40$, $\mathcal{M}_{I\ IV} = 11.70$, $\mathcal{M}_a = 1.00$, $\mathcal{M}_b = 0$, and $\mathcal{M}_c = 3.00\text{ cm}^{-1}$] and from a set of \mathcal{M}_{ij} which approximately fit the experimental function (solid curve) [$\mathcal{M}_{I\ II} = -1.55$, $\mathcal{M}_{I\ III} = 3.93$, $\mathcal{M}_{I\ IV} = 3.28$, and $\mathcal{M}_a = \mathcal{M}_b = \mathcal{M}_c = 0\text{ cm}^{-1}$].

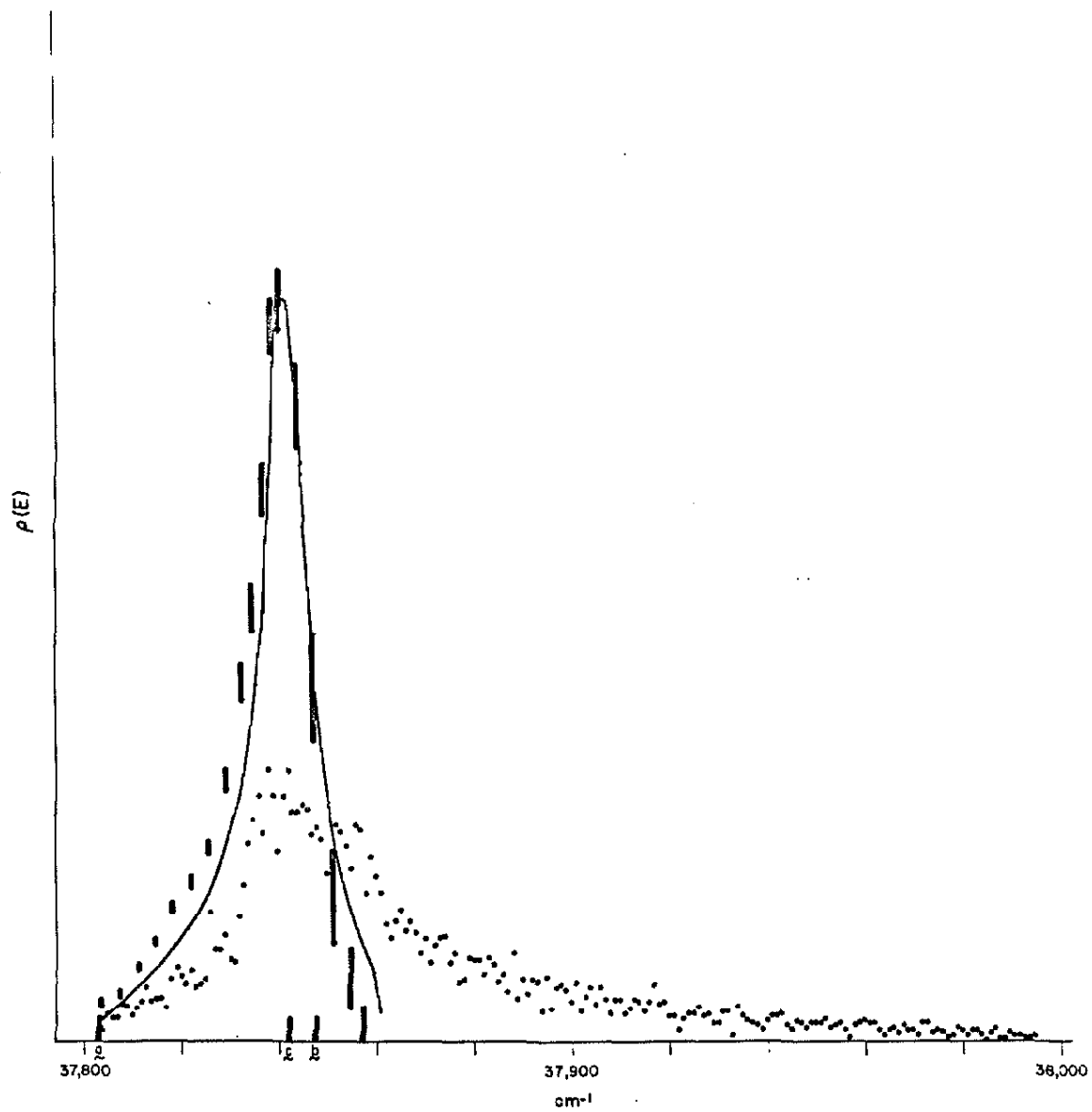
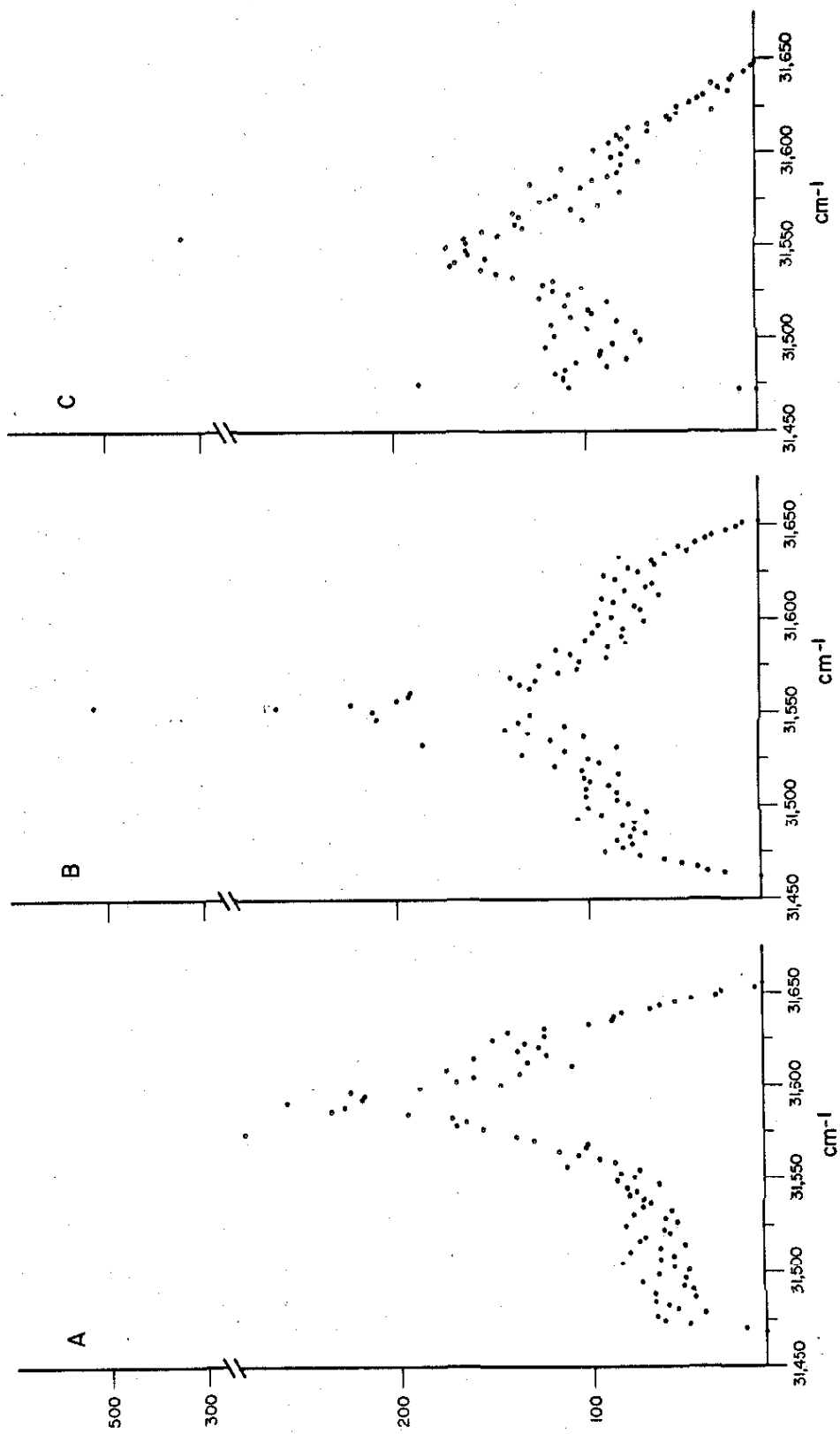


Fig. 18. Density functions giving the number of states per wave-number as determined from the dispersion relation [Eq. (4)] for various values of the excitation exchange integrals. (A) The octopole model: $\mathcal{M}_a = -4.8$, $\mathcal{M}_b = -3.9$, $\mathcal{M}_c = -2.4$, $\mathcal{M}_{12} = -21.1$, and $\mathcal{M}_{12'} = 1.6 \text{ cm}^{-1}$. These were obtained from Ref. 45, also see Ref. 8 b. (B) $\mathcal{M}_a = 2$, $\mathcal{M}_b = -1$, $\mathcal{M}_c = -1$, $\mathcal{M}_{12} = 22$, and $\mathcal{M}_{12'} = -2 \text{ cm}^{-1}$. (C) $\mathcal{M}_a = 10$, $\mathcal{M}_b = -6$, $\mathcal{M}_c = -4$, $\mathcal{M}_{12} = 22$, and $\mathcal{M}_{12'} = -2 \text{ cm}^{-1}$. The latter two density functions show the effect of translationally equivalent interactions. As shown in (C), a broad density function consistent with the experimental result can be obtained within the framework of the simple Frenkel approach.



the \mathcal{M} 's using a model crystal containing 128,000 molecules. The Davydov splitting ($\underline{k} = 0$) is given by $8 M_{\text{I II}}$ where $M_{\text{I II}}$ is the sum of the different interchange equivalent interactions over the entire lattice. Assuming nearest interactions dominate, $\mathcal{M}_{12} = 20 \text{ cm}^{-1}$. The density function for the case where the translationally equivalent interactions are nearly zero is very sharply peaked as shown in Fig. 18. The band structure of the octopole model has been presented by Craig and Philpott.^{8b} We have recalculated it for 128,000 molecules using the \mathcal{M} 's provided by R. G. Body.⁴⁵ The result of this calculation is also shown in Fig. 18. The fluorescence lineshapes at 77° and 20.4°K predicted from the above models are shown and compared with the experimental results in Fig. 14. Even though the octopole band structure is not in complete agreement with the experimental result (see Figs. 13, 14, 15 and 18), it cannot be eliminated due to the very qualitative estimate of the phonon component in the band \leftrightarrow band transitions.

VI. CONCLUSIONS

The recent theoretical developments concerning band \leftrightarrow band transitions in molecular crystals have been examined experimentally. The application of these theories has enabled us to evaluate the density function for the lowest excited singlet states of crystalline benzene and naphthalene as well as the temperature dependence and nature of the exciton-phonon coupling.

A comparison of the experimental density function with that obtained from semi-empirical calculations has provided information concerning the detailed nature of the excitation exchange interactions. Since the density function for naphthalene lies primarily between the Davydov components, it is concluded that the sum of the translationally equivalent interactions is small. The density function calculated when these terms are the same order of magnitude as the interchange equivalent interactions gives reasonable agreement with the experimental result. While the experimental results are only in qualitative agreement with the predictions of the octopole model, no comparison could be made with the model involving interaction with charge transfer states.

For benzene, a sharply peaked density function is found. Since there are four exciton branches of which at least two lie close together, such a function is not inconsistent with some translationally equivalent and interchange equivalent interactions being the same size. However, excellent agreement with the experimental result is obtained when the translationally equivalent interactions are neglected. Such a calculation places the forbidden A_u Davydov component above the observed components but not as far above as predicted by mixed crystal experiments.³ No theoretical model has been used to calculate a density function for the benzene crystal.

These results are not in any sense final, but they do indicate the power of Rashba's proposal as well as the necessity for the consideration of the entire band structure in theoretical calculations

and the need for an analysis of phonon effects in the spectra of aromatic molecular crystals.

FOOTNOTES

1. (a) L. P. Bouckaert, R. Smoluchowski, and E. Wigner, *Phys. Rev.* 50, 58 (1956); (b) J. M. Ziman, Principles of the Theory of Solids (Cambridge University Press, Cambridge, 1964).

2. (a) H. Winston and R. S. Halford, *J. Chem. Phys.* 17, 607 (1949); (c) Jon Mathews and R. L. Walker, Mathematical Methods of Physics (W. A. Benjamin, Inc., N. Y., 1964), Sec. 4.1.

3. G. C. Nieman and G. W. Robinson, *J. Chem. Phys.* 39, 1298 (1963).

4. D. M. Hanson, R. Kopelman, and G. W. Robinson, manuscript in preparation .

5. E. I. Rashba, *Soviet Phys. - Solid State* 5, 757 (1963).

6. S. D. Colson, R. Kopelman, and G. W. Robinson, *J. Chem. Phys.* 00, 000 (1967).

7. It should be noted that a 4 cm benzene crystal containing 10^{-5} parts phenol would be nearly opaque in the region of the observed absorption band \leftarrow band transition. Similarly β -methylnaphthalene absorbs in the region of the corresponding naphthalene transition.

8. (a) R. G. Body and I. G. Ross, *Aust. J. Chem.* 19, 1 (1966); (b) D. P. Craig and M. R. Philpott, *Proc. Roy. Soc. (London)* 290A, 583 (1966); (c) J. Jortner, S. A. Rice and J. I. Katz, *J. Chem. Phys.* 42, 309 (1965); and (d) A. S. Davydov and E. F. Sheka, *Phys. Stat. Sol.* 11, 877 (1965).

9. (a) R. Silbey, J. Jortner, M. T. Vala, and S. A. Rice, *J. Chem. Phys.* 42, 2948 (1965); (b) R. Silbey, S. A. Rice, and J. Jortner, *J. Chem. Phys.* 43, 3336 (1965).

10. (a) D. Fox and O. Schnepp, *J. Chem. Phys.* 23, 767 (1955); (b) T. Thirunamachandran (Doctoral Thesis, University of London, 1961).

11. The results of the calculations including interactions with the ion-pair states of crystalline benzene (Ref. 9a) place the A_u component near the B_{3u} Davydov component. R. Silbey, private communication.

12. The exciton states are optically pumped after which they come into thermal equilibrium with respect to the bottom of the band.

13. An exciton branch is composed of those k states which correspond to one of the representations of the interchange group. There are as many branches as molecules in the primitive unit cell.

14. D. A. Dows, Physics and Chemistry of the Organic Solid State, Vol. I, ed. by Fox, Labes, and Weissberger, (Interscience, N. Y., 1963), p. 609.

15. A. R. Gee and G. W. Robinson, *J. Chem. Phys.* 00, 000 (1967).

16. (a) D. P. Craig, J. M. Hollas, M. F. Redies, and S. C. Wait, Jr., *Phil. Trans. Roy. Soc.* A253, 543 (1961); (b) D. P. Craig and J. M. Hollas, *ibid.*, p. 569; (c) D. P. Craig and H. C. Wolf, *J. Chem. Phys.* 40, 2057 (1964); (d) A. R. Gee and D. M. Hanson, unpublished results.

17. The oriented site model only differs from the oriented gas model¹⁸ in that the transition moments for a molecule at the site (not in the gas) are used to predict the crystal moments.

18. R. M. Hochstrasser, Molecular Aspects of Symmetry (W. A. Benjamin, Inc., N. Y., 1966), pp. 312-13.

19. (a) A. S. Davydov, Theory of Molecular Excitons (McGraw-Hill, N. Y., 1962); (b) D. P. Craig and S. H. Walmsley, loc. cit. 14, p. 586 and references therein.

20. P. Sarti-Fantoni, Molecular Crystals 1, 457 (1966).

21. E. R. Bernstein, S. D. Colson, R. Kopelman, and G. W. Robinson (manuscript in preparation).

22. That is, the zero of energy is chosen at $\epsilon + \Delta$ (Ref. 21).

23. R. Kopelman, J. Chem. Phys. 00, 0000 (1967).

24. H. Winston, J. Chem. Phys. 19, 156 (1951).

25. A. S. Davydov, Usp. Fiz. Nauk 82, 393 (1964). [Engl. Tran. Soviet Physics-Uspekhi 7, 145 (1964).]

26. R. S. Knox, Theory of Excitons (Academic Press, N. Y., 1963).

27. S. D. Colson and E. R. Bernstein, J. Chem. Phys. 43, 2661 (1965).

28. D. M. Hanson and G. W. Robinson, J. Chem. Phys. 43, 4174 (1965).

29. V. L. Broude, E. I. Rashba, E. F. Sheka, Soviet Phys. Dokl 6, 718 (1962).

30. H. Maria and A. Zahlan, J. Chem. Phys. 38, 941 (1963).

31. (a) V. L. Broude, Usp. Fiz. Nauk 74, 577 (1962), [Engl. Tran. Soviet Physics-Uspekhi 4, 584 (1962).]; (b) V. L. Broude and M. I. Onoprienko, Opt. i Spektroskopiya 8, 629 (1960) [English transl. : Opt. Spectry. (USSR) 8, 332 (1960)].

32. Different crystals at the same temperature give quite different answers for the relative intensity of these transitions. In some crystals the peak height of the lowest energy component is about the same as that of the maximum of the phonon bands and, while the highest energy Davydov component is always the most intense, its intensity relative to the other two has appeared to vary by as much as a factor of 2-3. This is probably a manifestation of the difficulty inherent in a measurement of a very sharp absorption with moderate resolution. As the line width and energy of the Davydov components is very dependent upon crystal strains and stresses,³³ their apparent intensity could easily change from sample to sample as the strain induced line width changes. Or, to put it another way, if a very intense absorption line is narrower than the slit width, the narrower the line the weaker it appears at constant intensity and conversely.

33. S. D. Colson, J. Chem. Phys. 45, 4746 (1966).

34. A. Zmerli, J. Chim. Phys. 56, 387 (1959).

35. H. Maria, J. Chem. Phys. 40, 551 (1964).

36. A. F. Prihot'ko and M. S. Soskin, Opt. i Spektroskopiya 13, 522 (1962) [English transl. : Opt. Spectry. (USSR) 13, 291 (1962)].

37. V. N. Vatulev, N. I. Sheremet, and M. T. Shpak, *Opt. Spectry.* 16, 315 (1964).
38. A. Propstl and H. C. Wolf, *Z. Naturforsch.* 18, 724 (1963).
39. V. L. Broude, E. I. Rashba, and E. F. Sheka, *Phys. Stat. Sol.* 19, 395 (1967).
40. H. C. Wolf, *Solid State Physics* 9, 1 (1959).
41. V. L. Broude, V. S. Medvedev, and A. F. Prikhot'ko, *Opt. i Spek.* 2, 317 (1957).
42. T. A. Claxton (Doctoral Thesis, University of London, 1961) as quoted by O. Schnepp, *Annual Review of Physical Chemistry*, Vol. 14, ed. by H. Eyring (Annual Reviews, Inc., Palo Alto, Calif. 1963), p. 35.
43. A fourth line might be expected to be observed near or above the top of the band because of the presence of 6% (natural abundance) $^{13}\text{C}^{12}\text{C}_5\text{H}_6$, which has recently been shown to have its 0,0 shifted 3.7 cm^{-1} to the blue of the $^{12}\text{C}_6\text{H}_6$ isotope.
44. S. D. Colson, manuscript in preparation.
45. R. G. Body, private communication, also see Ref. 8a.

Location of the Fourth, Forbidden Factor Group Component
of the ${}^1B_{2u}$ State of Crystalline Benzene

by

STEVEN D. COLSON

Gates and Crellin Laboratories of Chemistry,
California Institute of Technology, Pasadena, California 91109

ABSTRACT

There have been two different experimental techniques used to locate the position of the fourth, forbidden factor group component of the ${}^1B_{2u}$ state of crystalline benzene. The method of variation of energy denominators gave a very wide exciton band, placing the forbidden, A_u component at $37,996\text{ cm}^{-1}$. More recently, the density of states function for the ${}^1B_{2u}$ exciton band has been determined and used to predict the A_u component to lie between $37,815$ and $37,875\text{ cm}^{-1}$. As both of these techniques rely upon the use of first or Frenkel theory, their disagreement might be interpreted to mean that a higher order theory is needed to explain the experiments. In fact, it has been shown that mixing with ion-pair crystal states could be important in determining the exciton band structure of this state. However, the lack of agreement between the two experimental techniques might only indicate that some of the assumptions, other than the applicability of a first or Frenkel theory, used in either approach are invalid for benzene crystals. To distinguish between these two alternatives, the method of variation of energy denominators is re-examined in this paper through improved and more extensive experiments. The

static gas-to-crystal shift for a guest in an isotopic mixed crystal is found to be a function of the isotopic substitution of the host crystal. Thus, the variation of energy denominators method, which assumes the static shift to be constant, is inappropriate for the study of the ${}^1B_{2u}$ state of crystalline benzene.

Additional evidence, based upon the vibronic spacings of a guest in a number of different isotopic hosts, is presented which indicates that there is no strong mixing between the ion-pair states and the ${}^1B_{2u}$ state of the crystal. In fact, this same evidence is used to independently predict the position of the forbidden, A_u component at about $37,860\text{ cm}^{-1}$, in agreement with the limits set by the experimental density of states function. The density function, calculated using first order Frenkel theory and the assuming nearest neighbor interactions dominate, is found to be in excellent agreement with the experimentally observed function. Thus, it is concluded that it is most likely not necessary to consider mixing with ion-pair states to explain the band structure of the lowest singlet state of benzene crystals.

I. INTRODUCTION

The exciton structure of the ${}^1B_{2u}$ excited state of crystalline benzene has been the subject of numerous calculations¹ and experimental works.² This problem is complicated over and above that of crystals with naphthalene-like crystal structures in that there are four Davydov components³ instead of two and, moreover, because one of them cannot be observed in the 0,0 absorption. For this reason, and because benzene crystals are harder to prepare, the benzene singlet exciton band structure is considerably less certain than that of naphthalene. The earliest predictions of the complete structure were those of Fox and Schnepf^{1a} who, using an octopole model for the exciton interactions, found the forbidden A_u level near the center of the exciton band; however, they were unsuccessful at getting the correct magnitudes of splitting for the observed levels. These calculations were followed by the isotopic mixed crystal experiments of Nieman and Robinson^{2b} (NR) through which they predicted the A_u level to lie well above the three observed Davydov components, i. e., at the top of the band. More recent octopole-octopole calculations,^{1b} in which the positions of the observed components were only approximately fit, confirmed the order of the observed levels predicted by Fox and Schnepf, but found the A_u level to lie at the top of the band. Silbey, Rice, and Jortner^{1c} concluded that mixing with ion-pair exciton states may play a considerable role in determining the Davydov structure of the ${}^1B_{2u}$ state. If such mixing is important, the A_u level could be expected to lie anywhere from the top to the bottom of the band,⁴ depending upon

the energy chosen for the ion-pair state. The most recent evidence has been that given by the experimentally determined density-of-states function.⁵ Comparison of the experimental function with that predicted by first-order Frenkel theory for several positions of the A_u level, shows that quite a range of values can be used to fit the experimental function. It was concluded, however, that the value predicted by NR is too high. Thus, the past work has not been fully successful in elucidating the ${}^1B_{2u}$ exciton band structure of benzene, as we find both experimental and theoretical questions that remain unanswered. In this paper the experimental conflicts are resolved and the implications of the experimental results concerning the various theoretical models are discussed.

II. THEORY

For simplicity, it will first be assumed that a first-order Frenkel theory is applicable and then possible complications due to mixing with ion-pair states or other higher crystal states will be considered. The theoretical framework necessary for the discussion of neat and isotopically mixed molecular crystals in the Frenkel limit has recently been discussed in detail,³ and will be briefly outlined below for completeness and clarity. The crystal energy states corresponding to the f excited molecular state can be expressed as,

$$E^{f\alpha}(\underline{k}) = \epsilon + D + L^{f\alpha}(\underline{k}). \quad (1)$$

In this expression, ϵ is the transition energy of a site-distorted molecule, D is a \underline{k} -independent band shift term, and $L^{f\alpha}(\underline{k}) = \sum_{q=1}^m a_q^\alpha L_{Iq}^f(\underline{k})$,

where the $L_{Iq}^f(\underline{k})$ are \underline{k} -dependent sums of excitation exchange integrals $M_{qq'} = \int \chi_q^f \chi_{q'}^0 |H' | \chi_q^f \chi_{q'}^0 d\tau$, and a_q^α are the coefficients corresponding to the α^{th} representation of the interchange group. The χ_i^f are the eigenfunctions of the i^{th} site distorted molecule in their f^{th} excited state, i. e., site functions, and H' is the intersite interaction Hamiltonian.

It will be of interest later to speak of the gas-to-crystal shift of the transition energy. For this purpose, as ϵ is not a gas phase transition energy and as shift terms higher than first order in χ_i^f have been neglected, it is necessary to rewrite Eq. (1) as

$$E^{f\alpha}(\underline{k}) = \bar{\epsilon} + \Delta + L^{f\alpha}(\underline{k}), \quad (2)$$

where $\bar{\epsilon}$ is the gas phase transition energy and Δ is $\epsilon - \bar{\epsilon} + D$ plus all other \underline{k} -independent contributions to the crystal transition energy.

Thus, the gas-to-crystal (site) shift is now given by Δ . As transitions connecting exciton states of the crystal with its ground state can only involve the states with $\underline{k} = 0$, the energy expressions for these \underline{k} states are of particular interest in considering low temperature absorption spectra. For benzene,⁶ with four molecules per unit cell and space group D_{2h}^{15} , there are four $\underline{k} = 0$ states whose energies relative to the mean of the \underline{k} band ($\bar{\epsilon} + \Delta$) are, using the \underline{D}_2 interchange group:

$$E^{f, A_u}(0) = 4(M_{I \text{ II}} + M_{I \text{ III}} + M_{I \text{ IV}}) + 2(M_a + M_b + M_c) \quad (3a)$$

$$E^{f, B_{1u}}(0) = 4(M_{I \text{ II}} - M_{I \text{ III}} - M_{I \text{ IV}}) + 2(M_a + M_b + M_c) \quad (3b)$$

$$E^{f, B_{2u}}(0) = 4(-M_{I \text{ II}} + M_{I \text{ III}} - M_{I \text{ IV}}) + 2(M_a + M_b + M_c) \quad (3c)$$

$$E^{f, B_{3u}}(0) = 4(-M_{I \text{ II}} - M_{I \text{ III}} + M_{I \text{ IV}}) + 2(M_a + M_b + M_c) \quad (3d)$$

where the M_{Iq} are algebraic sums of the \mathcal{M}_{Iq} integrals involving molecule I and each of the molecules translationally equivalent to molecule q; molecule q being generated from molecule I by one of the operations of the \underline{D}_2 interchange group⁷ (not the identity operation). Thus, they are called the interchange equivalent interactions. The M_a , M_b , and M_c terms are the corresponding sums of integrals involving molecules translationally equivalent to molecule I along the a, b, and c crystal axes respectively, i. e., translationally equivalent interactions.

As all the dipole allowed transitions for the benzene crystals are of the types $A \leftrightarrow B_1$, $A \leftrightarrow B_2$, $A \leftrightarrow B_3$, $B_1 \leftrightarrow B_2$, $B_1 \leftrightarrow B_3$, $B_2 \leftrightarrow B_3$, and $g \leftrightarrow u$, only the three B_u levels can be seen in transitions from the totally symmetric ground state. Thus, the 0,0 in absorption is expected to be a triplet of lines polarized along the \underline{a} , \underline{b} , and \underline{c} axes corresponding to the B_{1u} , B_{2u} , and B_{3u} levels respectively. However, as Eqs. (3b), (3c), and (3d) are not linearly independent, determining the corresponding $E^{fa}(0)$ does not allow one to solve for the M_{Iq} . Thus, either the A_u level or the mean of the four $\underline{k} = 0$ levels $[\bar{\epsilon} + \Delta + 2(M_a + M_b + M_c)]$ must be found before the magnitudes of the excitation exchange integrals can be extracted from the low temperature absorption spectrum. There are several experimental techniques which can be used to determine the M_{Iq} for those states which can be treated with Frenkel theory; the variation of energy denominators method, the determination of the density-of-states function, and the vibronic analysis of pure and isotopically mixed crystals. These techniques will now be discussed.

A. The Variation of Energy Denominators Method

This method was utilized by NR. They studied the absorption and emission spectra of an isotopic mixed crystal; $\sim 1\%$ C_6H_6 in 99% $C_6D_nH_{6-n}$. Their determination relied upon the assumption that Δ and M_{Iq} were independent of isotopic substitution. These approximations and their utilization in a determination of $E^{Au}(0)$ have recently been discussed in Ref. 3 in which the ideal mixed crystal concept is introduced. An ideal mixed crystal is one in which (a) the guest is infinitely dilute; (b) the only difference between guest and host is one of the isotopic substitution; (c) guest and host have the same symmetry and dimensions; (d) quasi-resonance interactions between guest and host and the effects of isotopic substitution on Δ are negligible. Thus, the isotopic guest absorption energy in an ideal mixed crystal is just $E = \bar{\epsilon} + \Delta$. The variation of energy denominators method is one in which the deviation δ from this energy due to quasi-resonance interactions between the guest and host states is determined and then used to calculate

$$\beta^2 = M_{I II}^2 + M_{I III}^2 + M_{I IV}^2 + \frac{1}{2}(M_a^2 + M_b^2 + M_c^2) \quad (4)$$

from the approximation $\delta = 4\beta^2/\Delta E$. ΔE was taken as the gas phase energy difference between the guest and the host 0,0 transitions. The experimental procedure was to determine

$$E(\text{guest}) = \bar{\epsilon} + \Delta + \delta \quad (5)$$

at two values of ΔE and solve for β^2 . Nieman and Robinson obtained the

value $\beta = 18 \pm 2 \text{ cm}^{-1}$. Knowing this and the positions of the observed Davydov components, they found $E^{Au}(0)$ to lie at $37,996 \text{ cm}^{-1}$,

which is outside the limits set by a later determination of $\rho(E)$ (see next section).

B. The Determination of the Density-of-States Function

It has recently been shown that, in a restricted Frenkel limit, the density-of-states function $\rho(E)$ (the number of \underline{k} states per unit of energy) can be derived from the intensity distributions of exciton band — exciton band transitions.⁵ An analysis of the benzene neat crystal fluorescence has shown that $\rho(E)$ is a peaked function that does not extend much beyond the limits set by the observed Davydov components. By calculating $\rho(E)$ from Eq. (4) with assumed $\mathcal{M}_{qq'}$, it was shown that the experimental data could be fit reasonably well if $37,815 \text{ cm}^{-1} \lesssim E^{A_u}(0) \lesssim 37,875 \text{ cm}^{-1}$, but not by the NR value. As this method relies upon Frenkel theory both for the determination of the "experimental" density-of-states function and for the subsequent prediction of $E^{A_u}(0)$, higher order mixing of crystal states could conceivably be responsible for the difference between the experimental $\rho(E)$ and that calculated with a $\beta = 18 \text{ cm}^{-1}$. However, the positions of the guest vibronic states in isotopic mixed crystals seems to rule out this possibility (see next section).

C. Vibronic Analysis of Pure and Isotopic Mixed Crystals

The mean of the exciton band $\bar{\epsilon} + \Delta$ can also be found by a completely independent method. In the Frenkel limit, the mean of the exciton band corresponding to a $0, 0 + \nu'_1$ gas phase transition will be $\Delta\nu'_1$ above that of the $0, 0$, where $\Delta\nu'_1$ is the crystal value of the excited state vibrational frequency. $\Delta\nu'_1$ can be determined from the isotopic

mixed crystal guest absorption spectrum if both the $0, 0$ and the $0, 0 + \nu'_1$ transitions are characteristic of an ideal mixed crystal. This follows naturally from the theory as the ideal mixed crystal energy for any crystal state is just the mean of the respective neat crystal exciton band $\bar{\epsilon} + \Delta$. (See Fig. 3 of Ref. 3) Thus, this technique will be applicable for cases where, for the $0, 0$ and at least one higher vibronic transition, Δ is independent of isotopic substitution and δ is either zero, the same for both states, or can be evaluated separately. The quasi-resonance interactions with host states which determine δ are not expected to be the same for both guest states as they depend upon the ΔE and β 's between the interacting guest and host states, both of which will generally be different for each vibronic state. However, if the $0, 0 + \nu'_1$ vibronic exciton band can be analyzed and the corresponding $\Delta\nu'_1$ determined, the band center of the $0, 0$ transition can be found by a simple subtraction.

At first, this would appear to be a fruitless approach since, in general, each vibronic exciton band will be just as difficult to analyze as the $0, 0$ band. However, in the limit of small crystal distortions of the molecule, the exciton splittings of vibronic bands involving non-totally symmetric vibrations will be zero since vibrational overlap integrals of the type $\langle \nu' | \nu'' \rangle$ vanish if the molecular symmetry classifications remain valid in the crystal.^{2b} However, in the benzene crystal, all site states are either u or g, and thus all vibronic states can have some exciton splitting. Nevertheless, if a vibronic state with little or no splitting can be found, and if its crystal $\Delta\nu'_1$ can somehow be determined, the band center of the $0, 0$ can be derived by merely subtracting $\Delta\nu'_1$ from the observed pure crystal transition. This method

was first utilized by Broude;^{2a} however, he made no attempt to calculate the energy of the A_u level from his data.

III. EXPERIMENTAL

The ${}^1B_{2u} \leftarrow {}^1A_{1g}$ absorption spectra of neat and isotopically mixed benzene crystals were taken at 4.2°K. The deuterated benzene isotopes were obtained from Merck, Sharp and Dohme Ltd., Montreal, Canada, and the perprotonated benzene was Phillips Research Grade purified by the methods of Colson and Bernstein.⁸ To minimize the effects of crystal strain⁹ on the spectra, relatively thick (20-30 μ) crystals were used. They were grown in evacuated cells by slowly cooling from the melt as described elsewhere.¹⁰ Most of the spectra were taken on a 2M Czerny-Turner stigmatic spectrograph utilizing the fourth order of a 600 line/mm Bausch and Lomb grating. Some of the spectra were also taken on a 3.4 M Jarrell-Ash Ebert spectrograph equipped with an equivalent grating. A 150 W Xe arc lamp, coupled with appropriate Kasha solution filters, was used as a light source. The neat crystal spectra and most of the mixed crystal spectra were observed with several crystals and, while the guest transition energies remained very nearly constant ($\pm .5 \text{ cm}^{-1}$), the neat crystal Davydov components were found to vary by as much as 3 cm^{-1} from sample to sample. The values reported are an average taken from selected spectra that exhibited the smallest linewidths and are believed accurate to $\pm 1 \text{ cm}^{-1}$. The data are all presented in Tables I through III, and Figs. 1 through 4. Fig. 1 shows a photograph of the C_6H_6 absorption spectrum of a $\sim 20 \mu$ thick crystal taken on the 2 M instrument at 4.2°K with the regions of interest indicated. Also included in Fig. 1 are some previously reported⁹ spectra of thin ($\sim 1 \mu$) strained crystals, taken at the same temperature.

Fig. 1. Absorption spectra of unstrained (A) and two different strained (B and C) crystals of C_6H_6 at $4.2^\circ K$. The high energy member of the 0-0 doublet in the strained crystals represents the unresolved b and c polarized absorptions.

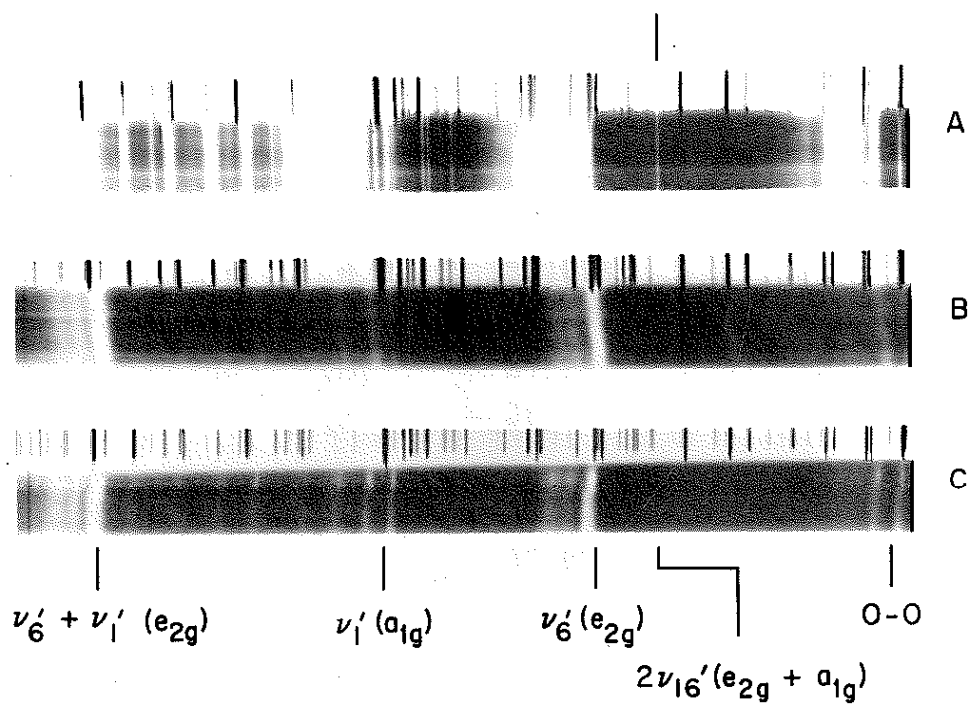


Table I. Guest 0, 0 Transition Energies of Isotopic Mixed Crystal

Host	Guest	E(Guest)	E(Guest)-E(Gas) ^a
		0, 0 (cm ⁻¹)	0, 0 (cm ⁻¹)
C ₆ D ₆	C ₆ H ₆	37,853	-233
C ₆ D ₅ H	"	37,852	-234
m-C ₆ D ₄ H ₂	"	37,850	-236
sym-C ₆ D ₃ H ₃	"	37,846	-240
p-C ₆ D ₂ H ₄	"	37,841	-245
C ₆ DH ₅	"	37,830	-253
C ₆ D ₆	C ₆ DH ₅	37,884	-240
"	p-C ₆ D ₂ H ₄	37,913	-242
"	sym-C ₆ D ₃ H ₃	37,949	-237
"	m-C ₆ D ₄ H ₂	37,981	-241
"	C ₆ D ₅ H	38,003	~ -257
C ₆ H ₆	C ₆ DH ₅	37,877	~ -247
"	m-C ₆ D ₄ H ₂	37,971	-251
"	C ₆ D ₅ H	38,001	-259
"	C ₆ D ₆	38,033	-256
C ₆ DH ₅	C ₆ D ₆	38,035	-254
p-C ₆ D ₂ H ₄	"	38,038	-251

^a Gas phase values for C₆H₆ and C₆D₆ are from Ref. 12. All others are from Ref. 2a.

Table II. C_6H_6 and C_6D_6 Neat Crystal Transition Energies

	Crystal		Gas ^b
	$\nu_{vac}(cm^{-1})$	Polarization ^a	$\nu_{vac}(cm^{-1})$
C_6H_6		a	
	0, 0	c	38, 086. 1
		b	
	$2\nu'_{18}$	—	38, 561. 0
C_6D_6		—	
	0, 0	—	38, 289. 1
		—	
	$2\nu'_{18}$	—	38, 703. 8

^a For a detailed explanation of this choice of polarizations see
Ref. 5 .

^b Ref. 12 .

Table III. Vibronic Spacings of a C_6H_6 Guest in Various Host Crystals

Host	0,0 + $2\nu'_{16}$	0,0 + ν'_6	0,0+ ν'_1
C_6D_6	392	519	927
C_6D_5H		520	
m- $C_6D_4H_2$		519	
sym- $C_6D_3H_3$		519	926
p- $C_6D_2H_4$		521	924
Gas ^a	475	522	925

^a The values for $2\nu'_{16}$ and ν'_6 are taken from Ref. 12 and that for ν'_1 from Ref. 15.

Fig. 2. Microphotometer tracings of the 0-0 absorption bands of neat C_6H_6 and 20% C_6H_5D in C_6H_6 at 4.2°K.

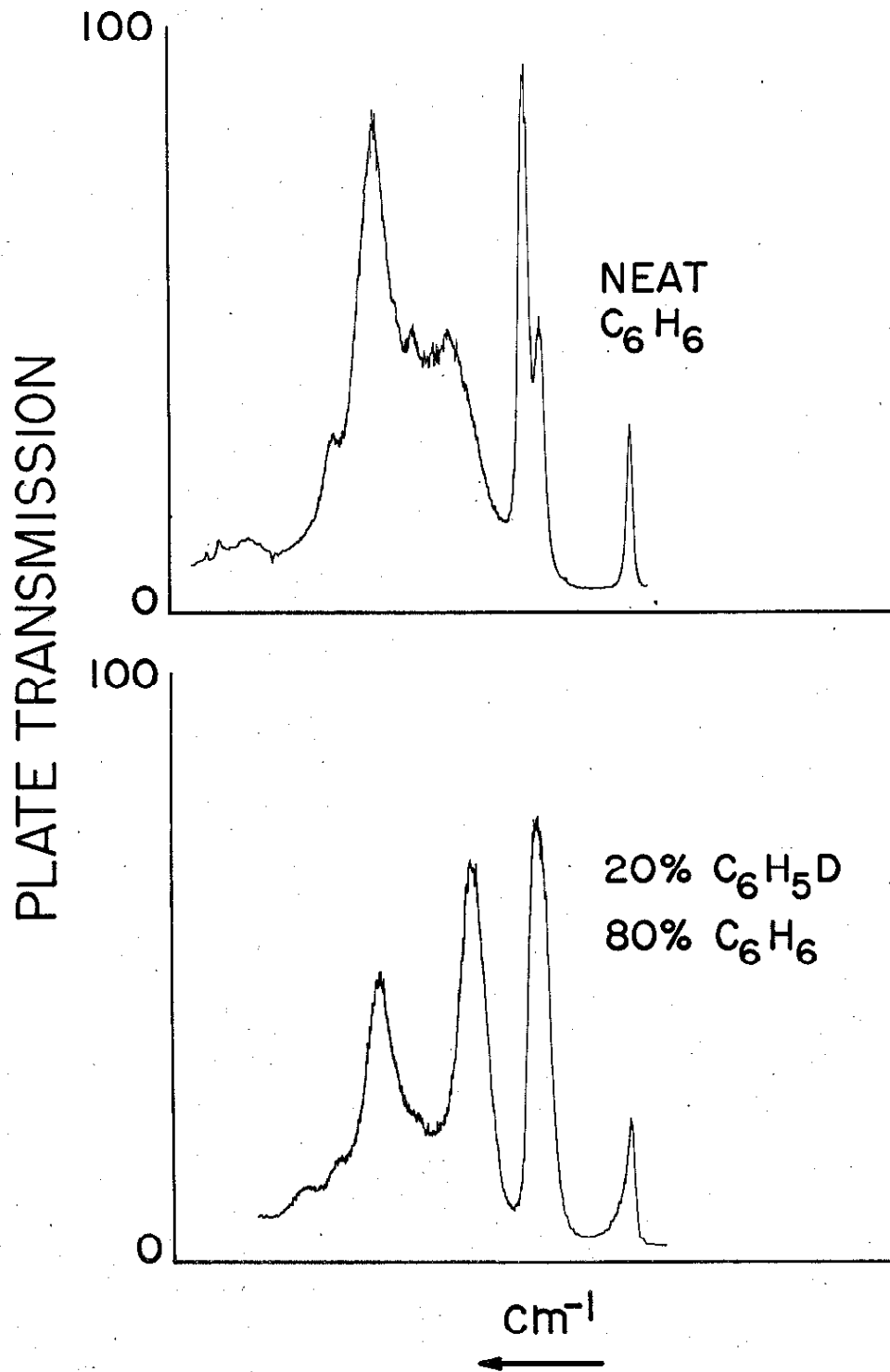
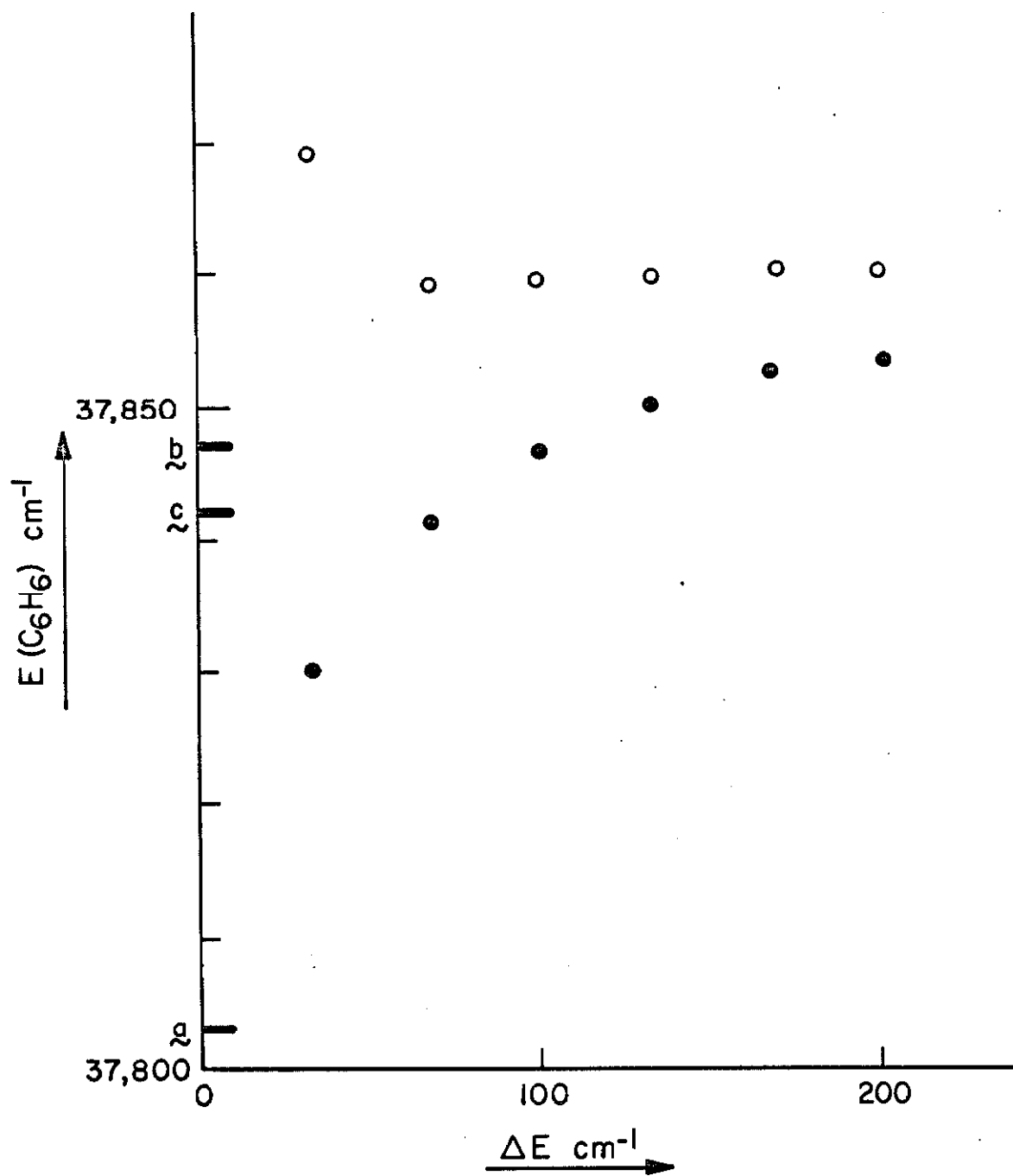


Fig. 3. Application of variation of energy denominators method to the 0, 0 energy of C_6H_6 in different hosts. The experimental points (dots) are from Table I. Each open circle represents a separate determination of $\bar{\epsilon} + \Delta$ from $\bar{\epsilon} + \Delta = E(\text{guest}) - 4\beta^2/\Delta E$ for $\beta = 18 \text{ cm}^{-1}$, and thus should form a horizontal, straight line.



These spectra illustrate the effects of improper sample preparation. The energy of the C_6H_5D in C_6H_6 0, 0 transition could only be approximately determined by studying the concentration dependence of mixed crystal spectra as it was masked by the phonon addition bands (see Fig. 2). The 0, 0 + $2\nu'_{16}$ transition of C_6H_6 in C_6D_6 was very weak and required $\sim 3\%$ C_6H_6 in a crystal $\sim 100 \mu$ thick for detection. The corresponding transition for a C_6D_6 guest could not be determined as it was masked by the host absorption for all choices of solvents.

IV. DISCUSSION

A. Variation of Energy Denominators Method

The first point to be discussed in light of these new data is that of the disagreement of the experimental $\rho(E)$ with that calculated from the data of Nieman and Robinson. The two functions are quite different and yet checking the more extensive data presented here shows that, indeed, the guest energy for C_6H_6 in several solvents can be fit to an expression of the form $E(\text{guest}) = \bar{\epsilon} + \Delta + 4\beta^2/\Delta E$ with $\beta = 18 \text{ cm}^{-1}$ (see Fig. 3). The only exception is the value of C_6H_6 in C_6H_5D where this approximation might not be expected to hold.¹¹ A difficulty is encountered, however, when one considers the energy of a C_6D_6 guest in solvents whose 0, 0 lie at lower energies. One should be able to predict the energy of the 0, 0 transition for C_6D_6 in a C_6H_6 solvent by adding 2δ (13 cm^{-1}) plus the gas phase energy difference¹² between C_6H_6 and C_6D_6 (203 cm^{-1}) to the energy of a C_6H_6 guest in a C_6D_6 host. That is, by assuming that the 0, 0 transitions of the C_6H_6 and C_6D_6 guests are only shifted relative to one another by interacting with the corresponding transition of the host. However, as the 0, 0 of C_6D_6 in C_6H_6 is $\sim 400 \text{ cm}^{-1}$ closer to the upper

vibronic bands of the host than that of C_6H_6 in C_6D_6 , interactions with these higher states can depress this energy difference. In fact, $E(\text{guest})$ for a C_6D_6 in C_6H_6 is only 180 cm^{-1} above that of C_6H_6 in C_6D_6 instead of the predicted 215 cm^{-1} . This apparent 36 cm^{-1} shift is surprisingly large, however, and most likely indicates either that:

1) The vibronic state responsible for this shift is very nearly degenerate with the C_6D_6 guest 0,0 transition; 2) There is also a considerable contribution to the shift of the C_6H_6 guest energy due to interactions with higher crystal states; or 3) That the assumption that Δ is independent of the isotopic substitution of the guest and host is not valid.

That (1) is not the case can be shown by the small change in the C_6D_6 guest 0,0 energy as the host energy increases (see Table I). Either (2) or (3) could explain the poor agreement between $\rho(E)$ calculated from the β of NR and that observed experimentally. Note, however, that there is no solution to the Eq.

$$\delta = \frac{4\beta_1^2}{\Delta E_1} + \frac{4\beta_2^2}{\Delta E_2}, \quad (6)$$

which will give a simultaneous solution for guests below the host and guests above the host, if one assumes the isotope effect on ΔE_1 and ΔE_2 is the same. Thus, several perturbing states must be conjectured to explain the data by a quasiresonance method. In any event, the conclusion that $\beta = 18 \text{ cm}^{-1}$ is certainly questionable since the assumptions of the variation of energy denominators method appear to be invalid for this state. The good fit to the experimental data for C_6H_6 in different hosts obtained with a $\beta = 18 \text{ cm}^{-1}$ is not too surprising as the functional

dependence of $E(\text{guest})$ on ΔE is slowly varying and only known over a short range and can thus be fit equally well by an exponential or other non-linear function.

From this discussion, we can conclude that the variation of energy denominators method is internally inconsistent and cannot be used to evaluate β for benzene.

B. Gas-to-Crystal Shifts for Different Isotopic Guests

A study of the gas-to-crystal shift $\Delta + \delta$ for a number of guests in a single host provides evidence that β is actually less than 18 cm^{-1} . In Table I, it can be seen that, with the exception of C_6HD_5 , $\Delta + \delta$ is nearly constant for all guests in a C_6D_6 host, contrary to the trend expected for a β of 18 cm^{-1} ; $\Delta + \delta = -237 \pm 4 \text{ cm}^{-1}$ for all isotopes in C_6D_6 . For the isotopes other than C_6H_6 and C_6D_6 , the gas phase 0,0 is known only to within $3\text{-}6 \text{ cm}^{-1}$, and thus the small fluctuations in $\Delta + \delta$ are of no significance, and might be masking a slight trend. The errors are such that the less accurate gas phase values are most likely higher in frequency than the actual ones as the rotational contours for C_6H_6 and C_6D_6 have maxima $3\text{-}5 \text{ cm}^{-1}$ to the blue of the zeroth rotational level.¹² The expected effects of the deuterium substitution on the rotational contours makes it impossible to say anything more definite, but the scatter in the Δ 's is reduced if $3\text{-}5 \text{ cm}^{-1}$ are subtracted from the values for $\text{C}_6\text{H}_5\text{D}$, $p\text{-C}_6\text{H}_4\text{D}_2$, $\text{sym-C}_6\text{H}_3\text{D}_3$ and $m\text{-C}_6\text{H}_2\text{D}_4$. From this we can conclude that β is less than 18 cm^{-1} since the expected change in $\Delta + \delta$ of 12 cm^{-1} in going from a C_6H_6 to a $\text{C}_6\text{H}_4\text{D}_2$ guest is not observed, and that the smaller value suggested by the experimental $\rho(E)$ ($\sim 5 \text{ cm}^{-1}$) is more realistic.



The mixed crystal data can all be explained in a consistent manner by assuming that Δ is a function of isotopic substitution of the host. The functional dependence is such that the magnitude of Δ decreases as deuteriums are substituted onto the host molecules. The dependence of the guest gas-to-crystal shift on the isotopic substitution of the host can most clearly be seen for the case of $m\text{-C}_6\text{H}_2\text{D}_4$. In a C_6H_6 host, $\Delta + \delta = -241 \text{ cm}^{-1}$. Any simple interaction scheme involving the observed states of the host crystals would have predicted the opposite order, because δ should be negative for a C_6H_6 host and positive for a C_6D_6 host. A difference in the van der Waals interactions in liquid C_6H_6 and C_6D_6 has been reported,¹³ but just how this will effect Δ cannot be predicted a priori.

The isotopic dependence of Δ for neat crystals cannot be readily determined by comparing the C_6H_6 and C_6D_6 Davydov structures. The two higher energy Davydov components of C_6D_6 are displaced (Table II) about 203 cm^{-1} from the corresponding transitions in C_6H_6 , while the lowest component is shifted by 209 cm^{-1} . The lowest component may be shifted as a result of interactions between the C_6D_6 host states and the C_6D_6 impurity states. The $\text{C}_6\text{D}_5\text{H}$ occurs as an impurity at $\sim 2\%$ in the C_6D_6 samples.¹⁴ From this, one might conclude that Δ is nearly independent of isotopic substitution for neat crystals. However, in that the A_u level is not observed, a dependence of $M_{qq'}$ on isotopic substitution cannot be ruled out as neither the nature of the excitation exchange integrals nor the crystal structure parameters for C_6D_6 are known. Thus, any conclusions about Δ based on the positions of the observed components should be made with caution.

C. Vibronic Analysis of the Pure and Isotopic Mixed Crystal Spectra

Measurements of the vibronic structure of neat and mixed crystals provide the best evidence that the $\rho(E)$ determined from exciton band \longleftrightarrow exciton band transitions is an accurate representation of the ${}^1B_{2u}$ state of crystalline benzene. The first absorption observed to the blue of the neat crystal 0,0 is a weak, sharp line; see Table II. Its assignment to the 0,0 + $2\nu'_{18}$ ($e_{2g} + a_{1g}$) transition is based on the following evidence: 1) the $2\nu_{18}$ overtone combines with the 0,0 in both the gas phase absorption¹² and emission¹⁵ and in the isotopic mixed crystal fluorescence;¹⁰ 2) there is no other absorption observed between 0,0 and the 0,0 + ν'_6 (e_{2g}) transition which is the next higher absorption expected from knowledge of the gas phase spectra; and 3) its intensity in the crystal relative to the 0,0 ($\sim 1:100$) is about what is expected from the mixed crystal fluorescence. Somewhat surprising is the fact that this band does not appear as a triplet as it does in the mixed crystal emission. As the site symmetry is only C_1 , the three-fold degeneracy of the corresponding ground state overtone is removed (site group splitting) giving a triplet in the fluorescence and phosphorescence spectra. Another unusual feature of the transition is its large gas-to-crystal shift, $\Delta = -330 \text{ cm}^{-1}$ for neat C_6H_6 and $\Delta = -338 \text{ cm}^{-1}$ for neat C_6D_6 . However, these effects may be related to the large difference between the excited and ground state frequencies of the $2\nu_{18}$ overtone; for C_6H_6 , $2\nu'_{18} = 474.9 \text{ cm}^{-1}$, while $2\nu''_{18} = 798.2 \text{ cm}^{-1}$.

The $0, 0 + \nu'_1$ and $0, 0 + \nu'_6$ crystalline transitions have been assigned previously by their frequencies and relative intensities. All three of these vibronic transitions for guest molecules can be seen in at least some of the possible hosts. Their frequencies relative to the $0, 0$ transition for a C_6H_6 guest in several hosts are given in Table III. As discussed in Sec. II, the vibronic spacings should change from solvent to solvent if there are measurable quasiresonance shifts of the respective levels. The C_6H_6 $0, 0$ shifts 12 cm^{-1} in going from a C_6D_6 to a $p\text{-}C_6H_4D_2$ solvent and yet the vibronic spacings remain constant to $\pm 2 \text{ cm}^{-1}$. It would be a surprising combination of events, indeed, if the differences of quasiresonance shifts and differences in isotopic effects on the Δ all combined to cancel for each vibronic state and for each solvent. Thus, it must be concluded that the vibronic spacings are independent of isotopic substitution and that β is much smaller than 18 cm^{-1} . The $\beta \approx 5 \text{ cm}^{-1}$ predicted from the experimental $\rho(E)$ would certainly be consistent with the above results, as then $\delta < 2 \text{ cm}^{-1}$ for $\Delta E = 70 \text{ cm}^{-1}$.

As these vibronic spacings are found to be independent of the isotopic substitution of the host, they can be used with some confidence in determining the mean of the $0, 0$ band. The $0, 0 + 2\nu'_{16}$ transition is the best suited for such a determination as it exhibits no measurable exciton splitting in the pure crystal. Subtracting 392 cm^{-1} from the pure crystal transition gives $37, 838 \text{ cm}^{-1}$ for the mean of the $0, 0$ band of C_6H_6 and, neglecting the translationally equivalent interactions, Eq. (3) gives $37, 860 \text{ cm}^{-1}$ for the energy of the A_u Davydov level, in excellent agreement with the limits set by the determination of $\rho(E)$.

Broude^{2a} used a similar technique. However, he utilized the $0, 0 + \nu'_{16}$ transition which occurs as a doublet split by 2.1 cm^{-1} in the mixed crystals¹⁰ and by 9 cm^{-1} in the neat crystal.^{2a} The resonance interactions giving rise to the increased splitting make the use of this band questionable. His value of $\bar{\epsilon} + \Delta = 37,835 \text{ cm}^{-1}$ is in reasonable agreement with that obtained above.

Finally, it should be remarked that the constancy of the guest vibrational frequencies in various solvents virtually eliminates any quasiresonance explanation of the difference in the gas-to-real mixed crystal energy shift for a given guest $0, 0$ above or below the host band. If this difference were caused by large quasiresonance interactions with other crystal states, including ion-pair states, such interactions would most likely cause solvent effects on the vibronic spacings.

CONCLUSION

From the previous discussion, it can be concluded that: 1) the data obtained from the variation of energy denominators method cannot be used to determine β for the ${}^1B_{2u}$ state; 2) the static gas-to-crystal shift of a guest is dependent upon the isotopic substitution of the host; 3) the vibronic spacings of the guest absorption spectrum are independent of the host energy for a guest-host $\Delta E > 70 \text{ cm}^{-1}$, implying that the singlet $\beta \approx 5 \text{ cm}^{-1}$; and 4) the mean of the singlet exciton band is at $37,838 \text{ cm}^{-1}$.

Using the new value for mean of the exciton band, the A_u level can only be determined if the magnitude of the translationally equivalent interactions are negligible. However, the separations between the translationally equivalent molecules are quite large when compared to those between the interchange equivalent molecules. Thus, since the interchange equivalent interactions must be small for a $\beta \approx 5 \text{ cm}^{-1}$, it will be a good first approximation to neglect the $2(M_a + M_b + M_c)$ portion of Eq. 3. Doing so, and using the pure crystal absorption data (Table II), one predicts the $E^{A_u}(0)$ level to lie at $37,860 \text{ cm}^{-1}$ in agreement with the limits set by the density of states function ($37,815 \text{ cm}^{-1} \approx E^{A_u}(0) \approx 37,875 \text{ cm}^{-1}$). This position of the A_u level gives $M_{I \text{ II}} = -1.55$, $M_{I \text{ III}} = 3.93$, and $M_{I \text{ IV}} = 3.28 \text{ cm}^{-1}$ for the values of the interchange equivalent interactions, and 5.3 cm^{-1} for β . From these values, the density of states function can be calculated as in Ref. 5. The results of this calculation for a crystal of 32,000 molecules are in excellent agreement with the experimental density function as can be seen in Fig. 4. The various predictions of the factor group structure are compared in Table IV.

Fig. 4. Comparison of the 20.4°K experimental (solid bars) density-of-states function with that calculated from the \mathcal{M}_{ij} of this work (solid curve) [$\mathcal{M}_{I II} = -1.55$, $\mathcal{M}_{I III} = 3.93$, $\mathcal{M}_{I IV} = 3.28$ and $\mathcal{M}_a = \mathcal{M}_b = \mathcal{M}_c = 0 \text{ cm}^{-1}$].

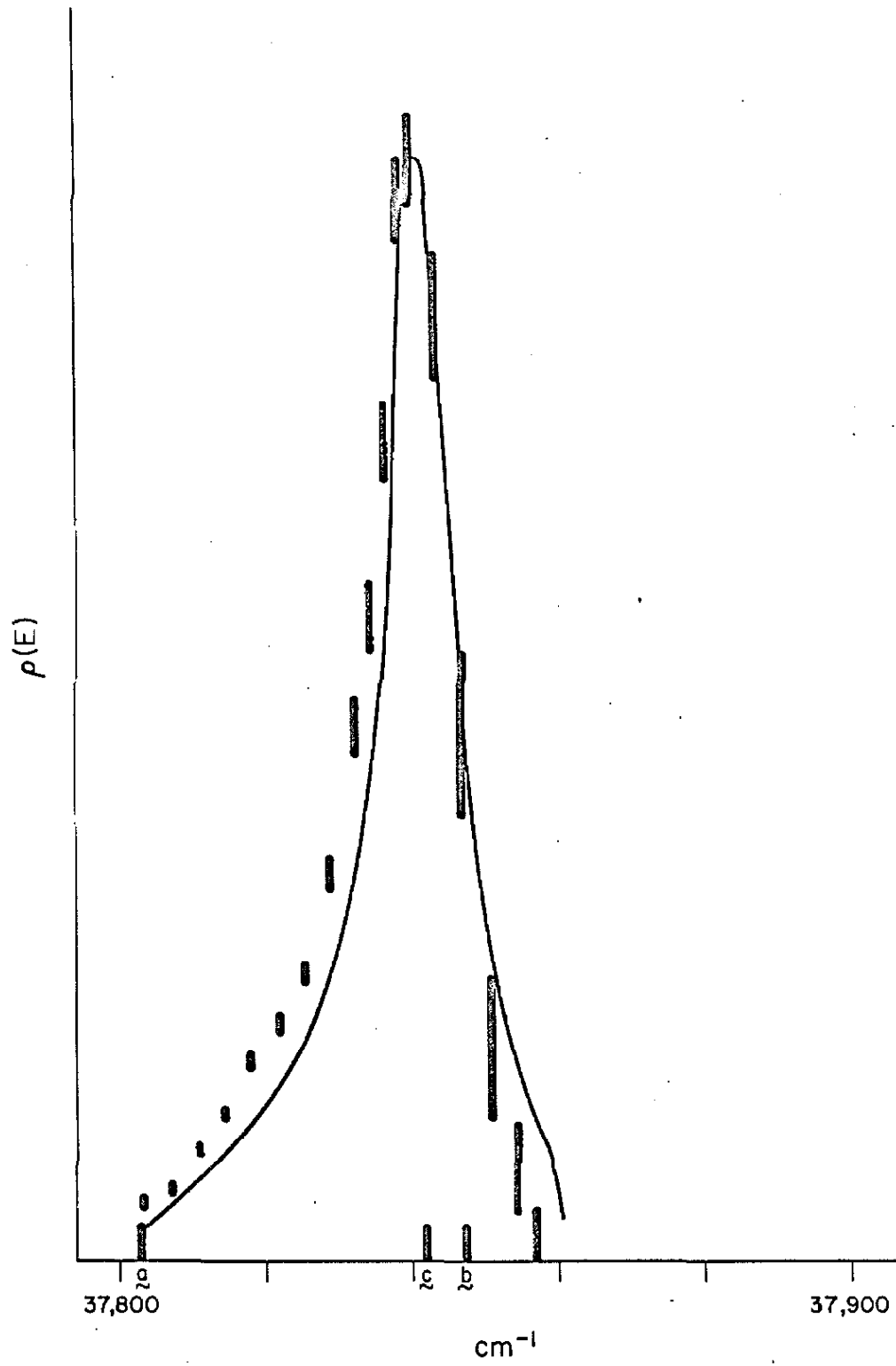


Table IV. Comparison of the Different Determinations of the Factor Group Structure of the ${}^1B_{2u}$ State of Crystalline Benzene. (The Energies (cm^{-1}) are given with respect to the center of the band.)

Reference	Factor Group Component			
	A_u	B_{1u}	B_{2u}	B_{3u}
Fox and Schnepf ^a	(+7)	(-29)	(+29)	(-7)
	+1.8	-7.2	+7.2	-1.8
Thirunamachandran ^b	+30	-44	+28	-14
Nieman and Robinson ^c	+124	-68	-25	-31
This work	+22	-35	+9	+4

^a The values in () are those reported by Ref. 1a; however, these values are for the entire electronic interaction and have been divided by a Franck-Condon factor (~ 4) to give the lower value for comparison with the other predictions. See Ref. 1c in this regard.

^b Ref. 1b.

^c Ref. 2b.

It should be emphasized that the use of first-order Frenkel theory would not be valid if mixing with the ion-pair exciton states were important. However, recent experiments on naphthalene¹⁶ have shown that there is considerable doubt as to the importance of such mixing with the lowest singlet of crystalline naphthalene. The agreement between the experimental density-of-states function and that predicted herein with a Frenkel approach and the constancy of the guest vibronic spacings in mixed crystals is also felt to be good evidence for neglecting the charge-transfer state in considering the excitation exchange interactions for the lower excited states of such molecular crystals.

References

- ¹(a) D. Fox and O. Schnepp, *J. Chem. Phys.* 23, 767 (1955);
(b) T. Thirunamachandran (Doctoral Thesis, University of London, 1961);
(c) R. Silbey, S. A. Rice, and J. Jortner, *J. Chem. Phys.* 43, 3336 (1965).
- ²(a) V. L. Broude, *Usp. Fiz. Nauk* 74, 577 (1961) [Engl. Transl. *Sov. Phys. --USP* 4, 584 (1962)];
(b) G. C. Nieman and G. W. Robinson, *J. Chem. Phys.* 39, 1298 (1963).
- ³E. R. Bernstein, S. D. Colson, R. Kopelman, and G. W. Robinson, (manuscript in preparation).
- ⁴The results of the calculations including interactions with ion-pair states of crystalline benzene (Ref. 1c) place the A_u component near the B_{2u} Davydov component. R. Silbey, private communication.
- ⁵S. D. Colson, D. M. Hanson, R. Kopelman, and G. W. Robinson, (manuscript in preparation).
- ⁶E. G. Cox, *Rev. Mod. Phys.* 10, 159 (1958); E. G. Cox, D. W. J. Cruickshank, and J. A. S. Smith, *Proc. Roy. Soc. (London)* A247, 1 (1958); G. E. Bacon, N. A. Curry, and S. A. Wilson, *Proc. Roy. Soc. (London)* A279, 98 (1964).
- ⁷R. Kopelman, *J. Chem. Phys.* 00, 0000 (1967).

- ⁸ S. D. Colson and E. R. Bernstein, *J. Chem. Phys.* 43, 4174 (1965).
- ⁹ S. D. Colson, *J. Chem. Phys.* 45, 4746 (1966).
- ¹⁰ E. R. Bernstein, S. D. Colson, D. Tinti, and G. W. Robinson (manuscript in preparation).
- ¹¹ R. G. Body and I. G. Ross, *Aust. J. Chem.* 19, 1 (1966).
- ¹² J. H. Callomon, T. M. Dunn, and J. M. Mills, *Phil. Trans. Roy. Soc. (London)* 259A, 499 (1966).
- ¹³ I. B. Rabinovich, *Zh. Fiz. Khim.* 34, [Engl. Transl. Russ. *J. Phys. Chem.* 34, 198 (1960)]
- ¹⁴ Determined from the I. R. spectrum of crystalline C_6D_6 , E. R. Bernstein, private communication.
- ¹⁵ F. M. Garforth, C. K. Ingold, and H. G. Poole, *J. Chem. Soc.* 1948, 508.
- ¹⁶ D. M. Hanson, R. Kopelman, and G. W. Robinson, (manuscript in preparation).

PART III

TRIPLET EXCITONS IN CRYSTALLINE BENZENE:
LOCATION OF THE FIRST AND SECOND TRIPLETS;
PHOSPHORESCENCE AND TRAP - TRAP
ENERGY TRANSFER IN ISOTOPIC MIXED CRYSTALS

Reprinted from THE JOURNAL OF CHEMICAL PHYSICS, Vol. 43, No. 8, 2661-2669, 15 October 1965
 Printed in U. S. A.

First and Second Triplets of Solid Benzene*

STEVEN D. COLSON AND ELLIOT R. BERNSTEIN

Gates and Crellin Laboratories of Chemistry,† California Institute of Technology, Pasadena, California

(Received 1 March 1965)

Absorption spectra have been taken of the O₂-perturbed first (³B_{1u}) and second (³E_{1u}) triplets of solid benzene at 4.2°K. Spectra of both C₆H₆ and C₆D₆ were obtained. The (0-0) bands of the first triplet occur at 29 674±25 cm⁻¹ for C₆H₆ and 29 851±25 cm⁻¹ for C₆D₆. For the second triplet they lie at 36 560 cm⁻¹±50 for C₆H₆ and 36 784±50 cm⁻¹ for C₆D₆. The result for the first triplet of C₆H₆ compares very favorably with Evans' gas-phase O₂-perturbed spectrum. It is also in satisfactory agreement with Nieman's accurate phosphorescence measurements on isotopic mixed crystals of benzene which place the C₆H₆ (0, 0) band position in the crystal at 29 657.1 cm⁻¹. Many precautions were taken to eliminate the possibility of misidentification of the second triplet. The observation that the O₂-enhanced first triplet and the O₂-enhanced bands in the 36 600-cm⁻¹ region always appear together and with approximately the same relative intensities is considered to be the best evidence for the assignment. However, the rather broad structure obtained by the O₂-perturbation technique does not allow all the uncertainties in the identification to be completely removed, nor does it allow a detailed study of this interesting state.

A detailed evaluation of the purity of the benzene is made, and a method is described for the preparation of material having ultrahigh spectroscopic purity. Crystals, up to 5 cm in length, of this very highly purified C₆H₆ and C₆D₆ were studied at 4.2°K to ascertain if the singlet-triplet absorptions could be seen in the absence of a perturbation. The long crystals showed some sharp and some broad ($\Delta\nu \approx 150$ cm⁻¹) absorptions starting at 36 947±50 cm⁻¹ in C₆H₆ and at 37 147±50 cm⁻¹ in C₆D₆. The broad absorptions correlate reasonably well with the features assigned to the second triplet in the O₂-perturbation experiments. The first triplet is too weak to be observed in the long-crystal experiments. The position of the second triplet lies about 3000 cm⁻¹ above that given by the Pariser-Parr calculation. This places the second triplet about nine-tenths rather than half of the distance from the lowest triplet to the lowest excited singlet.

INTRODUCTION

FOR many years the location of the second triplet state of benzene has been the object of much research, both theoretical and experimental.^{1,2} This intense interest has been generated by theoretical predictions, many and varied, of the energies of the excited states of aromatic hydrocarbons. All theoretical predictions identify the second triplet of benzene as the orbitally degenerate ³E_{1u} state, and most of these predictions place the second triplet in the experimentally accessible region between the lowest triplet and the

lowest singlet.³ Semiempirical theories^{4,5} for these energy levels, which are based partially on spectral data, have seemed fairly promising. Thus it becomes of great importance to fix experimentally as many of the states of the lowest π - π^* manifold of benzene as possible. Up to now, all three singlet states, but only one triplet state, the lowest, have been identified.⁶

¹ J. W. Moskowitz and M. P. Barnett, *J. Chem. Phys.* **39**, 1537 (1963); note that the use of a Goeppert-Mayer-Sklar core, accurate integrals, and extensive configuration interaction (Column e of Table I in this reference) places the second triplet above the first singlet.

² R. Pariser and R. G. Parr, *J. Chem. Phys.* **21**, 466, 767 (1953).

³ H. E. Simmons, *J. Chem. Phys.* **40**, 3554 (1964).

⁴ G. W. Robinson, in *Methods of Experimental Physics*, edited by D. Williams (Academic Press Inc., New York, 1962), Vol. 3, p. 244.

* Supported in part by the U. S. Atomic Energy Commission.
 † Contribution No. 3211.

¹ J. R. Platt, *J. Mol. Spectry.* **9**, 288 (1962).

² D. R. Kearns, *J. Chem. Phys.* **36**, 1608 (1962).

DETECTION OF HIGHER TRIPLETS IN AROMATIC HYDROCARBONS

Phosphorescence

The lowest triplet can be studied in emission (phosphorescence) since it can be populated by excitation into nearby singlets. The lowest triplet is the lowest excited state, and, even though the radiative transition probability for the emission process is extremely small, competing nonradiative processes are themselves sufficiently slow to allow detectable quantum yields of light emission. For higher triplets, however, nonradiative paths to lower triplets are so much more important than the highly forbidden radiative process back to the ground singlet state that quantum yields are vanishingly small.

Triplet-Triplet Absorption

Triplet-triplet absorption from the long-lived, lowest triplet state of benzene could yield information about higher triplets, just as it has done in other aromatic hydrocarbons.⁷ However, $g \leftrightarrow u$ selection rules would not allow strong absorption into the nearby higher triplets since these have the same parity as the lowest triplet. This selection rule is weakened if the molecule distorts and its center of symmetry is lost. The distortion may occur through molecular vibrations, solvent effects, or simply because the equilibrium configuration for the triplet is distorted. In any case the transition is not expected to be strong. This fact combined with the inconveniently low energy of the transition would cause detection of the second triplet in benzene by this technique to be difficult. Actually no evidence has yet been obtained for any kind of triplet-triplet absorption in benzene.⁸

Heavy-Atom Perturbations

Passing over phosphorescence and triplet-triplet absorption, there remain three other experimental methods which can be used to study the second triplet state of benzene: heavy-atom perturbation, O₂ perturbation,

⁷ G. Porter and M. W. Windsor, Proc. Roy. Soc. (London) A245, 238 (1958).

⁸ The most favorable system in which to search for the triplet-triplet absorption is probably the C₆D₆-argon system at 4.2°K. Here a gaseous mixture of less than 1% C₆D₆ with argon is condensed on a liquid-helium-cooled surface. The ³B_{1u} lifetime in this system is nearly 30 sec, and all observed vibronic components are quite sharp. The study in our laboratory of this system using intense, steady illumination for triplet excitation plus a continuum for detection of triplet-triplet absorption showed negative results for the region 2650–7000 Å. In contrast, using the same technique for naphthalene, the ³B_{1u} ← ³B_{2u} absorption in the 4000-Å region could be detected routinely with much greater intensity than that of the 3200-Å ¹B_{2u} ← ¹A_{1g} absorption even though the latter transition involves the ground state! No attempt was made to search for the ³E_{1u} ← ³B_{1u} transition of benzene which, according to results presented in this paper, should have its origin near 1.5μ.

and direct unperturbed absorption studies. Heavy-atom perturbations can arise from the environment or from substituents. Assuming the theoretical ideas of Robinson⁹ concerning environmental heavy-atom perturbations to be correct, perturbed oscillator strengths of not much more than $f \approx 10^{-7}$ may be obtained from solvent perturbations.¹⁰ If the heavy atom is chemically substituted onto the benzene ring, much larger oscillator strengths may result.¹¹ Even though future work may concern pure-crystal studies at 4.2°K of benzenes containing heavy-atom substituents, the primary interest in this paper revolves about the second triplet of benzene itself or of externally perturbed benzene.

Unperturbed Absorption

The experimental value of the oscillator strength for the spin and orbitally forbidden transition ³B_{1u} ← ¹A_{1g} (the first triplet) is $f \approx 10^{-10}$. This value has been derived from phosphorescence-lifetime measurements^{9,12} on both C₆H₆ and C₆D₆ combined with the accurate quantum-yield results of Lim.¹³ Purely theoretical values¹⁴ of 10⁻⁹–10⁻¹⁰ for the oscillator strength of the spin-forbidden but orbitally allowed second-triplet transition therefore seem too small. Such calculations may be plagued by cancellation effects in the spin-orbit energy of aromatics,¹⁵ in which case small wavefunction

⁹ G. W. Robinson, J. Mol. Spectry, 6, 58 (1961).

¹⁰ See Ref. 9, pp. 71–77. It is envisioned that the heavy-atom enhancement is caused by weak exchange interactions that couple the triplet state of the molecule to a Russell-Saunders triplet component of the electronically excited heavy-atom perturber. The triplet component of the perturber is in turn coupled to the singlet component of the perturber through strong spin-orbit mixing. In this manner the triplet state of the perturbed molecule borrows some singlet character from the perturber. For heavy-rare-gas perturbations, second-order perturbation theory yields,

$$f_p = [z\delta^2\zeta^2/2(F_0 - \bar{E}_T)^4] (\bar{E}_T/F_0)f_r$$

for the perturbed oscillator strength caused by the lowest ³P₁, ¹P₁ pair of the rare gas. Here z is the coordination number of solvent atoms around the perturbed molecule, δ is the electrostatic "excitation transfer" matrix element which is of the exchange type, ζ is the spin-orbit coupling constant for the ¹P₁ and ³P₁ states of the rare gas, F_0 is the term value for the rare gas, \bar{E}_T is the average triplet-state energy of the perturbed molecule, and f_r is the oscillator strength for the rare gas. A summation of such terms should be made over all perturbing states. For the most effective rare-gas perturber, solid xenon, the observed f_p for benzene is roughly 2.5×10^{-8} compared with the unperturbed value $f \approx 10^{-10}$. Here $z \approx 10$, $\delta \approx 50$ cm⁻¹, $\zeta = -6086$ cm⁻¹, $F_0 = 71\,095$ cm⁻¹, and $\bar{E}_T \approx 29\,800$ (see Table II of Ref. 9). Neglecting other states as a first crude approximation, a rare-gas ¹P₁ ← ¹S₀ oscillator strength of $f_r \approx 0.4$ would be required to explain the experimental result. This is a very reasonable value for f_r . To find a "clean" perturber which would push the perturbed oscillator strength to a factor of, say, more than 100 of what it is in xenon, would be difficult.

¹¹ A chemically bound heavy-atom substituent is expected to yield a δ which is 10–100 times larger than that for an intermolecularly bound entity.

¹² M. R. Wright, R. P. Frosch, and G. W. Robinson, J. Chem. Phys. 33, 934 (1960).

¹³ E. C. Lim, J. Chem. Phys. 36, 3497 (1962).

¹⁴ E. Clementi, J. Mol. Spectry, 6, 497 (1961).

¹⁵ D. S. McClure, J. Chem. Phys. 20, 682 (1952). Deviation of the molecular eigenfunction from a $2p$ (carbon) representation in the D_{6h} molecule or in a distorted form of the molecule would cause the cancellation to be inexact.

errors would give rise to serious errors in the oscillator strengths. Semiempirical estimates can, however, be made and are probably more reliable. For example, assume that the primary singlet-triplet mixing mechanism is spin-orbit coupling between $^1E_{1u}$ and $^3E_{1u}$ with further vibronic coupling between $^3E_{1u}$ and $^3B_{1u}$.¹⁶ The vibronic coupling constants for benzene singlets can be computed from the observed oscillator strengths and excitation energies for the $^1E_{1u}$, $^1B_{1u}$, $^1B_{2u} \leftarrow ^1A_{1g}$ transitions.⁶ One obtains $\langle ^1E_{1u} | ^1B_{1u} \rangle \approx 2000 \text{ cm}^{-1}$ and $\langle ^1E_{1u} | ^1B_{2u} \rangle \approx 800 \text{ cm}^{-1}$. Assuming the same kind of values hold in the triplet manifold and taking the energy separation between the $^3B_{1u}$ and $^3E_{1u}$ states to be roughly 7000 cm^{-1} , one finds that absorption into the $^3E_{1u}$ state should be from 12-75 times more intense than absorption into the $^3B_{1u}$ state.

It has been estimated that well over a meter of path length of liquid benzene would be required for the detection of the unperturbed first triplet transition.⁹ According to the above semiempirical estimate, the $^3E_{1u} \leftarrow ^1A_{1g}$ transition would presumably require 12-75 times less path, providing the line breadths were comparable. In such long paths of benzene, impurity absorption and hot-band structure from nearby intense singlet-singlet transitions become dominant. The hot-band structure is an especially severe problem when searching for the second triplet of benzene, since this state lies virtually in the shadow of the first singlet. The hot-band structure can be eliminated completely by working at liquid-helium temperatures.

The sharpening of structure is an added bonus at these low temperatures. Spectral line sharpening increases the chance of observing weak transitions. For instance, consider the oscillator strength for a transition

$$f = 4.3 \times 10^{-9} \int \epsilon_{\nu} d\nu, \quad (1)$$

where the integration is carried out over the extinction coefficient for all vibronic components, the units of ν being cm^{-1} . Taking a Gaussian line shape for each of m vibronic components, assumed for simplicity all to have equal intensity, one has⁶

$$f = (4.3 \times 10^{-9}) (m) (1.06 \epsilon_{\text{max}} \Delta\nu_{1/2}), \quad (2)$$

where $\Delta\nu_{1/2}$ is the width (in cm^{-1}) at half-maximum of each component, and ϵ_{max} is the extinction coefficient at maximum absorption. If half of the incident light is absorbed at the maximum extinction, detection of the absorption is well above threshold. In that case the required path length in centimeters is given by,

$$l(\text{cm}) = 1.4 \times 10^{-9} (m \Delta\nu_{1/2} / Cf), \quad (3)$$

¹⁶ A. C. Albrecht, J. Chem. Phys. 33, 156, 169 (1960); 38, 354 (1963).

where C is the concentration of the absorber in moles per liter.

There are about five intense components in the benzene $^1B_{2u} \leftarrow ^1A_{1g}$ absorption spectrum. Assume the same holds true for the triplets; thus $m \approx 5$. In pure crystalline benzene $C \approx 12$, and for the benzene transitions thus far observed at 4.2°K , the narrowest absorptions have $\Delta\nu_{1/2} \approx 2 \pm 1 \text{ cm}^{-1}$. This means that a path length of about 5-20 cm would be necessary to give $(I/I_0)_{\text{max}} = 0.5$ for absorption into the first triplet providing the absorption components were sharp. At room temperature in the liquid, the $\Delta\nu_{1/2}$ of each of the five most intense components is around 500 cm^{-1} , and Eq. (3) yields a path length of 30 m.¹⁷ This simple estimate illustrates the great advantages of working at low temperatures where the lines are of minimum width. For the second triplet, as noted earlier, one expects an increase of around one to two orders of magnitude in the oscillator strength compared with that of the first triplet. Thus it would seem to be a relatively easy matter to detect the second triplet in long-path absorption at low temperatures. It will be seen, however, that line broadening substantially lessens the ease with which the absorption can be detected.

O₂ Enhancement

In our initial search for the second triplet state of benzene, the method of O₂ enhancement¹⁸ was decided upon because of the extremely small oscillator strengths for unperturbed, multiplicity-forbidden transitions in aromatic hydrocarbons. In the present work, the O₂-perturbation method has been extended to low temperature in order to sharpen structure and to remove hot-band interference from the nearby $^1B_{2u}$ state. A perturbed oscillator strength of 10^{-5} would allow detection of the triplets in 0.01-cm paths of solid benzene even though the respective $\Delta\nu_{1/2}$ were as broad as 150 cm^{-1} . Such path lengths can easily be obtained through deposition techniques.⁹ The O₂-perturbation method, while yielding broad absorption lines and inaccurate vibrational spacings, would fix, within experimental accuracy, the position of the (0-0) band for the high triplets of aromatic hydrocarbons.

EXPERIMENTAL

Purification of Benzene

In the study of emission spectra or weak absorption spectra of organic molecules, the question of chemical

¹⁷ An earlier estimate of 1.5 m by Robinson, Ref. 5, was based on a detection threshold suggested by Craig *et al.*, J. Chem. Phys. 29, 974 (1958). It is felt that for the broad spectra, on top of a rapidly rising background absorption, such a threshold is unrealistic. The 30-m value above, it should be stressed, is not a threshold value. It is the path at which $(I/I_0)_{\text{max}} = 0.5$.

¹⁸ D. F. Evans, J. Chem. Soc. 1957, 1351

purity must always be carefully considered. For this reason a section devoted to the benzene purification methods used in this work seems appropriate.

Sources of the raw starting material were as follows. The C_6H_6 was obtained from three different sources: from the Phillips Petroleum Company, from D. R. Davis of the Chemistry Department, UCLA, and from the National Bureau of Standards. Two different samples of Phillips research-grade benzene were employed, one sample stated to have 99.93 mole % purity and another reportedly being 99.89 mole % pure. This material is furnished in capped bottles and is therefore air contaminated. It is stated that toluene is the major impurity, but it has been reported that about half of the impurity is water.¹⁹ The sample from UCLA had been twice purified by vapor-phase chromatography, degassed, and vacuum sublimed into a tube which was then sealed under vacuum. The NBS sample was prepared by carrying out a large number of careful recrystallizations using the Phillips research-grade benzene as starting material. Freezing-point data were used to set the purity level of the NBS benzene at 99.999 mole %.

Long-crystal absorption spectra provide a sensitive test for spectroscopic impurities, i.e., those impurities which alter the absorption or emission spectrum of an otherwise pure material. If the absorption spectrum of the contaminant is sharp, and its oscillator strength is high, impurity levels in the 10^{-7} – 10^{-10} -mole fraction range can be detected in a 5-cm path of crystalline benzene.²⁰ Because of extensive impurity absorption, in none of the three types of raw starting material mentioned above was it possible to get sufficient radiation through a 5-cm crystal to study absorption in the 2650–2800-Å region! A series of experiments on 2-cm crystals was therefore carried out to determine the nature of these contaminants. The UCLA sample was by far the most inferior, showing strong, broad absorption well to the long wavelength side of 3000 Å, and perhaps indicating the inadequacy of VPC purification for the removal of trace impurities. The major spectroscopic impurity in both the NBS sample and the Phillips sample was found to be phenol. An estimate made from absorption intensity indicated that the NBS sample contained 10^{-5} parts of phenol and little else that was spectroscopically observable. Interestingly enough, the Phillips research-grade benzene showed the smallest amount of impurity absorption. However, a wide variety of chemical impurities seemed to be present in the Phillips samples. Again, the major spectroscopic impurity was phenol, but it was present

to only about $\frac{1}{3}$ the extent of that in the NBS sample. A broad absorption band near 2690 Å is perhaps due to monochlorobenzene, while an underlying, nearly continuous absorption might be caused by toluene plus other unidentified impurities in the mole-fraction range 10^{-5} – 10^{-6} .

The C_6D_6 was obtained from Merck, Sharp & Dohme, of Canada, Ltd. It was said to be 99.5 at. % isotopically pure. The chemical purity was much like that of the NBS C_6H_6 sample, showing a mole fraction of about 10^{-5} perdeuterophenol as the major spectroscopic impurity.

The occurrence of phenol as a trace impurity in benzene has been noted previously.²¹ Its wide occurrence suggests that benzene may react with O_2 from the atmosphere. The reaction must be autoinhibited, however, since large amounts of phenol never seem to be produced. Care must therefore be exercised when handling high-purity benzene, just as it must be for higher aromatic homologs, so as not to allow atmospheric contamination.

It should be stressed that impurities at the concentration levels existing in the Phillips research-grade or NBS C_6H_6 , or the Merck C_6D_6 caused no problems for sample thicknesses up to about 0.2 mm. That is, in the absence of O_2 , only extremely weak impurity absorption could be detected in such samples at wavelengths through the near ultraviolet all the way down to the benzene cutoff at 2650 Å. Certain spectra appeared when 2% O_2 was present. They are discussed more fully later on.

For spectroscopic investigation of 5-cm benzene crystals much better purity is required than exhibited by any of the "raw starting materials." The benzene used in the long-crystal experiments is purified in the following manner. From the beginning of the process until after the crystal is grown, the benzene is kept in a vacuum system. A schematic diagram of the apparatus is shown in Fig. 1. The vacuum system is isolated from the oil diffusion and mechanical pumps by a $\frac{1}{2}$ -in. Kerotest metal valve (a) having a Teflon gasket. The benzene is transferred from a breakseal tube (b) to a vessel (c) where it is dried over vacuum distilled potassium. It is then degassed and transferred by two vacuum distillations through (e_1) to a vessel (i) mirrored with vacuum-distilled high-purity cesium (j). After the initial reaction, the sample is degassed and the cesium reaction vessel is sealed off at the constriction (f_5) from the rest of the vacuum system. The benzene is then refluxed over the cesium at about 100°C for 1 h. Conditions very much more severe than these were found to degrade the benzene and produce a large amount of undesirable impurity absorption. During the cesium refluxing, the parts of the system previously used are "pulled off" under vacuum at the constrictions (f_1), (f_2), and (f_3). The remainder of the

¹⁹ International Union of Pure and Applied Chemistry, Commission on Physico-Chemical Data and Standards, "Cooperative Determination of Purity by Thermal Methods," Report of the Organizing Committee, July 14, 1961, Vol. I.

²⁰ For example, 0.1% phenol can easily be detected as an impurity in a $10\text{-}\mu$ -thick crystal of benzene. For a 5-cm crystal, which is 5000 times thicker, 2×10^{-7} parts of phenol would be easily detected. The oscillator strength of the phenol transition is roughly 0.03.

²¹ V. L. Broude, Soviet Phys.—Uspekhi 4, 584 (1962) [Usp. Fiz. Nauk 74, 577 (1961)].

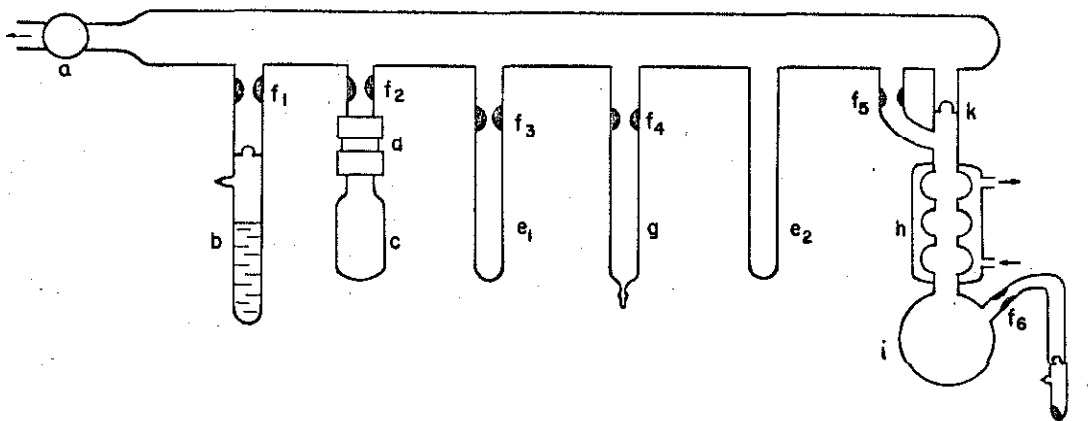


FIG. 1. Benzene purification manifold. (a) Kerotest (Kerotest, Inc., Pittsburgh, Pennsylvania) metal valve to cold traps, gauges, and oil-diffusion pump. (b) Benzene to be purified. (c) Potassium mirrored drying vessel. (d) Swagelok union, $\frac{1}{4}$ in., (Crawford Fitting Company, Cleveland, Ohio) for adding potassium. (e) Receiving vessel for primary vacuum distillations. (f) Constrictions for pulling off under vacuum. (g) Bridgman crystal-growing tube (14 mm \times 10 cm). (h) Water-cooled condenser. (i) Cesium reflux vessel (\sim 30 cc). (j) Cesium. (k) Breakseal.

system is thoroughly flamed until the limiting vacuum of 2×10^{-6} mm of Hg is attained. By means of a breakseal (k), the cesium vessel is reopened to the main vacuum manifold. The benzene is degassed thoroughly, and by two vacuum distillations through the intermediate tube (e_2) it is transferred into a Bridgman crystal-growing tube (g).²² It is then cooled to liquid-nitrogen temperature, and the tube is pulled off at (f_4). A 5-cm crystal purified in this way showed little or no absorption throughout the ultraviolet down to the 2700-Å region. In particular the mole fraction of phenol was estimated to be less than 10^{-3} !

Benzene-O₂ Experiments

The central idea here is to observe the spectrum of a mixture of benzene and oxygen in the region just to the long-wavelength side of the singlet-singlet system ($^1B_{1u} \leftarrow ^1A_{1g}$; $f \approx 0.0014$) whose origin lies near 2650 Å. Since thin (<0.2-mm) samples are used, purity is not a problem for the O₂-perturbed experiments. Phillips research-grade benzene, degassed but without further purification, was therefore used for these experiments.

As mentioned earlier, low temperatures are required to eliminate hot-band structure associated with the relatively much stronger singlet-singlet system.²³ Liquid-helium temperature is used in all of

²² D. Fox, M. M. Labes, and A. Weissburger, *Physics and Chemistry of the Organic Solid State* (Interscience, Publishers Inc., New York, 1963) p. 267.

²³ For example, according to this paper, the separation of the unperturbed (0, 0) bands of the first singlet and the second triplet is only about 900 cm⁻¹. At room temperature, hot band structure from the first singlet in the vicinity of the (0, 0) band of the second triplet is therefore expected to be down in intensity by only a factor of 150. Since even under O₂ perturbation the second triplet is at least 100 times weaker than the first singlet, there would be no chance whatsoever of detecting the second triplet at room temperature. The very highest temperature at which one can expect to separate the second triplet from the hot-band structure of the first singlet is 100°K, and much lower temperatures are to be preferred.

the experiments reported here. Another advantage of low temperatures, the sharpening of band structure, is not realized to its fullest extent in the O₂-perturbation experiments.

Because of the broad structure, a spectrograph of relatively low resolution is adequate for this portion of the work. The instrument used was a Bausch & Lomb medium quartz prism spectrograph. A 150-W Xe lamp was used as source for the absorption studies, while a Bausch & Lomb $f/3.5$ grating monochromator, in conjunction with the Xe lamp, was used to excite emission. Combinations of bromine gas, Corning Glass #9863, and aqueous nickel sulfate filters were used to reduce stray light from longer wavelength radiation.

Some earlier experiments in our laboratory attempted to detect the second triplet state of benzene by depositing at liquid-helium temperature benzene with excess oxygen; i.e., benzene in an oxygen "matrix." Only the well-known visible and near-ultraviolet bands of condensed oxygen²⁴ were discernible. Besides, in oxygen-rich systems it is very difficult, because of scattering, to get light through the thick deposits necessary for such low concentrations of benzene.

To avoid the problem of O₂ absorption which is caused by O₂-O₂ interactions and simultaneously to increase the path length of benzene, a mixture rich in benzene containing a few percent O₂ was used. In order for most of the benzene molecules in the solid to have nearest-neighbor contact with at least one oxygen molecule, an optimum concentration of oxygen would lie perhaps in the 5%-10% range. However, the maximum amount which was actually used was 2%, since higher concentrations seem to give deposits which strongly scatter the light.

The gaseous mixture containing 98% benzene and 2% oxygen was deposited on a window cooled to liquid-

²⁴ L. J. Schoen and H. P. Broida, *J. Chem. Phys.* **32**, 1184 (1960).

TABLE I. First and second triplet-state energies (in cm^{-1}) of C_6H_6 and C_6D_6 in O_2 -perturbed systems and pure crystals.

	O_2 perturbed		Benzene crystals	
	C_6H_6^a	C_6D_6	C_6H_6	C_6D_6
$^3B_{1u}$	29 674 \pm 25	29 851 \pm 25	29 657.1 ^b	29 855.1 ^c
	30 581	30 628		
	31 446	31 446		
	32 258	32 362		
$^3E_{1u}$	36 560 \pm 50	36 784 \pm 50	36 947 \pm 50	37 147 \pm 50
	37 170	37 495	37 496	not identified

^a Evans's¹⁸ values in the gas phase for this system are 29 440, 30 350, 31 250, and 32 100 cm^{-1} .

^b G. C. Nieman, Ph.D. thesis, California Institute of Technology, 1965, observed in 1% C_6H_6 in 99% C_6H_6 mixed-crystal phosphorescence. The corresponding value of the (0, 0) band position for the $^1B_{2u} \rightarrow ^1A_{1g}$ transition is 37 855 cm^{-1} . It should be noted that the pure-crystal value would be lower by about 50 cm^{-1} [see G. C. Nieman and C. W. Robinson, *J. Chem. Phys.* **39**, 1298 (1963)].

^c Obtained from C_6H_6 value by adding 198 cm^{-1} [see Ref. (b)].

helium temperature in a manner similar to that described by Robinson.⁹ Because of light scattering, the maximum deposit thicknesses that could be used were somewhere around 200 μ . This value was estimated from absorption intensities of the singlet-singlet systems of pure benzene and of a phenol-in-benzene standard sample. It is known that when pure benzene is deposited from the vapor phase at 4.2°K, the electronic spectrum appears very broad compared with the spectrum of a crystal of benzene more carefully prepared. It was discovered that benzene deposited at liquid-nitrogen temperature and then cooled to 4.2°K shows a sharp spectrum, just as in the case of a good crystal. Unfortunately, attempts revealed that little oxygen could be trapped in the benzene under these conditions. Furthermore, strong fluorescence emission from crystalline regions in this deposit masked any weak absorption bands which otherwise might have appeared. Therefore, this technique was abandoned in favor of the 4.2°K deposition experiments. No fluorescence occurred from the 4.2°K depositions containing O_2 . Perhaps deposit temperatures intermediate between 4.2° and 77°K would have been optimum, but no attempt was made to check this point.

Long-Crystal Experiments

Thick crystals of benzene are prepared in the following manner. The crystal-growing tube containing the ultrapure benzene is lowered into a -20°C cold room through a temperature gradient of 30°C/in. at a rate of $\frac{1}{4}$ in./h. The over-all temperature differential is about 50°C. The crystal is removed from the growing tube and both ends are cut off with a hot wire. The crystal is then polished with a warm brass block and

the 5-cm sample is placed in a loosely fitting Teflon holder, the crystal being kept in an inert atmosphere during all these manipulations. At this stage the crystal is completely transparent with only minor imperfections. During radiation cooling in two stages, first to 77°K, then to 4.2°K, the crystals become somewhat cracked. However, they remain fairly translucent in spite of this difficulty.

All spectra are taken at 4.2°K with the sample in a horizontal position. The optical arrangement and light sources were the same as before. However, a 2-m grating spectrograph having a resolution of about 35 000 was utilized in place of the low-resolution prism instrument in the event that sharp structure, such as factor-group structure, exists in the $^3E_{1u} \leftarrow ^1A_{1g}$ transition in the crystal.

IDENTIFICATION OF SECOND-TRIPLET ABSORPTION

There are three major problems in determining a weak absorption such as the second triplet of benzene. The absorption can be due to an impurity; a photoproduct can be produced during the experiment; or there can be broad but structured emission whose inverse may appear to be weak absorption. The experimental procedure is aimed at the elimination of these possibilities.

Benzene- O_2 System

The benzene- O_2 mixtures were prepared in the manner described in a previous section. A summary of absorption spectra obtained from these mixtures is presented in Table I. It is gratifying that the first triplet ($^3B_{1u}$) is easily detected by this technique. In addition to the first-triplet bands, two broad ($\sim 300\text{-cm}^{-1}$) features in the 36 600- cm^{-1} region of the spectrum occur under O_2 perturbation. Microdensitometer

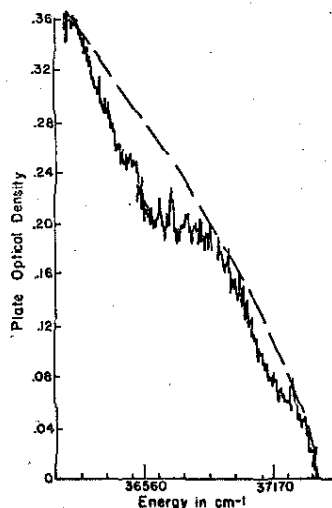


FIG. 2. Densitometer tracing of O_2 -perturbed second triplet of benzene; ---, assumed base line.

tracings of these features are depicted in Fig. 2. It is these features which are attributed to the second triplet (${}^3E_{1u}$). No absorption except that assigned to the first- and second-triplet bands occurs for wavelengths longer than the benzene first-singlet cutoff near 2650 Å.

After first observing the absorption thought to be caused by the second triplet, the system was completely taken apart and cleaned, and the experiment was repeated in the clean system. The absorption appeared as before. Then a completely different deposit Dewar (one previously used only for NH_3 , ND_3 , NH_2D , etc., and HCl and DCl) was used with an entirely new glass manifold. Again the same results were obtained.

To check for an impurity in the benzene, two different sources of C_6H_6 , the Phillips and the NBS, and one sample of C_6D_6 , the Merck, were tried, all giving consistent, corroborating results. An absorption spectrum of 1% phenol in C_6H_6 was taken, the second-triplet absorption was compared with this, and the two were found to be entirely different.

Spraying on benzene without O_2 showed absolutely no absorption for $\lambda > 2650$ Å. This fact combined with the simultaneous observation, when O_2 is added, of the well-known first-triplet absorption and the 36 600- cm^{-1} bands provides fairly convincing evidence for the existence of the second triplet in the 36 600- cm^{-1} region.

Three different supplies of O_2 were used; two types of Linde high-purity O_2 and an O_2 of standard purity. No evidence for the absorption spectrum of condensed O_2 was found.

The possibility of a photoproduct being formed during the experiment was also explored. Plates were taken of the O_2 -benzene mixtures after sample exposure times of from less than 1 sec to 1 h using a 150-W Xe lamp, and the absorption intensity was not seen to increase or decrease. No new absorptions were produced. Furthermore, varying the light intensity over a rather wide range by means of filters and a monochromator, showed no detectable change in the observed absorptions. This fact indicates that the absorptions are not caused by transitory photoproducts. The possibility that the absorption is an artifact due to broad emission was eliminated by using a Bausch & Lomb $f/3.5$ grating monochromator with a 150-W Xe source. Fluorescence spectra using 252- μ exciting light (bandpass of 200 Å) from this monochromator were searched for. In a $\frac{1}{2}$ -h exposure, no emission in the region of interest was observed. Typical absorption exposure times are of the order of 1 sec, so we have convinced ourselves that neither photoproducts nor stray emission can account for the 36 600- cm^{-1} bands.

Based on deposit times and bandwidths, it is possible to determine the relative perturbed intensities of the two triplet states. Our estimates give

$$I({}^3E_{1u}) : I({}^3B_{1u}) \approx 10-100 \quad (\text{O}_2 \text{ perturbed}).$$

It is interesting, and perhaps even surprising, that the ratio of the perturbed intensities is so similar to that expected on the basis of our earlier semiempirical estimates for the unperturbed intensities.

Crystalline-Benzene Experiments

As mentioned earlier, impurities are of much more concern in this system than in the previous one because of the long path length required for detection of the weak, unperturbed singlet-triplet absorption. It can be estimated that a sharp-lined impurity absorption with an oscillator strength of $f \approx 0.1-1.0$ could be detected for an impurity concentration of 1 part in 10^{10} ! For this reason, a positive assignment of an absorption caused by the ${}^3E_{1u} \leftarrow {}^1A_{1g}$ transition without a knowledge of detailed vibronic structure in the spectrum or without the O_2 -perturbation results would be impossible. Since the ${}^3E_{1u}$ state is so close to the relatively strong ${}^1B_{2u}$ state, little vibronic structure can be observed. Thus one must rely on a correspondence between any observed bands and the O_2 -perturbed spectrum.

Several absorptions, some sharp and some broad, were observed in the 2650-to-2800-Å region in both C_6H_6 and C_6D_6 . However, only two broad absorption features could be consistently identified in both samples, considering the expected perdeutero shift of about 200 cm^{-1} to higher energy. The intensity of these two features has always been observed to follow, in an expected manner, any changes in benzene path length. Furthermore, the intensity of these bands was found not to be dependent on the extent of purification of the sample, while the intensity of impurity lines change according to the purification method used. The most extensive purification was obtained with cesium refluxing, as described earlier in this paper. For one 5-cm crystal of C_6H_6 so purified, all impurity absorption was reduced to below or barely above the level of detection, while the two broad absorptions showed the same intensity as in less well purified samples.

The broad absorptions, which appear to belong to benzene itself, lie at $36\,947 \pm 50 \text{ cm}^{-1}$, and $37\,496 \pm 50 \text{ cm}^{-1}$ in C_6H_6 , and at $37\,147 \pm 50 \text{ cm}^{-1}$ in C_6D_6 . The second absorption feature in C_6D_6 was obviously present but was strongly overlapped by a series of sharp impurity lines and was therefore difficult to measure. The impurity was perhaps an isotopic or a chemical impurity that was not completely removed by the purification technique.

The broadness of the absorption was disappointing and somewhat unexpected at first, considering the sharpness of emission and absorption lines in other crystalline-benzene transitions. After a little reflection, however, one can find many mechanisms that could broaden the ${}^3E_{1u} \leftarrow {}^1A_{1g}$ transition. For instance, it is certain that the orbital degeneracy of the ${}^3E_{1u}$ state is removed by the crystalline field whose symmetry is

only C_2 . (This effect may be called *electronic site-group splitting*.) Further contributions to the degeneracy removal from the Jahn-Teller effect may also be important. The removal of this twofold degeneracy on top of the expected 100–200 cm^{-1} factor-group splitting²⁵ divides the (0-0) band and other totally symmetric vibronic bands into eight components, transitions to six of which are allowed. It is noteworthy that the observed 150- cm^{-1} total breadth of each band is of reasonable magnitude on the basis of such contributions. Further line-broadening mechanisms must be postulated, however, in order to explain the complete lack of resolution of any of this fine structure, since, ordinarily, individual components are not more than about 5–10 cm^{-1} broad, and the instrumental resolving power of the 2-m spectrograph used is not a limiting factor. The nature of this extra broadening is not known at the present time, but crystal strain to which the site-group splitting is sensitive may be responsible.

Estimating from the plates that $(I_0/I)_{\text{max}}$ for the second-triplet absorption bands is about 1.3 and applying Eq. (2) yields an oscillator strength of

$$f(^3E_{1u} \leftarrow ^1A_{1g}) \approx 7 \times 10^{-9} \quad (\text{unperturbed}).$$

It has been assumed that $\Delta\nu_1 \approx 150 \text{ cm}^{-1}$ and that $m=5$, but that three of the bands are overlapped by the singlet. The oscillator strength so obtained is wholly reasonable.

In all fairness it must be pointed out that the absorptions observed in the long-crystal experiments, in spite of all our precautions, could still be due to impurities. If this were the case, one would have to conclude that either the oscillator strength and breadth of the $^3E_{1u} \leftarrow ^1A_{1g}$ bands are such that the absorption could not be observed in crystals of this length, or that the transition energy lies above that of the first excited singlet. However, the correlation between the long-crystal absorptions and the O_2 -perturbed bands makes the second-triplet identification plausible. The $^3B_{1u}$ state was never observed in these long crystals. This fact is consistent with the oscillator strength $f \approx 10^{-10}$ for this transition.

SUMMARY

The following constitutes a summary of the reasons that the absorption bands in C_6H_6 and C_6D_6 , whose origins lie, respectively, at 36 560 and 36 784 cm^{-1} in the O_2 -perturbed system and at 36 947 and 37 147 cm^{-1} in the pure crystals, are believed to belong to the second-triplet ($^3E_{1u}$) transitions in these molecules.

(1) Evidence that the bands are not caused by impurity absorptions.

(a) The bands in C_6D_6 are shifted $220 \pm 50 \text{ cm}^{-1}$ to higher energy from those in C_6H_6 . The size of the

shift compares reasonably well, considering the accuracy of the measurements, with the deuterium shift in the other benzene transitions. This is not a binding argument, however, since protonated vs deuterated chemical impurities may well behave in the same manner.

(b) The absorption was seen in two sources of C_6H_6 and a totally different source of C_6D_6 .

(c) Varying the source of O_2 produced no effect.

(d) *Except for the 5-cm crystals, the absorption is not seen without O_2 in the sample.* This is the case not only for a deposited sample but also for a 2-cm-thick crystal of C_6H_6 or C_6D_6 .

(e) After making various checks, the sample used in the O_2 -perturbation experiments was found to be much too thin to show impurity absorption from C_6H_6 , C_6D_6 , or O_2 .

(f) The O_2 -perturbed absorption was seen in two entirely different deposit systems.

(g) Varying the exposure time and the light intensity produced no change whatever in the observed spectra, indicating that photoproducts are not responsible for the absorption.

(2) After careful investigation, the possibility was eliminated that the weak, broad absorption is an artifact caused by the presence of broad emission.

(3) Absorption spectra of 5-cm crystals of ultrapure benzene indicate that the $^3E_{1u} \leftarrow ^1A_{1g}$ transition lies higher than 36 900 cm^{-1} providing its oscillator strength is of the expected magnitude.

(4) That this absorption is the second triplet is evidenced by the following facts:

(a) *In the O_2 -perturbed system, the second triplet and the first triplet were observed in all instances during the same experiment in the same sample, and with approximately constant relative intensities.*

(b) The relative intensities of the three absorptions ($^1B_{2u}$, $^3B_{1u}$, $^3E_{1u} \leftarrow ^1A_{1g}$) are roughly of the expected magnitude.

(c) The absorption is indeed O_2 enhanced. This meets a criterion for a multiplicity-forbidden transition.

(d) The position of the absorptions is reasonable.

CONCLUSIONS

In the past, the search for the second triplet of benzene has usually been carried out at room temperature and in the liquid phase,²⁶ using O_2 - and heavy-atom-perturbation methods.²⁷ In all of these attempts no great pains were taken to purify the benzene or the perturbers. It is obvious from the earlier discussion that experiments of this nature are not likely to give positive evidence about higher triplet states in benzene. Hot bands, impurities, and spreading out of intensity are just a few of the reasons that data from such experi-

²⁵ G. C. Nieman and G. W. Robinson, *J. Chem. Phys.* **39**, 1298 (1963); E. R. Bernstein, S. D. Colson, R. Kopelman, and G. W. Robinson (to be published).

²⁶ A. C. Pitts, *J. Chem. Phys.* **18**, 1416 (1950); J. S. Ham and K. Ruedenberg, *ibid.* **25**, 1 (1956).

²⁷ For a general review of these experiments see Ref. 1.

ments are not definitive. Bands observed by Ham²⁸ at 77°K in a carbon tetrachloride glass have been assigned^{29,30} as the (0, 0) progression of the ${}^1B_{2u} \leftarrow {}^1A_{1g}$ transition intensified by solvent-solute interactions. We consider this assignment to be much more reasonable than the original suggestion that the Ham bands are the second triplet.

Even though positive identification of the broad absorptions observed in our 5-cm samples of pure benzene, as belonging to the ${}^3E_{1u} \leftarrow {}^1A_{1g}$ transition, is not possible, these experiments are very useful in placing a lower limit to the energy of this state. The ${}^3E_{1u}$ state of crystalline C_6H_6 cannot lie below 36 900 cm^{-1} . In the O_2 -perturbed C_6H_6 system no absorption (aside from the first triplet) was observed below 36 560 cm^{-1} . These results are consistent with the empirical lower limit of 37 000–38 000 cm^{-1} for the ${}^3E_{1u} \leftarrow {}^1A_{1g}$ transition as discussed by Platt.¹

Pariser-Parr theory⁴ places the position of maximum intensity of the ${}^3E_{1u} \leftarrow {}^1A_{1g}$ transition exactly halfway between the maxima of the ${}^3B_{1u} \leftarrow {}^1A_{1g}$ and the ${}^1B_{2u} \leftarrow {}^1A_{1g}$ transitions. Due to the lack of experimental data, these authors were forced to employ empirically evaluated integrals derived from the energies of observed singlet states to calculate triplet-state energies. There is no theoretical justification for this, since singlet and triplet wavefunctions, even though from a common configuration, are expected to require a different basis representation. The discrepancy between our experimental energy and that calculated for the ${}^3E_{1u}$ state on the basis of Pariser-Parr theory is about 3000 cm^{-1} . This value is based on (0, 0) band positions (see Table I) rather than on absorption maxima as specified in the theory, but for the states in question there should be no great difference.³¹ Thus, the second triplet lies

nearly $\frac{1}{3}$ rather than $\frac{1}{2}$ of the way from the lowest triplet to the lowest excited singlet state of benzene.

It should be noted that from our experiments no information can be obtained concerning the energy of the proposed O_2 -benzene charge-transfer states.³⁰ These states would have a continuous absorption spectrum and therefore could not be differentiated from light loss due to scattering in the deposit experiments.

Note added in proof: It is conceivable that the absorption observed in the 37 000- cm^{-1} region of the O_2 -perturbed system is due to the benzene- O_2 "double" transition [${}^3B_{1u} \leftarrow {}^1\Delta_g$] \leftarrow [${}^1A_{1g} \leftarrow {}^3\Sigma_g^-$]. Addition of the gas-phase value of the ${}^1\Delta_g \leftarrow {}^3\Sigma_g^-$ transition to the crystal-phase value of the ${}^3B_{1u} \leftarrow {}^1A_{1g}$ transition "predicts" the double transition to lie about 1000 cm^{-1} above that observed. This is not particularly close. Nevertheless, it would be unrealistic to exclude this as a possibility, considering the assumptions inherent in the prediction. Observing the transition using NO perturbation would eliminate this possibility. Deposit experiments were attempted in which the O_2 was replaced by NO. These proved to be unproductive as NO is a weaker perturber than O_2 , neither the first nor second triplet being observed. We are now working on new techniques that will hopefully yield long, transparent crystals of benzene containing NO. NO-benzene mixed crystals about 2 cm long have been produced, but so far have been so badly cracked that they are opaque in the 37 000- cm^{-1} region. The first triplet has, however, been detected in such crystals. We are also trying to grow crystals long enough to observe the first triplet (${}^3B_{1u} \leftarrow {}^1A_{1g}$) transition in the absence of external perturbations. We acknowledge B. Stevens of Sheffield University for suggesting the double transition to Robinson as a possible cause of the 37 000- cm^{-1} absorptions in the benzene- O_2 mixed crystal. It should not be forgotten, however, that similar absorptions have been seen in 5-cm crystals containing no O_2 where, of course, the double transition cannot occur.

ACKNOWLEDGMENTS

The many hours of discussion with and advice from Professor G. W. Robinson are greatly appreciated by the authors. Preliminary O_2 -perturbation work was done on this project by Mrs. Lelia Coyne.

²⁸ J. S. Ham, J. Chem. Phys. 21, 756 (1953).

²⁹ E. C. Lim and V. L. Kowalski, J. Chem. Phys. 36, 1729 (1962).

³⁰ N. S. Bayliss and L. Hulme, Australian J. Chem. 6, 257 (1953).

³¹ A recent theoretical calculation (Ref. 5) which employs more extensive configuration interaction within the framework of the Pariser-Parr theory, appears to give very good agreement with our experimental ${}^3E_{1u}$ energy. However, the calculated energies refer to intensity maxima. The theoretical (0-0) band position is 1000 to 2000 cm^{-1} lower than our experimental value. It should also be noted that "experimental values" for the ${}^3E_{1u}$ energy reported in Refs. 3 and 5 are not experimental values at all, only semiempirical estimates.

Reprinted from THE JOURNAL OF CHEMICAL PHYSICS, Vol. 45, No. 10, 3873, 15 November 1966
 Printed in U. S. A.

Observation of the Second Triplet of Solid Benzene Using NO Perturbation*

ELLIOT R. BERNSTEIN AND STEVEN D. COLSON

*Gates and Crellin Laboratories of Chemistry†
 California Institute of Technology, Pasadena, California*

(Received 14 July 1966)

AS mentioned in our previous paper on the first and second triplets of solid benzene,¹ the absorptions observed in the 37 000-cm⁻¹ region under O₂ perturbation could conceivably be "due to the benzene-O₂ 'double' transition [³B_{1u} ¹A_g] \leftarrow [¹A_{1g} ³Σ_g⁻]." To eliminate this possibility, benzene-NO mixed crystals have been grown and their spectra taken. The mixed crystals were prepared in the following manner: The benzene was purified as before and checked for purity by taking its spectrum. No impurity absorptions in the 37 000-cm⁻¹ region were observed in 2-cm-thick crystals at 4.2°K. The NO was purified by a series of vacuum sublimations until the originally multicolored solid was white. NO, thus purified and placed in a hydrocarbon glass at 77°K, shows no absorption in the 37 000-cm⁻¹ region. However, in the 40 000-cm⁻¹ region a strong cutoff was observed, believed to be caused by the γ bands of NO, indicating that NO had dissolved in the glass.

Several NO-benzene mixed crystals were prepared by loading a sample cell containing purified benzene with 10⁻¹ to 10⁻² liter·atm of the purified NO gas. Crystals were grown by lowering the cell at the rate of 1 mm/h through a temperature gradient of about 100°C/cm (10° to ~-100°C), and then directly into liquid N₂. This technique gives excellent pure benzene crystals

but the mixed crystals were highly cracked. The mixed crystals containing large amounts of NO were so cracked that only the (0-0) band of the first triplet absorption system could be seen. However, the crystals more dilute in NO were sufficiently less scattering to be investigated in the 37 000-cm⁻¹ region.

New absorptions are observed at 36 983±50 and 37 324±50 cm⁻¹. These are assigned to the second triplet transition (³E_{1u} \leftarrow ¹A_{1g}) of the perturbed solid benzene system. The reason for the difference between the energy of these absorptions and those observed under O₂ perturbation (36 560±50 and 37 170±50 cm⁻¹) is not obvious. It does not appear to be large enough to justify a new interpretation. It therefore seems improbable that the absorptions observed in the O₂-perturbed system are due to a benzene-O₂ "double" transition. The absorptions both in the benzene-O₂ and the benzene-NO systems in the 37 000-cm⁻¹ region are, as concluded earlier,¹ most likely caused by the perturbed second triplet of benzene.

The support and encouragement from Professor G. W. Robinson is gratefully acknowledged by the authors.

* Supported in part by the U.S. Atomic Energy Commission.

† Contribution No. 3395.

¹ S. D. Colson and E. R. Bernstein, *J. Chem. Phys.* **43**, 2661 (1965).

Static Crystal Effects on the Vibronic Structure of the Phosphorescence,
Fluorescence, and Absorption Spectra of
Benzene Isotopic Mixed Crystals

E. R. BERNSTEIN, S. D. COLSON, D. S. TINTI, and G. W. ROBINSON

Gates and Crellin Laboratories of Chemistry,
California Institute of Technology, Pasadena, California 91109

The phosphorescence, fluorescence and absorption spectra of the isotopic benzenes C_6H_6 , C_6H_5D , $p-C_6H_4D_2$, and $sym-C_6H_3D_3$, present as dilute guests in a C_6D_6 host crystal at 4.2°K, are obtained with sufficient spectral resolution to ascertain the magnitude of the crystalline site effects. Two such effects are emphasized: site splitting of degenerate fundamentals and orientational effects. The former can occur for the isotopes C_6H_6 and $sym-C_6H_3D_3$, while the latter is possible only for isotopes with less than a molecular three-fold rotation axis. The observations show that both site-splitting and orientational effects do occur as a general rule on vibronic and vibrational states in benzene isotopic mixed crystals. We conclude, therefore, that the site interactions are not negligible.

An empirical correlation of the magnitudes of the site splitting, orientation effect and site (gas-to-crystal) shifts for in-plane and out-of-plane modes is noted. Our results for the ground state vibrations are in good agreement with the findings of Bernstein from infrared spectra in those cases where levels can be observed by both techniques.

In order to characterize completely the above mentioned site effects it was necessary to analyze in some detail both the emission and absorption spectra of the isotopic guest molecules. The phosphorescence of C_6H_6 and sym- $C_6H_3D_3$ has been completely analyzed out to $0, 0-(\nu_8 + \nu_1)$ while for that of C_6H_5D , the analysis of only the more intense bands near the electronic origin has been carried out. Some ground state vibrations of p- $C_6H_4D_2$ are presented but the phosphorescence spectrum, complicated greatly by both ground and excited state orientational effects, is not analyzed in this present work. The fluorescence of these isotopes was used only to corroborate and supplement the conclusions and assignments extracted from the phosphorescence analysis and is not presented in detail. The relative vibronic intensities in the fluorescence spectrum are compared to those in the phosphorescence. From the general analysis it is possible to conclude that the effect of the crystal site on the molecule, while spectroscopically measurable, is quite small.

On heavily exposed photographic plates it has been possible to assign the $^{13}CC_6H_6$ emission spectra in both the pure electronic and a few vibronic bands. Absorption spectra of these mixed crystals have yielded information concerning

the orientational effect on the first excited singlet state of C_6H_5D and $p-C_6H_4D_2$ as well as site splitting of the ν'_6 vibrational levels of C_6H_6 . The $^{13}CC_5H_{6-n}D_n$ 0,0 absorption spectra have also been identified. New absorptions, in the region of the 0,0 of C_6H_6 and C_6H_5D have been tentatively assigned to resonance pair lines and $^{13}C_2C_4H_{6-n}D_n$ on the basis of their intensity behavior as a function of guest concentration

I. INTRODUCTION

Since the classic work of Halford,¹ Hornig,² and Winston and Halford³ in the late 1940's, the effect of the crystal environment on molecular spectra has been of much interest. These early works deal in part with the effect of the crystal site on the degenerate molecular states. More recently, Bernstein⁴ and Strizhevsky⁵ have considered further site interactions not limited only to degenerate states, viz., orientational effects,⁴ gas-to-crystal shifts,⁴ and enhanced Fermi resonance^{4,5} in the solid. For experimental as well as historical reasons, most of these investigations concern the ground state vibrations observable by means of infrared spectroscopy. Since it is of theoretical importance to know whether or not such effects are present for all the vibration classes and types, in the present work we look for the above effects in the vibronic transitions of C_6H_6 and some of its deuterated isotopes: that is, the phosphorescence, fluorescence, and absorption spectra of various benzene isotopic mixed crystals. This allows us to study site interactions in vibrations which are not seen by infrared absorption.

For the case of a C_6H_6 guest in the C_i site of a C_6D_6 host crystal, the molecular $\underline{u}, \underline{g}$ classification of guest states is retained, imposing the $\underline{u} \leftrightarrow \underline{g}$ dipole selection rule for the C_6H_6 transitions. Thus, in the infrared absorption spectra from the \underline{g} -ground state, only \underline{u} -vibrations are observed, while vibronic transitions involving \underline{u} -excited states can be utilized to study \underline{g} -vibrations. The emission spectra also supplement the vibrational data obtained employing the Raman effect. On the other hand, in an isotope that does not have inversion symmetry, the infrared absorption and the UV emission spectra can involve the same vibrations, and thus the data complement each other. For example, in the case of site splitting of degenerate fundamentals, the infrared and UV data for C_6H_6 should supplement one another due to the $\underline{u} \leftrightarrow \underline{g}$ selection rule, while for the case of sym- $C_6H_3D_3$ these data should overlap and check one another. Similarly, for the orientation effect, the C_6H_5D data should overlap with both techniques while for p- $C_6H_4D_2$, there would be no direct overlap of data. It was from these considerations that C_6H_6 , C_6H_5D , p- $C_6H_4D_2$, and sym- $C_6H_3D_3$ were chosen for this work. These were all studied as dilute guests in a C_6D_6 host crystal at 4.2°K. By such a study we hope to provide a complete picture of crystal effects on vibrations of the benzene molecule for all classes and types and, therefore, furnish a good test for theoretical calculations of intramolecular and intermolecular force fields and potentials in solid benzene.

A vibrational analysis of the benzene phosphorescence spectrum in EPA at 77°K was first published by Shull.⁷ Sveshnikov and co-workers⁸ and Leach and Lopez-Delgado⁹ have compared the vibronic structure of phosphorescence and fluorescence, again in glasses at 77°K. Nieman¹⁰ and Nieman and Tinti (NT)¹¹ have analyzed the benzene phosphorescence under low resolution for many benzene isotopes in a C_6D_6 host crystal at 4.2°K.

The benzene emission spectra in amorphous solids do not generally show resolvable crystal effects on the ground state vibrations. While a few of the larger of these effects were observed in the lower resolution crystal spectra of NT, it is only with the higher resolution employed here that the effects are discernible on nearly all vibronic bands as a general occurrence and can be quantitatively discussed with confidence.

II. THEORETICAL CONSIDERATIONS OF CRYSTAL EFFECTS ON VIBRATIONS

Crystal effects on vibrations have been considered in great detail previously both in our laboratory and others. We will only discuss the general results as needed here, referring the reader to the more detailed work when necessary. Site splitting^{1,2} for a molecular energy state occurs if this level has a degenerate representation in the group of the molecule which maps into one or more nondegenerate representations in the group of the crystal site. Thus, the doubly degenerate vibrations of C_6H_6 and sym- $C_6H_3D_3$ are mapped into two nondegenerate components in the \tilde{C}_i site of the benzene crystal. The energy difference between these two components in an "ideal mixed crystal" is defined as the site group splitting δ_{SS} .^{4,12} The concept of an "ideal mixed crystal" implies the absence of all resonance and quasi-resonance intermolecular interactions, while all other interactions remain as in the pure crystal. Dilute (<1%) isotopic mixed crystals of benzene have been shown to be an excellent approximation to the "ideal mixed crystal" for ground state vibrations.⁴ This is found not to be true, however, for the lowest excited singlet state of benzene.¹³

For benzene isotopes without a molecular threefold axis, a different effect occurs.⁴ It is clear that in the \tilde{C}_i site there are three possible

orientations with respect to rotation about the original C_6H_6 sixfold axis for the isotopic molecule that, at least in principle, could have different energies. Therefore, a nondegenerate molecular vibration could give rise in the spectrum to three lines, each of which is due to differently oriented molecules in three physically equivalent but distinct sites. For other site symmetries, in general a different number of physically distinct orientations are possible. Thus, the number of lines observed in the spectrum for a given vibration is an indication of the effective site symmetry. Table I summarizes the number of orientations group theoretically possible for benzene isotopes in various sites.

The observations of either effect measures the effect of the static field on the guest molecule. However, certain interaction terms present in one are absent in the other. In the orientational effect, which involves two or more guest molecules on different sites, the ground state terms do not necessarily cancel. These terms must cancel in transitions to the two site split components. Moreover, the two site split components have the same symmetry in the crystal site and can interact with each other, increasing the first-order splitting given by interaction with the static crystal field. This latter interaction can not, of course, occur for molecules on widely separated sites, i. e. for the orientational effect. Because of these differences, a direct comparison of the respective magnitudes of these effects is difficult at best and could be misleading.

III. EXPERIMENTAL

The benzenes were obtained from Merck, Sharp and Dohme, Ltd., of Montreal, Canada. The mixed isotopic solutions were purified by the method described by Colson and Bernstein¹⁴ and directly vacuum distilled into modified "Bridgman type" growing tubes, of the type depicted in Fig. 1. Two

TABLE I. Number of possible orientations for benzene isotopes in sites of different symmetries.

Molecule	Molecular Symmetry	Site Symmetry			
		\tilde{C}_1	\tilde{C}_i	\tilde{C}_{2h}	\tilde{D}_{2h}
C_6H_6	D_{6h}	1	1	1	1
C_6D_6	D_{6h}				
sym- $C_6H_3D_3$	D_{3h}	2	1	1	1
p- $C_6H_4D_2$	D_{2h}	3	3	3, ^a 2	2
C_6H_5D					
o- $C_6H_4D_2$	C_{2v}	6	3	3, ^a 2	2
m- $C_6H_4D_2$					
vic- $C_6H_3D_3$					
asym- $C_6H_3D_3$	C_s	12	6	6, ^a 3	3

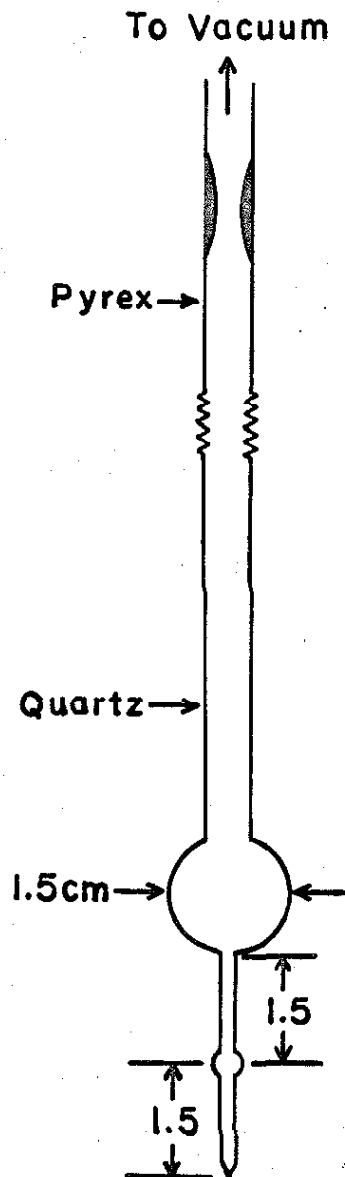
^aPlane of the site same as the molecular plane.

Caption for Fig. 1.

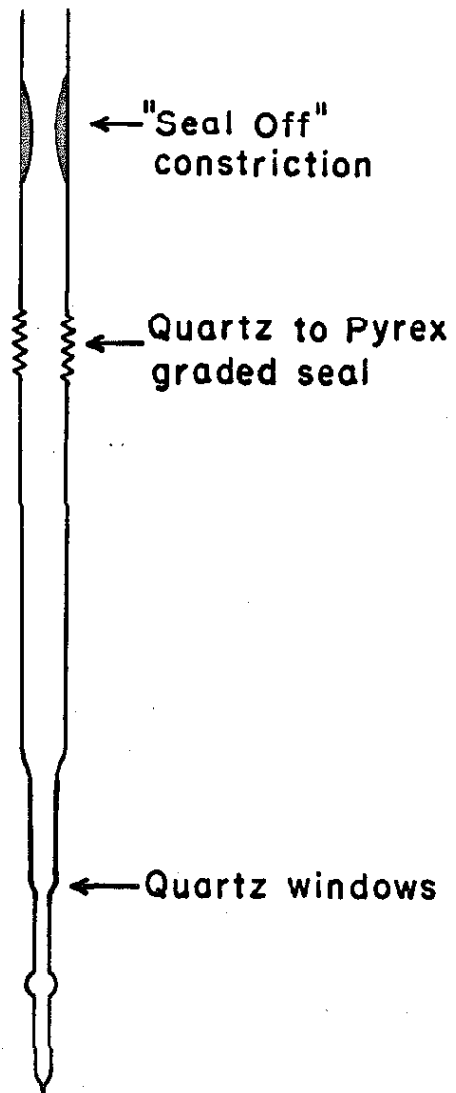
Modified "Bridgman-type" sample cell.

SAMPLE CELL

FRONT VIEW



SIDE VIEW



thicknesses of crystal were used: 3 mm and $\sim 20 \mu$. The thick crystals were grown by lowering the optical cells through a temperature gradient of about $100^\circ\text{C}/\text{cm}$ directly into a liquid N_2 cooled chamber at the rate of roughly 1 cm/day. These crystals, which are usually transparent and nearly free of cracks, are then cooled to 4.2°K with little decrease in quality. This same technique has been successful in growing crystals up to 3 cm in length. The thin crystals are grown in the same type tube by suspending the holder in a dewar approximately 20 cm above the liquid N_2 surface and subsequently cooling to helium temperatures. Once the crystal holder is completely submerged under the liquid helium, the cell is broken open above the graded seal to insure good thermal contact with the coolant. If this is not done, the sample temperature has been found to remain well above 4.2°K for some length of time and increases when the sample is irradiated.

The emission spectra of the guest triplet and singlet states were excited by absorbing into the C_6D_6 host singlet exciton band from which the excitation energy is rapidly transferred to the lowest excited singlet and triplet states of the guest. These lie approximately 30 cm^{-1} to lower energy for each hydrogen substituted into C_6D_6 . The guests thus serve as effective energy traps from which emission is observed at low temperatures. Both low and high pressure Hg lamps were employed as excitation sources. Order sorting, where necessary, was accomplished by liquid Kasha or Corning glass filters in conjunction with 0.1 m-atm Cl_2 and Br_2 filters. When high orders were used, a small Bausch and Lomb monochromator was used as a predispersing element or as an order sorter.

The phosphorescence spectra of the mixed isotopic crystals were photographed at 4.2°K on a Jarrell-Ash 3.4 meter Ebert spectrograph. Two gratings were employed. The first had 15000 line/in yielding a plate

factor of roughly $1.62 \text{ \AA}/\text{mm}$ in the third order. Exposure times for the more intense vibronic lines were about 5 min with 20μ entrance slits. The weaker lines required approximately one hour exposures. A second grating was used in the eighteenth order where the plate factor was $0.32 \text{ \AA}/\text{mm}$. Only the more intense vibronic lines of C_6H_6 were photographed, requiring exposure times with 40μ entrance slits of four hours.

All fluorescence and some of the survey phosphorescence spectra were obtained on a 2.0 meter Czerny-Turner spectrograph, constructed in our laboratory, with a 15000 line/in grating blazed at 1.0μ . Spectra were taken in third order where the dispersions are $2.4 \text{ \AA}/\text{mm}$ and $3.7 \text{ \AA}/\text{mm}$ in the phosphorescence and fluorescence regions, respectively. The exposure times for 5μ slits were roughly 5 min. Some of the very weak phosphorescence lines were measured from these plates.

Absorption spectra were taken on the 3.4 meter instrument utilizing the fourth order of the lower resolution grating which gives a dispersion of roughly $1.23 \text{ \AA}/\text{mm}$ at 2650 \AA . A few spectra were also photographed with the higher resolution grating.

IV. EMISSION SPECTRA

Both fluorescence and phosphorescence emissions have been photographed for the isotopic guest in a C_6D_6 host crystal at 4.2°K . Exposure times for the more intense features are roughly equal for the two emissions at lower dispersions, implying nearly equal quantum yields for the singlet and triplet emissions of the guest molecule for the isotopes studies. Furthermore, the measured phosphorescence lifetime of the guest molecule for C_6H_6 , $\text{C}_6\text{H}_5\text{D}$, $p\text{-C}_6\text{H}_4\text{D}_2$, and $\text{sym-C}_6\text{H}_3\text{D}_3$ is independent of the isotopic composition of the guest and its concentration for less than about 1% guest by weight.

The phosphorescence intensity, followed over the first decade change for isolated vibronic lines, decayed exponentially within experimental error with an average lifetime of 8.7 sec. This constant triplet lifetime implies that the quantum yields remain approximately constant independent of the guest and thus appear to be crystal determined.

The phosphorescence does have somewhat sharper lines and is thus easier to photograph at higher dispersions. Due to this smaller linewidth and the greater cm^{-1} dispersion available in the phosphorescence spectral region, we have concentrated mainly on the phosphorescence spectrum as a means of studying ground state vibrations. The larger of the site splittings to be discussed is resolved in both emissions and we have used the fluorescence to complement the phosphorescence where possible.

The narrowest phosphorescence linewidth at the highest resolution employed was approximately 0.1 cm^{-1} and seemed to be limited by the quality of the crystal. This linewidth was observed only once in a very transparent, seemingly near perfect, crystal of 0.04% C_6H_6 in C_6D_6 . The linewidth of 0.1 cm^{-1} was superimposed on a weaker background whose width was approximately 0.5 cm^{-1} . This latter width probably corresponds to residual crystal imperfections. It should be noted that the narrowest linewidth we obtained roughly equals the expected zero-field splitting in the triplet state. Thus, the vibronic linewidth which would result from the uncertainty broadening of the ground state excited vibrational level may be much less than 0.1 cm^{-1} , implying that the vibrational relaxation time in the ground state is $\geq 5 \times 10^{-11}$ sec.

The lowest benzene triplet state most likely has B_{1u} symmetry in point group \underline{D}_{6h} .¹⁵ It is thus both spin and electronically forbidden. This double forbiddenness can be formally removed in a second-order perturbation scheme

by some combination of spin-orbit and vibronic mixing such that the active vibrations must have symmetries contained in $\Gamma_T \times \Gamma_S \times \Gamma_R$ where Γ_i is the irreducible representation in point group \underline{D}_{6h} of the phosphorescing triplet state, the dipole allowed singlet state, and the spin-orbit operator for $i = T, S,$ and $R,$ respectively. In this way $e_{2g}, b_{2g},$ and e_{1g} vibrations are group theoretically predicted to be active in the phosphorescence spectrum for the free \underline{D}_{6h} molecule.

Albrecht¹⁶ has analyzed various first- and second-order mechanisms for bringing dipole-allowed singlet character into the triplet state. From the polarized phosphorescence spectrum in solid glass at 77 °K, he concludes that the bulk of the transition probability arises from vibronic mixing, utilizing the e_{2g} vibrations ν_8 and ν_9 ¹⁷ of the lowest triplet with the $^3E_{1u}$ state which is spin-orbit coupled to the dipole-allowed singlet states $^1A_{2u}$ and $^1E_{1u}$. Assuming this mixing route and that the lowest excited singlet has B_{2u} symmetry, the vibronic structure of the phosphorescence implies the $^3B_{1u}$ assignment for the lowest triplet state in point-group \underline{D}_{6h} .

For the lowest excited benzene singlet state,¹⁸ B_{2u} symmetry in point-group \underline{D}_{6h} has been established with greater certainty than the triplet symmetry. The spatial forbiddenness of the transition between the ground $^1A_{1g}$ state and the lowest excited $^1B_{2u}$ state can be formally removed by vibronic mixing with the dipole allowed $^1E_{1u}$ and $^1A_{2u}$ states. The latter route requires a b_{1g} fundamental of which benzene has none. However, e_{2g} vibrations can mix a B_{2u} and an E_{1u} state. Thus, vibrations of species e_{2g} are group theoretically predicted to be active in the fluorescence and singlet absorption spectra. Vibronic calculations¹⁹ predict that the e_{2g} vibration ν_8 should dominate.

In the \underline{C}_i site of the C_6D_6 host crystal, only the u, g-classification of molecular states is retained and, therefore, the above group-theoretical arguments are no longer rigorously correct. However, it is found experimentally (*vide infra*) that the above scheme predicts the dominant features of the spectrum, implying that the molecular classification of states is still approximately valid. The effect of the site is demonstrated by the appearance in both the fluorescence and phosphorescence of a totally symmetric progression built on a relatively weak 0, 0 band.

One feature common to both emissions is the activity of a 72 cm^{-1} lattice phonon. This frequency is apparently determined primarily by the C_6D_6 host, independent of the guest, since the value does not measurably change for different isotopic guests. The phonon emission band is quite broad ($\sim 5\text{ cm}^{-1}$) and is usually photographed only for the stronger molecular bands. Crystalline C_6D_6 does have two observed²⁰ optical phonons in this range with frequencies of 62 and 77 cm^{-1} at 4.2°K . Some unobserved optical phonons are also estimated²⁰ to have very similar frequencies so that the species of the phonon is not known with certainty. Symmetry arguments require that it be a gerade type.

1. C_6H_6

The more active vibrations in the phosphorescence spectrum of C_6H_6 in a C_6D_6 host are the same as previously assigned in the solid glasses. However, the much sharper lines in the mixed crystal allow a more nearly complete analysis. For example, some of the fundamentals of $^{13}C^{12}C_5H_6$ can be assigned (*vide infra*). C_6H_6 has four degenerate fundamentals of e_{2g} symmetry in \underline{D}_{6h} -- ν_6 , ν_7 , ν_8 , and ν_9 --of which ν_8 dominates the phosphorescence in all solvents, being roughly a factor of five more intense than the

next strongest vibronic origin built on ν_9 . In a C_6D_6 host many other weaker "false" origins are resolved and assigned. Progressions of the totally symmetric 990 cm^{-1} (a_{1g}, ν_1) quantum are also found built on ν_6 , on the two b_{2g} fundamentals ν_4 and ν_5 , the single degenerate e_{1g} fundamental ν_{10} , the electronic 0, 0 and combinations and overtones of overall symmetry e_{2g} , b_{2g} , and e_{1g} .

Figure 2 shows a microphotometer tracing of the phosphorescence spectrum of C_6H_6 from the 0, 0 to 0, 0 - 2500 cm^{-1} . The analysis of the C_6H_6 phosphorescence is given in Table II for energies greater than 0, 0 - $(\nu_8 + \nu_1)$. Table III compares the relative intensity of the stronger vibronic origins in the C_6H_6 phosphorescence and fluorescence spectra as determined from microphotometer tracings of photographic plates.

Fig. 2 and Tables II and III show the general dominance of e_{2g} vibrations, and in particular of ν_8 and ν_9 in activating the triplet emission spectrum in qualitative agreement with vibronic theory.^{16,19} The almost exclusive activation of the benzene phosphorescence by the modes ν_8 and ν_9 is partially carried over to all the lower symmetry isotopes with an increase in the activity of certain other vibrations qualitatively predictable from mixing of the normal coordinates in the other isotopes. The only e_{2g} fundamental not assigned in the phosphorescence is ν_7 . The fundamental ν_6 is quite weak. However, when in combination with ν_1 it steals intensity from ν_8 by Fermi resonance. The totally symmetric progression built on the $\nu_{10}(e_{1g})$ origin is the weakest progression analyzed, being weaker than some progressions based on combinations or overtones of u-fundamentals of overall symmetry e_{2g} . The only g-fundamentals which were not assigned in the phosphorescence of C_6H_6 are $\nu_2(a_{1g})$, $\nu_3(a_{2g})$, and $\nu_7(e_{2g})$. However, ν_2 and ν_7 are assigned from the fluorescence spectrum. No u-vibrations are seen in either emission.

Caption for Fig. 2.

Microphotometer tracing of a lower resolution plate of the C_6H_6 phosphorescence. The bands labeled "a" are due to $^{13}C^{12}C_5H_6$ and discussed in the text.

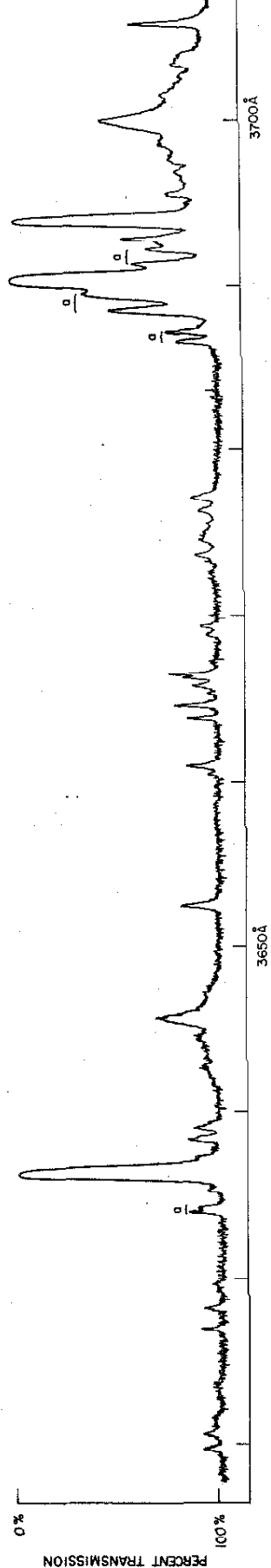
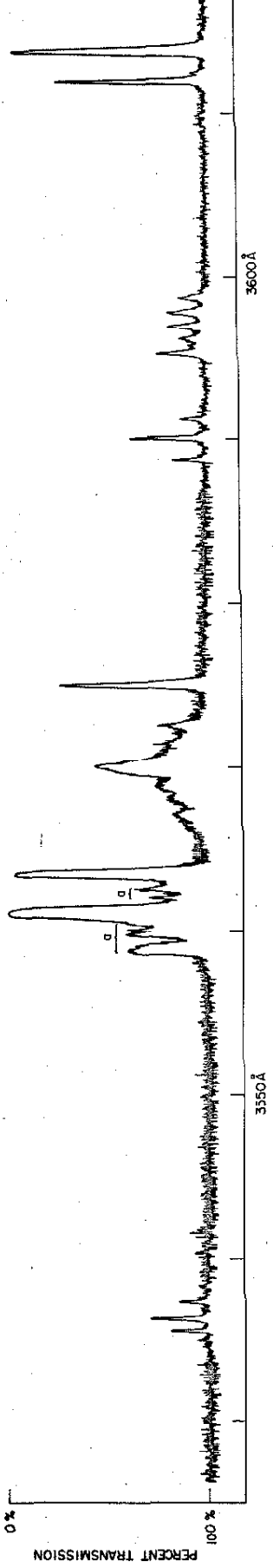
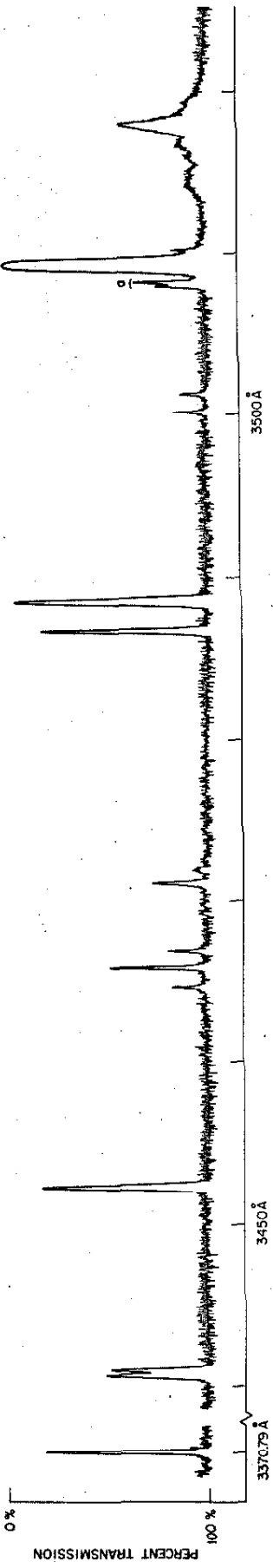


TABLE II. Analysis of the C_6H_6 phosphorescence.

$\lambda_{\text{air}} (\text{\AA})$	$\nu_{\text{vac}} (\text{cm}^{-1})$	Relative intensity	$\Delta\nu (\text{cm}^{-1})$	Assignment ^a	Vibrational symmetry in D_{6h}	Predicted harmonic value (cm^{-1})	
3369.90	29666.0	VVW		$^{13}\text{C } 0,0$			
70.79	658.2	m	0	0,0			
3441.13	051.9	mW	606.3	ν_6	e_{2g}		
41.49	048.8	mW	609.4				
52.85	28953.3	m	704.9	ν_4	b_{2g}		
65.22	849.9	w	808.3	$2\nu_{16}$		809.6	
66.40	840.1	mW	818.1			$e_{2g} + a_{1g}$	817.8
67.45	831.4	w	826.8				826.0
71.75	795.7	w	862.5	ν_{10}	e_{1g}		
72.57	788.9	VW	869.3				
87.25	667.7	m	990.5	ν_1	a_{1g}		
87.90	662.4	VW	995.8	$^{13}\text{C } \nu_5$			
89.00	653.3	s	1004.9	ν_5	b_{2g}		
3500.82	556.6	w	1101.6	$\nu_{11} + \nu_{16}$		1101.7	
01.96	547.3	w	1110.9			e_{2g}	1109.9
08.58	493.4	w	1164.8	$^{13}\text{C } \nu_{9a,b}$			
08.83	491.4	w	1166.8				
09.79	483.6	VS	1174.6	ν_9			
10.84	475.1	VW	1183.1	?	e_{2g}		
18.63	412.0	w,b	1246.2	$\nu_9 + 71.6$			

TABLE II. (Cont'd)

$\lambda_{\text{air}} (\text{\AA})$	$\nu_{\text{vac}} (\text{cm}^{-1})$	Relative intensity	$\Delta\nu (\text{cm}^{-1})$	Assignment ^a	Vibrational symmetry in D_{6h}	Predicted harmonic value (cm^{-1})
3535.51	28276.4	w	1381.8			1383.1
36.21	270.8	mw	1387.4			1387.5
36.8	266.	vw	1392.	$\nu_{16} + \nu_{17}$	$e_{2g} + a_{2g} + a_{1g}$	1391.3
37.25	262.5	w	1395.7			1395.7
58.53	093.4	mw	1564.8			
59.01	089.6	mw	1568.6			
59.65	084.6	mw, b	1573.6	$^{13}\text{C} ?$		
60.43	078.4	mw, b	1579.8			
61.00	073.9	vs	1584.3	ν_8	e_{2g}	
62.56	061.7	mw, b	1596.5	$^{13}\text{C} ?$		
63.35	055.4	s	1602.8			1596.8
63.51	054.2	s	1604.0	$\nu_6 + \nu_1$	e_{2g}	1599.9
64.32	047.8	vw	1610.4			1611.2
64.52	046.2	vw	1612.0	$\nu_6 + \nu_5$	e_{1g}	1614.3
70.10	002.4	w, b	1655.8	$\nu_8 + 71.5$		
72.59	27982.9	w, b	1675.3	$\nu_6 + \nu_1 + 71.3$		
74.99	964.1	m	1694.1	$\nu_4 + \nu_1$	b_{2g}	1695.4
88.75	856.9	w	1801.3			1800.1
90.08	846.5	mw	1811.7			1808.3
91.20	837.9	w	1820.3	$2\nu_{16} + \nu_1$	$e_{2g} + a_{1g}$	1816.5
95.31	806.0	w	1852.2			1853.0
96.24	798.8	vw, b	1859.4	$\nu_{10} + \nu_1$	e_{1g}	1859.8

TABLE II. (Cont'd)

$\lambda_{\text{air}} (\text{\AA})$	$\nu_{\text{vac}} (\text{cm}^{-1})$	Relative intensity	$\Delta\nu (\text{cm}^{-1})$	Assignment ²	Vibrational symmetry in D_{6h}	Predicted harmonic value (cm^{-1})
3597.02	27792.8	w	1865.4	$\nu_{10} + \nu_5$	e_{2g}	1867.4
97.86	786.3	w	1871.9			1874.2
98.77	779.3	w	1878.9	$\nu_9 + \nu_4$	e_{1g}	1879.5
3611.63	680.4	vw, sh	1977.8	$^{13}\text{C } \nu_5 + \nu_1$		
11.89	678.4	m	1979.8	$2\nu_1$	a_{1g}	1981.0
12.42	674.4	vw	1983.8	?		
13.78	664.0	s	1994.2	$\nu_5 + \nu_1$	b_{2g}	1995.4
19.30	621.8	w	2036.4			2037.1
20.35	613.8	w	2044.4	$\nu_{10} + \nu_9$	$e_{1g} + b_{2g} + b_{1g}$	2043.9
26.75	565.1	w	2093.1	$\nu_{11} + \nu_{16} + \nu_1$		2092.2
28.00	555.6	w	2102.6			2100.4
29.39	545.0	vw	2113.2	?		
33.76	511.8	w	2146.4			
34.05	509.6	w	2148.6	$^{13}\text{C } \nu_{9a}, b + \nu_1$		
35.32	500.0	vw	2158.2	$\nu_{12} + \nu_{15}$?	a_{2g}	2158.2
36.13	493.9	vs	2164.3	$\nu_9 + \nu_1$	e_{2g}	2165.1
37.23	485.6	vw	2172.6	?		
38.20	478.3	w	2179.9	$\nu_9 + \nu_5$	e_{1g}	2179.5
38.35	477.1	w, sh	2181.0			2181.7
38.90	473.0	w	2185.2	$\nu_{15} + \nu_{18}$	e_{2g}	2185.5
45.57	422.7	w, b	2235.5	$\nu_9 + \nu_1 + 71.2$		
52.47	370.9	w	2287.3	$\nu_8 + \nu_4$	e_{1g}	2289.2

TABLE II. (Cont'd)

$\lambda_{\text{air}} (\text{\AA})$	$\nu_{\text{vac}} (\text{cm}^{-1})$	Relative intensity	$\Delta\nu (\text{cm}^{-1})$	Assignment ^a	Vibrational symmetry in D_{6h}	Predicted harmonic value (cm^{-1})
3660.46	27311.2	vw	2347.0	$\nu_{14} + \nu_{18}$	e_{2g}	2347.4
60.98	307.3	w	2350.9			2351.2
63.87	285.8	w	2372.4	$\nu_{16} + \nu_{17} + \nu_1$	$e_{2g} + a_{2g} + a_{1g}$	2373.6
64.65	280.0	w	2378.2			2378.0
65.31	275.1	vw	2383.1			2381.8
65.83	271.2	w, b	2387.0			2386.2, 2387.2
66.31	267.6	w	2390.6	$2\nu_6 + \nu_9$	$2e_{2g} + a_{2g} + a_{1g}$	2390.3
66.53	266.0	w	2392.2			2393.4
68.94	248.1	w	2410.1	?		
69.46	244.2	w	2414.0	?		
73.73	212.5	w	2445.7	$\nu_8 + \nu_{10}$	e_{1g}	2446.8
74.58	206.2	w, b	2452.0			2453.6
76.39	192.8	w	2465.4	$\nu_6 + \nu_1 + \nu_{10}$	e_{1g}	2465.9
77.15	187.2	w, b	2471.0			2472.7
86.68	116.9	mw	2541.3	$^{13}\text{C} ?$		
87.24	112.8	mw	2545.4			
88.60	102.8	m	2555.4			
89.58	095.6	m	2562.6			
90.34	090.1	vs	2568.1	$\nu_8 + \nu_1$	e_{2g}	2574.8
91.38	082.4	mw	2575.8			$^{13}\text{C} ?$
92.27	075.9	mw	2582.3			
93.00	070.6	mw	2587.6	$\nu_8 + \nu_5$	e_{1g}	2589.2

TABLE II. (Cont'd)

$\lambda_{\text{air}} (\text{\AA})$	$\nu_{\text{vac}} (\text{cm}^{-1})$	Relative intensity	$\Delta\nu (\text{cm}^{-1})$	Assignment ^a	Vibrational symmetry in D_{6h}	Predicted harmonic value (cm^{-1})
3693.91	27063.9	s	2594.3	$\nu_6 + 2\nu_1$	e_{2g}	2587.3
94.07	062.7	s	2595.5			2590.4
95.54	052.0	vw	2606.2	$\nu_6 + \nu_1 + \nu_5$	e_{1g}	2601.7
95.70	050.8	vw	2607.4			2604.8
3700.06	018.9	w, b	2639.3	$\nu_8 + \nu_1 + 71.2$		
05.92	26976.2	mw	2682.0	$\nu_4 + 2\nu_1$	b_{2g}	2685.9

^aBands in Fermi resonance are connected by square brackets.

TABLE III. Relative intensity estimates for the stronger vibronic origins in the C_6H_6 phosphorescence and fluorescence spectra.

Symmetry	Vibration	${}^3B_{1u} \rightarrow {}^1A_{1g}$	${}^1B_{2u} \rightarrow {}^1A_{1g}$
e_{2g}	ν_6	1	100
	ν_7	—	3
	ν_8^a	100	20
	ν_9	25	3
	$2\nu_{16}$	1	3
	$\nu_{11} + \nu_{16}$	<1	5
b_{2g}	ν_4	1+	<1
	ν_5	6	—
a_{1g}	ν_1	1	22
	ν_2	—	1
e_{1g}	ν_{10}	<1	—
	0,0	1	b

^aUncorrected for Fermi resonance with $\nu_8 + \nu_1$.

^bDue to appreciable reabsorption, no relative intensity estimate is given.

In general the same ground state vibrations are observed in the fluorescence spectrum as in the phosphorescence. However, the relative vibronic activity is substantially different, as can be seen from Table III. The relative intensities in the fluorescence also agree generally with the prediction of vibronic theory outlined earlier. In comparing the two emissions the following features seem noteworthy. The b_{2g} modes, both fundamentals and combinations, are relatively much more intense in the phosphorescence. The only b_{2g} mode we have assigned in the fluorescence is the fundamental ν_4 , which appears very weakly. No vibrations of species b_{2g} are seen in the gas phase ${}^1B_{2u} - {}^1A_{1g}$ spectrum.¹⁸ However, its intensity is so much less than ν_1 and, therefore, the electronic 0,0, that it is not possible to draw definitive conclusions from its appearance. The presence of a b_{2g} vibronic origin in the free molecule would support a B_{1u} assignment for the lowest singlet state, but in the crystal the b_{2g} origin could easily be due to crystal site interactions.

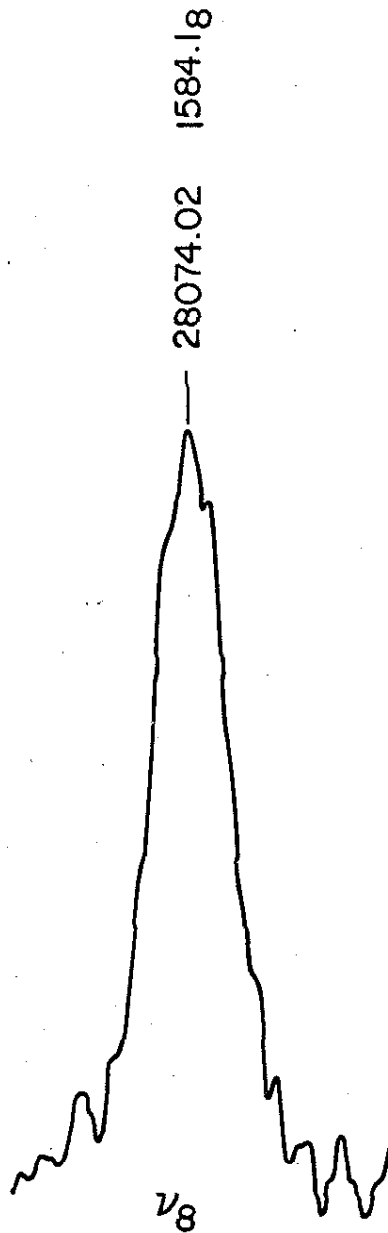
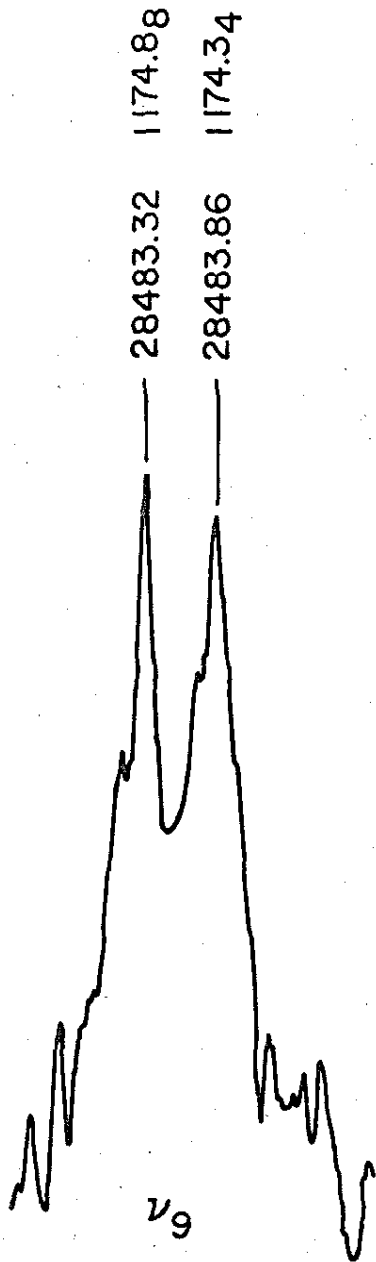
The intensity of the totally symmetric fundamental ν_1 relative to the most intense vibronic origin is much greater in the fluorescence than in the phosphorescence. It seems reasonable to attribute this to a greater enhancement of the 0,0 in the fluorescence since the transition is only symmetry and not spin forbidden. However, the possibility that vibronic mixing by ν_8 in the phosphorescence is enhanced simultaneously with the 0,0 in the crystal can not be eliminated.

Site splitting δ_{SS} defined in Sec. II is observed for the degenerate e_{2g} fundamentals ν_6 , ν_7 , and ν_9 amounting to 3.1 cm^{-1} , 5.5 cm^{-1} , and 0.54 cm^{-1} , respectively. The splitting of ν_9 is seen only with the highest resolution employed and is not shown in Table II. Fig. 3 is a densitometer tracing of ν_9 and ν_8 with this highest resolution. No distinct splitting is seen in ν_8 , but, as seen in the Fig. 3, the ν_8 linewidth is roughly equal to the total bandwidth of the split ν_9 fundamental. ν_8 could be much more sensitive to

Caption for Fig. 3.

Microphotometer tracing of the $0, 0-\nu_9$ and $0, 0-\nu_8$
 C_6H_6 phosphorescence lines at the highest
resolution employed.

PLATE TRANSMISSION



crystal quality than ν_9 so that its greater linewidth (0.5 cm^{-1}) need not completely represent unresolved site splitting. On the other hand, the absence of a splitting in ν_8 supports the assignment of the splitting in ν_9 as a genuine site splitting rather than a splitting due to different sites in a non-perfect crystal. A very weak line, which has not been assigned, is observed ca. 8.5 cm^{-1} to low energy of the very strong $0, 0 - \nu_9 - n\nu_1$ progression. The intensity ratio of ν_9 to the unassigned line is > 100 and much larger than the intensity ratio (≤ 10) for the two components of any other observed site-split fundamental. We thus feel that this weak feature does not represent the other component of ν_9 .

The e_{1g} fundamental ν_{10} is also split ($\delta_{SS} = 6.8 \text{ cm}^{-1}$). The vibronic intensity of the two components is different in the fundamental (see Fig. 2), but in the observed combinations of ν_{10} with ν_5 ($e_{1g} \times b_{2g} = e_{2g}$) and with ν_9 , ν_8 and $\nu_6 + \nu_1$ ($e_{1g} \times e_{2g} = b_{1g} + b_{2g} + e_{1g}$) the splitting repeats itself. The intensity of the components also tends to equalize in these combinations. For the totally symmetric progression built on ν_{10} the intensity difference remains. The mode ν_{10} is not observed in the fluorescence, apparently since it has e_{1g} symmetry in \underline{D}_{6h} , but the overtone $2\nu_{10}$ (e_{2g}) is seen very weakly and a site splitting of 7 cm^{-1} can be inferred. Thus, even though the vibronic intensities of the site split components of ν_{10} in the phosphorescence is different, the reported site splitting and the frequencies of the components are certainly correct.

In the combination and overtone vibronic bands, site splitting in many u-fundamentals can be inferred. Consider for example the three lines at 808.3 , 818.1 , and 826.8 cm^{-1} removed from the $0, 0$ which are assigned as $2\nu_{16}$, $(e_{2u})^2 = e_{2g} + a_{1g}$ in \underline{D}_{6h} . The observed splitting could arise by two different routes, both yielding three lines. The first mechanism assumes

the degenerate fundamental ν_{16} is not split, but that the site and intramolecular anharmonic terms removes the threefold degeneracy of the overtone $2\nu_{16}$. If this were the case, the expected splitting would be small and the pattern not necessarily symmetric. If, however, the fundamental ν_{16} is split in the site, then the overtone would be three symmetrically spaced lines for small anharmonicities with intensities determined by the binomial coefficients, i. e., 1:2:1, for equal vibronic activity among the three components. As seen from Fig. 2 and Table II the intensities are roughly in this ratio in the phosphorescence and the splitting nearly symmetrical. The fundamental ν_{16} is thus predicted to occur at 404.2 cm^{-1} and 413.0 cm^{-1} with a site splitting δ_{SS} of 8.8 cm^{-1} . In the infrared spectrum of C_6H_6 in a C_6D_6 host crystal,^{4a} ν_{16} consists of a doublet at 404.8 cm^{-1} and 413.0 cm^{-1} ($\delta_{SS} = 8.2 \text{ cm}^{-1}$) in excellent agreement with the values inferred from the emission spectra. A small deviation is expected both from anharmonicities and from Fermi resonance among the trio of lines corresponding to $2\nu_{16}$ each of which rigorously has only symmetry a_g in the C_1 site. The same band observed in the fluorescence, however, does not show this intensity pattern, the high-energy component at 827 cm^{-1} being more intense relative to the other two.

Similarly, the doublet at 1101.6 and 1110.9 cm^{-1} , which is assigned to $\nu_{11} + \nu_{16}$, is the combination of ν_{11} with each of the site-split components of ν_{16} . Assuming no anharmonic corrections or resonances, the inferred value of ν_{11} is 697.4 cm^{-1} which compares with 696.9 observed in the infrared. The quartet assigned to $\nu_{16} + \nu_{17}$ at about 1390 cm^{-1} yields for the degenerate fundamental ν_{17} the frequencies 978.3 cm^{-1} and 982.8 cm^{-1} for an inferred site splitting of 4.5 cm^{-1} . This should be compared with 5.6 cm^{-1} observed in the infrared.

TABLE IV. Summary of C₆H₆ data (cm⁻¹).

D _{6h} symmetry class	Vibration number and type ^a	Fundamental frequency			Site splitting
		gas ^b	liquid ^c	solid ^d	
a _{1g}	ν ₁ (CC)	995.4 (3073)	(993) (3062)	990.5 3063.3	
a _{2g}	ν ₃ (H)	(1350)	1346		
b _{2g}	ν ₄ (C [⊥])	(707)	(707)	704.9	
	ν ₅ (H [⊥])	(990)	(991)	1004.9	
e _{2g}	ν ₆ (C)	608.0	(606)	606.3, 609.4	3.1
	ν ₇ (CH)	(3056)	(3048)	3042.0, 3047.5	5.5
	ν ₈ (CC) ^e	(1590)	1586	1584.2	≤0.3
	ν ₉ (H)	(1178)	1177	1174.3 ₄ , 1174.8 ₈	0.5 ₄
e _{1g}	ν ₁₀ (H [⊥])	(846)	850	862.5, 869.3	6.8
a _{2u}	ν ₁₁ (H [⊥])	674.0	675	696.9 [697]	
b _{1u}	ν ₁₂ (C)	(1010)	1010	1011.3 [1011]	
	ν ₁₃ (CH)	(3057)	(3048)		
b _{2u}	ν ₁₄ (CC)	(1309)	1309	1312.6 [1313]	
	ν ₁₅ (H)	(1146)	1146	1146.9 [1147]	
e _{2u}	ν ₁₆ (C [⊥])	398.6	404	404.8, 413.0 [404, 413]	8.2
	ν ₁₇ (H [⊥])	(967)	969	978.3, 983.9 [978, 983]	5.6

TABLE IV. (Cont'd)

D_{6h} symmetry class	Vibration number and type ^a	Fundamental frequency			Site splitting
		gas ^b	liquid ^c	solid	
e_{1u}	$\nu_{18}(H^{\parallel})$	1037	1035	1034.8, 1038.6 [1034, 1038]	3.8
	$\nu_{19}(CC)$	1482	1479		
	$\nu_{20}(CH)^e$	3047	3036		

^aThe vibrational numbering for this and the other isotopes follows Refs. 17 and 26.

^bTaken from summary given in Ref. 26. () indicates calculated values.

^cRef. 18.

^dThe frequencies of the \underline{u} -fundamentals are from Ref. 4. The values inferred from the u. v. spectra, rounded-off to the nearest cm^{-1} , are given in parentheses.

^eUncorrected for Fermi resonance.

Table IV summarizes the fundamental ground state frequencies of C_6H_6 in a C_6D_6 host crystal and the site splittings for the degenerate fundamentals. The g-fundamentals were obtained directly from the emission spectra as false origins for totally symmetric progressions. For the u-fundamentals both the values inferred in this work from combinations and overtones and the values observed directly in the infrared are given. The latter should, of course, be taken for the frequencies of the u-fundamentals. Sixteen of the twenty benzene fundamentals are therefore accurately known and the site splitting of eight of the ten degenerate fundamentals is established for a crystalline benzene environment. For comparison, Table IV also includes the vapor and liquid phase fundamentals.

2. $^{13}C^{12}C_5H_6$

The isotope ^{13}C is present in natural abundance in the amount of 1.1%. Thus, roughly 6.6% of any benzene will contain at least one ^{13}C atom. For all the partially deuterated benzenes, more than one isomer with the chemical formula $^{13}C^{12}C_5H_nD_{6-n}$ exists. The corresponding vibrational frequencies of each of these isotopes will be very similar and difficult to resolve. However, only one isomer $^{13}C^{12}C_5H_6$ exists. Electronic spectra provide a means of obtaining some of the vibrational frequencies of $^{13}C^{12}C_5H_6$ as an "impurity" in the C_6H_6 guest in the C_6D_6 crystal. This may have a definite advantage over a conventional infrared spectrum since in an electronic transition the corresponding vibronic lines are separated not by the vibrational energy difference, but by the vibrational energy difference plus the zero-point energy contribution. Thus, even if a particular vibrational frequency is unchanged by introducing ^{13}C , the corresponding vibronic lines will be separated in energy by zero-point effects which may be much larger than any individual shift in a vibration. In actuality, however, the electronic

emission spectra have been only of limited usefulness in these mixed crystals for several reasons. Although $\sim 6\%$ of the isotopic guest is ^{13}C -benzene, the ^{13}C to ^{12}C phosphorescence intensity ratio is less than 6% since the transition energy for ^{13}C -benzene lies above that of ^{12}C -benzene. Thus, at low temperatures excitation energy transfer to the lowest lying trap, i. e., the ^{12}C -benzene, can reduce the relative intensity of emission from the ^{13}C -isotope. Definitive assignments of all but the more intense ^{13}C -lines are further hampered by the intense background of ^{12}C -lines along with phonon structure on very heavily exposed plates.

Since $^{13}\text{C}^{12}\text{C}_5\text{H}_6$ has vibrational symmetry $\underline{\text{C}}_{2v}$, the degenerate vibrations of $^{12}\text{C}_6\text{H}_6$ are split into a and b components. In the $\underline{\text{C}}_i$ site the vibrations of $^{13}\text{C}^{12}\text{C}_5\text{H}_6$ can be further perturbed by orientational effects and thus give rise to further apparent splittings or line broadening. However, the orientation effects due to one ^{13}C -atom should be much smaller than that for one D-atom since the guest-host interaction is more sensitive to changes on the periphery of the interacting molecules. The orientation effects for $^{12}\text{C}_6\text{H}_5\text{D}$, discussed in a following section, are in general $\lesssim 1 \text{ cm}^{-1}$ and, thus, are expected to be vanishingly small for $^{13}\text{C}^{12}\text{C}_5\text{H}_6$. Therefore, the only new vibrational structure anticipated is the removal of the $^{12}\text{C}_6\text{H}_6$ vibrational degeneracies.

A somewhat surprising result for $^{13}\text{C}^{12}\text{C}_5\text{H}_6$ is that the isotope shifts from $^{12}\text{C}_6\text{H}_6$ in the electronic origins of the phosphorescence and fluorescence are quite different, contrary to the observations for the deuterium substituted isotopes.^{21, 11} These shifts to high energy from the corresponding $^{13}\text{C}_6\text{H}_6$ transitions are 3.7 and 7.8 cm^{-1} in the $^1\text{B}_{2u} - ^1\text{A}_{1g}$ and $^3\text{B}_{1u} - ^1\text{A}_{1g}$ $0, 0$ lines, respectively. The electronic origin in the singlet transition, as will be discussed in Section V, is determined from the $0, 0$ line observed in

absorption. The assignment is confirmed by the presence in the fluorescence spectrum of a progression built on this origin involving a known fundamental^{22,23} of $^{13}\text{C}^{12}\text{C}_6\text{H}_6$, viz. ν_1 of species a_1 . The mixed crystal value observed for this fundamental is 982.0 cm^{-1} compared to a liquid value²² of 984 cm^{-1} .

The other $^{13}\text{C}^{12}\text{C}_6\text{H}_6$ fundamentals assigned with some certainty are ν_4 , ν_5 , ν_{9a} , and ν_{9b} . These were obtained from the phosphorescence wherein they serve as origins for progressions in ν_1 . The $0,0$ and $0,0-\nu_4$ lines are very weak and, thus, were only photographed with the faster, lower resolution spectrograph. The bands involving $\nu_{9a,b}$ are seen in Fig. 2 as a weak doublet to high energy of the very strong $0,0-\nu_9-n\nu_1$ progression of $^{12}\text{C}_6\text{H}_6$. The progressions built on ν_4 and ν_5 are too weak to see on the exposure corresponding to Fig. 2 as is the $^{13}\text{C}^{12}\text{C}_6\text{H}_6$ $0,0$. The fundamental frequencies are presented in Table V. The observed ^{13}C -shifts are also tabulated and compared with the shift calculated from Whiffen's²⁴ force field employing the modifications of Albrecht.²⁵ The agreement between the predicted and observed shifts for the fundamentals ν_1 , ν_4 , ν_5 , and $\nu_{9a,b}$ is excellent and generally within the experimental error limits of $\pm 0.3\text{ cm}^{-1}$. This range is imposed mainly by the uncertainty in the phosphorescence electronic origin. The vibronic bands terminating in the ground state fundamentals are nearly as sharp as the $^{12}\text{C}_6\text{H}_6$ lines at the same resolution, confirming our expectations of a very small orientation effect for $^{13}\text{C}^{12}\text{C}_6\text{H}_6$.

Other lines are observed in both emissions which seem due to ^{13}C -benzene, but the analysis leaves some doubt. For example, ν_8 is expected to be stronger than the assigned ν_1 in the fluorescence (cf. Table III). A single line of about the correct intensity relative to ν_8 of ^{12}C -benzene is seen 599.5 cm^{-1} from the ^{13}C - $0,0$. If the $\nu_{9a,b}$ -splitting is greater than about 5 cm^{-1} and if the low energy component is the one observed, the other

TABLE V. Some observed and calculated fundamental frequencies of $^{13}\text{C}^{12}\text{C}_5\text{H}_6$.

$^{13}\text{C}^{12}\text{C}_5\text{H}_6$ fundamental frequency (cm $^{-1}$) ^a	$\Delta\nu(^{12}\text{C} - ^{13}\text{C})$		
	observed ^b	predicted ^c	
ν_1 982.0	8.5	8.4	
ν_4 702.0	2.9	3.5	
ν_5 1003.8	1.1	1.0	
$\nu_{9a, b}$ {	1174.6	0.0	0.3
	1172.6	2.0	2.4

^aThe experimental error is ± 0.3 cm $^{-1}$.

^bThe mean of the site-split fundamental ν_9 of $^{12}\text{C}_6\text{H}_6$ was used to calculate the $\Delta\nu$ observed.

^cSee text.

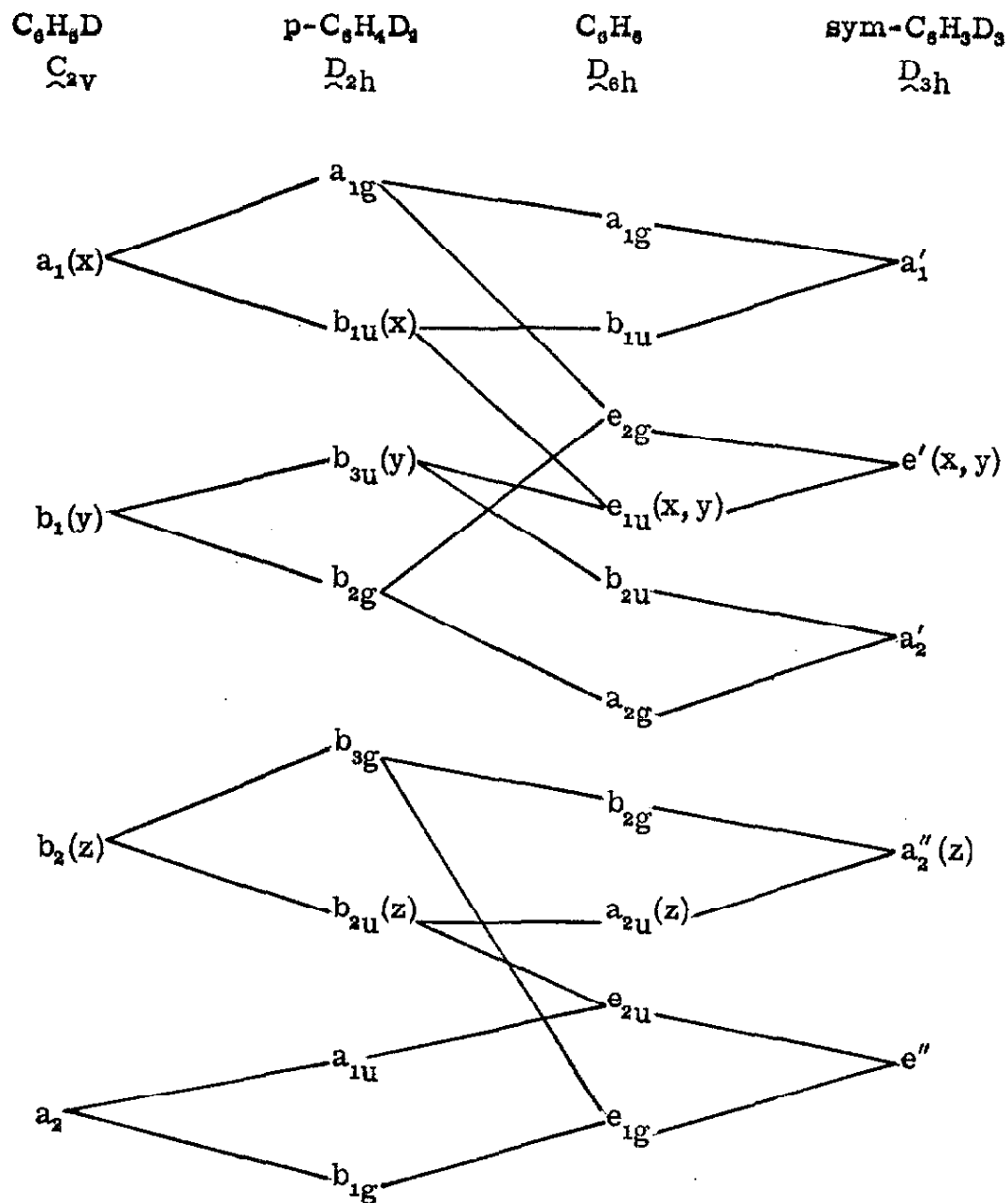
component of ν_6 would be unresolved from the overexposed ν_6 band of ^{12}C -benzene. Two very weak lines are seen in the phosphorescence at 600 and 606 cm^{-1} from the ^{13}C -0,0 and, thus, seemingly support the assignment to $\nu_{6a,b}$. However, this analysis can not be confirmed by a progression of ν_1 built on $\nu_{6a,b}$. Moderately intense lines are seen in the correct spectral region in both the fluorescence and phosphorescence emissions, but they are not easily assignable to $\nu_{6a,b} + \nu_1$. Because of the different ^{13}C -shifts in the phosphorescence and fluorescence electronic origins, the ^{13}C -lines are shifted relative to the ^{12}C -lines in the two emissions. Some lines show the correct shift, but a sufficient number do^{not}/or are absent, to make an analysis difficult. Moreover, $\nu_{6a,b} + \nu_1$ is most likely in Fermi resonance with $\nu_{8a,b}$ and possibly also $\nu_{6a,b} + \nu_{12}$. Therefore, we do not conjecture a possible assignment for $\nu_{8a,b}$, even though in the phosphorescence it is expected to be stronger than the assigned $\nu_{9a,b}$, and present the results for $\nu_{6a,b}$ only as tentative.

For the other $^{13}\text{C}^{12}\text{C}_5\text{H}_n\text{D}_{6-n}$ isotopes, which are of course present in the other isotopic benzenes, no assignments to ^{13}C -benzene are made. However, some of the unassigned weak lines, especially in the spectrum of sym- $\text{C}_6\text{H}_3\text{D}_3$, could easily be due to $^{13}\text{C}^{12}\text{C}_5\text{H}_3\text{D}_3$.

3. sym- $\text{C}_6\text{H}_3\text{D}_3$

From the correlation diagram shown in Fig. 4, the active vibrations in the phosphorescence of sym- $\text{C}_6\text{H}_3\text{D}_3$ (point group $\underline{\text{D}}_{3h}$) are predicted to have symmetry a_2'' , e' , and e'' . However, only vibrations which correlate directly to the active C_6H_6 vibrations given in Table III, viz. ν_4 , ν_5 , ν_6 , ν_8 , and ν_9 , or are strongly mixed with them in the lower symmetry isotope are intense vibronic origins in the phosphorescence. For the mixing to be strong the vibrations must have similar frequencies and the same symmetry in the

FIG. 4. Correlation diagram for the groups of benzene isotopes^a.



^a z -axis always perpendicular to the plane of molecule; y -axis through C_1 ; and x -axis between C_2 and C_3 .

Caption for Fig. 5.

Microphotometer tracing of a lower resolution plate of the sym- $C_6H_3D_3$ phosphorescence. The bands labeled "a" are from a plate exposed 1/20 as long as the rest of the spectrum; "b" denotes bands assigned to m- $C_6H_4D_2$ and m- $C_6H_2D_4$ impurities.

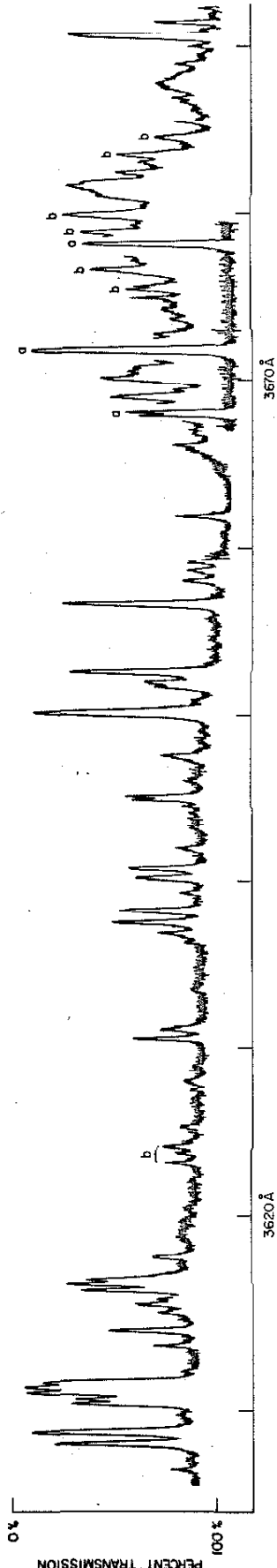
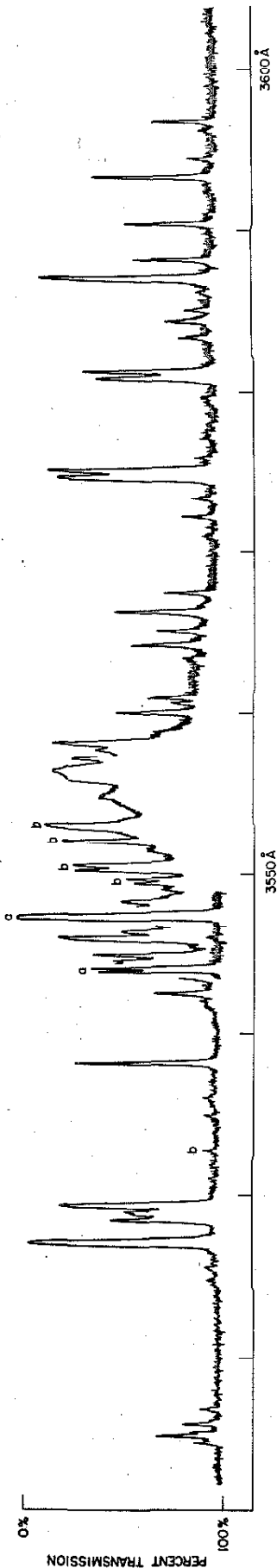
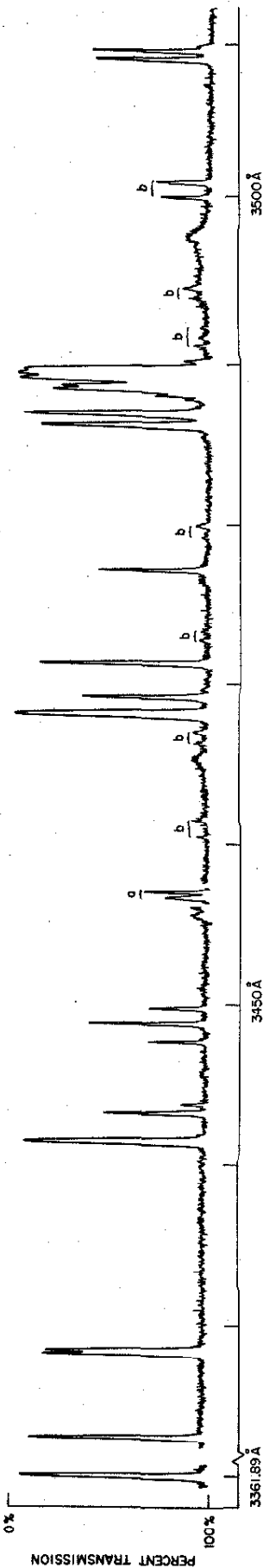


TABLE VI. Analyses of the sym-C₆H₃D₃ phosphorescence.

$\lambda_{\text{air}} (\text{\AA})$	$\nu_{\text{vac}} (\text{cm}^{-1})$	Relative Intensity	$\Delta\nu (\text{cm}^{-1})$	Assignment †	Vibrational symmetry in D_{3h}	Predicted harmonic value (cm^{-1})
3361.89	29,753.8	m	0			
3422.78	29,207.6	m	546.2	ν_{11}	a_2''	
28.14	162.0	m	591.8	ν_6	e'	
28.33	160.3	m	593.5			
41.33	050.2	m	703.9	ν_4	a_2''	
43.06	035.6	mw	718.2	ν_{10}	e''	
43.59	031.1	vw	722.7			
47.55	28,997.8	w	756.0	$2\nu_{16}$	$a_1' + e'$	
48.65	988.6	mw	765.2			
49.70	979.7	w	774.1			
56.55	922.3	ms	831.5	ν_{18}	e'	
56.97	918.8	ms	835.0			
68.10	825.9	m	927.9	ν_5	a_2''	
69.17	817.1	mw	936.7	ν_{17}	e''	
69.66	813.1	vww	940.7			
71.33	799.2	m	954.6	ν_1	a_1'	
77.15	750.9	mw	1002.9	ν_{12}	a_1'	
86.06	677.5	m	1076.3	$\nu_4 + \nu_{16} ?$	e'	1081.9
86.80	671.3	ms	1082.5			
87.89	662.4	vw	1091.4	$2\nu_{11} ?$	a_1'	1090.9
						1092.4

TABLE VI. (Cont'd)

$\lambda_{\text{air}} (\text{\AA})$	$\nu_{\text{vac}} (\text{cm}^{-1})$	Relative intensity	$\Delta\nu (\text{cm}^{-1})$	Assignment	Vibrational symmetry in D_{3h}	Predicted harmonic value (cm^{-1})
3488.02	28,661.4	vw	1092.4	?		
88.35	658.6	m	1095.2	} ν_9 and $\nu_{10} + \nu_{16}$	e'	
88.60	656.5	m	1097.3			
88.99	653.4	ms	1100.4			
89.35	650.4	ms	1103.4		$e' + a'_1 + a'_2$	
89.65	848.0	m	1105.8			
90.19	643.5	vw	1110.3			
3508.92	490.6	mw	1263.2	} $\nu_{11} + \nu_{10}$	e'	1263.0
09.46	486.3	mw	1267.5			
14.70	443.8	vw	1310.0	} $\nu_{16} + \nu_5,$ $\nu_{10} + \nu_6,$ $\nu_{16} + \nu_{17}$	$e'' + a''_1 + a''_2$	
15.22	439.6	w	1314.2			
15.44	437.8	vw	1316.0			
15.97	433.5	vw	1320.3		$e' + a'_1 + a'_2$	
16.88	426.2	vw	1327.6			
27.23	342.8	ms	1411.0	ν_{19}	e'	
28.63	331.5	mw	1422.3	} $\nu_6 + \nu_{18}$	$e' + a'_1 + a'_2$	
29.02	328.3	w	1425.5			
29.52	324.4	m	1429.4	$\nu_4 + \nu_{10}$	e'	
35.07	279.9	vww	1473.9	$\nu_{11} + \nu_5$	a'	1474.1
36.18	271.0	vww	1482.8	$\nu_{11} + \nu_{17}$	e'	1482.9
38.32	253.9	mw	1499.9	$\nu_{11} + \nu_1$	a''_2	1500.8

TABLE VI. (Cont'd)

$\lambda_{\text{air}}(\text{\AA})$	$\nu_{\text{vac}}(\text{cm}^{-1})$	Relative intensity	$\Delta\nu(\text{cm}^{-1})$	Assignment	Vibrational symmetry in D_{2h}	Predicted harmonic value (cm^{-1})
3542.63	28,219.5	w	1534.3	?		
43.90	209.5	s	1544.3	$\nu_6 + \nu_1$	e'	1546.5
44.13	207.6	s	1546.2			1548.2
44.67	203.3	w	1550.5			1549.1
45.00	200.7	mw	1553.1	$\nu_{11} + \nu_{12}$	a_2''	
45.98	192.9	m	1560.9	$\nu_{18} + \nu_{10}$	$e'' + a_1'' + a_2''$	
46.43	189.3	w	1564.5	?		
47.28	182.6	vs	1571.2	ν_8	e'	
47.41	181.6	vs	1572.2			
48.39	173.7	w	1580.1	?		
49.12	168.0	vw	1585.8	?		
56.44	110	m, vb	1644	$\nu_8 + 72$		
57.24	103.6	w	1650.2	$\nu_5 + \nu_{10}$	e'	1646.0
57.82	99.1	vw	1654.7			1650.5
58.22	95.9	mw	1657.9	$\nu_4 + \nu_1$	a_2''	1658.5
60.09	81.2	w	1672.6	$\nu_{10} + \nu_1$	e''	1672.8
60.68	76.5	vw	1677.3			1677.3
61.01	73.9	w	1679.9	?		
64.26	48.3	w	1705.5	$\nu_4 + \nu_{12}$	a_2''	1706.8
65.09	41.8	w	1712.0			1710.6
66.29	32.3	mw	1721.5	$2\nu_{16} + \nu_1$	$a_1' + e'$	1719.8
67.42	23.5	w	1730.3			1728.7

TABLE VI. (Cont'd)

$\lambda_{\text{air}}(\text{\AA})$	$\nu_{\text{vac}}(\text{cm}^{-1})$	Relative intensity	$\Delta\nu(\text{cm}^{-1})$	Assignment	Vibrational symmetry in D_{3h}	Predicted harmonic value (cm^{-1})
3570.96	27,995.7	vvw	1758.1	$2\nu_{16} + \nu_{12}$	$a'_1 + e'$	1758.9
72.14	986.4	vw	1767.4			1768.1
73.28	977.5	vvw	1776.3			1777.0
74.54	967.6	m	1786.2	$\nu_{18} + \nu_1$	e'	1786.1
75.00	964.0	m	1789.8			1789.2
80.71	919.6	mw	1834.2	$\nu_{18} + \nu_{12}$	e'	1834.4
81.14	916.1	mw	1837.7			1837.5
83.19	899.9	vw	1853.9	$2\nu_5$?	a'_1	1855.8
84.27	891.7	vw	1862.1	$\nu_5 + \nu_{17}$	e'	1864.5
84.93	886.6	vw	1867.2			1868.6
86.83	871.8	m	1882.0	$\nu_5 + \nu_1$	a''_2	1882.4
87.97	863.0	w	1890.8	$\nu_{17} + \nu_1$	e''	1891.3
90.45	845.3	w	1908.5	$2\nu_1$	a'_1	1909.2
93.05	823.5	mw	1930.3	$\nu_5 + \nu_{12}$	a''_2	1930.8
94.18	814.8	vw	1939.0			1939.5
96.52	796.7	w	1957.1	$\nu_{17} + \nu_{12}$	e''	1957.5
3604.60	734.4	vvw	2019.4	$\nu_{12} + \nu_1$	a'_1	
				?		
06.13	722.6	mw	2031.2	$\nu_4 + \nu_{16} + \nu_1$?	e'	2036.0
06.91	716.6	m	2037.2			2043.5
08.03	708.0	vvw	2045.8	?		

TABLE VI. (Cont'd)

$\lambda_{\text{air}} (\text{\AA})$	$\nu_{\text{vac}} (\text{cm}^{-1})$	Relative intensity	$\Delta\nu (\text{cm}^{-1})$	Assignment	Vibrational symmetry in \underline{D}_{3h}	Predicted harmonic value (cm^{-1})
3608.59	27,703.7	mw	2050.1	$\left. \begin{array}{l} \nu_9 + \nu_1 \\ \nu_{10} + \nu_{16} + \nu_1 \end{array} \right\}$	e'	2084.8
08.88	701.5	mw	2052.3			
09.27	698.8	m	2055.0			
09.67	695.8	m	2058.0			
09.92	693.5	m	2060.3			
12.23	675.8	vw	2078.0			
13.08	669.3	w	2084.5	$\nu_4 + \nu_{16} + \nu_{12}$?	e'	2093.8
13.74	664.3	vww	2089.5	?		
14.12	661.4	vw	2092.4	?		
14.62	657.5	vww	2096.3	$\left. \begin{array}{l} \nu_9 + \nu_{12} \\ \nu_{10} + \nu_{16} + \nu_{12} \end{array} \right\}$	e'	2084.8
14.95	655.0	vww	2098.8			
15.45	651.2	w	2102.6			
15.80	648.5	mw	2105.3			
16.05	646.6	w	2107.2			
17.42	636.1	vww	2117.7			
23.59	589.1	vww	2164.7	?		
24.33	583.4	vww	2170.4	?		
26.60	566.2	vww	2187.6	?		
27.37	560.3	vww	2193.5	?		
28.83	549.2	vww	2205.6	?		

TABLE VI. (Cont'd)

$\lambda_{\text{air}} (\text{\AA})$	$\nu_{\text{vac}} (\text{cm}^{-1})$	Relative intensity	$\Delta\nu (\text{cm}^{-1})$	Assignment	Vibrational symmetry in \tilde{D}_{3h}	Predicted harmonic value (cm^{-1})
3630.37	27,537.6	w	2216.2	$\nu_{11} + \nu_{10} + \nu_1$	e'	2219.0
30.93	533.3	vw	2220.5			2223.5
36.21	493.3	vvw	2260.5	$\nu_{11} + \nu_{10} + \nu_{12}; \nu_{10} + \nu_6 + \nu_1$]	
36.69	489.7	vw	2264.1	$\nu_7; \nu_{16} + \nu_5 + \nu_1$		
37.32	484.9	w	2268.9	$\nu_8 + \nu_4; \nu_{16} + \nu_{17} + \nu_1$		
38.09	479.1	w,b	2274.4			
39.14	471.2	vw	2282.6	ν_{13}		
40.08	464.1	w,b	2289.7	$\nu_8 + \nu_{10}$	$e'' + a_1'' + a_2''$	
40.64	459.9	w,b	2293.9			
41.80	451.1	vw	2302.7			
43.14	441.1	vw,b	2312.7	$\nu_6 + \nu_{12} + \nu_{14}$]	
44.41	431.5	vvw	2322.3	$2\nu_{16} + \nu_{12} + \nu_{11}$		
44.97	427.2	vvw	2326.6	$2\nu_{16} + \nu_8$		
45.93	420.0	vvw	2333.8	$\nu_{19} + \nu_{17}$		
47.40	409.0	w	2344.6			
47.55	407.1	w	2346.6			
48.44	401.2	vw, b	2352.6			
50.02	389.3	m	2364.5	$\nu_{19} + \nu_1$	e'	2365.4
50.82	383.3	w	2370.5	$\nu_6 + \nu_{18} + \nu_1; \nu_4 + \nu_{10} + \nu_1$	$e' + a_1' + a_2'$	
51.81	375.9	w	2377.9		e'	
52.40	371.5	mw	2382.3			

TABLE VI. (Cont'd)

$\lambda_{\text{air}} (\text{\AA})$	$\nu_{\text{vac}} (\text{cm}^{-1})$	Relative intensity	$\Delta\nu (\text{cm}^{-1})$	Assignment	Vibrational symmetry in D_{3h}	Predicted harmonic value (cm^{-1})
3656.52	27,340.6	mw	2413.2	$\nu_{19} + \nu_{12}$	e'	2413.7
57.86	330.6	vw	2423.2	$\nu_6 + \nu_{18} + \nu_{12}$	$e' + a'_1 + a'_2$	
58.50	325.8	vw	2428.0	$\nu_4 + \nu_{10} + \nu_{12}$	e'	
59.04	321.8	vw	2432.0	$\nu_{11} + \nu_5 + \nu_1$	a'_1	
60.84	308.4	vvw, b	2445.4	?		
61.79	301.3	vw	2452.5	$\nu_{11} + 2\nu_1$	a''_2	2455.4
64.49	281.2	vw, vb	2472.6	?		
65.85	273.0	vvw	2480.8	?		
65.96	270.2	vvw	2483.6	$\nu_{11} + \nu_{12} + \nu_{17}$	e'	2484.4
67.63	257.8	ms	2496.0	$\nu_6 + 2\nu_1$	e'	
67.83	256.3	ms	2497.5	$(\nu_8 + \nu_5)$	e''	
68.71	249.7	vw	2504.1	?		
69.15	246.4	mw	2507.4	$\nu_8 + \nu_{17} (?)$	$e'' + a''_1 + a''_2$	2508.3
69.89	241.0	vw	2512.8			2512.4
70.49	236.6	mw, vb	2517.2	?		
71.54	228.8	vs, b	2525.0	$\nu_8 + \nu_1$	e'	2525.8
72.56	221.2	vw	2532.6	?		
73.46	214.5	vw	2539.1	?		
74.04	210.2	vw	2543.6	?		

TABLE VI. (Cont'd)

λ_{air} (Å)	ν_{vac} (cm ⁻¹)	Relative intensity	$\Delta\nu$ (cm ⁻¹)	Assignment	Vibrational symmetry in D_{3h}	Predicted harmonic value (cm ⁻¹)
3677.84	27, 182.2	s	2571.6	$\nu_8 + \nu_{12}$	e'	2574.1
81.34	156.3	mw, vb	2597.5	$\nu_8 + \nu_1 + 72.0$		
82.77	145.7	vw	2608.1	$\nu_4 + 2\nu_1$	a ₂ ''	2613.1
85.19	127.9	vw	2625.9	$\nu_{10} + 2\nu_1$?		2632.0
86.44	118.7	vw	2635.1	$\nu_6 + 2\nu_{11} + \nu_1$	e'	2638.9
86.66	117.1	vw	2636.7			
87.5	111.3	w, vb	2643.5	$\nu_8 + \nu_{12} + 71.9$		
88.67	102.4	vww	2651.4	?		
89.22	98.3	vww	2655.5	?		
89.71	94.7	vww	2659.1	?		
90.32	90.3	m-b	2663.5	$\nu_8 + 2\nu_{11}$	e'	2664.1

† Square brackets connect possible Fermi resonances.

‡ Splitting only resolved at higher resolution.

free molecule. Thus, as shown by the normal coordinate analysis of Brodersen and Langseth,²⁶ relatively strong mixing occurs between ν_9 and ν_{18} , ν_4 and ν_{11} , and ν_8 and ν_{19} . Weaker mixing does occur to some extent among all vibrations of the same symmetry, and in particular in the C_{2v} site symmetry among all the vibrations of sym- $C_6H_3D_3$. This latter mixing, however, does not appear to be very strong since the predicted vibrations are the more intense. Figure 5 shows a microphotometer tracing of the phosphorescence spectrum of sym- $C_6H_3D_3$ in crystalline C_6D_6 near the electronic origin. All of the observed fundamentals serve as false origins for totally symmetric ν_1 (a_1' , 955 cm^{-1}) and ν_{12} (a_1' , 1003 cm^{-1}) progressions. The analysis of the sym- $C_6H_3D_3$ phosphorescence out to $0, 0 - (\nu_8 + \nu_1)$ is given in Table VI. Some of the lines shown in Fig. 5 are due to m- $C_6H_4D_2$ and m- $C_6H_2D_4$ impurities. These were identified from the phosphorescence of the corresponding isotopes in a C_6D_6 host. The frequencies are not included in Table VI. The possibility that some of the unassigned lines might be due to isotopic impurities other than the two above has not been investigated.

The vibrational degeneracies in sym- $C_6H_3D_3$, as in C_6H_6 , can also be removed by the low symmetry crystalline field, giving rise to site splittings. Nine of the ten degenerate vibrations have been assigned from the phosphorescence and fluorescence spectra. Site splitting is directly observed on four e' and two e'' (vide infra) fundamentals and inferred for the third e'' fundamental. ν_{20} was obtained from the fluorescence. Because of the greater linewidth in the fluorescence, the site splitting in ν_{20} could be as large as 3 cm^{-1} and not be resolvable. For ν_{19} the site splitting must be $< 1\text{ cm}^{-1}$ assuming roughly equal intensities for the two components since only one line was observed. The results are summarized in Table VII.

TABLE VII. Summary of the sym-C₆H₃D₃ data (cm⁻¹)

D _{3h} symmetry class	Vibration number	Fundamental frequency			Site splitting	
		gas ^a	liquid ^a	solid ^b		
a ₁ '	ν ₁	(956)	955	954.6		
	ν ₂	(3074)	(3062)	3046.3		
	ν ₁₂	(1004)	1003	1002.9		
	ν ₁₃	(2294)	2282	2281.4		
a ₂ ''	ν ₄	697	697	703.9		
	ν ₅	917	918	927.8		
	ν ₁₁	531	533	546.2		
e'	ν ₆	594	594	591.8	593.5	1.7
	ν ₇	2282	2274	2269.0	2274	5
	ν ₈	1580	1575	1571.2	1572.2	1.0
	ν ₉	1101	1101	FR		
	ν ₁₈	833	833	831.5	834.6	3.1
	ν ₁₉	1414	1412	1410.8		<1
	ν ₂₀	3063	3553	3060.6		<3
e''	ν ₁₀	(707)	711	718.2	722.7	4.5
	ν ₁₆	(370)	375	[378]	[387]	[8.5]
	ν ₁₇	(924)	(926)	936.6	940.7	4.1 ^c

^a Ref. 26. Values in parentheses are calculated.

^b Not corrected for possible Fermi resonance (FR). Values in brackets are inferred from combinations.

^c See text.

None of the three possible a_2' vibrations -- ν_3 , ν_{14} , and ν_{15} -- were assigned from the emission spectra. These were observed in the infrared for sym- $C_6H_3D_3$ in both C_6H_6 and C_6D_6 hosts and are reported in Ref. 4. For the ground state fundamentals that are seen both in the infrared spectrum and in the electronic emission spectra the agreement is within experimental error except for ν_{17} . The site split components of the fundamental ν_{17} in the phosphorescence have quite different intensities and the high energy component of the vibration is too weak to observe in most combinations.

The two components are seen only in ν_{17} and in the doublets tentatively assigned to $\nu_{17} + \nu_8$ and to $\nu_{17} + \nu_5$, where the splitting repeats but the intensities become more nearly equal. This behavior is similar to ν_{10} in both C_6H_6 and sym- $C_6H_3D_3$, but for ν_{17} the intensity difference is greater. The more intense component of ν_{17} agrees with one of the infrared values in a C_6D_6 host, but the weaker component differs from the other infrared value by ca. 2 cm^{-1} which is outside the combined experimental errors. The infrared values for this sym- $C_6H_3D_3$ vibration in the two hosts C_6H_6 and C_6D_6 show larger than usual shifts (ca. 1 cm^{-1}), but this borders on the reported experimental error. Considering the weakness of the high energy component in the phosphorescence, the assignment to ν_{17} may be questioned, but, if this is not the correct assignment and the other component of ν_{17} is unobserved, then the vibronic intensities of the two components must be greatly different as ν_{17} is seen as a doublet in the mixed crystal infrared spectrum.

An alternate assignment of the very weak 940.7 cm^{-1} component would be to ν_1 of either one (or both) of the two $^{13}C^{12}C_5H_3D_3$ species present.

Brodersen and Langseth have assigned a Raman line at 947 cm^{-1} , observed in liquid sym- $C_6H_3D_3$, to $^{13}C^{12}C_5H_3D_3$. If the ^{13}C -isotope shift in the phosphorescence 0, 0 of $^{13}C^{12}C_5H_3D_3$ is roughly equal to the 7.8 cm^{-1} ^{13}C -shift seen for

$^{13}\text{C}^{12}\text{C}_5\text{H}_6$, then the line at $\Delta\nu = 940.7 \text{ cm}^{-1}$ becomes $\Delta\nu = 948.5 \text{ cm}^{-1}$ based on the unobserved $^{13}\text{C}-0, 0$. This near agreement with the Brodersen and Langseth value and the weakness of the vibronic line suggests that perhaps the assignment to ^{13}C is correct. We choose to report in Table VII a site splitting of 4.1 cm^{-1} based on (1) the few tentative combinations involving both components of ν_{17} in the phosphorescence and (2) the observation of a comparable site splitting in the infrared.

At $\Delta\nu \approx 1100 \text{ cm}^{-1}$ the fundamental $\nu_9(e')$ is in resonance with the combination $\nu_{10} + \nu_{16}(e' + a' + a_2')$. The strongest two lines in this region, which might be assigned to ν_9 since this fundamental is expected to be strong in the phosphorescence, are degenerate with two of the harmonic values for $\nu_{10} + \nu_{16}$. Since six lines are observed, the ν_9 component of the Fermi multiplet is apparently responsible for two of these lines; however, unambiguous assignments can not be made. Similar problems occur 2270 cm^{-1} to the red of the $0, 0$. The fundamental ν_7 is expected to occur in this region, but again overlapping combinations make a unique assignment difficult especially from the phosphorescence (see Table VI). However, in the sym- $\text{C}_6\text{H}_3\text{D}_3$ fluorescence, as in that of C_6H_6 , the relative vibronic intensity of ν_7 is increased and, therefore, the lines assigned to ν_7 stand out more clearly. Of course the higher the energy of the ground state vibration, i. e., the further it is removed from the $0, 0$, the more severe these problems become. Furthermore, for all the isotopes the emission lines at the same time become broader and an underlying continuum appears. Thus, the assignments to ν_2 and ν_{20} in the 3050 cm^{-1} region are the least certain. As seen by comparing Figs. 3 and 5, the density of lines is less in the C_6H_6 emissions and these complications are not so prevalent.

4. C_6H_5D

C_6H_5D has vibrational symmetry C_{2v} for a hexagonal carbon framework. As seen from the correlation diagram in Fig. 4, degenerate vibrations are split into a and b components in this lower symmetry and all vibrations group theoretically can be active in the phosphorescence spectrum. However, those vibrations which correlate directly to the more intense vibrations in the phosphorescence of C_6H_6 or are strongly mixed with one of these active vibrations²³ again dominate. For example, the b_2 vibrations ν_{11} and ν_{17b} are mixed with ν_4 and ν_5 , respectively. For the b_1 vibrations strong mixing occurs among ν_{9b} , ν_{15} , and ν_{18b} and between ν_3 and ν_{14} . Thus, besides the strong vibrations corresponding to those shown in Table III, the vibrations ν_{11} , ν_{17b} , ν_{15} , and ν_{18b} also serve as relatively strong vibronic origins of totally symmetric progressions. The weakness of the remaining vibrations again suggests that the molecular symmetry classifications are still approximately valid in the C_i site.

As a result of this mixing, the actual numbering of the fundamentals is somewhat arbitrary in a number of cases. We have generally followed Brodersen and Langseth, deviating from their labeling scheme only in one of the more arbitrary cases where the vibronic activity seemed to suggest a different assignment, i. e., ν_{9b} and ν_{15} are interchanged.

Since there are no degenerate species in point group C_{2v} , site splitting cannot occur. As pointed out in Section II an apparently similar and related effect can and does occur. The latter has been termed the orientational effect.⁴ The expected line pattern is given in Table I for the different isotopes for different choices of the effective site symmetry.

The phosphorescence spectrum near the electronic origin for 0.5% C_6H_5D in a C_6D_6 host crystal is shown in Fig. 6. Table VIII gives the complete analysis for the measured bands out to $0,0 - (\nu_{s a, b} + \nu_1)$. The electronic origin consists of a pair of lines separated by 6.5 cm^{-1} and all other vibronic bands are doublets or triplets with a total band width of approximately 7 cm^{-1} . These general features have been previously described by NT. They assigned the $0,0$ doublet to different orientations of the guest in the crystal, the 6.5 cm^{-1} "splitting" representing the difference in zero-point energies among distinct guest molecules with different orientations of the deuterium atoms in the nearly C_{2h} site. Thus, based on each member of the $0,0$ band vibronic lines appear with energy separations corresponding to vibrational frequencies. Due to the complications of the reduced molecular symmetry and of the orientational effect, the overall density of lines is greatly increased in the C_6H_5D phosphorescence. Therefore, we have primarily concentrated on the lower energy fundamentals and the more intense combinations.

For example, consider the doublet assigned to $0,0 - \nu_1(a_1)$ in Fig. 6. Each of these represents the subtraction of a quantum of the totally symmetric mode ν_1 from its respective $0,0$ line. NT have been able to show from concentration studies that for some of the more intense lines, the high (low) energy member of a vibronic doublet corresponds to the high (low) energy member of the $0,0$ band. Therefore, in the analysis for ν_1 presented in Table VIII the subtractions are made assuming this correlation holds for all vibronic bands. Two values are in this manner obtained for ν_1 , 979.0 cm^{-1} and 979.4 cm^{-1} . The difference in these two values results from the inequivalence of the guest-host interactions when two guest molecules undergo the same vibration in two physically different crystal directions corresponding

Caption for Fig. 6.

Microphotometer tracing of the stronger bands of the C_6H_5D phosphorescence. The $\nu_{a, b}$ bands are taken from a plate exposed 1/5 as long as the rest of the spectrum. Lines under the trace indicate assignments.

262

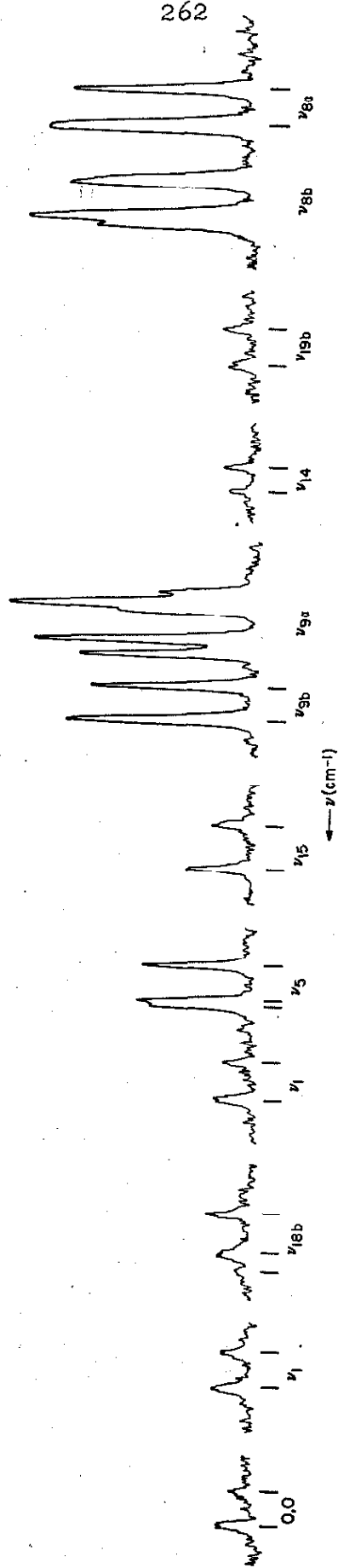


TABLE VIII. Analysis of the C₆H₅D phosphorescence

λ_{air} (Å)	ν_{vac} (cm ⁻¹)	Relative intensity	$\Delta\nu$ (cm ⁻¹)	Assignment ^a	Vibrational symmetry in C _{2v}	Predicted harmonic value (cm ⁻¹)
3367.85	29690.3	w	0	0, 0 ¹		
67.11	683.8	w	6.5	0, 0 ²		
3436.53	090.8	vw, b	599.5	600.1	ν_{ea}	a ₁
37.37	083.7	vw, b	606.6		ν_{eb}	b ₁
39.14	068.8	vw, b	621.5	623.2	ν_{11}	b ₂
40.11	060.6	vw, b	629.7			
48.81	28987.2	w	703.1	703.2	ν_4	b ₂
49.60	980.6	w	709.7			
66.88	836.1	vw	854.2	857.1	(ν_{10a})	a ₂
67.23	833.2	w	857.1		ν_{18b}	b ₁
68.15	825.6	w	864.7	858.2		
76.86	755.3	vw	937.0		ν_{17b}	b ₂
77.56	747.5	vw	942.8	936.3		
81.95	711.3	w	979.0		ν_1	a ₁
82.78	704.4	w	985.9	979.4		
84.09	693.7	w	996.6			
84.21	692.7	w	997.6	997.6	ν_5	b ₂
84.99	686.2	mw	1004.1			

TABLE VIII. (Cont'd)

λ_{air} (Å)	ν_{vac} (cm^{-1})	Relative intensity	$\Delta\nu$ (cm^{-1})	Assignment ^a	Vibrational symmetry in C_{2v}	Predicted harmonic value (cm^{-1})
3493.76	28614.3	w	1076.0	1077.7	b_1	ν_{15}
94.76	606.1	w	1084.2			
3503.58	534.1	m	1156.2	1156.3	b_1	ν_{9b}
04.39	527.5	mw	1162.8			
05.09	521.8	mw	1168.5	1168.5	b_2	$3\nu_{16}$
05.43	519.0	mw	1171.3	1171.3	a_1	ν_{9a}
06.07	513.8	w	1176.5	1176.5	b_1	$(\nu_{16b} + \nu_{10a})$
06.21	512.2	m	1178.1		a_1	ν_{9a}
07.51	510.3	w	1180.0	1180	b_2	$3\nu_{16}$
07.90	499.0	vw	1191.3	1184.8	b_1	$(\nu_{16b} + \nu_{10a})$
21.08	392.3	vvw	1297.5	1298.5	b_1	ν_8
21.95	385.3	vvw	1305.0			
23.88	369.7	vw	1320.6	1320.6	b_1	ν_{14}
24.43	365.2	vw	1325.1	1318.4		
39.72	242.8	vw	1447.5			
40.56	236.1	vw	1454.2	1417.7	b_1	ν_{19b}
53.27	135.0	vw, b	1555.3	1555.7		$\nu_{11} + \nu_{17b}$
54.15	128.1	vw, b	1562.7		a_1	1558.6 1566.0

TABLE VIII. (Cont'd)

λ_{air} (Å)	ν_{vac} (cm^{-1})	Relative intensity	$\Delta\nu$ (cm^{-1})	Assignment ^a	Vibrational symmetry in C_{2v}	Predicted harmonic value (cm^{-1})
3555.41	28118.1	s	1572.2	$(\nu_6 + \nu_1)$	b_1, a_1	
55.68	115.9	s	1574.4	ν_{8b}	b_1	
56.39	110.3	s	1580.0	1573.5 $(\nu_6 + \nu_1)$	b_1, a_1	
56.55	109.1	s	1581.2	1574.7 ν_{8b}	b_1	
57.67	100.2	s	1590.1	1590.3 ν_{8a}	a_1	
58.52	093.5	s	1596.8			
64.38	047.3	$\nu\nu, b$	1643.0	$\nu_{8b} + 69.7$		
66.52	030.5	$\nu\nu, b$	1659.8	$\nu_{8a} + 69.7$		
69.31	008.6	w	1681.7	1683.1 $\nu_4 + \nu_1$	b_2	1682.1
70.19	001.7	w	1689.6			1689.1
81.91	27910.1	$\nu\nu$	1780.2	1778.8 $(\nu_{10b} + \nu_1)$	b_2	
82.57	905.0	$\nu\nu$	1785.3			1833.2
89.19	853.5	$\nu\nu, b$	1836.8	1837.6 $\nu_{18b} + \nu_1$	b_1	1836.1
90.13	846.2	$\nu\nu$	1844.1			1844.1
99.29	775.4	$\nu\nu$	1914.9	1915.5 $\nu_{17b} + \nu_1$	b_2	1916.0
3600.21	768.3	$\nu\nu$	1922.0			1922.0
04.73	733.4	$\nu\nu$	1956.9	1957.3 $2\nu_1$	a_1	1958.0
05.68	726.1	$\nu\nu$	1964.2			1965.3

TABLE VIII. (Cont'd)

λ_{air} (Å)	ν_{vac} (cm^{-1})	Relative intensity	$\Delta\nu$ (cm^{-1})	Assignment ^a	Vibrational symmetry in C_{2v}	Predicted harmonic value (cm^{-1})
3607.12	27715.0	w	1975.3	1975.3		1975.6
07.25	714.0	w	1976.3	1976.3	$\nu_5 + \nu_1$	1976.6
08.09	707.6	w	1982.7	1975.7	$\nu_5 + \nu_1$	1983.5
17.50	635.5	vw	2054.8	2056.8	$\nu_{15} + \nu_1$	2055.0
18.62	627.0	vw	2063.3	2056.8	$\nu_{15} + \nu_1$	2063.6
28.03	555.3	m	2135.0	2135.2	$\nu_{9b} + \nu_1$	2135.2
28.92	548.6	mw	2141.7	2135.2	$\nu_{9b} + \nu_1$	2142.2
29.67	542.9	mw	2147.4	2147.4	$3\nu_{16} + \nu_1$	
30.04	540.1	m	2150.2	2150.2	$\nu_{9a} + \nu_1$	
30.86	533.9	vw	2156.4		$(\nu_{16a} + \nu_{10a}) + \nu_1$	
30.95	533.2	m	2157.1	2149.2	$\nu_{9a} + \nu_1$	
31.30	530.5	vw	2159.8	2149.2	$3\nu_{16} + \nu_1$	
49.54	392.9	vw	2297.4		$(\nu_3 + \nu_1), \nu_{7a}$	
49.87	390.4	vw	2299.9	2299.9		2299.6
50.38	386.6	vw	2303.7	2297.7	$\nu_{14} + \nu_1$	2304.3
66.64	265.0	vw	2425.3	2425.7	$\nu_{19b} + \nu_1$	2426.5
67.60	258.1	vw	2432.2	2425.7	$\nu_{19b} + \nu_1$	
83.06	143.6	s	2546.7	2548.8	$\nu_{8b} + \nu_1$	
83.34	141.5	s	2548.8	2548.8	$\nu_{6} + 2\nu_1$	
84.18	135.3	s	2555.0	2547.5	$\nu_{6} + 2\nu_1$	

TABLE VIII. (Cont'd)

λ_{air} (\AA)	ν_{vac} (cm^{-1})	Relative intensity	$\Delta\nu$ (cm^{-1})	Assignment ^a	Vibrational symmetry in C_{2v}	Predicted harmonic value (cm^{-1})
3686.20	27120.5	s	2569.8	2569.8		2569.1
87.18	113.3	s	2577.0	2570.5	a_1	2582.7

^a Bands in Fermi resonance are connected by square brackets.

to the two different guest orientations. This apparent splitting, namely 0.4 cm^{-1} for ν_1 , is the orientational effect on this vibration for $\text{C}_6\text{H}_5\text{D}$ in a C_6D_6 host crystal. If this vibration were observed in the infrared or by the Raman effect with sufficient resolution, it would appear as a close doublet with a splitting of 0.4 cm^{-1} , instead of the apparent 6.9 cm^{-1} splitting observed in the phosphorescence.

Since the crystallographic site symmetry is $\underline{\text{C}}_i$ and not $\underline{\text{C}}_{2h}$, triplets are predicted in Table I instead of the generally observed doublets. In fact, triplets are observed for some bands, e. g., ν_{18b} and ν_5 in Fig. 6, and inferred for many doublets since the high-energy line is broader. From this and the concentration studies of NT, two of the three electronic origins are assigned to the higher energy component of the $0,0$. In Table VIII this nearly degenerate pair are designated as $0,0^1$ and $0,0^2$; the third origin 6.5 cm^{-1} to lower energy is called $0,0^3$.

For the vibronic bands which appear as doublets, the vibrational energy quantum corresponding to origins $0,0^1$ and $0,0^2$ are again nearly degenerate. If the vibronic band is a triplet, the two lines at higher energy are subtracted from the assumed degenerate electronic origins $0,0^1$ and $0,0^2$ to obtain the respective vibrational quantum for these two guest orientations. The vibrational energy in the third orientation is obtained by

subtracting the low-energy line of the triplet vibronic band from $0, 0^3$. In this fashion, three different frequencies are generally obtained for a given vibrational mode as shown in Table VIII.

The results are summarized in Table IX which gives all the directly observed fundamental frequencies and the orientational effects determined. The near equivalence of the $0, 0^1$ and $0, 0^2$ orientations is demonstrated by the fact that only two of the fifteen observed fundamentals show a triplet structure and thus have non-zero entries in column 6 of Table IX. This indicates that the effective site symmetry is very nearly C_{2h} . However, the effect on the vibrational energy in these two cases is quite large, amounting to $1-3 \text{ cm}^{-1}$, compared to an average orientation splitting of 0.7 cm^{-1} between $0, 0^3$ and $0, 0^2$. It should be noted that both positive and negative energy shifts are observed for the orientational effect. Where the fundamentals reported here overlap with bands observed directly in the infrared the agreement is excellent. No orientation effect has been reported for ν_{9a} or ν_{9b} as it is difficult to conclusively assign all the lines in these regions (1170 and 1575 cm^{-1} removed from the $0, 0$ band, respectively). It appears that these fundamentals are in Fermi resonance with combinations (see Table VIII).

Since these orientational effects are all small, it is necessary to carefully analyze the sources and the magnitudes of the errors and their propagation in obtaining the final result. The first consideration is, of course, the validity of the subtractions. These have been made subject to the following restrictions: the concentration studies referred to earlier and the fact that where the assignments are unambiguous the orientational effects are usually small (vide infra and Ref. 4). These considerations lead to the method of subtraction given above. Besides this fundamental problem, experimental errors in line frequencies can distort the final result. Such an analysis leads to an uncertainty in the orientational effect of $\lesssim 0.5 \text{ cm}^{-1}$.

TABLE IX. Summary of C₆H₅D data (cm⁻¹)

C _{2v} symmetry class	Vibration number	Gas ^a			Liquid ^a			Solid sites			Orientational effect (arbitrary)			Comments ^b
a ₁	ν_1	(983)		979.0	(983)		979.4					+0.4	FR: ν_5	
	ν_{8a}	(1600)		1590.1	1593		1590.3					+0.2	FR: ν_{8a} , ν_{8b} and ($\nu_6 + \nu_1$)	
	ν_{9a}	(1177)		1171	1177		-						FR: ($\nu_{10} + \nu_{16b}$) and 3 ν_{16b} ; F	
b ₁	ν_8	(1295)		1297.5	1291		1298.5					0	+1.0	
	ν_{6b}	(607)		599.5	602		600.1					0	+0.6	ν_{6a} and ν_{6b} in resonance
	ν_{8b}	(1590)		1575.2	1576		-					0	FR: ν_{8a} , ν_{8b} and ($\nu_6 + \nu_1$); F	
	ν_9	(1157)		1156.2	1158		1156.3					0	+0.1	
	ν_{14}	(1327)		1320.6	(1325)		1318.4					0	-2.2	
	ν_{15}	1077		1076.0	1077		1077.7					0	+1.7	
ν_{18b}	858		854.2	857.1	857		858.2				+2.9	+1.1	FR: ν_{10a}	
ν_{19b}	1440- 1490		1447.5	1448	1448		1447.7				0	+0.2	FR: ν_{19a}	

TABLE IX. (Cont'd)

C _{2v} symmetry class	Vibration number	Gas ^a		Liquid ^a			Solid sites			Orientational effect (arbitrary)		Comments
		Gas ^a	Liquid ^a	1	2	3	2-1	3-2				
b ₂	ν_4	698	699	703.1		703.2	0	+0.1				
	ν_6	(984)	978	996.6	997.6	997.6	+1.0	0			FR: ν_1	
	ν_{11}	607	602	621.4		623.6	0	+2.2			FR: ν_6 in liquid	
	ν_{17}	924	925	937.0		936.3	0	-0.7				

^a Ref. 26 () indicates calculated values.

^b FR = Fermi resonance; F = frequency observed in the fluorescence.

This is a consequence mainly to the three differences involved and round-off error in the absolute energy of any given vibronic line which is reported only to $\pm 0.1 \text{ cm}^{-1}$.

5. p-C₆H₄D₂

For p-C₆H₄D₂, which has vibrational symmetry D_{2h} for a hexagonal carbon framework, the correlation diagram in Fig. 4 shows that all the g-vibrations a_{1g} , b_{1g} , and b_{3g} can group theoretically be active in the phosphorescence spectrum. Besides those vibrations which correlate directly to the more active vibrations of C₆H₆, a significant activity is also seen of the vibrations $\nu_{10} b(b_{3g})$ and $\nu_3(b_{2g})$ which mix with $\nu_4(b_{3g})$ and $\nu_9 b(b_{2g})$, respectively. As in C₆H₅D, no degeneracies remain in the vibrational manifold of p-C₆H₄D₂. However, inversion symmetry is preserved in the latter isotope so that in general the same fundamentals are not observed in the infrared and emission spectra.

As can be seen from the phosphorescence spectrum of 0.5% p-C₆H₄D₂ shown in Fig. 7, the electronic 0,0 and apparently all other vibronic bands are triplets. Because of the complex nature of this spectrum, it was not completely analyzed. A partial analysis of the spectrum is given in the figure, where the average band width of the triplets is about 13 cm^{-1} . The origin of the electronic splittings and their relative magnitude for various isotopes has been discussed by NT. Proceeding as in C₆H₅D, in general three different frequencies corresponding to $0, 0^1$, $0, 0^2$, and $0, 0^3$ are observed for each vibrational mode summarized in Table X. These bands are the only ones for which an unambiguous assignment of the orientation effect could be made.

Caption for Fig. 7.

Microphotometer tracing of the stronger bands of the p-C₆H₄D₂ phosphorescence. The ν_8 region is taken from a plate exposed 1/5 as long as the rest of the spectrum. Lines under the trace indicate assignments.

274

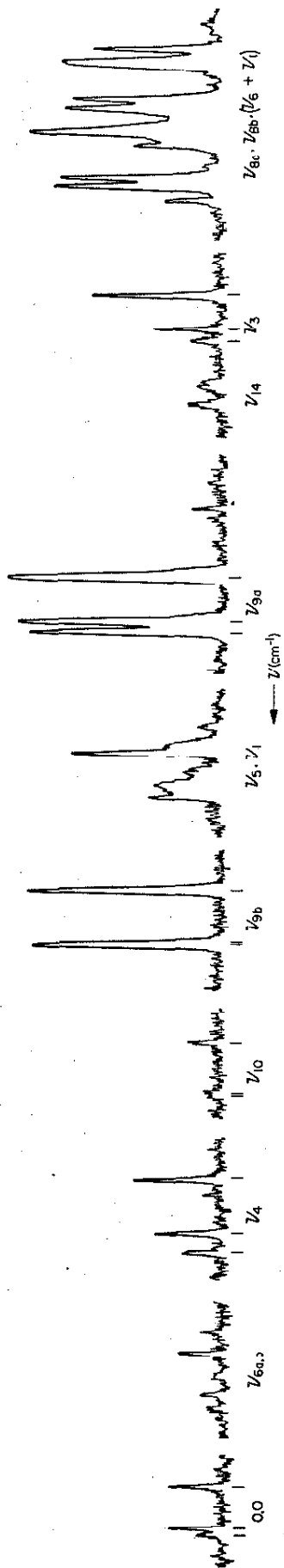


Table X. Summary of p-C₆H₄D₂ Data (cm⁻¹)

D _{2h} symmetry class	Vibration number	Gas ^a			Liquid ^a			Solid sites			Orientational effect (arbitrary)	
								1	2	3	2-1	3-2
b _{3g}	ν ₄	(633)	633	637.9	641.2	643.6					+3.3	+2.4
	ν _{10b}	(739)	736	744.3	742.4	742.9					-1.9	+0.5
	ν ₃	(1307)	1311	1310.2	1311.5	1308.1					+1.3	-3.4
a _{1g}	ν _{9a}	(1177)	1173	1171.4	1172.9	1171.8					+1.5	-1.1
	ν _{9b}	(913)	908	908.4	906.5	909.1					-1.9	+2.6
¹ B _{3u}	0,0			29721.4	29723.3	29734.9					+1.9	+12.6

^aRef. 26 () indicates calculated values.

V. ${}^1B_{2u} \leftarrow {}^1A_{1g}$ ABSORPTION SPECTRA

The vibronic absorption spectra of the guest in an isotopic mixed crystal also provides a useful tool for studying the effects of the crystal environment on the molecular energy levels. Not only can some excited state vibrations be studied but the orientational structure of the 0,0 band can be observed directly. Unlike the fluorescence, the guest singlet \leftarrow singlet absorption spectra can be very sharp in properly prepared crystals. Care must be exercised to avoid straining the crystal to obtain maximum sharpness.²⁷ In the thicker crystals of C_6H_6 in C_6D_6 , absorption linewidths as narrow as 0.6 cm^{-1} have been measured. The structure of the guest 0,0 absorption bands is given in Table XI for mixed crystals of C_6H_6 , C_6H_5D , $p\text{-}C_6H_4D_2$, and $\text{sym-}C_6H_3D_3$ at $\lesssim 0.005\%$ in C_6D_6 at 4.2°K . This structure represents the differences in the orientational effects of the ground and lowest excited singlet states, including both the vibrational contribution to their zero-point energies and any electronic effect. That is, if the net contribution to the energy of the zeroth vibronic level for a given orientation were the same for both states and if this were true for all orientations, the 0,0 band would consist of one line. From a comparison of Tables VIII, X, and XI one can see that this difference for the ${}^1B_{2u} \leftarrow {}^1A_{1g}$ transition is about 1/5 that of the ${}^3B_{1u} \leftarrow {}^1A_{1g}$ transition, but in both transitions the overall splitting for $p\text{-}C_6H_4D_2$ is about twice that for C_6H_5D . For a detailed discussion of the significance of these differences, see NT.

The thin crystals ($\sim 20 \mu$) are required to observe the higher vibronic guest transitions as such absorptions are completely masked by the host absorption in the thick samples. Such guest lines are usually sharper than the fluorescence lines even in these "poorer" crystals. The vibrational frequencies obtained from these absorption lines are less significant than

Table XI. ${}^1B_{2u} \leftarrow {}^1A_{1g}$ Electronic Transition Energy for Isotopic
 Guests in a C_6D_6 Host Crystal at 4.2°K.

	mixed crystal ^a (cm ⁻¹)		gas ^b (cm ⁻¹)
	${}^{12}C_6H_nD_{6-n}$	${}^{13}C\ {}^{12}C_5H_nD_{6-n}$	${}^{13}C_6H_nD_{6-n}$
C_6H_6	37853.3	37856.9	38086.1
C_6H_5D	37885.2 37884.0	37888.8 37887.7	38124
p- $C_6H_4D_2$	37915.7 37912.9		38154
sym- $C_6H_3D_3$	37947.9	37951.4	38184

^a Uncorrected for interaction with the C_6D_6 host.

^b The C_6H_6 value is from Ref. 18. For the other isotopes the
 0, 0 is taken from Ref. 21.

Table XII. Analysis of the ${}^1B_{2u} \leftarrow {}^1A_{1g}$ Absorption Spectrum of
1% C_6H_6 in C_6D_6 at 4.2°K.

λ_{air}	ν_{vac}	$\Delta\nu$	Assignment	Gas $\Delta\nu$
2641.00	37,853.3	0	0-0	
2605.34	38,371.3	518.0	} ν_6'	522.4 ^a
2605.20	38,373.4	520.1		
2577.89	38,779.8	926.5	ν_1'	923 ^b
2543.9	39,297(b)	1444	$\nu_1' + \nu_6'$	

^aRef. 18.

^bF. M. Garforth and C. K. Ingold, J. Chem. Soc., 1948, 417

those of ground state vibrations as excited state levels are more apt to be shifted by interactions with the host. The excitation exchange interactions are typically larger for the singlet vibronic bands than for the ground state vibrational bands and thus quasisonance interactions²⁸ with nearby host bands could cause a different shift in each vibronic level. A few C_6H_6 in C_6D_6 levels are given in Table XII from which it can be seen that the ν'_6 site splitting (2.1 cm^{-1}) is less than that of the ν''_6 (3.1 cm^{-1}). This splitting should not necessarily be the same as that of the ν'_6 in a pure C_6H_6 crystal, which has been reported²⁹ to be 9 cm^{-1} , since resonance interactions must contribute to the splitting in the pure crystal.

Absorptions due to ^{13}C -containing benzene have also been observed (see Table XI). In thick crystals of about 0.04% C_6H_6 , considerable fine structure is seen surrounding the 0,0 line. The spectrum is shown in Fig. 8 and analyzed in Table XIII. The additional absorptions are tentatively assigned to ^{13}C -benzene, $^{13}C_2$ -benzene, and to pairs of guest molecules in adjacent sites ("dimers" or "resonance pairs"). The line at 37856.9 cm^{-1} is assigned to $^{13}C^{12}C_5H_6$ based on the presence of a 982 cm^{-1} (ν_1, a_1) progression built on this origin in the $^1B_{2u} \rightarrow ^1A_{1g}$ emission spectrum, as described earlier, and on its intensity relative to the $^{12}C_6H_6$ 0,0 absorption at very low concentrations. The $^{13}C_2$ -benzene assignment is made from an analogy with the deuterium isotope effect,^{11,21} that is, the $^{13}C_2$ -line is expected to be shifted twice as much as the $^{13}C_1$ -line. Also in analogy with the deuterium effect, the o-, m-, or p- $^{13}C_2$ -shifts are expected to be nearly equal (within 10% of one another). The assignment of the line at 37848.6 cm^{-1} to a resonance pair is made on the basis of its concentration dependence; that is, its intensity decreases more rapidly than that of the C_6H_6 "monomer" absorption with decreasing C_6H_6 concentration. The line at 37851.2 cm^{-1} , which may also be due to a dimer on a different pair of crystallographic sites, has not been shown to have the expected concentration dependence since it is

Caption for Fig. 8.

Microphotometer tracing of the C_6H_6 electronic origin at two concentrations in a 2 mm. thick C_6D_6 host crystal. See Table XIII for the frequencies.

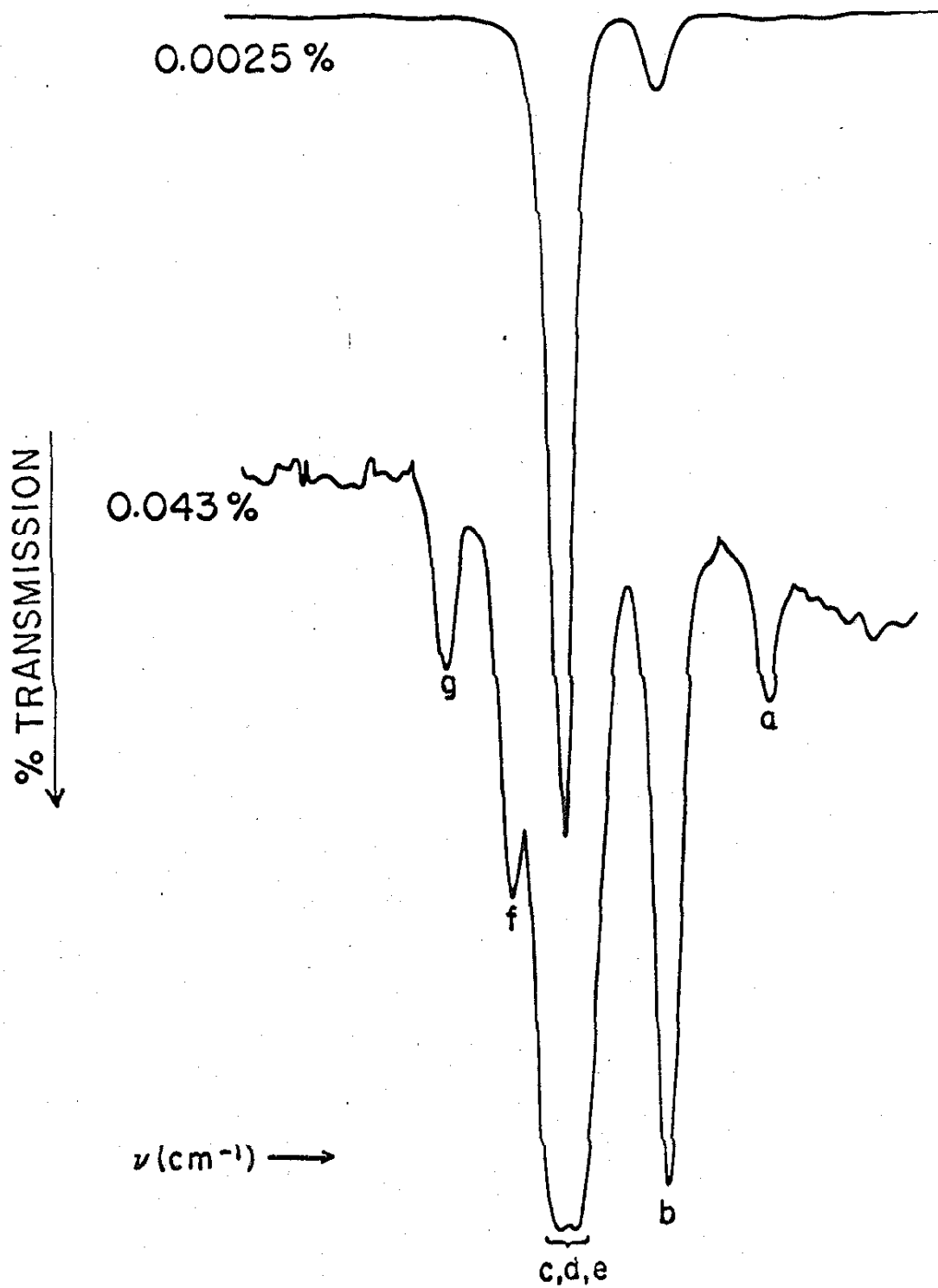


Table XIII. Structure Observed Near the Electronic Origin for C_6H_6 and C_6H_5D at Higher Concentrations in a C_6D_6 Host.

$C_6H_6^\dagger$			$C_6H_5D^\dagger$		
ν cm^{-1}	I	Assignment	ν cm^{-1}	I	Assignment
a^\ddagger 37,860.9	w	$^{13}C_2^{12}C_4H_6$	37,892.5	w	$^{13}C_2^{12}C_4H_5D$
			37,891.6	w	
b 37,856.9	s	$^{13}C C_5H_6$	37,888.8	s	$^{13}C^{12}C_5H_5D$
			37,887.7	s	
c \sim 37,854.1	w,sh		—		
d 37,853.3	vs	Monomer	37,885.2	vs	Monomer
			37,884.0	vs	
e 37,852.3	w		—		
f 37,851.2	w		37,882.7	w	
			37,881.8	w	
g 37,848.6	w	Resonance Pair	37,880.0	w,b	Resonance Pair

† 0.04% guest in a \sim 2 mm C_6D_6 host crystal.

‡ See Fig. 8.

too near the intense monomer absorption. At the highest resolution employed, additional absorption lines very near the monomer line are resolved. These are given in Table XIII, but are unresolved in the lower resolution spectrum shown in Fig. 8. Their concentration dependence and, therefore, their definite assignment is unknown. Similar lines were seen for the other deuterated isotopes. The C_6H_5D data is also given in Table XIII; note the consistency of the orientational effects.

It should be pointed out that polarized absorption spectra of pairs of molecules in isotopic mixed crystals allow the magnitudes and relative signs of pairwise intermolecular excitation exchange interactions to be determined directly, and therefore may be quite important in the interpretation of the pure crystal spectrum. Within the Frenkel limit, assuming short range terms dominate, these interactions are responsible for exciton mobilities and Davydor splittings, as well as for the full exciton band structures of molecular crystals.³⁰

VI. DISCUSSION AND CONCLUSIONS

From the results presented in the summary Tables, both site splittings and orientational effects are seen to be a general occurrence in the benzene crystal. The magnitude of the effects are generally insensitive to isotopic substitution, u- or g-symmetry classification, or to the vibration type as long as the vibration is either in- or out-of-plane. Even the gas-to-crystal frequency shifts (vide infra) follow this general pattern. However, differences are seen comparing in-plane and out-of-plane vibrations. Apparent exceptions for the site shifts are the particular in-plane vibrations ν_2 , ν_7 , ν_8 , and ν_{13} . However, the anomalously large gas-to-crystal shift for these vibrations parallels an anomalously large gas-to-liquid shift, while for the

other fundamentals the gas-to-liquid shifts are very small. This implies that the gas-to-solid shifts for these vibrations are due to environmentally induced interactions among the molecular vibrations, rather than, for example, repulsive interactions in the solid phase. The average site shift for the in-plane vibrations is very nearly zero and certainly within gas phase experimental error ($2-3 \text{ cm}^{-1}$) for unresolved bands. For the out-of-plane vibrations the average site shift (solid-gas) is greater than 10 cm^{-1} .

This trend is followed in the site splittings (see Tables IV and VII). The average site splitting for the out-of-plane vibrations is $\sim 7 \text{ cm}^{-1}$ while the in-plane vibrations have an average site splitting of roughly 3 cm^{-1} . For the orientational effect the distinction between in-plane and out-of-plane bands is less clear and it appears that the effect is more dependent on the particular vibrational mode. We note, however, that for $\nu_{16}(\text{CC}^{\perp})$ the orientational effect as seen in the infrared⁴ in $\text{C}_6\text{H}_5\text{D}$ and $p\text{-C}_6\text{H}_4\text{D}_2$ is the largest observed. Furthermore, the average maximum splitting among the orientational components is generally less than site splitting.

We suggest that the distinction between in-plane and out-of-plane modes is probably due to the greater vibrational amplitudes²⁴ for the out-of-plane displacements. This could imply that interaction with the crystal environment is greater and, therefore, larger site shifts, site splittings, and orientational effects result for larger vibrational displacements. For the lower symmetry isotopes which exhibit orientational effects, the mixing among vibrations, especially in the C_1 site, tends to equalize the vibrational amplitudes. Hence, one might not expect a clear distinction into certain vibrational classes or types, but rather a general effect larger only for certain motions with large vibrational amplitudes.

The site splitting observed in the fundamental ν_6 for C_6H_6 is 3.1 cm^{-1} .

Table XIV: Change in the 1600 cm^{-1} ν_6 and $\nu_6 + \nu_1$ Fermi Couple Splitting with Totally Symmetric $n\nu_1$ Additions

n	$\nu_6 + \nu_1$ (cm^{-1})	$(\nu_6 + \nu_1) + n\nu_1$ (cm^{-1})	Site splitting (cm^{-1})	Fermi splitting (cm^{-1})	
				solid ^a	gas ^b
0	1584.3	1602.8	1.2	19.1	20
		1604.0			
1	2568.1	2594.3	1.2	26.8	26
		2595.5			
2	3551.6	3583.5	1.3	32.5	31
		3584.8			
3	4534.1	4571.5 ^c		37.4	37
ν_6		606.3	3.1		
		609.4			

^aThe mean of the split $(\nu_6 + \nu_1) + n\nu_1$ component is used to calculate the Fermi splitting.

^bF. M. Garforth, C. K. Ingold and H. G. Poole, J. Chem. Soc., 1948, 427.

^cThis band is too weak to observe any splitting.

When totally symmetric additions are made to ν_6 , $(\nu_6 + \nu_1) + n\nu_1$ comes into Fermi resonance with $\nu_6 + n\nu_1$ and the measured splitting decreases to roughly 1.2 cm^{-1} as shown in Table XIV. The assignment of the " ν_6 component" in the Fermi doublet is made by comparison of the intensities of the members of the Fermi couple with the ν_6 fundamental in the fluorescence and phosphorescence emissions (cf. Table III and Fig. 3). The decrease in the measured splitting of ν_6 for C_6H_6 in the Fermi couple is apparently due to the resonance. Note, however, that the "lost splitting" does not appear in the other half of the couple ν_8 . In $\text{sym-C}_6\text{H}_3\text{D}_3$ this same resonance does not appear to be as strong since the observed value for $\nu_6 + \nu_1$ is closer to the harmonic value. The site splitting in this progression is more nearly constant and equals 1.7 , 1.9 and 1.5 cm^{-1} for $n = 0$, 1 , and 2 respectively. Furthermore, ν_8 in $\text{sym-C}_6\text{H}_3\text{D}_3$ is split by 1.0 cm^{-1} .

Even though the site-split components of a degenerate fundamental usually have very nearly equal vibronic intensities, the fundamentals ν_{10} in both C_6H_6 and $\text{sym-C}_6\text{H}_3\text{D}_3$ and ν_{17} in $\text{sym-C}_6\text{H}_3\text{D}_3$ are exceptions. Exactly how to evaluate this difference in vibronic intensities is not clear at present. An unknown amount of mixing and Fermi resonance between the components contributes to the site splitting and, if substantial, these interactions would tend to equalize the vibronic intensities. Therefore, one might conclude that for the bands where significant intensity differences are seen such intra-site interactions are small. The inverse, however, need not be true; that is, nearly equal intensities does not necessarily imply strong intra-site interactions. It may just be that in these cases the site-split components are equally good "intensity stealers." In combination and overtone bands the relative intensity of the components is variable. For example, the components of $(\nu_{16} + \nu_{11})$ and $2\nu_{16}$ in C_6H_6 appear as expected in the phosphorescence,

but in the fluorescence $2\nu_{16}$ differs from this intensity pattern, whereas $(\nu_{11} + \nu_{16})$ does not. Other examples are evident both from the approximate intensities given in Tables IV and VII and Figs. 2 and 5. Some of these have been previously discussed.

One would also expect an increased mixing and interaction among different molecular vibrations. These effects are expected to show up most clearly where they are symmetry forbidden or weak in the molecule but allowed in the crystal site. For example, for the well known case of $(\nu_6 + \nu_1) + n\nu_1$ interacting with $\nu_6 + n\nu_1$, as given in Table XIV, crystal effects are not obvious. However, for sym- $\text{C}_6\text{H}_3\text{D}_3$ $\nu_{16} + \nu_{10}$ and ν_9 (see Fig. 5 and Table VI) and ν_{20} and ν_2 seem to be examples of crystal site induced interactions. A further possible indication of the magnitude of the crystal site induced effects can be obtained from anharmonicities. Observing $n\nu_1$ out to $n = 5$ in the C_6H_6 fluorescence, the anharmonic effects are small in accordance with the above observations. The only other vibrations whose overtones are observed are ν_{16} and ν_{10} , but in these cases Fermi resonance in the crystal site among the three components of the overtone complicates the analysis of the anharmonicities. Similar difficulties are encountered in the combination bands.

The general conclusion from the gross vibrational structure is that neither the energies nor the symmetry classifications of the vibrations are strongly perturbed by the crystal. This is specifically shown by the magnitude of the site shifts, splittings, and orientational effects and by the dominance of the e_{2g} vibrations in the singlet and triplet spectra. The most pronounced effect of the crystal is the appearance of the 0, 0 progressions in the two emissions. This, along with the observation of site splittings, indicates that the molecular symmetry is not strictly \underline{D}_{6h} , but these effects could correspond to very small molecular distortions.

References

- ¹R. S. Halford, J. Chem. Phys. 14, 8 (1946).
- ²D. F. Hornig, J. Chem. Phys. 16, 1063 (1948).
- ³H. Winston and R. S. Halford, J. Chem. Phys. 17, 607 (1949).
- ^{4(a)}E. R. Bernstein, "Site Effects in Molecular Crystals--Site Shift, Site Splitting, Orientational Effect and Intermolecular Fermi Resonance for Benzene Crystals," J. Chem. Phys. (to be published). ^(b)E. R. Bernstein and G. W. Robinson, "Vibrational Exciton Structure in Crystals of Isotopic Benzenes," J. Chem. Phys. (to be published). ^(c)E. R. Bernstein, "Calculation of the Ground State Vibrational Structure and Phonons of the Isotopic Benzene Crystals," J. Chem. Phys. (to be published).
- ⁵V. L. Strizhevsky, Opt. i Spektroskopiya 8, 86 (1960).
- ⁶E. G. Cox, Rev. Mod. Phys. 30, 159 (1958); E. G. Cox, D. W. J. Cruickshank, and J. A. S. Smith, Proc. Roy. Soc. (London) A247, 1 (1958).
- ⁷H. Shull, J. Chem. Phys. 17, 295 (1949).
- ⁸B. Ya. Sveshnikov and P. P. Dikun, Dokl. Akad. Nauk SSSR 65, 637 (1949); Zhur. Eksperim. i Teor. Fiz. 19, 1000 (1949); T. V. Ivanova and B. Ya. Sveshnikov, Opt. i Spektroskopiya 11, 322 (1961).
- ⁹S. Leach and R. Lopez-Delgado, J. chim. phys. 61, 1636 (1964).
- ¹⁰G. C. Nieman, Thesis, California Institute of Technology, 1964.
- ¹¹G. C. Nieman and D. S. Tinti, J. Chem. Phys. 46, 1432 (1967).
- ¹²E. R. Bernstein, S. D. Colson, R. Kopelman, and G. W. Robinson (manuscript in preparation).
- ¹³S. D. Colson, "Electronic Absorption Spectra of Isotopic Mixed Benzene Crystals," J. Chem. Phys. (to be published).
- ¹⁴S. D. Colson and E. R. Bernstein, J. Chem. Phys. 43, 2661 (1965).
- ¹⁵See, however, G. Castro and R. M. Hochstrasser, J. Chem. Phys. 46, 3671 (1967), who suggest that the lowest triplet is ${}^3B_{2u}$.

- ¹⁶A. C. Albrecht, *J. Chem. Phys.* 38, 1326 (1963).
- ¹⁷Here and elsewhere in this work, the normal coordinates are numbered after E. B. Wilson, J. C. Decius, and P. C. Cross, Molecular Vibrations, McGraw-Hill Book Co., Inc., New York, New York, 1955.
- ¹⁸J. H. Callomon, T. M. Dunn, and I. M. Mills, *Phil. Trans. Roy. Soc. (London)* A259, 499 (1966).
- ¹⁹A. C. Albrecht, *J. Chem. Phys.* 33, 156, 169 (1960); D. P. Craig, *J. Chem. Soc.* 1950, 59 2146; J. N. Murrell and J. A. Pople, *Proc. Phys. Soc. (London)* A69, 245 (1956); A. Liehr, *Z. Naturforsch.* A16, 641 (1961).
- ²⁰M. Ito and T. Shigeoka, *Spectrochim. Acta* 22, 1029 (1966).
- ²¹F. M. Garforth, C. K. Ingold, and H. G. Poole, *J. Chem. Soc.* 1948, 508.
- ²²A. Langseth and R. C. Lord, Jr., *J. Chem. Phys.* 38, 203 (1938); W. Gerlach, *Ber. d. Bayr. Akad. d. Wiss.* 1, 39(1932).
- ²³A. R. Gee and G. W. Robinson, *J. Chem. Phys.* 46, 4847 (1967).
- ²⁴D. H. Whiffen, *Phil. Trans. Roy. Soc. (London)* A248, 131 (1955).
- ²⁵A. C. Albrecht, *J. Mol. Spectry.* 5, 236 (1960).
- ²⁶S. Brodersen and A. Langseth, *Danske Videnkab. Selskab, Mat. Fys. Skrifter Kgl.* 1, No. 1 (1956).
- ²⁷S. D. Colson, *J. Chem. Phys.* 45, 4746 (1966).
- ²⁸G. C. Nieman and G. W. Robinson, *J. Chem. Phys.* 38, 1928 (1963).
- ²⁹V. L. Bronde, *Usp. Fiz. Nauk* 74, 577 (1961) [English transl. *Soviet Phys.-Usp.* 4, 584 (1962)].
- ³⁰A. S. Davydov, *Usp. Fiz. Nauk.* 82, 393 (1964) [English transl. *Soviet Phys.-Usp.* 6, 145 (1964)].

Trap-Trap Triplet Energy Transfer in Isotopic
Mixed Benzene Crystals

S. D. COLSON AND G. W. ROBINSON

Gates and Crellin Laboratories of Chemistry
California Institute of Technology, Pasadena, California 91109

ABSTRACT

The phosphorescence and fluorescence spectra of three component (two different guests in a C_6D_6 host crystal) isotopic mixed benzene crystals are studied as a function of guest concentration, excitation lamp intensity, and temperature. The energy relaxation processes in these systems are discussed and it is established that few, if any, host triplet excitons are produced during the interconversion of "trapped" singlet excitation into "trapped" triplet excitation. Triplet-triplet excitation transfer from one guest (trap) to the other lower energy guest (supertrap) is observed at temperatures where the host guest ΔE is greater than 30 KT. The concentration dependence of the trap-supertrap triplet energy transfer is interpreted in terms of a Perin model to indicate that the energy can be transferred over $\sim 20 \text{ \AA}$ in this system. At high lamp intensities, the phosphorescence intensity is found to depend upon the square root of lamp intensity. This is discussed in terms of a guest-guest annihilation model. Evidence is also presented for the generation of impurities at these high lamp intensities.

I. INTRODUCTION

Intermolecular transfer of electronic excitation has been subject to numerous investigations. The transfer of triplet excitation has been studied in systems ranging from chemically mixed¹ to pure (neat) crystals,² using both optical³ and EPR¹ spectroscopy. The primary mechanism for the transfer of triplet excitation from one guest molecule to another in dilute chemically mixed crystals is that of thermal "boiling out" of the trapped excitation into the host triplet exciton band. The host crystal excitons can then migrate through the crystal and be retrapped by another chemical impurity.¹ As the chemical impurities usually form quite deep ($\sim 2000 \text{ cm}^{-1}$) traps, this type of transfer is strongly temperature dependent and occurs only at relatively high temperatures. On the other hand, excitation transfer in neat crystals (exciton transfer) relies upon the direct interaction of the initial and final molecules and, neglecting complications from phonons, defects and impurities, is very rapid² and nearly temperature independent. In fact, triplet exciton transfer and the resultant triplet-triplet annihilation⁴ are so rapid, compared to the triplet radiative lifetime of aromatic molecules, that there are few examples of phosphorescence from aromatic molecular crystals.⁵ For this reason, the exchange interactions that are responsible for the transfer of triplet excitation, are much more difficult to determine than the interactions giving rise to singlet excitation transfer.

It has been shown,³ however, that the transfer of excitation among shallow traps formed by isotopic guests is very similar to that in neat crystals and, yet, is slow enough at low temperatures to allow one to observe phosphorescence from the traps. The transfer mechanism is similar to that in neat crystals in that, when the trap is much deeper than KT , the transfer rate is nearly independent of temperature and can be quite rapid. In that the transfer rate depends upon the exchange interactions between the host molecules and the host and guest molecules,³ it provides a direct measure of these interesting quantities. The transfer of excitation from one isotopic trap to another is determined by using two different isotopic guests that produce traps of different depths (a trap and a supertrap). The deviation of the trap-supertrap intensity ratio from the concentration ratio is taken to indicate energy transfer. Nieman and Robinson³ reported the phosphorescence intensity ratio for a 0.4% C_6H_6 , 0.4% C_6H_5D in C_6D_6 mixed crystal to be $I_p(C_6H_6)/I_p(C_6H_5D) \approx 10$ at 4.2°K, indicating a considerable amount of triplet energy transfer even though $\Delta E/KT \sim 60$.

The object of this paper is to present new experiments on isotopically mixed benzene crystals. The phosphorescence and fluorescence of mixed crystals containing two different isotopic traps are studied as a function of concentration and lamp intensity. Some very interesting effects are observed at high light levels.

II. EXPERIMENTAL

a. Preparation of Samples

Isotopic mixed benzene crystals were grown in evacuated crystal cells of $\sim 20\mu$ to 2 mm thickness by a technique which has been previously reported.⁶ The normal benzene was Phillips research grade (99.89 mole percent pure), and the deuterated benzenes were obtained from Merck, Sharp and Dohme, Ltd., Montreal, Canada. The C_6D_6 was reported to be 99.5 atom percent pure and in its absorption spectrum the various other isotopes were seen to be present at the following approximate mole fractions: $C_6HD_5 \sim .02$, $C_6H_2D_4 \sim .005$, $C_6H_3D_3 \sim .0005$, and C_6H_5D and $C_6H_6 \sim 10^{-5}$. All crystals were prepared from benzene which had been further treated to remove chemical impurities by refluxing over cesium as described in Ref. 7. Some mixed crystals were prepared from components that were separately purified while others were purified as a mixture. There was no evidence of isotope exchange during purification as long as the refluxing temperature was kept below $\sim 100^\circ C$.

b. Recording the Spectra

The emission spectra were recorded on a 1.83 M Jarrell-Ash Ebert spectrometer equipped with an EMI 6256s photomultiplier and with a 600 line/mm grating blazed at 1μ . The phosphorescence line widths for these mixed crystals are known⁶ to be too sharp ($\sim 0.05 \text{ cm}^{-1}$) to be accurately displayed by this instrument. In order to provide the maximum signal for intensity measuring purposes and, at the same time, to resolve clearly the emission from the different

Figure 1. Experimental setup. The sample S is positional in a quartz tipped helium dewar and "surrounded" by low pressure G. E. , 4 watt mercury lamps L_2 , L_3 , L_4 . To collect more of the light from these lamps, they are placed inside a magnesium oxide coated cylinder in which appropriate holes are cut for observing the emission and for exciting the sample with L_1 . L_1 is a Hanovia Model LO 735 A-7, low pressure 12 watt mercury discharge lamp. Photomultiplier P_1 is used to monitor the stability of L_1 and P_2 is used to record the benzene emission apectrum.

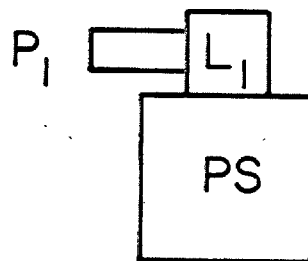
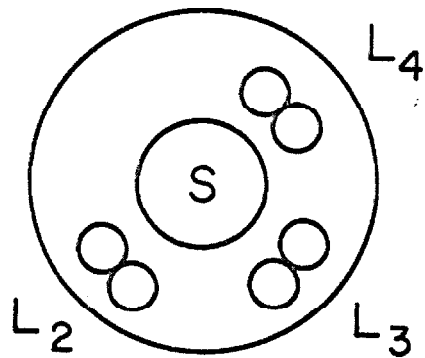
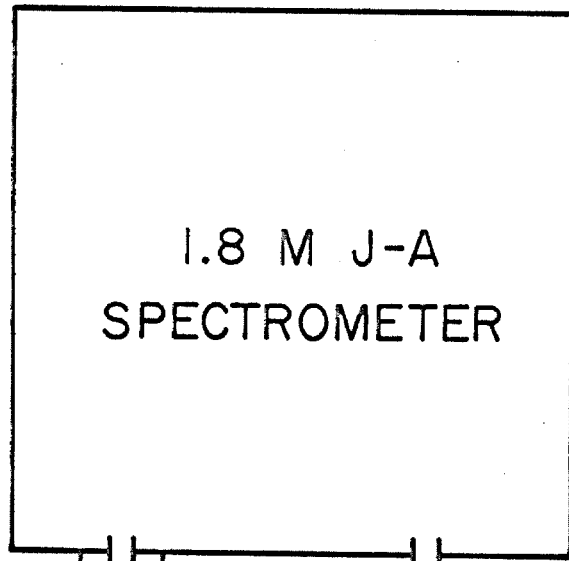
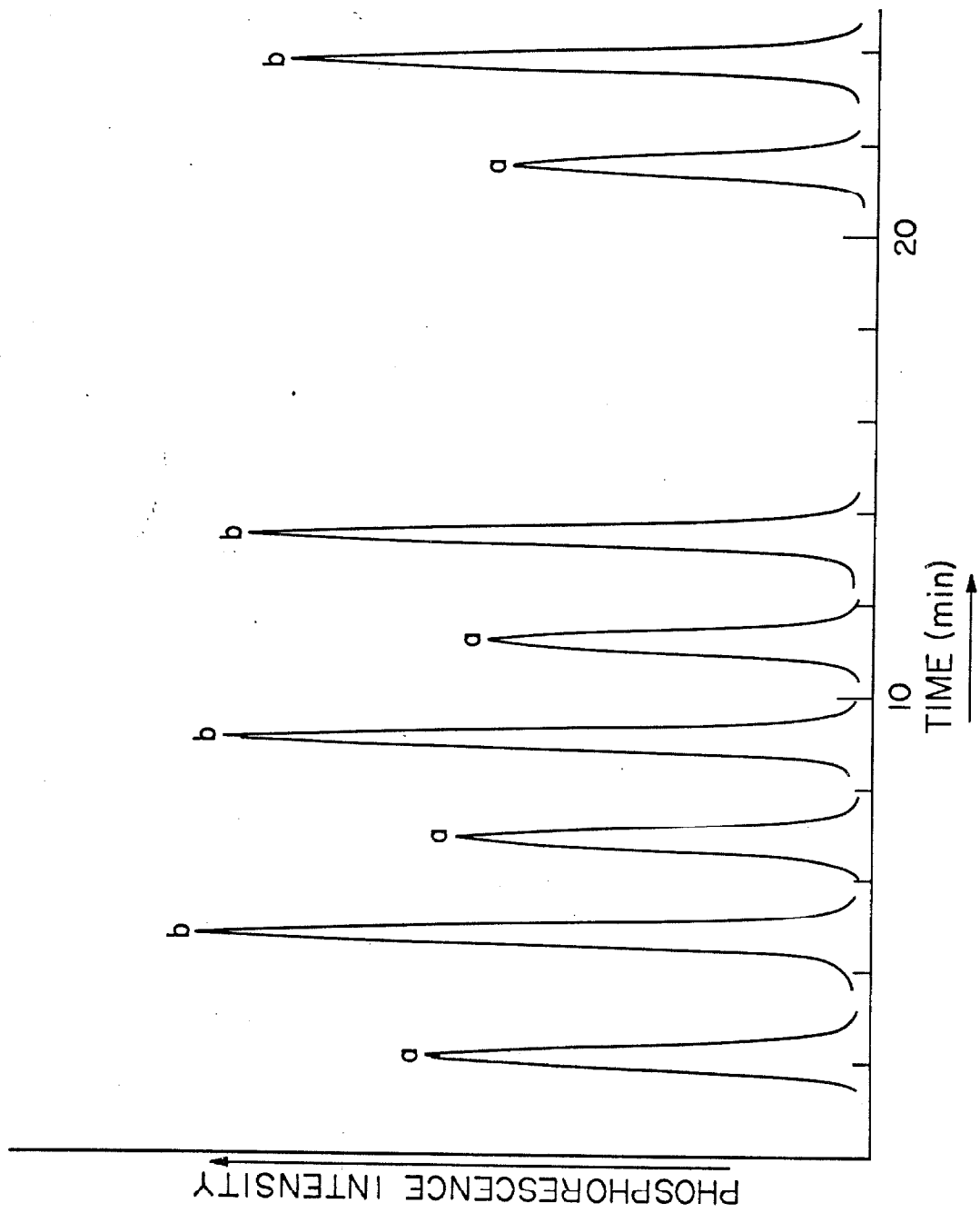


Figure 2. Time dependence of the phosphorescence intensity at the highest excitation light level. 0.2% sym- $C_6H_3D_3$, 0.2% C_6H_6 in C_6D_6 . Here, (a) is the $0,0 - \nu_8$ transition of sym- $C_6H_3D_3$ and (b) is the corresponding transition of C_6H_6 .



either by extrapolating back to the time the lamps were turned on or by turning them off and evaluating the amount of degradation by re-measuring the emitted intensity at lower light levels. Either method worked equally well giving an increased uncertainty in the measurement of $\sim 3\%$. This decreased quantum efficiency was found to be irreversible but it had no effect on the relative intensities of the trap and supertraps. After correcting for this phenomena, it was found that all other changes in the quantum efficiency with changing light level were completely reversible.

c. Measurement of Intensities

As the half widths of all lines were very nearly the same, their intensities were taken to be proportional to their peak heights. Because of changes in molecular symmetry, the number of lines and the distribution of emitted intensity among these lines changes markedly in going from one sample to another.⁶ Thus, no attempt was made to measure the total intensity emitted by each sample. The relative intensities of the various emitting traps as a function of concentration was determined as follows: The highest concentration to be studied was prepared from the pure liquids. This solution was then used to prepare the more dilute solutions, being careful to properly mix each sample to keep the concentration ratio of the two isotopic guests from changing upon dilution. All concentrations were determined by weighing in small, glass stoppered weighing flasks. The intensities of the more intense emission lines from each

guest were then measured, and a trap-supertrap intensity ratio determined at each concentration. This concentration dependent ratio was then extrapolated to determine its value at infinite dilution, and this value was used as a reference for determining the amount of excitation transfer from the trap to the supertrap. This procedure corrects for a number of possible evils in that one does not need to assume that the trap-supertrap concentration ratio is precisely known, that the emission quantum yields are independent of isotopic substitution, or that all or a specific fraction of the total emitted intensity of each trap has been accounted for. The largest source of error seems to be in the determination of the intensity ratios, which are found to be dependent upon sample preparation and upon the portion of a given crystal from which the intensity originates. For some crystals, the intensity ratio has been found to vary by as much as $\sim 3\%$ from one portion to another. As any determination of transfer distances relies heavily upon an accurate determination of the infinite dilution ratio (vide infra), only rough estimates could be determined from this work.

d. Temperature Effects on the Intensities

A controllable factor, which was found to strongly effect the phosphorescence intensity ratio, was the sample temperature. While it was found that the change in the ratio in going from 4.2°K to 1.8°K was not outside the experimental error, this ratio could be appreciably changed by heating of the sample with the excitation source. If the evacuated cells containing the 2 mm thick crystals were not broken

open, little if any trap phosphorescence could be detected, even though the same crystal when in direct contact with liquid helium gave a trap-supertrap phosphorescence ratio near unity. Similar but less dramatic effects were observed for the fluorescence intensity ratio. This problem was even more serious at the highest light levels used in some of these experiments. It was found that, even for the $20\ \mu$ thick crystals in direct contact with boiling He, the triplet energy transfer could be enhanced measurably ($\sim 10\%$) at these light levels. The change was attributed to heating of the sample since the effect was not observed for crystals in contact with superfluid He at any light levels. Thus, all intensity ratios were measured for samples in direct contact with either boiling or superfluid helium at normal light levels and with superfluid helium at the higher light levels employed.

III. DISCUSSION

a. Energy Relaxation Mechanism

Before undertaking a detailed discussion of the experimental results, it is important to understand clearly the inter- and intramolecular relaxation mechanisms that are operative in these somewhat complicated systems. A typical isotopic mixed crystal would be composed of 0.2% C_6H_6 , 0.2% sym- $C_6H_3D_3$, and 99.6% C_6D_6 . The replacement of each hydrogen with a deuterium atom results in an $\sim 33\ \text{cm}^{-1}$ blue shift of the 0,0 transition for the lowest excited singlet and triplet states of benzene.⁶ Thus, the C_6H_6 and sym- $C_6H_3D_3$

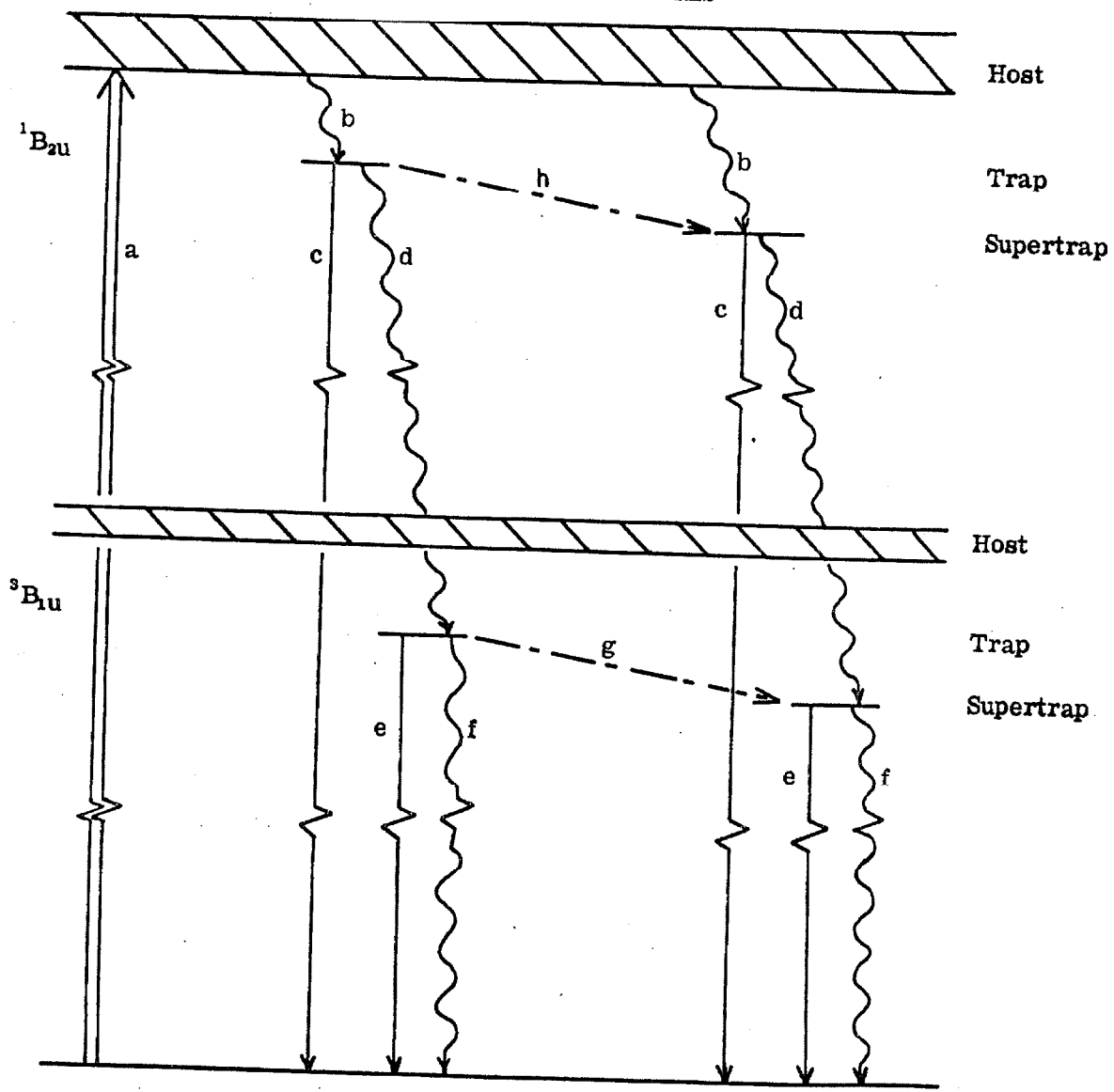
impurities form, respectively, 200 and 100 cm^{-1} traps for the host singlet or the host triplet excitons. These are designated as supertraps and traps (see Fig. 3). The crystal is usually excited by nearly monochromatic ultraviolet light that is absorbed by the $^1\text{B}_{2\text{u}}$ state of the host. That this excitation is very rapidly ($\sim 10^{-8}$ sec) trapped by the singlet traps and supertraps, is shown by the lack of host fluorescence at total impurity concentrations as low as 0.1 mole percent.

For traps in isotopic mixed crystals, the intersystem crossing rate (from the singlet to form triplet molecules) is of the same order as the fluorescence rate. Thus, making the plausible assumption that the intersystem crossing rates for host and guest molecules are nearly the same, it is possible to conclude that few, if any, host triplet excitons are generated from the host singlet excitons. In fact, under these conditions, no host triplet excitons will be produced unless either 1) there is intermolecular intersystem crossing from the guest singlets into the host triplet manifold, 2) there is guest-host triplet excitation transfer during the relaxation process subsequent to guest intramolecular intersystem crossing, or 3) triplet excitation is thermally pumped out of the triplet excited guests and into the host exciton band.

That none of these mechanisms is very important for the benzene system at 4.2°K can be seen from the following experiment. An ~ 2 mm thick crystal of 0.2% C_6H_6 , 0.2% sym- $\text{C}_6\text{H}_3\text{D}_3$ in 99.6% C_6D_6 at 4.2°K was excited with nearly monochromatic ($\Delta\nu_{\frac{1}{2}} \sim 30 \text{ cm}^{-1}$) light obtained from a 150 watt Xe lamp and a 0.75 M Jarrell-Ash monochromator. The phosphorescence (p) and fluorescence (f) were monitored photo-

Figure 3. Energy relaxation processes in three component isotopic mixed crystals. The various steps are designated by the arrows as follows: (a) the absorption process, (b) trapping of singlet excitons, (c) fluorescence, (d) intersystem crossing to produce triplets, (e) phosphorescence, (f) non-radiative relaxation to the ground state, (g) trap-supertrap, triplet-triplet energy transfer, and (h) trap-supertrap, singlet-singlet energy transfer.

MIXED CRYSTAL ENERGY LEVELS



graphically with a medium quartz spectrograph. When the 0, 0 transition of the host was excited, the supertrap-trap emission intensity ratios were $I_p(\text{C}_6\text{H}_6)/I_p(\text{C}_6\text{H}_3\text{D}_3) \approx 2$, and $I_f(\text{C}_6\text{H}_6)/I_f(\text{C}_6\text{H}_3\text{D}_3) \approx 1$. However, when the supertrap (C_6H_6) alone was excited, the only emission observed was the supertrap phosphorescence and fluorescence. If any of the above three mechanisms were very important at this temperature, phosphorescence from the sym- $\text{C}_6\text{H}_3\text{D}_3$ trap would have been observed.

The only other possible relaxation processes are those resulting from trap-trap, supertrap-supertrap, and trap-supertrap interactions and from radiative and nonradiative degradation to the ground state. All of these relaxation routes are shown schematically in Fig. 3.

b. Phosphorescence Lifetimes

To aid in the interpretation of the phosphorescence intensity ratios in light of the expected isotope effect on the phosphorescence efficiencies, the lifetimes of the various traps were measured with and without the presence of a second trap. The intensity was measured for one decade after the steady state illumination was shut off. It was found to be exponential, as can be seen in Fig. 4, and independent of the isotopic substitution of the host⁶ and guest. The time required for the intensity to fall to $1/e$ of its original value for the cases studied is given in Table I. The constancy of these lifetimes is a somewhat surprising result in light of the findings of Wright, Frosch, and Robinson.⁸ They found that the lifetime of C_6H_6 in an argon matrix is

Figure 4.

Triplet Lifetimes

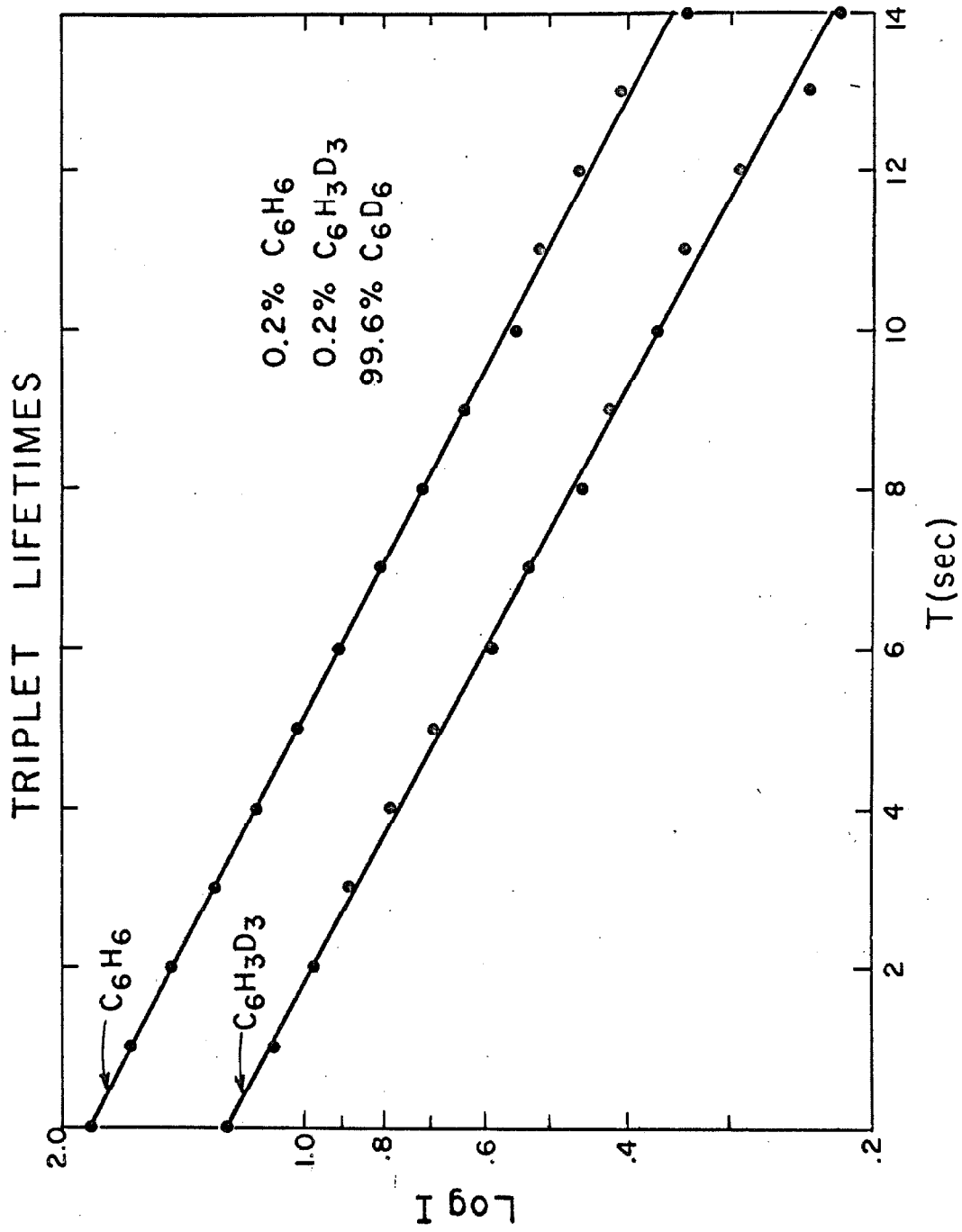


TABLE I
 TRIPLET LIFETIMES OF ISOTOPIC TRAPS IN C_6D_6
 τ (sec)*

Other Trap Measured \ Trap	$C_6H_3D_3$	$C_6H_4D_2$	C_6H_5D	C_6H_6	—
$C_6H_3D_3$		8.08	8.30	8.23	8.80
$C_6H_4D_2$	8.87		8.08		8.92
C_6H_5D	8.62	8.68		8.37	8.50
C_6H_6	8.51		8.51		8.54

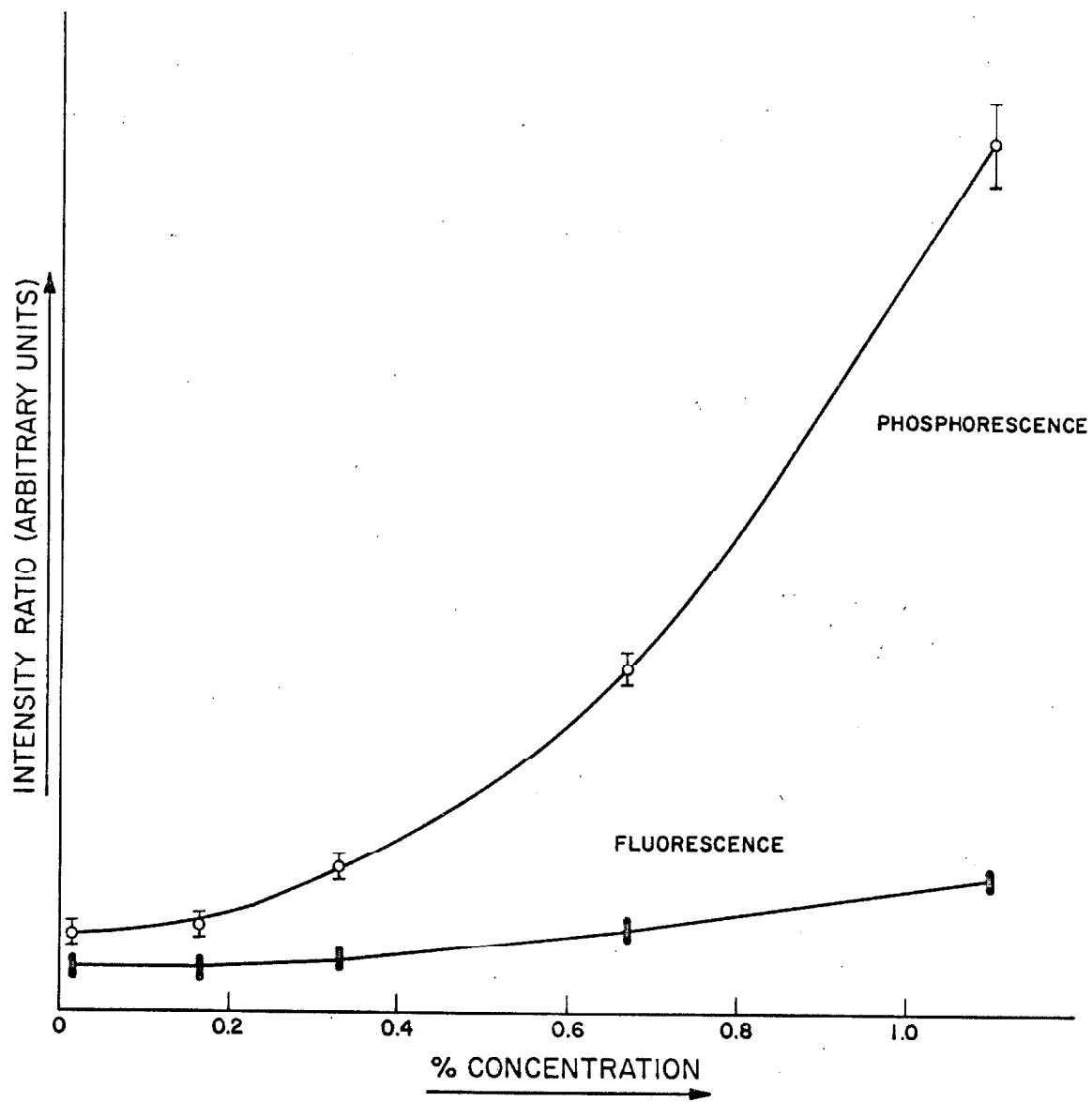
* ± 0.3 sec

16 sec while that of C_6D_6 is 26 sec. This isotope effect has been explained⁸ as a change in the lifetime for nonradiative decay to the ground state. Not observing this effect for the triplet lifetimes of benzene isotopic mixed crystals could indicate that the radiative decay process has been sufficiently shortened by the effects of the crystal field that the slower nonradiative decay processes can no longer favorably compete. In any case, as the lifetimes are found to be constant, they need not be considered further in the interpretation of the phosphorescence intensity ratios. The tendency for the trap lifetimes to be shorter than those of the supertraps might be real but is just outside the experimental uncertainty. Trap-supertrap energy transfer by an exchange mechanism is not expected to significantly alter the respective emission lifetimes if they are determined by extinguishing a steady state excitation source.⁹

c. Concentration Dependence of the Supertrap-Trap Ratios

The concentration dependence of the phosphorescence and fluorescence supertrap-trap ratios is given in Fig. 5 for mixed crystals of C_6H_6 and C_6H_5D in a C_6D_6 host crystal. The simplest theory that can be used to relate the concentration dependence of the intensity ratios is that of Perrin.¹⁰ In this theory it is assumed that, if there is a supertrap within an "active sphere" of radius R_0 around an excited trap, the excitation will be transferred to the supertrap, and if not it will not be transferred to any supertrap. As the transfer probability drops off exponentially for an exchange interaction, this

Figure 5. Concentration dependence of the supertrap-trap emission ratios for equal molar solutions of C_6H_6 and C_6H_5D in C_6D_6 at 4.2°K and moderate light levels. The concentration scale gives the value for each trap.



will be a reasonable first approximation. Using this approach, Nieman¹¹ has derived an expression for the fraction γ of traps that, after excitation, transfer their excitation to a supertrap:

$$\gamma = \frac{1 - (1 - f_s)^N}{1 - [(1 - f_s)^N - (1 - f_s - f_t)^N]} \quad (1)$$

where f_s and f_t are, respectively, the concentrations of supertraps and traps expressed as mole fractions, and N is the total number of molecules in the active sphere.

In terms of the supertrap-trap ratios, γ for triplet transfer is,

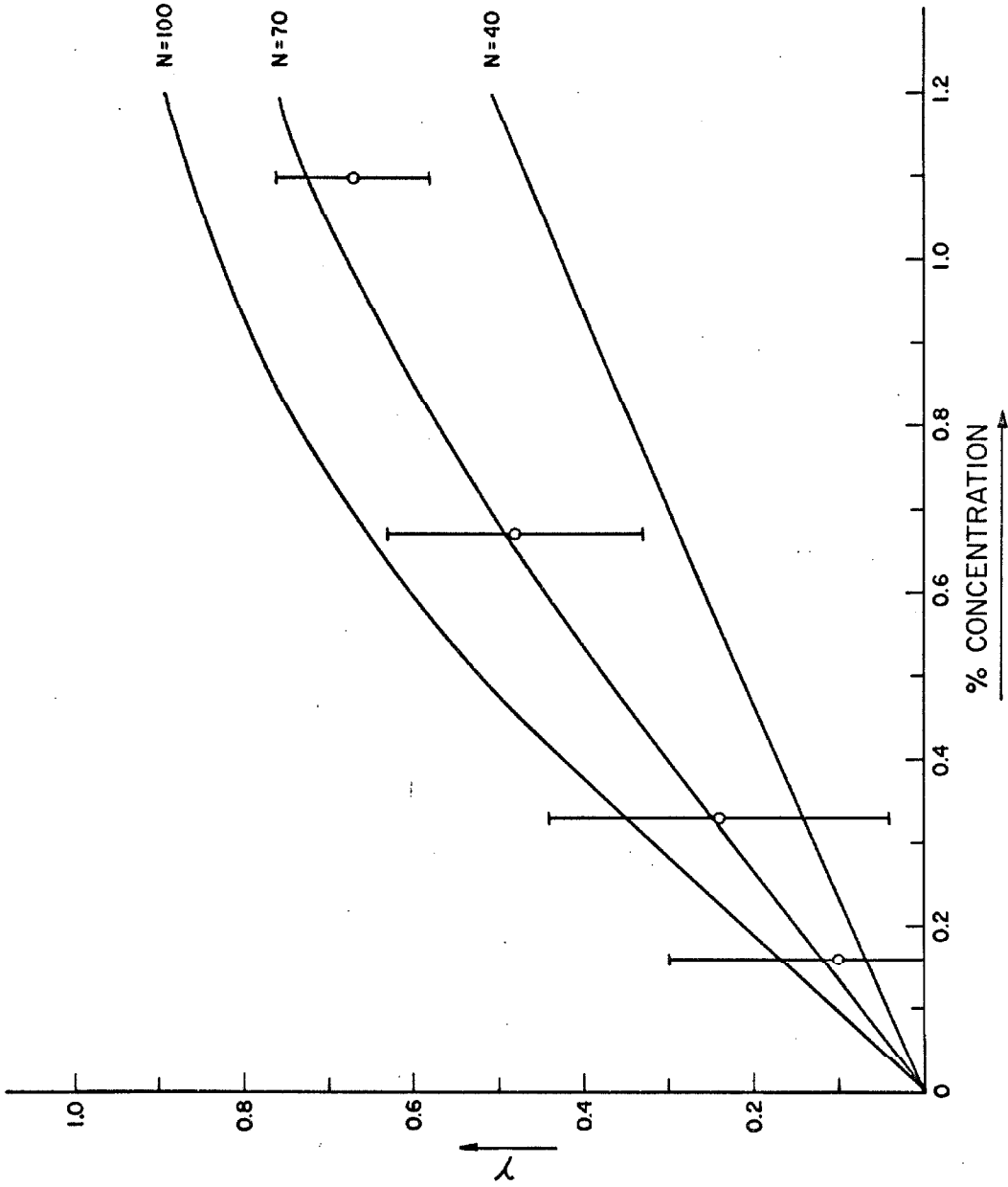
$$\gamma_x = \frac{P_x - F_x}{P_x + 1} \quad (2)$$

where P_x is the phosphorescence intensity ratio at concentration x divided by the ratio at infinite dilution, and F_x is the corresponding ratio for fluorescence. F_x is included to account for the distortion of P_x by singlet-singlet transfer. A plot of γ for various values of N and of γ_x from the data given in Fig. 5 is shown in Fig. 6.

These expressions take into account, by the way, intermediate trap to trap transfer steps that lead eventually to supertrapping. This feature is particularly important in the limit of high trap, low super-trap concentrations where most supertrapping involves many trap to trap steps.

Because of the large experimental uncertainties, one can only

Figure 6. γ (solid curve) and γ_x (open circle) as a function of guest concentration for an isotopic mixed crystal containing equal amounts of C_6H_6 and C_6H_5D in C_6D_6 . The concentration scale gives the value for each trap.

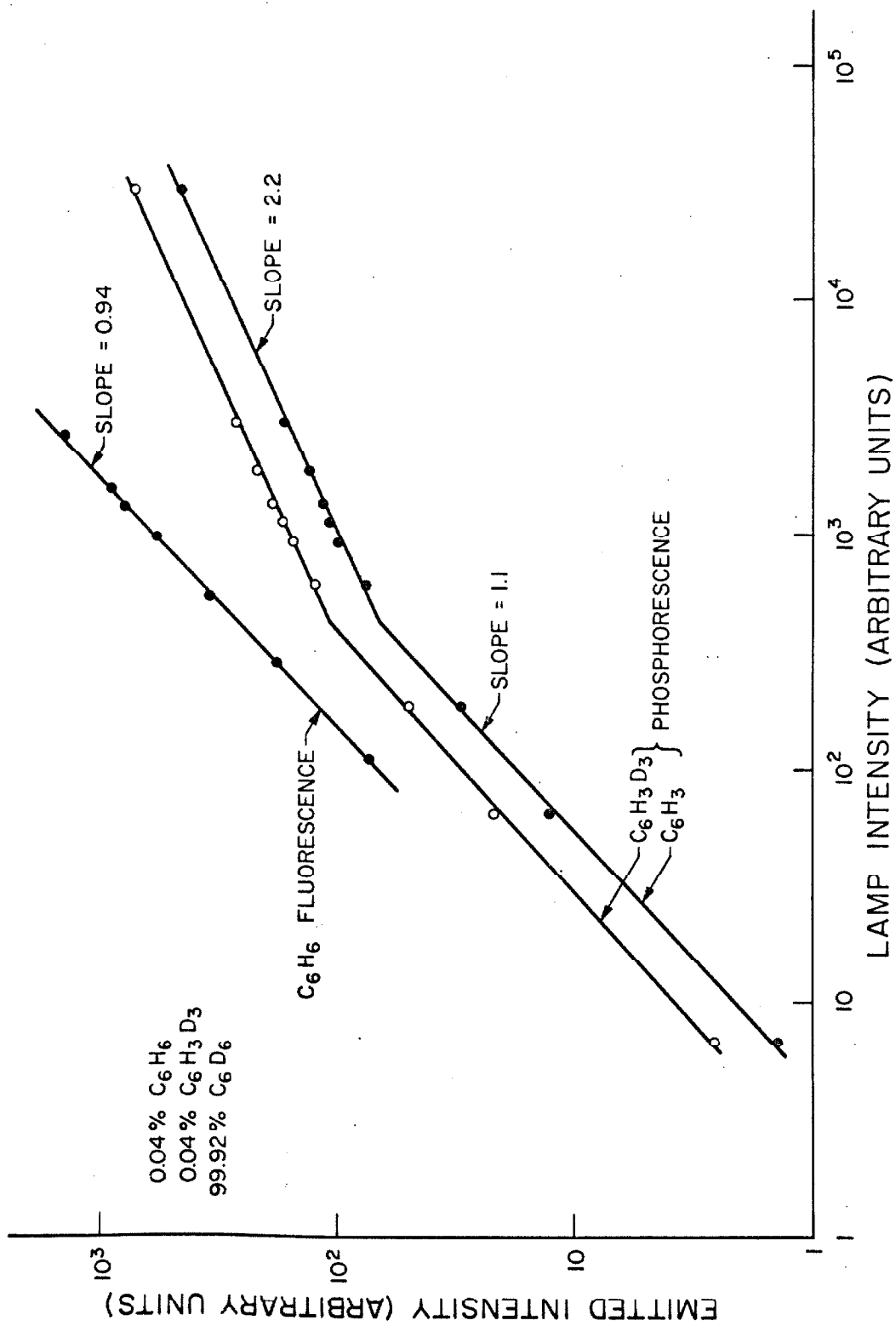


conclude that the active sphere contains ~ 70 molecules. In order to interpret this result in terms of an average distance R_0 over which triplet excitation can be transferred, one must make an assumption about the anisotropy of the pertinent exchange interactions in the benzene crystal. If the transfer probability is assumed to be nearly isotropic (i. e., the "active sphere" is nearly spherical) one finds from the crystal structure of benzene that $R_0 \sim 15 \text{ \AA}$, the "second neighbor" distance. However, if a two-dimensional model is assumed to be characteristic of the anisotropy (i. e., the "active sphere" is a planar figure) one finds $R_0 \sim 30 \text{ \AA}$, i. e., one must go to 4th nearest neighbor to circumscribe an area containing this many molecules in a two-dimensional. Because of the approximate nature of the entire approach, the most that can be concluded is that if a triplet excited trap and an unexcited supertrap are within $\sim 20 \text{ \AA}$ of each other in the host crystal, the excitation will most likely be exchanged. These transfer distances, in particular the one associated with the now probably isotropic model, are considerably shorter than those first estimated by Nieman and Robinson.³

d. Dependence of the Emitted Intensity on the Lamp Intensity

Perhaps the most interesting finding of this study is the effect of light on the relative emission quantum yields. This effect is shown in Fig. 7 for a 0.04% C_6H_6 , 0.04% $C_6H_3D_3$ in C_6D_6 mixed crystal, where it can be seen that $I(\text{phos.}) \propto [I(\text{lamp})]^{-\frac{1}{2}}$ at high light levels. The same relationship is found to hold for a mixed crystal containing only one type of trap. The degradation of the emission yield with

Figure 7. The dependence of the phosphorescence and fluorescence intensity on the lamp intensity at 1.8°K.



time at high lamp intensities has already been accounted for in preparing Fig. 7.

The dependence of the emitted intensity on the lamp intensity has the following characteristics. 1) There is no change in the supertrap-trap phosphorescence or fluorescence intensity ratios at the highest lamp intensity, even at guest concentrations as high as 1%. 2) The fluorescence intensity is linearly dependent upon the light level for all lamp intensities. 3) The high intensity slope was found to vary somewhat from sample to sample, its value averaged over several samples being $2 \pm .3$, i. e., $I(\text{phos.}) = K [I(\text{lamp})]^{0.5 \pm .07}$. This scatter probably represents the accuracy with which the phosphorescence and lamp intensities can be measured.

The dependence of the phosphorescence intensity on the lamp intensity at high light levels suggests that triplet-triplet annihilation processes might be determining the steady state concentration of triplets. As we have already established that few, if any, host triplets are formed in these mixed crystals (see Sec. III-a), any such annihilation must be occurring between excited trap or supertrap species. If this is true, it is somewhat surprising that annihilation can readily occur at concentrations where there is effectively no trap-supertrap triplet energy transfer. This would imply that the probability for annihilation is due to much longer range interactions than the probability for transfer. In fact, it must be considerably longer range as only a small fraction of the existing traps and supertraps are excited even at the highest light levels. That a small percentage of the guests are excited is known from the fact that the supertrap-trap

phosphorescence intensity ratios do not change with lamp intensity. If a large fraction of the supertraps were excited, the probability for trap to supertrap transfer would be markedly reduced. In the limit of complete saturation, the phosphorescence ratio would be the same as that of infinite dilution. Nothing like this has been observed and estimates of the amount of radiation absorbed by the crystal show that indeed only a few percent of the guest molecules can be excited under the steady state conditions possible with the exciting intensities used.

Long range triplet-triplet annihilation is not out of the question and, in fact, would be expected if there were a strong triplet-triplet absorption at the same frequency as the emission. Such an absorption would play the role of the strong singlet-singlet absorption in the long range triplet-singlet transfer mechanism established by Ref. 12. However, as no triplet-triplet absorption has been found in the region, if the annihilation is indeed long range, it most likely goes by a different mechanism.

It should be mentioned that not seeing trap to supertrap excitation transfer does not mean there is no trap to trap or supertrap to supertrap transfer. In fact "resonance" transfer is expected to be more probable than a transfer that requires energy to be given up to the lattice. In the language of Robinson and Frosch,¹³ the transfer of energy from a trap to a supertrap requires the supertrap to be excited to an electronic plus phonon state that is degenerate with the trap state. That this is 10 to 100 times less probable than a purely electronic excitation can be seen from the emission spectrum. The

phosphorescence of these isotopic mixed crystals consists of very sharp lines and the phonon addition bands are considerably weaker (~ 50 times) than the zero phonon lines.⁶ Thus the annihilation mechanism might actually be much shorter range than supposed above if rapid "resonance" transfer of excitation among traps and supertraps could effectively bring the excitations close to one another.

Different annihilation mechanisms, involving a trapped triplet excitation and either a host singlet exciton or a lamp photon obviously cannot be eliminated. Even though the singlet excitons are very short lived, the triplet state is so long lived that there is a fair probability of a singlet exciton being generated near by. However, as the probability for singlet-triplet annihilation is completely unknown, nothing more quantitative can be said about the validity of this explanation. Annihilation of a trapped triplet excitation by a 2537 \AA photon from the lamp is likewise a possible explanation since the positions of the higher lying triplet states have yet to be established.

The data could also be explained by conjecturing that a transient impurity is generated by some absorption process involving two photons. This impurity would have to have a lifetime no longer than a few seconds since the phosphorescence intensity at the "instant" the lamp is turned on is used in preparing Fig. 7. It also would have to be ineffective in quenching the fluorescence. Even though this combination of circumstances possibly exists, it seems much less probable than the annihilation mechanism.

IV. CONCLUSIONS

It has been confirmed that electronic excitation is transferred from one isotopic guest to another at very low temperatures. The benzene triplet state exchange interactions are such that an isotopic trap $\sim 200 \text{ cm}^{-1}$ deep can transfer its excitation to a slightly lower lying impurity roughly 20 \AA away. Evidence is also presented for even longer range transfer between degenerate isotopic guests and for annihilation of the trapped excitation at high light levels. The formation of impurities is also found at these very high light levels.

The energy relaxation processes in these crystals have been discussed and it has been established that few, if any, host triplet excitons are produced during the interconversion of "trapped" singlet excitation into "trapped" triplet excitation.

REFERENCES

- ¹ N. Hirota and C. A. Hutchison Jr., J. Chem. Phys. 42, 2869 (1965)
- ² R. G. Kepler, J. C. Caris, P. Avakian, and E. Abramson, Phys. Rev. Letters. 10, 400 (1963).
- ³ G. C. Nieman and G. W. Robinson, J. Chem. Phys. 37, 2150 (1962).
- ⁴ H. Sternlicht, G. C. Nieman, and G. W. Robinson, J. Chem. Phys. 38, 1326 (1963) and J. Chem. Phys. 39, 1610 (1963).
- ⁵ Exciton phosphorescence has been reported for p-dichloro- and p-dibromobenzene crystals. G. Castro and R. M. Hochstrasser, J. Chem. Phys. 46, 3617 (1967).
- ⁶ E. R. Bernstein, S. D. Colson, D. S. Tinti and G. W. Robinson, (manuscript in preparation).
- ⁷ S. D. Colson and E. R. Bernstein, J. Chem. Phys. 43, 2661 (1965).
- ⁸ M. R. Wright, R. P. Frosch, and G. W. Robinson, J. Chem. Phys. 33, 934 (1960).
- ⁹ M. Inokuti and F. Hirayama, J. Chem. Phys. 43, 1978 (1965).
- ¹⁰ F. Perrin, Compt. Rend. 178, 1978 (1924).
- ¹¹ G. C. Nieman, Thesis, California Institute of Technology (1965).
- ¹² R. P. Schwenker, R. G. Bennett, and R. E. Kellogg, J. Chem. Phys. 41, 3040 (1964).
- ¹³ G. W. Robinson and R. P. Frosch, J. Chem. Phys. 38, 1187 (1963).

Proposition I

A study of the PtH "molecule" and its relation to heterogeneous catalysis.

The need for an improved understanding of the fundamental concepts involved in heterogeneous catalysis has been recently pointed out by Brennan¹. Little is known about the nature of the simplest catalytic reactions involving atomization of diatomic molecules and, in particular, about the state of the adsorbed atom (adatom) on a metal surface. It is proposed that the methods of attenuated-total-reflection (ATR) spectroscopy² and matrix isolation spectroscopy³ be applied to the study of the interaction between Pt and H. Previous direct evidence as to the nature of the Pt-H "complex" has only been obtained from the optical absorption spectra of finely divided solids⁴. The solids are used as a support for metallic catalysts. Indirect evidence has been obtained by studying a large number of properties of metal surfaces exposed to a variety of reactants,⁵ and by following the kinetics of catalytic atomization on hot wires through pressure measurements in a flow system¹. However, none of the experiments to date have been successful in presenting a clear picture of the adsorbed state of H. It is hoped that the new, more quantitative experiments outlined below will lead to an improved understanding of the basic concepts governing catalytic hydrogenation. The ATR techniques will not only provide a much more sensitive method of taking the IR absorption spectrum of adsorbed hydrogen

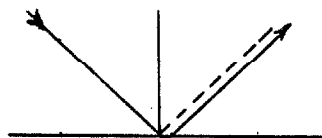
but will allow one to utilize clean, single crystal surfaces. This should make any conclusions more reliable than those previously drawn from the spectra of H adsorbed on small Pt particles which are in turn supported on alumina. The interpretation will be further aided by an infrared spectroscopic investigation of the PtH molecule isolated in an inert matrix.

Even though ATR spectroscopy is based upon a rather simple application of classical optics, it has only come into use during the past few years. The many advantages of this method over conventional IR reflection methods and often over transmission methods are yet to be realized by spectroscopists in general. Maxwell's theory for light propagation in semiconductors predicts that the electric field of a totally internally reflected plane wave penetrates the rarer medium with exponentially decreasing intensity such that it has been reduced to one half power at

$$x_{\frac{1}{2}} = \frac{0.693 \lambda_1}{2\pi(\sin^2\theta - n_{21}^2)^{\frac{1}{2}}}, \quad n_{21} = \frac{n_2}{n_1} < 1$$

$\theta > \theta_{\text{critical}}$

It has been verified experimentally that the resultant wave actually appears to be reflected from beneath the reflecting surface.⁶



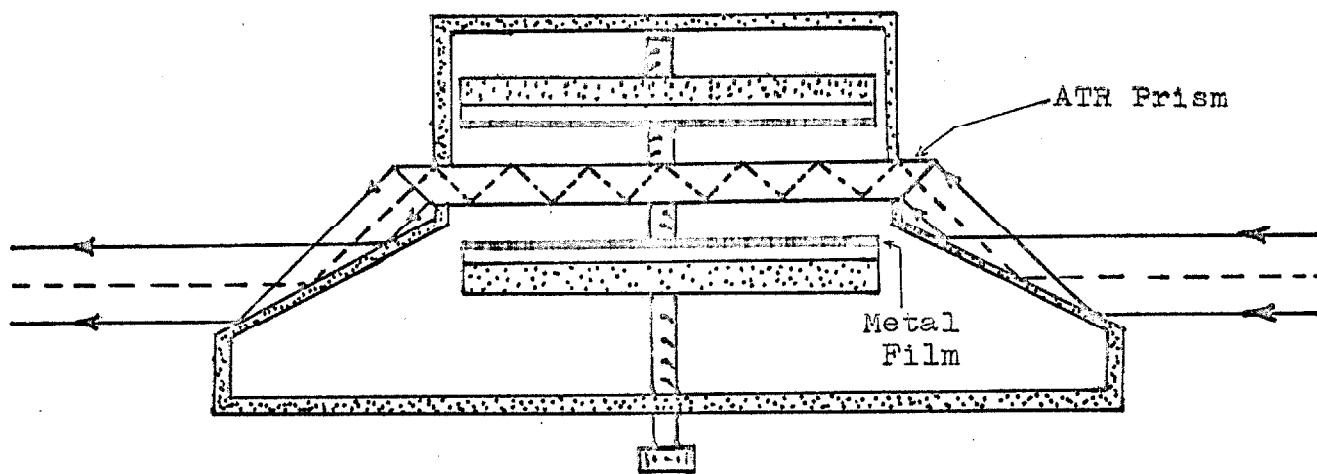
ATR spectroscopy is based upon the attenuation of the incident beam by placing a spectrally absorbing medium on or near the rarer side of the reflecting surface. Obviously, the substance to be studied must have a lower refractive index than the ATR crystal or there will be no reflection at any wave length.

Many of the advantages of internal reflection methods (ATR) over those based upon external reflection are given by Harrick.⁷ Since the intensity loss for total internal reflection is significantly less than that for external reflection, many more internal than external reflections are feasible without significant power losses. Indeed, this is found to be the case. ATR optics utilizing up to 350 reflections have been successfully used, and, in fiber optics, as many as 2×10^4 reflections have been reported.⁷ This results in a marked improvement in the signal to noise ratio. Another problem, other than light scattering, associated with the spectroscopy of adsorbed species is that of obtaining significant light intensity at the reflecting surface. Since the radiant density near the surface (0 to $\lambda/10$ Å) is greater for internal than for external reflection,⁷ if the light beam could somehow be internally reflected at the metal surface, the interaction with the chemisorbed species would be greater than if the beam had been externally reflected. One possible way of obtaining such an internal reflection spectrum would be to deposit a metallic film directly on the surface of a high refractive

index prism designed to give many internal reflections. The refractive index of thin metallic films is a function of their thickness and, thus, by carefully controlling the film thickness ($\sim 25 \text{ \AA}$), one could match the refractive index of the metal with that of the supporting crystal and observe internal reflection at the exterior metal surface. However, this method is beset by complications. The metal film, being an absorber itself, could significantly damage the important signal to noise ratio. Twenty reflections would require the light to pass through a total of 1000 \AA of metal for a 25 \AA thick film. This would result in a power loss of about 50%. Preparing the metallic films and controlling their thickness would be tedious at best. Furthermore, the interpretation of such spectra would be questionable since there may be no direct relationship between the catalyst-reactant interactions for such thin films with those for the more general case of thicker films. However, it would be at least as meaningful as that based on the presently available data. As these problems are not insurmountable, one should still try this technique since it lends itself so well to the study of the kinetics of reactions at the metal surface.

Such spectra could also be obtained by pressing a thick metal film (1 to 100μ), which had previously been exposed to hydrogen gas, against an ATR prism. (Figure 1) The metal film could be formed on a malleable support such as Teflon to improve the contact with the crystal surface.

Figure I

Schematic of ATR Cell
Top View

The sample holder should be built evacuable so that reactant pressures could be controlled precisely and foreign impurities eliminated. The major complications expected for such a system would arise from reactant-prism interactions and possible pressure effects if high "vise" pressures are required to obtain intense signals. Intense spectra at low pressures are anticipated if carefully milled and aligned surfaces are used.

It is, therefore, proposed that the method of ATR Spectroscopy be applied to obtain the IR absorption spectrum of chemisorbed H_2 on platinum films. H_2 , HD, and D_2 isotopes should be used and it is felt that a marked improvement in the resolution could be gained by working at low temperatures ($77 - 4^\circ K$). Pliskin and Eischens⁴ observed

considerable sharpening of their spectra by lowering the temperature to -50°C . The line shape of the absorption peaks can be followed as a function of temperature and of adatom surface concentration. The observed changes in line width should allow one to differentiate between the free translation and hopping models for the migration of adatoms. The time dependence of the absorption intensity can also be used to study the kinetics of the adsorption and desorption processes.

There is presently no spectral data available for the PtH molecule to use in the interpretation of the above mentioned experiments. All that is known is that complex hydrides of platinum exhibit absorptions in the 4.5 to 4.9μ region which have been attributed to excitation of the PtH stretching mode.⁸ The IR PtH spectrum is therefore of considerable interest, both from a fundamental standpoint and to aid in the interpretation of the catalysis experiments. It is proposed that isolated PtH molecules be obtained as follows. Pt vapor from a hot wire and an inert gas can be simultaneously deposited on an optical window which is cooled to 4°K by contact with liquid He. An $\sim 1\%$ Pt mixture prepared in this way can then be impregnated with H atoms generated from H_2 by an RF field. The small, "hot" H atoms are capable of penetrating into the solid deposit and can thus seek out and react with the dissolved Pt atoms. Alternately, a few percent of H_2 can be mixed with

the rare gas and then deposited simultaneously with the Pt. Ne and N₂ matrices should be used as they are known^{3,9} to give the narrowest line widths in other matrix isolation spectra, and as the use of such different hosts will help one understand the matrix effects on the observed transitions. The study of the spectra as a function of H concentration could be very illuminating as there have been numerous suggestions as to the nature and number of Pt-H complexes. While Eley¹⁰ has presented kinetic evidence for a



complex, the spectroscopic evidence of Pliskin⁵ and Eichens⁴ could not confirm it. The spectrum of Pt in an H₂ matrix should also be taken with this thought in mind. If deposits of high Pt concentration can be obtained in inert and hydrogen matrices, the IR spectra of platinum - hydrogen complexes containing different numbers of platinum and hydrogen atoms will be observed.

It is hoped that the combination of these ATR and matrix isolation spectra, covering a wide variety of platinum-hydrogen "molecules", will result in an improved understanding of the fundamental concepts governing the bonding of hydrogen to a platinum surface.

REFERENCES

1. D. Brennen, Adv. In Catalysis 15, 1 (1964)
2. J. Fahrenfort, Spectrochimica Acta 17, 698 (1961)
3. G.W. Robinson, J. Mol. Sect. 6, 58 (1961)
4. W.A. Pliskin and R.P. Eischens, Z. Phys. Chem. N.F. 24, 11 (1960)
5. See the Advances in Catalysis series for numerous examples.
6. F. Goos and H. Hänchen, Ann. Phys. 1, 333 (1947)
7. N.J. Harrick, Ann. N.Y. Acad. Sci. 101, 928 (1963)
8. J. Chatt, L.A. Duncanson and B.L. Shaw, Proc. Chem. Soc. (1957) 343
9. Y. Diamant, R.M. Hexter, and O. Schnepp, J. Mol. Spec. 18, 158 (1965)
10. D.D. Eley, Catalysis and the Chemical Bond, (University of Notre Dame Press, 1954), p.10

Proposition II

Neutron diffraction of metal surfaces contaminated by deuterium

The low energy electron diffraction study of the contamination of clean, single crystal surfaces by simple gases has been very important in the development of the present understanding of these heterogeneous reactions¹. For instance, using this technique, it has been established that oxygen molecules undergo surface diffusion on metallic Ni and that the reaction of O₂ with Ni is catalyzed by surface defects. In addition, strong evidence has been presented to indicate that the reaction of O₂ with the Ni results in the replacement of some of the surface nickel atoms by oxygen atoms.¹ However, the low energy electron diffraction technique cannot be applied to the study of adsorbed hydrogen or deuterium because of their low electron scattering power.¹ Thus, the study of this very important class of systems has been limited to less direct methods (see Proposition I).

In contrast, the scattering cross-sections of neutrons are not determined by the atomic number of the element. In fact, the cross-section for coherent scattering of thermal neutrons from deuterium is larger than from palladium and nearly as large as from platinum.² Thus, the pattern for neutrons scattered from a clean metal surface will be significantly different from that obtained

from a surface contaminated with deuterium. (Deuterium has been chosen for this discussion because of its low incoherent scattering cross-section in comparison to hydrogen².)

Neutron scattering spectroscopy also has the advantage of being a cleaner technique than electron diffraction because of the low neutron absorption cross-section of many elements. The neutron source can be external to the evacuable chamber containing the metal to be studied where as the electron "gun" has to be mounted inside the chamber¹, greatly increasing the probability of impurity contamination of the metal surface. However, this penetrating ability is probably the main reason neutrons have not previously been used for these studies. While electrons are strongly scattered by the surface, the primary signal from neutron scattering will be from the bulk of the sample. At high deuterium levels where a considerable number of deuterium atoms have "dissolved" into the bulk of a crystal such as platinum, the spectra of the bulk might be very interesting. However, if one is also to gain information about the surface reactions, the standard neutron scattering techniques must be refined.

It is proposed that the scattering from the bulk of the metal can virtually be eliminated by replacing all but the first few atomic layers of the metal with a strong neutron absorber. For instance, a thin film

of palladium can be formed on a cadmium crystal. The cadmium, being a strong absorber², will not reflect neutrons and, thus, any scattering will be due to the metallic film.

Another shortcoming of the neutron diffraction approach is due to the relatively small neutron scattering cross-sections. The neutron intensity scattered from a few atomic layers will be very difficult to detect using the relatively feeble neutron source available from ordinary thermal reactors. However, there have recently been numerous advances in the production of pulsed neutron sources with very high flux³, the use of which would make the experiment considerably easier. In fact, neutron pulses from underground nuclear explosions are presently being used in neutron spectroscopy⁴. These extremely intense pulses are thermalized with boron containing plastics and have been used to obtain diffraction patterns of higher quality from a single burst than can be obtained after several hours of counting using an ordinary thermal reactor.

Thermal neutrons can also be inelastically scattered from the surface by exciting a vibrational mode of the crystal or of the metal-deuterium complex bond. Thus the study of the inelastic scattering of neutrons from metal surfaces contaminated with deuterium will be complementary to the experiments outlined in Proposition I.

It is therefore proposed that the elastic and inelastic neutron scattering of deuterium contaminated metal films deposited on cadmium crystals be studied as outlined above.

REFERENCES

1. H.E. Farnsworth, Advances in Catalysis, Vol. 15 (Academic Press, New York, 1964), p.31.
2. G.E. Bacon, Neutron Diffraction (Oxford at the Clarendon Press, 1962)
3. R.H. Stahl, J.L. Russell, JR., and G.R. Hopkins, Advances in Nuclear Science and Technology, Vol. 3 (Academic Press, New York, 1966), p.329.
4. R.M. Brugger, (Idaho Nuclear Corporation), Private communication.

Proposition III

The effect of high pressures on the crystal structure and spectrum of molecular crystals

A number of organic molecules have been shown to crystallize under high pressures, and in some cases, the IR spectrum of the resulting crystal has been significantly different from that of solids normally produced by low-temperature crystallization.¹ This suggests an interesting technique by which one might learn more about the excitation exchange integrals which result in the exciton band structure² of molecular crystals. Presently, the assumptions of a given theoretical model for calculating these integrals are checked by calculating the exciton structure for a number of crystals of different molecules³. A much more meaningful approach would be to do the calculation for a number of different crystals of the same molecule. That is, if, by the application of pressure, a molecule could be caused to crystallize into a different structure, one would be able to compare the theory and experiments for a new set of intermolecular orientations and distances. One, of course, must consider the effects of pressure on the validity of the theoretical model. An assumption that is an excellent approximation for a crystal whose intermolecular distances are controlled by London dispersion forces may not be

valid at all for a crystal whose density has been drastically increased by external pressure. A low pressure phase change would be ideal for avoiding such complications.

The benzene crystal is a particularly interesting case to which this technique might be applied. Not only is it known to form high pressure crystals which are stable at pressures much below 5 K bar¹, but its exciton structure has been shown to be sensitive to external crystal strains.⁴ Unfortunately, the structure of the high pressure crystal is not known, but its IR spectrum indicated that this crystal (like the low temperature one) can be assumed, to first order, to be an ordered array of benzene molecules¹. That is, the theoretical assumptions applicable for one form will most likely apply to the other.

In order for this technique to work, the crystal symmetry need not change, only the lattice parameters. However, it would be especially interesting to study benzene crystals whose symmetry is different from that of the ordinary crystals. The symmetry based selection rules prevent one from observing all of the Davydov components of the 0,0 exciton band of ordinary benzene crystals and, as a result, one is forced to resort to indirect methods to obtain any quantitative data from the spectrum.² If a crystal structure with less restrictive symmetry properties can be formed at high pressures,

the interpretation of the data would be easier and the comparison with theory would be a more critical check of the theoretical assumptions.

There are two difficult problems associated with this type of experiment; obtaining a "high pressure crystal" at low temperatures (4.2°K) and determining the crystal structure at these low temperatures. Without a knowledge of the crystal structure, the pressure perturbations on the spectra are almost impossible to interpret. The X-ray techniques presently used for high pressure studies⁵ can be adapted for low temperature work by using a dewar similar to that used for low temperature studies of normal crystals.⁶

The high pressure crystals are most easily prepared in a diamond anvil press⁵ to which the pressure is mechanically applied. A simple modification of this device in which the pressure is applied by compressed He gas would be adequate for low temperature experiments. A typical experiment might be performed as follows: A single, high pressure crystal 20 μ thick is first prepared at room temperature (as described in Ref. 1) in a diamond anvil press that is attached to a cold finger of a liquid He dewar. The dewar will have to be such that the cold finger can be rotated into one position for optical absorption studies and into another for the X-ray analysis. The crystal is then cooled over a period of several hours

to 77°K and then to 4.2°K by blowing cold He gas through the liquid helium reservoir of the dewer. A constant "vice pressure" can be maintained during cooling by keeping the pressure of the pressure inducing He gas at a constant value. The absorption spectrum and X-ray scattering pattern can then be determined for comparison with the corresponding findings for normal benzene crystals.

The crystal will most likely crack quite badly during cooling but, hopefully, the applied pressure will be sufficient to prevent a phase change to the normal crystalline form.

The literature is barren of any but preliminary studies of the effects of pressure on the crystal structure and spectra of organic molecular crystals. There have been no experiments combining the crystal structure determinations with optical spectroscopy at low temperatures. Thus, it is proposed that these studies be undertaken to provide a deeper understanding of the intermolecular interactions in the solid phase. There are numerous very interesting systems to be studied; the benzene example discussed above merely serves as an illustration. If the crystal growing techniques can be developed, the simpler diatomic molecular crystals, where the theory is more tractable, would also be interesting examples.

REFERENCES

1. J.W. Brasch, *Spectrochimica Acta* 21, 1183 (1965)
2. For a detailed discussion of the relationship between the intermolecular excitation exchange integrals and the exciton band structure of molecular crystals, see Part II of this thesis.
3. R. Silbey, S.A. Rice, and J. Jortner, *J. Chem. Phys.* 43, 3336 (1965); R. Silbey, J. Jortner, M.T. Vala, and S.A. Rice, *J. Chem. Phys.* 42, 2948 (1965); D.P. Craig and M.R. Philpott, *Proc. Roy. Soc. (London)* 290A, 583 (1966); J. Jortner, S.A. Rice, and R. Silbey, Modern Quantum Chemistry, Part II (Academic Press, 1965), p.139.
4. S.D. Colson, *J. Chem Phys.* 45. 4746 (1966).
5. L.S. Whatley and A. Van Valkenburg, Advances in High Pressure Research, Vol. 1 (Academic Press, 1966), p.143.
6. W.E. Streib and W.N. Lipscomb, *Proc. Natl. Acad. Sci. (V.S.)* 48, 911 (1962).

Proposition IV

The spectra of "transition state molecules"

The kinetic theory of bimolecular reactions has generated considerable interest in molecules which have yet to be detected. An assumption of the absolute rate theory is that an activated complex is in complete equilibrium with the reactive species¹. The success of this theory has caused many to wonder if metastable intermediates are involved in these reactions. It is the object of this proposition to point out that, if there is any potential for the formation of stable intermediates, this potential will most likely be ^enhanced in a solid matrix by the repulsive interactions with the surrounding molecules. If this is the case, and if the reaction can be performed in solid matrices, the resultant "frozen" intermediates can be characterized spectroscopically. Even if such an intermediate does not have a stable ground state, it could have numerous bound excited states that can combine radiatively with the dissociative ground state. If emission from the bound excited states can somehow be observed, the nature of the repulsive potential can be obtained directly from the spectrum.

To impliment these ideas, it is proposed that simple bimolecular reactions be carried out in the solid phase at low temperatures and that the spectra of trapped intermediates be searched for and analyzed.

One interesting experiment would be to deposit a gas mixture of ~1% Cl_2 in H_2 on an optical window which is cooled by contact with liquid He. The IR spectrum of the solid deposit could then be taken to characterize the unreacted state. If the sample is then exposed to UV excitation, the Cl_2 molecules which are excited to the dissociative ${}^1\Pi_u$ state² will interact with the surrounding H_2 lattice with considerable energy ($\sim 20,000 \text{ cm}^{-1}$) and, thus, a number of possible products can be produced. The result will depend upon the final states available and the rates of relaxation into these final states. The formation of new species such as H_2Cl would be observable in the IR spectrum. A shallow attractive potential will result in dissociation limits in the vibrational or rotational structure from which the stability of the products in the matrix can be determined.

Luminescence from bound excited states of these new molecules could be searched for by using higher energy excitation. Perhaps a cleaner system for this purpose would be a 1% mixture of HCl in solid H_2 . If the sample were irradiated with a pulse of high energy electrons, the highly excited H atoms formed might react with HCl forming H_2Cl in an electronically excited state. If this species then relaxes radiatively to the ground state, the nature of the emission will characterize the ground state potential function.³ A dissociative ground state will yield a continuous emission spectrum while a weakly bound final state will produce a partially discrete spectrum with dissociation limits in the

vibrational progressions. The extent of the continuous emission will display the nature of ground state repulsive forces in that a strongly repulsive state will result in a broad continuum emission and the converse will be observed for a weakly repulsive one.

The formation of new species with stable ground states, should be searched for by exciting an appropriate mixture of gases (HCl in H₂) with radio frequency radiation. Discrete spectra (not due to hydrogen or chlorine) superimposed on the hydrogen continuum could be analyzed to give the stability of these species in the gas phase. Continuous emission spectra from species with unstable ground states could only be detected in spectral regions where the hydrogen continuum was very weak. Even then, unless it had some structure, its assignment to a specific species would be very difficult at best.

REFERENCES

1. K.J. Laidler and J.C. Polangi, Progress in Reaction Kinetics, (Pergamon Press, N.Y., 1965), P.1.
2. G. Herzberg, Molecular Spectra and Molecular Structure I. Spectra of Diatomic Molecules, (D. Van Nostrand Co., Inc. 1950), P. 392.
3. Ref. 2, P.387.

Proposition V

The Exciton Band Structure and Mobility of the Lowest Excited Triplet States of the p-dihalogenated Benzenes

Some very interesting and puzzling questions have been raised by the spectroscopic studies of Castro and Hochstrasser on the p-dihalogenated benzenes. They found that, while the lowest triplet state of p-diiodobenzene (DIB) exhibited large Davydov splittings¹ ($\sim 120 \text{ cm}^{-1}$), no measurable splitting ($< 0.3 \text{ cm}^{-1}$) was observed for the p-dibromobenzene (DBB) or p-dichlorobenzene (DCB) crystals.² This in itself is not too surprising in light of the large differences in the crystal structures. The DIB crystal has a D_{2h}^{15} space group with four molecules (translationally inequivalent) per primitive unit cell, each at a physically equivalent site.³ Both p-dichlorobenzene⁴ and p-dibromobenzene⁵ crystalize in the space group C_{2h}^5 with two molecules (translationally inequivalent) per unit cell. The dimensions of these unit cells are given in Table I. Two of the four translationally inequivalent (TI) molecules in the DIB unit cell are very nearly parallel and have a small center-to-center distance (3.5 \AA), where as the two TI-molecules in the DBB and DCB crystals are nearly perpendicular and have a relatively large center-to-center distance (7.9 \AA). Thus, as it is the interaction between the TI-molecules that determines the magnitude of the Davydov splittings⁶, one would expect quite different results for the two types of crystals. The observed

differences are certainly in qualitative agreement with these expectations.

TABLE I

Dihalogenated Benzene Unit Cell Dimensions			
	P-Dichlorobenzene	P-Dibromobenzene	P-Diodobenzene
\underline{a} (Å)	14.80	15.36	17.01
\underline{b} (Å)	5.75	5.75	7.32
\underline{c} (Å)	3.99	4.10	5.95

A surprising feature of their studies is that relatively intense exciton phosphorescence was observed² from neat crystals of DBB and DCB but no such emission could be detected¹ from the DIB crystal. Not observing phosphorescence from DIB is consistent with findings for benzene and naphthalene crystals. The lack of emission is explained⁷ by allowing for triplet-triplet annihilation of two triplet excitons to yield one highly excited molecule and one molecule in its ground state. The migration of the triplet excitons through the crystal is said to be so rapid that the annihilation rate is much faster than the radiative transition to the ground state and, thus, the equilibrium concentration of triplets is too low to yield detectable emission. The shorter radiative lifetimes of the halogenated benzenes ($\sim 10^{-3}$ sec) might make the observation of exciton phosphorescence possible as exciton fluorescence ($\sim 10^{-8}$ sec) is a common occurrence in molecular crystals. However, the $T_1 \rightarrow S_0$ transition of DIB is stronger

than that of either DBB or DCB. Thus, unless the intermolecular interactions of DIB are much larger (including those between translationally equivalent molecules) than those of DBB or DIB, the iodo compound should have the higher phosphorescence yield if one assumes that the excitation migration mechanisms are the same for both systems. From crystal structure considerations alone, the translationally equivalent (TE) interactions along the g crystal axes of both DBB and DIB are expected to be nearly as large as the largest interactions in the DIB crystal. In fact, there is reasonably strong experimental evidence to support such an expectation as part of the phosphorescence of DBB is very broad and shifted to the red from the sharp exciton phosphorescence. Since these features are characteristic of excimer (excited dimer) emission, the broad portion has been assigned to excimer phosphorescence from a strongly interacting TE-pair of molecules by Castro and Hochstrasser.⁸ Thus, as TE-interactions and TI-interactions both lead to excitation migration, no explanation has been given for the appearance of phosphorescence from DBB and DCB crystals.

It is the purpose of this proposition to offer an explanation for the appearance of $T_1 \rightarrow S_0$ emission from DBB and DCB and to indicate experiments by which the explanation can be verified.

The phosphorescence abilities of these crystals can be explained very reasonably in terms of the anisotropy in the intermolecular interactions. For the DBB and DCB crystals,

since there is virtually no interaction between TI-molecules, an excited molecule can only transfer its excitation along the a, b, or c crystal axes. However, as the excitation exchange integrals for weak transitions fall off very rapidly with distance, the interaction between a molecule and its neighbor along the a axis (15 \AA) can be neglected. Similarly the interaction with its neighbor along the c axis (4 \AA) is expected to be considerably larger than that along the b axis (5.7 \AA). Thus, the excitation will effectively travel along the c axis of the crystal, greatly reducing the probability for annihilation. The only opportunity for annihilation will be when two excitons are generated on the "same c axis" and then subsequently come together. As the fraction of molecules in the sample which are excited with normal excitation sources is of the order of 10^{-4} , such a coincidence is highly unlikely and even a slight amount of spreading along the b axis will probably lead to negligible annihilation.

If this is the correct interpretation of the data, it provides an excellent opportunity for differentiating between the random walk and coherent models for excitation transfer. There has been no direct measurement of the spread of excitation transfer through a crystal, even though the subject has generated numerous discussions in the literature ranging from the very qualitative⁹ to the purely theoretical.¹⁰ The two limiting models of excitation transfer have recently been compared by Robinson¹¹. He concluded that the coherent model, which neglects scattering from phonons and defects, will be

closer to reality for molecular crystals than the random walk model which assumes a scattering process occurs after every "jump" of the excitation. The real situation undoubtedly lies somewhere between these two limits which predict quite different rates for the spread of the excitation through the crystal. If the initial distribution is Gaussian, the coherent¹¹ and random walk¹² models predict the respective widths for the probability distribution functions

$$X \text{ (Coherent)} \approx \frac{am\tau}{\hbar},$$

$$X \text{ (Random)} \approx a \left(\frac{2m\tau}{\hbar} \right)^{\frac{1}{2}},$$

where a is the distance traveled during a single jump, m is the value of the excitation exchange integral, and τ is the average lifetime. For DBB, estimating $m \sim 10 \text{ cm}^{-1}$ and setting $a = \underline{c} = 4 \text{ \AA}$ and $\tau = 0.0003 \text{ sec}$ ¹³, one finds

$$X \text{ (Coherent)} = 24 \text{ cm},$$

$$X \text{ (Random)} = 5 \times 10^{-4} \text{ cm},$$

and for DCB, setting $\tau = 0.02 \text{ sec}$ ¹³, one finds

$$X \text{ (Coherent)} = 160 \text{ cm}$$

$$X \text{ (Random)} = 1.1 \times 10^{-2} \text{ cm}$$

Thus it is reasonable to assume that X will actually be of the order of 1 cm. Such a spread of the excitation can easily be measured by the following experiment. A long single crystal can be grown and oriented such that the ab face can be

illuminated with light which will only be absorbed by the lowest excited singlet state. The singlet excitons generated in this manner will be found in the first few mm of the crystal because of the strong $^1S \leftarrow ^0S$ transition probability and because even the coherent model would predict their spreading out to be less than one mm. Thus, the triplet excitons formed by intersystem crossing will be initially located in a well defined region of the crystal. The intensity of the phosphorescence as a function of distance from the excited end along the c axis can then be studied either under pulsed or steady state excitation conditions and compared to the various theoretical models. The temperature dependence of the transfer rate can be used to evaluate the scattering of thermally populated phonons with the exciton. Naturally, extreme care should be taken in the experiment to eliminate scattered light from the excitation source and from different emitting regions of the sample. The large differences expected when the crystal is oriented such that the transfer rate along the a and b axes can be measured should provide a good test of the experimental techniques. In this regard, the temperature dependence of the width of the exciton band \rightarrow exciton band transitions should be measured so that the total triplet exciton band width can be independently measured and utilized in the interpretation of the excitation transfer data. For a complete discussion of this latter technique see Part II of this thesis where it is applied to the lowest singlet states of benzene and naphthalene.

REFERENCES

1. G. Castro and R.M. Hochstrasser, *Molecular Crystals* 1, 139 (1966).
2. G. Castro and R.M. Hochstrasser, *J. Chem. Phys.* 46, 3617 (1967).
3. L. Dun-choi and Yu T. Struchkov, *IZvest. AKad. Nauk SSSR, OKhN*, 12, 2095 (1959).
4. V. Croatto, S. Bezzi, and E. Bua, *Acta Cryst.* 5, 825 (1952).
5. S. Bezzi and V. Croatto, *Gazz. Chim. Ital* 72, 318 (1942).
6. For a detailed discussion of the origin of Davydov splittings in molecular crystals see Sec.II of this thesis.
7. H Sternlicht, G.C. Nieman, and G.W. Robinson, *J. Chem. Phys.* 38, 1326, (1963).
8. G.C. Castro and R.M. Hochstrasser, *J. Chem. Phys.* 45, 4352 (1966).
9. D.L. Dexter and R.S. Knox, Excitons (Interscience, New York, 1965) p. 89.
10. J. Jortner, S.A. Rice, and J.L. Katz, *J. Chem. Phys.* 42, 309 (1965)
11. G.W. Robinson, Energy Conversion by the Photosynthetic Apparatus (Brookhaven Symposia in Biology : No. 19, 1966) p.16.
12. N. Davidson, Statistical Mechanics (McGraw-Hill, New York, 1962) p.283.
13. D.S. McClure, *J Chem. Phys.* 17, 905 (1949).